Neutrosophic Knowledge

Journal of Modern Science and Arts

Volume 9, 2026

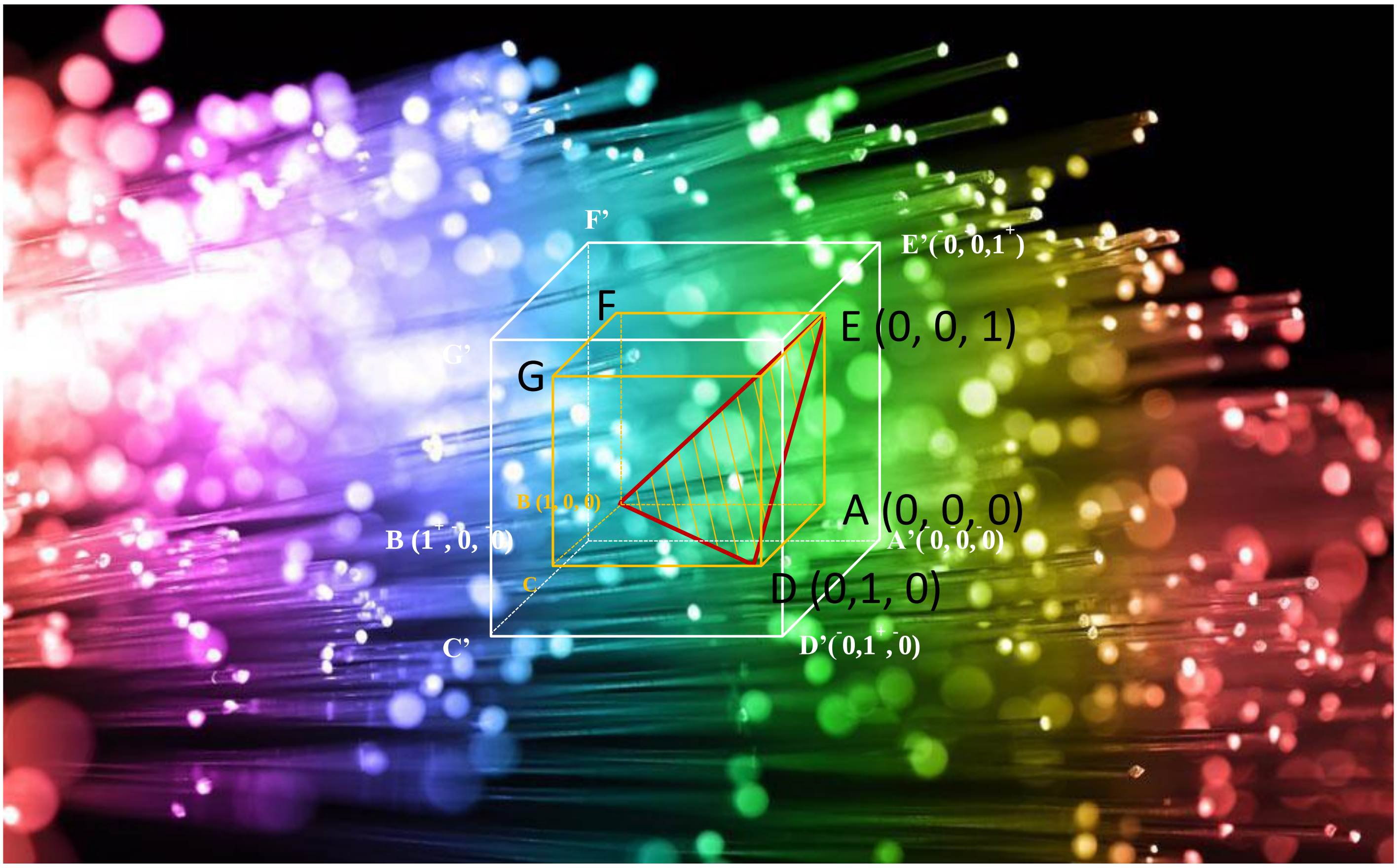

Editors-in-Chief

Salah Bouzina, Florentin Smarandache, Ahmed Hatip

ISSN 2767-0619 (Print)

ISSN 2767-0627 (Online)

Neutrosophic Science
International Association (NSIA)

Published by the UNIVERSITY OF NEW MEXICO, United States

Neutrosophic Knowledge

JOURNAL OF MODERN SCIENCE AND ARTS

Editors-in-Chief

Salah Bouzina, Florentin Smarandache, Ahmed Hatip

ISSN 2767-0619 (Print)

ISSN 2767-0627 (Online)

ISSN 2767-0627 (online) ISSN 2767-0619 (Print)

Neutrosophic Knowledge

An international Journal concerned with publishing in all scientific and literary fields

Papers Published in Arabic, Turkish, English and French

Copyright Notice

Information for Authors and Subscribers

*"*Neutrosophics Knowledge*"* has been created for publications on advanced studies in neutrosophy, neutrosophic set, neutrosophic logic, neutrosophic probability, neutrosophic statistics that started in 1995 and their applications in any field, such as the neutrosophic structures developed in algebra, geometry, topology, etc.

The submitted papers should be professional, in good Arabic, Turkish, English and French containing a brief review of a problem and obtained results.

Neutrosophy is a new branch of philosophy that studies the origin, nature, and scope of neutralities, as well as their interactions with different ideational spectra.

This theory considers every notion or idea <A> together with its opposite or negation <antiA> and with their spectrum of neutralities <neutA> in between them (i.e. notions or ideas supporting neither <A> nor <antiA>). The <neutA> and <antiA> ideas together are referred to as <nonA>.

Neutrosophy is a generalization of Hegel's dialectics (the last one is based on <A> and <antiA> only).

According to this theory every idea <A> tends to be neutralized and balanced by <antiA> and <nonA> ideas - as a state of equilibrium.

In a classical way <A>, <neutA>, <antiA> are disjoint two by two. But, since in many cases the borders between notions are vague, imprecise, Sorites, it is possible that <A>, <neutA>, <antiA> (and <nonA> of course) have common parts two by two, or even all three of them as well.

Neutrosophic Set and *Neutrosophic Logic* are generalizations of the fuzzy set and respectively fuzzy logic (especially of intuitionistic fuzzy set and respectively intuitionistic fuzzy logic). In neutrosophic logic a proposition has a degree of truth

(*T*), a degree of indeterminacy (*I*), and a degree of falsity (*F*), where *T, I, F* are standard or non-standard subsets of *]-0, 1+[*.

Neutrosophic Probability is a generalization of the classical probability and imprecise probability.

Neutrosophic Statistics is a generalization of the classical statistics.

What distinguishes the neutrosophics from other fields is the <neutA>, which means neither <A> nor <antiA>.

<neutA>, which of course depends on <A>, can be indeterminacy, neutrality, tie game, unknown, contradiction, ignorance, imprecision, etc.

All submissions should be designed in MS Word format using our template file:
http:// fs.unm.edu/NK/Nk-paper-template.doc.

A variety of scientific books in many languages can be downloaded freely from the Digital Library of Science:
http:// fs.unm.edu/ScienceLibrary.htm.

To submit a paper, mail the file to the Editor-in-Chief. To order printed issues, contact the Editor-in-Chief. This journal is non-commercial, academic edition. It is printed from private donations.

Information about the neutrosophics you get from the UNM website:
http:// fs.unm.edu/neutrosophy.htm.. The home page of the journal is accessed on http://fs.unm.edu/NK.

ISSN 2767-0627 (online) *ISSN 2767-0619 (Print)*

Editors-in-Chief

Associate Editors

ISSN 2767-0627 (online) ISSN 2767-0619 (Print)

Editors

ISSN 2767-0627 (online) ISSN 2767-0619 (Print)

Content

Neutrosophic Knowledge, Vol. 9, 2026
University of New Mexico

Article

Unmatter in High Energy Physics: Theoretical Foundations, Experimental Verification, and Emerging Applications

Florentin Smarandache[1,*]

[1] University of New Mexico, Mathematics, Physics, and Natural Sciences Division, 705 Gurley Ave., Gallup, NM 87301, USA
* Correspondence: smarand@unm.edu

Received: Month Day, Year; *Accepted:* Month Day, Year; *Published:* Month Day, Year

Abstract: Unmatter—a state of matter defined by the stable or quasi-stable coexistence of intertwined matter and antimatter components—represents a significant departure from classical annihilation paradigms. Emerging from the nexus of neutrosophic logic, paradoxist philosophy, and high-energy particle physics, the concept provides a framework for understanding indeterminate material states. This paper synthesizes the conceptual evolution of unmatter and reviews the seminal 2015 Rutherford Appleton Laboratory (RAL) experiment, which successfully generated a high-density, charge-neutral electron-positron ($e^- e^+$) plasma, serving as the experimentum crucis for macroscopic unmatter. Furthermore, we survey contemporary research (2024–2025) that integrates unmatter into Quantum Chromodynamics (QCD), exotic plasma dynamics, and neutrosophic computational models. Finally, we propose future research trajectories, including the application of super-hypergraph modeling to complex unmatter systems and the exploration of novel energy-generation architectures.

Keywords: Unmatter, Neutrosophic Logic, High-Energy Physics, Antimatter, Electron-Positron Plasma, Rutherford Appleton Laboratory (RAL), Quantum Chromodynamics (QCD), Super-Hypergraph Modeling, Bound States.

1. Introduction

The conceptual framework of **unmatter** [11, 12] was first introduced by Smarandache as a physical extension of **neutrosophy**—a branch of philosophy concerned with the nature of neutralities and the spectrum of indeterminacy [10]. In neutrosophic logic, any proposition is characterized by a triad of truth (T), indeterminacy (I), and falsity (F). When mapped onto the ontologies of high-energy physics [1], this triad challenges the traditional binary of matter versus antimatter.

Classical particle physics generally views matter and antimatter as mutual antagonists that undergo rapid annihilation upon contact. In contrast, unmatter posits the existence of **stable or metastable configurations** where matter and antimatter components coexist in a bound or intertwined state. This transition from "annihilation partners" to "coexistence partners" marks a paradigm shift in how we categorize composite particles and exotic states of matter.

The relevance of unmatter to contemporary **High-Energy Physics (HEP)** [15] is demonstrated through several critical intersections:

- **Quantum Chromodynamics (QCD)** [7] **and Meson Physics** [18]: At the subatomic level, mesons—composed of a quark (q) and an antiquark ($\bar{q}$)—serve as the most fundamental realization of unmatter. Because they are neither purely matter nor purely antimatter, they embody the neutrosophic "neutral" state.

- **Unparticle Physics** [4, 5]: The theoretical construct of "unparticles," which exhibit scale-invariance and fractional excitations, can be interpreted as a specialized manifestation of unmatter. In this context, the indeterminate component (I) describes the non-integer nature of the particle's scaling dimension.
- **Exotic Plasma Dynamics** [19]: On a macroscopic scale, the generation of **charge-neutral electron-positron** (e^-e^+) **plasmas** via ultra-intense laser-matter interactions provides a laboratory for studying unmatter in bulk. These plasmas do not immediately annihilate but instead exhibit collective electromagnetic behaviors, creating a macroscopic "unmatter environment."
- **Computational and Mathematical Modeling:** Beyond physical particles, the neutrosophic triplet (T, I, F) offers a robust logical substrate for modeling the stochastic and indeterminate interactions within complex particle systems, leading to the development of **neutrosophic computational frameworks** for HEP data analysis.

By synthesizing these diverse domains, the study of unmatter moves beyond speculation into a rigorous inquiry of the fundamental symmetries—and asymmetries—of the universe.

2. Conceptual Foundations

2.1. Neutrosophic Logic and the Neutral State

At its core, **neutrosophy** defines three independent components for any logical statement or physical system: **Truth (*T*)**, **Indeterminacy (*I*)**, and **Falsity (*F*)**. Unlike classical fuzzy logic, these components range over the non-standard unit interval $]^-0, 1^+[$, and are not necessarily constrained by the sum $T + I + F = 1$. [10]

In the context of high-energy physics, we map these components onto the material composition of a system:

- ***T* (Matter):** The presence of matter particles (e.g., quarks, electrons).
- ***F* (Antimatter):** The presence of antimatter particles (e.g., antiquarks, positrons).
- ***I* (Indeterminacy/Unmatter):** The degree of binding, neutral coexistence, or "neutrality" where the identity of the system as purely matter or antimatter is lost.

The **neutral element (*n*)** corresponds to a region where I is maximized and $T \approx F$. Mathematically, an unmatter entity U can be represented by a composition vector:

$$V_U = \begin{pmatrix} M \\ I \\ A \end{pmatrix}$$

where M is the matter percentage, A is the antimatter percentage, and I represents the indeterminate interaction term. For a perfectly balanced unmatter system, such as a neutral pion (π^0), the vector approaches (α, I, α), where the interaction term I accounts for the gluon field and binding energy that prevents immediate annihilation.

2.2 Physical Realizations: From Microscopic to Macroscopic

Unmatter is not merely a speculative construct; it manifests across various energy scales. The following descriptions categorize these realizations by their physical structure:

- **Mesons (π, K, …):** These are the most common microscopic realizations. As bound states of a quark (q) and an antiquark ($\bar{q}$), they exist in a state of constant "internal tension" between matter and antimatter, governed by the Strong Force.
- **Unatoms:** In the realm of nuclear physics, unatoms are hypothetical nuclei consisting of both nucleons and antinucleons (e.g., a system of $p + \bar{p}$). While highly unstable, they represent a complex "neutral" material state.
- **Electron-Positron** (e^-e^+) **Beam Plasma:** This represents a **macroscopic** realization. When ultra-intense lasers interact with high-Z targets, they create a dense, charge-neutral plasma where matter and antimatter are spatially intertwined. Unlike individual particle pairs, this plasma exhibits collective electromagnetic modes (see §4).

- **Unparticles:** Emerging from scale-invariant sectors of theoretical physics, unparticles can be modeled as a continuous superposition of unmatter states. Their lack of a definite mass shell reflects the "indeterminacy" (I) component of neutrosophic logic.

These realizations demonstrate that unmatter is an essential category for describing particles and states that do not fit the binary "matter vs. antimatter" classification.

3. Historical Development

The trajectory of unmatter research is characterized by an increasing convergence between abstract logic and high-energy experimental physics. The following milestones delineate this evolution:

3.1. The Ontological Proposal (2004)

The term "unmatter" was formally introduced by **Smarandache** in 2004 [11]. Grounded in the principles of **neutrosophy**, the original proposal argued that the exclusion of "neutral" states in particle physics was a limitation of binary logic. By defining unmatter as a combination of matter and antimatter that is neither purely one nor the other, Smarandache provided a theoretical bridge for understanding complex bound states that do not undergo immediate annihilation.

3.2. The Unparticle Connection (2008)

A pivotal theoretical expansion occurred when **Goldfain and Smarandache** (2008) [6] linked unmatter to the emerging field of **unparticle physics**. Unparticles represent a scale-invariant sector of physics that does not consist of standard particles with definite mass. By interpreting these fractional field quanta as mixed matter-antimatter states, the researchers suggested that unmatter could provide the physical substrate for non-standard scaling dimensions in quantum field theory.

3.3. Dissemination via the American Physical Society (2008–2017)

Throughout the period of 2008–2017, a series of technical abstracts were presented at **American Physical Society** (APS) meetings, covering various facets of unmatter. These range from nuclear models (the Brightsen Nucleon Cluster Model) to the 2017 interpretation of the "Angel Particle" as an experimental manifestation of unmatter. This persistent presence in APS proceedings—spanning the divisions of Plasma, Nuclear, and Atomic physics—underscores a sustained dialogue between neutrosophic theory and the broader high-energy physics community. (See *Supplemental References, 20-31*, for a detailed list of these proceedings.)

3.4. The "Experimentum Crucis" at RAL (2015)

The year 2015 marked the transition from theoretical conjecture to empirical verification. Conducted at the **Rutherford Appleton Laboratory (RAL)** using the **Astra Gemini laser**, a landmark experiment [9, 17] led to the generation of a high-density, charge-neutral electron-positron ($e^{-}e^{+}$) plasma.

- This achievement was hailed as the "experimentum crucis" for unmatter, as it realized a macroscopic state where matter and antimatter components coexisted and exhibited collective behavior before annihilation.
- Unlike individual pair production, this "unmatter plasma" allowed for the study of global electromagnetic properties of intertwined matter-antimatter systems [13].

3.4. Modern Synthesis and Super-Hypergraphs (2024–2025)

In recent years, interest in unmatter has shifted toward **computational and structural modeling**. Recent publications in journals such as *Neutrosophic Sets and Systems* (https://fs.unm.edu/NSS/) have integrated unmatter into:

- **Super-hypergraph models**: Used to map the multidimensional interactions within unmatter-related systems.
- **Decision-making under uncertainty:** Applying the *I* (Indeterminacy) component of unmatter to model high-risk variables in energy-analysis frameworks.
- **Exotic Plasma Engineering:** Exploring the potential for unmatter states to serve as precursors for novel energy-generation schemes.

4. Experimental Verification: The 2015 RAL "Experimentum Crucis"

The experiment was conducted at the **Central Laser Facility (CLF)** using the **Astra Gemini laser system**. Led by Gianluca Sarri (Queen's University Belfast) and an international team, the study successfully generated a high-density, quasi-neutral electron-positron (e^-e^+) plasma. This result provided the first empirical evidence that macroscopic "unmatter" could be sustained long enough to exhibit collective plasma dynamics. [9, 17]

4.1 Technical Methodology

The experiment utilized a two-stage approach to overcome the traditional difficulty of creating and merging separate matter and antimatter populations:

1. **Laser-Driven Acceleration:** The Astra Gemini laser (delivering ultra-short pulses of ≈40fs) was focused onto a gas jet (helium and nitrogen). This created a **Laser Wakefield Accelerator (LWFA)**, propelling a beam of electrons to ultra-relativistic energies (ranging from 500 to 600 MeV).
2. **The Cascade Process:** This high-energy electron beam was directed into a thick, high-*Z* target (specifically **lead**). As the electrons traversed the lead, they underwent a two-step electromagnetic cascade:
    - **Bremsstrahlung:** Electrons interacted with the electric fields of the lead nuclei, emitting high-energy gamma-ray photons.
    - **Pair Production:** These photons, in turn, interacted with the nuclear fields to produce electron-positron pairs (e^-e^+).

4.2 Results and "Unmatter" Characteristics

The experiment yielded a beam consisting of an approximately equal number of electrons and positrons. Key parameters included:

- **Charge Neutrality:** The resulting beam achieved a positron-to-electron ratio near unity.
- **High Density:** The pair density reached $\approx 10^{15}$cm^3, with a total yield of $\approx 10^9$ to 10^{10} pairs per shot.
- **Collective Behavior:** Crucially, the **Debye length** (the scale over which charges screen each other) was much smaller than the beam size. This is the defining characteristic of a **plasma** versus a collection of individual particles, confirming that the system was a single, intertwined "unmatter" state.

4.3 Why "Experimentum Crucis"?

In neutrosophic terms, this experiment moved the study of unmatter from the microscopic (individual mesons) to the **macroscopic**. By creating a bulk state where matter and antimatter are not merely "annihilation partners" but are part of a shared, stable-velocity plasma, RAL demonstrated that the *Indeterminacy (I)* component—the neutral coexistence of the system—is a controllable physical reality.

5. Theoretical Implications

5.1 Quantum Chromodynamics (QCD) and Confinement [16]

Unmatter serves as a unique laboratory for probing the **confinement mechanism** of quarks. In classical Lattice QCD, simulations often struggle with the "sign problem" when dealing with high-density systems. However, unmatter configurations—by maintaining approximate matter-antimatter neutrality—can be modeled to enforce $T \approx F$ (Truth ≈ Falsity), potentially simplifying the study of gluon-mediated bound states. This allows for:

- **Probing the Flux Tube:** Analyzing how the "indeterminate" (*I*) energy of the gluon field fluctuates in stable $q\bar{q}$ clusters.
- **Mixed-System Confinement:** Testing if exotic neutral mesons (such as the hypothesized **X17** or **E38** particles) follow the structural rules of macroscopic unmatter.

5.2 Neutrosophic Computational Models: Super-HyperGraphs [3]

A major breakthrough has been the application of **Neutrosophic Super-HyperGraphs (NSHG)** [14] to model the hierarchical complexity of unmatter plasmas.

- **Super-Vertices:** Instead of individual particles, super-vertices represent **clusters of particles** that act as coherent units within the plasma.
- **Super-Edges:** These represent the collective fields (electromagnetic and nuclear) that bind the vertices together.

This mathematical framework allows researchers to propagate uncertainty across scales, from the subatomic level up to the macroscopic plasma bulk, providing a more accurate representation of the "Indeterminacy" inherent in unmatter.

5.3 Energy-Release Scenarios

The traditional view of matter-antimatter interaction is one of pure loss (conversion to gamma-ray photons). Unmatter theory suggests that **controlled collisions** between unmatter plasma and conventional matter may follow different decay channels. By utilizing the collective shielding effects of the e^-e^+ plasma, energy may be released through directed kinetic channels rather than isotropic radiation.

5.4 Case Studies in Material Engineering

The transition from unmatter theory to material engineering has been facilitated by the development of **Physical Super-HyperStructures**. Recent 2025 studies demonstrate the following applications:

- **Grain Boundary Networks & Crystal Graphs:** Engineers have introduced **Grain Boundary Super-HyperNetworks** to model the hierarchical architecture of polycrystalline materials. [2] By treating grain boundaries as "super-edges" in a **Crystal Super-HyperGraph**, it is now possible to perform multi-scale analysis of how microscopic defects influence the macroscopic structural integrity of high-strength alloys.
- **Thermoelectric Material Discovery:** Researchers are combining **Crystal Graph Neural Networks** with neutrosophic logic to map the relationship between atomic structures and thermoelectric efficiency (η). [8] This "material mapping" accounts for structural indeterminacy—a key characteristic of unmatter states—facilitating the discovery of novel superconductors and high-efficiency thermal conductors.
- **Sustainable Power Plant Synthesis:** A 2025 paper formalized the use of **Physical Super-HyperStructures** to model "meta-ensembles" of steady-state power plants. [3] This framework captures the inherent uncertainty in energy balances (analogous to the dynamics in **unmatter plasma reactors**) and propagates it through multi-layered hierarchical interactions to optimize plant-wide synthesis.

6. Emerging Applications

The convergence of neutrosophic modeling and high-energy experiment has led to several prospective applications:

Table 1: *Emerging Trajectories for Unmatter Technologies: From Medical Diagnostics to Deep-Space Propulsion*

Domain	*Potential Role of Unmatter*
Space Propulsion	**High-Density Fuel:** Using unmatter-matter collisions to generate thrust. The neutral nature of unmatter reduces the magnetic shielding weight required for storage compared to pure antiproton fuels.
Medical Imaging	**Neutrosophic PET:** Enhanced diagnostics using "mixed-state" signatures. Instead of simple annihilation counts, unmatter-informed algorithms can filter signal noise (Indeterminacy) to provide higher-resolution voxel mapping.
Material Science	**Neutrosophic Metamaterials:** Designing materials guided by Super-HyperGraph models whose electromagnetic responses mimic the neutral distributions of unmatter.
Smart-Grid Optimization	**Indeterminate Dispatch:** Using neutrosophic algorithms to manage the "indeterminate" power output from theoretical **unmatter-based micro-reactors**, allowing grids to balance supply/demand in real-time under extreme volatility.

7. Conclusion

Unmatter bridges philosophical notions of neutrality with tangible high-energy phenomena. The 2015 RAL electron-positron plasma experiment substantiates its existence at macroscopic scales, while ongoing theoretical work situates unmatter within QCD, unparticle physics, and neutrosophic computation. By leveraging super-hypergraph representations and uncertainty-aware decision frameworks, researchers can explore novel energy-conversion schemes, advanced diagnostic technologies, and materials with engineered neutral charge characteristics. Continued interdisciplinary effort—uniting particle physics, logic theory, and computational modeling—will be essential to unlock the full scientific and technological potential of unmatter.

References

1. Braibant, S.; Giacomelli, G.; Spurio, M. (2009). *Particles and Fundamental Interactions: An Introduction to Particle Physics*. Springer.
2. Fujita, Takaaki. (2025). "Unifying Grain Boundary Networks and Crystal Graphs: A HyperGraph and SuperHyperGraph Perspective in Material Sciences." *Asian Journal of Advanced Research and Reports*, 19:344-379. DOI: 10.9734/ajarr/2025/v19i51023.
3. Fujita, Takaaki. (2025). "Toward a Formal Framework of Physical SuperHyperStructures: Multi-Layered Extensions of Hyperstructures in Physics." *Neutrosophic Optimization and Intelligent Systems*, 8:1-18. DOI: 10.61356/j.nois.2025.8631.
4. Georgi, Howard (2007). "Unparticle physics." *Physical Review Letters*, 98(22), May 2007.
5. Georgi, Howard (2007). "Another odd thing about unparticle physics." *Physics Letters B*, 650(4):275–278, July 2007.
6. Goldfain, E., & Smarandache, F. (2008). "On Emergent Physics, Unparticles and Exotic Unmatter States." *Progress in Physics*, 4:10-15, 2008, https://fs.unm.edu/PP-15-02.pdf .
7. Greiner, Walter; Schramm, Stefan; Stein, Eckart (2007). *Quantum Chromodynamics*. Springer.
8. Jia, X., Aziz, A., Hashimoto, Y. et al. (2024). "Dealing with the big data challenges in AI for thermoelectric materials." *Sci. China Mater.* 67, 1173–1182.

9. Sarri, G., Poder, K., Cole, J. et al. "Generation of neutral and high-density electron–positron pair plasmas in the laboratory." *Nature Communications* 6, 6747 (2015). https://doi.org/10.1038/ncomms7747
10. Smarandache, Florentin (2002). *A Unifying Field in Logics: Neutrosophic Logic. Neutrosophy, Neutrosophic Set, Neutrosophic Probability* (3rd edition), Am. Res. Press. www.gallup.unm.edu/~smarandache/eBook-Neutrosophics2.pdf
11. Smarandache, Florentin (2004). "Matter, antimatter, and unmatter." CERN, EXT-2004-142, 1-4. https://cds.cern.ch/record/798551/files/ext-2004-142.pdf
12. Smarandache, Florentin (2005). "A New Form of Matter — Unmatter, Composed of Particles and Anti-Particles." *Progress in Physics*, 1:9-11. https://digitalrepository.unm.edu/math_fsp/51
13. Smarandache, Florentin (2015). "Unmatter Plasma Discovered." *Progress in Physics*, 3:246-246. https://digitalrepository.unm.edu/math_fsp/50
14. Smarandache, Florentin (2020). "Introduction to the n-SuperHyperGraph - the most general form of graph today." *Neutrosophic Sets and Systems*, 33:289-295. https://doi.org/10.5281/ZENODO.3783103
15. Smarandache, Florentin (2024). "Partial Collisions of Unmater-Matter, Unmatter-Antimatter, and $Unmatter_1$-$Unmatter_2$ to Generate High Energy." *Progress in Physics*, 20(1):33-35, https://fs.unm.edu/Physics/PartialCollisionsUnmaterMatter.PDF
16. Smith, C.H.L. (1980). *Topics in Quantum Chromodynamics*. In: Mahanthappa, K.T., Randa, J. (eds) *Quantum Flavordynamics, Quantum Chromodynamics, and Unified Theories*. NATO Advanced Study Institutes Series, vol 54. Springer. https://doi.org/10.1007/978-1-4613-3099-8_2
17. Warwick, J.; et al., "Experimental observation of a current-driven instability in a neutral electron-positron beam," *Physical Review Letters*, Vol. 119, 185002, 2017. https://doi.org/10.1103/PhysRevLett.119.185002
18. Weinberg, Steven (1983). *The Discovery of Subatomic Particles*. Scientific Amer.
19. Xian, Y., Zhang, P., Lu, X. et al. (2013). "From short pulses to short breaks: exotic plasma bullets via residual electron control." *Sci. Rep*. 3, 1599. https://doi.org/10.1038/srep01599

Supplemental References (International Conference Abstracts from the American Physical Society, https://www.aps.org/)

20. Florentin Smarandache, Dmitri Rabounski: *Discovered "Angel Particle", which is Both Matter and Antimatter, as a New Experimental Proof of Unmatter*. 2017 Annual Meeting of the Far West Section, Friday–Saturday, November 3–4, 2017; Merced, California. http://meetings.aps.org/Meeting/FWS17/Session/E1.16
21. Florentin Smarandache: *Unmatter Plasma revisited*. 59th Annual Meeting of the APS Division of Plasma Physics, Volume 62, Number 12, Monday–Friday, October 23–27, 2017; Milwaukee, Wisconsin. http://meetings.aps.org/Meeting/DPP17/Session/YP11.35
22. Florentin Smarandache, Mumtaz Ali: *Neutrosophic Triplet as extension of Matter Plasma, Unmatter Plasma, and Antimatter Plasma*. 69th Annual Gaseous Electronics Conference, Volume 61, Number 9, Monday–Friday, October 10–14, 2016; Bochum, Germany. http://meetings.aps.org/Meeting/GEC16/Session/HT6.111
23. Florentin Smarandache: *Unmatter Plasma*, 57th Annual Meeting of the APS Division of Plasma Physics, Volume 60, Number 19, Monday–Friday, November 16–20, 2015; Savannah, Georgia, http://meetings.aps.org/Meeting/DPP15/Session/UP12.46
24. Florentin Smarandache, Mumtaz Ali: *Neutrosophic Triplet as extension of Matter Plasma, Unmatter Plasma, and Antimatter Plasma*, 69th Annual Gaseous Electronics Conference, Volume 61, Number 9, Monday–Friday, October 10–14, 2016; Bochum, Germany, http://meetings.aps.org/Meeting/GEC16/Session/HT6.111
25. Florentin Smarandache: *Unparticle, a special case of unmatter*, Bulletin of the American Physical Society, 53rd Annual Meeting of the APS Division of Plasma Physics, Volume 56, Number 16, Monday–Friday, November 14–18, 2011; Salt Lake City, Utah, http://meetings.aps.org/Meeting/DPP11/Event/153509
26. Ervin Goldfain, Florentin Smarandache: *Connection between `unparticle' and `unmatter'*, Bulletin of the American Physical Society, 2010 Annual Meeting of the California-Nevada Section of the APS Volume 55, Number 12, Friday–Saturday, October 29–30, 2010; Pasadena, California, http://meetings.aps.org/Meeting/CAL10/Event/135968
27. Dmitri Rabounski, Florentin Smarandache: *The Brightsen Nucleon Cluster Model Predicts Unmatter Entities inside Nuclei*, Bulletin of the American Physical Society, 2008 Annual Meeting of the Division of Nuclear Physics Volume 53, Number 12, Thursday–Sunday, October 23–26, 2008; Oakland, California, http://meetings.aps.org/Meeting/DNP08/Event/87738

28. Ervin Goldfain, Florentin Smarandache: *On Emergent Physics, Unparticles and Exotic Unmatter States*, Bulletin of the American Physical Society, 2009 Joint Spring Meeting of the New England Section of APS and AAPT Volume 54, Number 5, Friday–Saturday, May 8–9, 2009; Boston, Massachusetts, http://meetings.aps.org/link/BAPS.2009.NES.APSP.2
29. Florentin Smarandache: *Verifying Unmatter by Experiments, More Types of Unmatter, and a Quantum Chromodynamics Formula*, Bulletin of the American Physical Society, 62nd Annual Gaseous Electronics Conference Volume 54, Number 12. Tuesday–Friday, October 20–23, 2009; Saratoga Springs, New York, http://meetings.aps.org/link/BAPS.2009.GEC.KTP.110
30. Florentin Smarandache: *A New Form of Matter -- Unmatter, Composed of Particles and Anti-Particles*, Bulletin of the American Physical Society, 40th Annual Meeting of the APS Division of Atomic, Molecular and Optical Physics Volume 54, Number 7. Tuesday–Saturday, May 19–23, 2009; Charlottesville, Virginia, http://meetings.aps.org/link/BAPS.2009.DAMOP.E1.97
31. Florentin Smarandache: *Unparticle, a special case of unmatter*, Bulletin of the American Physical Society, 53rd Annual Meeting of the APS Division of Plasma Physics Volume 56, Number 16. Monday–Friday, November 14–18, 2011; Salt Lake City, Utah, http://meetings.aps.org/Meeting/DPP11/SessionIndex3/?SessionEventID=158034

Neutrosophic Knowledge, Vol. 9, 2026
University of New Mexico

Article

Appurtenance and Inclusion Equations in Neutrosophic Numbers: Foundations, Theoretical Development, and Practical Applications

Florentin Smarandache[1,*]

[1] University of New Mexico, Mathematics, Physics, and Natural Sciences Division, 705 Gurley Ave., Gallup, NM 87301, USA
* Correspondence: smarand@unm.edu

Received: Month Day, Year; *Accepted:* Month Day, Year; *Published:* Month Day, Year

Abstract: Neutrosophic statistics extends classical statistical theory to accommodate indeterminate, vague, or incomplete data by representing quantities as **real neutrosophic numbers** $N = a + bI$, where $I \subset \mathbb{R}$ denotes an indeterminacy set. To manipulate such numbers consistently, this short review consolidates two novel equation types: the **Appurtenance Equation** (using the symbol "∈") and the **Inclusion Equation** (using "⊂" or "⊆"), introduced by Smarandache [5] in 2023. This paper presents a self-contained exposition of these equations as well, derives their fundamental algebraic rules, demonstrates solution techniques through worked examples, and surveys a range of practical domains—quality control, financial planning, electrical engineering, and broader neutrosophic statistical modelling—where the equations provide a rigorous framework for handling uncertainty.

Keywords: Decision-making, Indeterminacy, Interval analysis, Neutrosophic arithmetic, Neutrosophic statistics, Quality control, Set-valued equations, Uncertainty quantification.

1. Introduction

Classical statistics assumes that each datum is a precise real number. In many scientific and engineering contexts, however, measurements are reported as intervals, fuzzy ranges, or sets due to instrument tolerance, expert judgement, or incomplete information. **Neutrosophic statistics** addresses this gap by allowing data points to be expressed as *real neutrosophic numbers*

$$N = a + bI, a, b \in \mathbb{R}, I \subset \mathbb{R},$$

where the *indeterminate part* bI captures the inherent vagueness [1]. Standard algebraic equalities are insufficient for manipulating such objects; the operations must respect the set-valued nature of the indeterminacy [3].

We therefore proposed two families of equations that replace the ordinary equality sign [4, 5]:

- **Appurtenance Equation** – expresses *membership* of a quantity in a neutrosophic set (symbol "∈").
- **Inclusion Equation** – expresses *set inclusion* between neutrosophic expressions (symbols "⊂", "⊆").

These equations constitute the logical backbone of neutrosophic arithmetic and enable the formulation of statistical models, hypothesis tests, and optimisation problems under uncertainty [2].

The present paper consolidates the definitions, algebraic theorems, solution strategies, and illustrative applications of these equations, providing a ready reference for researchers and practitioners.

2. Preliminaries

2.1. Real Neutrosophic Numbers

A **real neutrosophic number** is a pair (a, b) together with an indeterminacy set $I \subset \mathbb{R}$. The notation

$$N = a + bI$$

means that the deterministic component is a and the uncertain component spans the interval $bI = \{b\,v \mid v \in I\}$. Typical choices for I are open intervals (α, β), closed intervals $[\alpha, \beta]$, or more general subsets of $\mathbb{R}$.

2.2. Set Arithmetic Notation

For two subsets $A, B \subset \mathbb{R}$ we define

$$\begin{aligned} A + B &= \{a + b \mid a \in A,\ b \in B\}, \\ A - B &= \{a - b \mid a \in A,\ b \in B\}, \\ A \cdot B &= \{a\,b \mid a \in A,\ b \in B\}, \\ A/B &= \{a/b \mid a \in A,\ b \in B,\ b \neq 0\}, \\ A^n &= \{a^n \mid a \in A\}, n \in \mathbb{Z}_+. \end{aligned}$$

These constructions allow interval (or more general set) arithmetic to be performed component-wise.

3. Appurtenance Equations

3.1. Definition

An **Appurtenance Equation** has the generic form

$$f(x) \ \in \ g(x),$$

where f and g are *hyper-functions* whose values are subsets of $\mathbb{R}$. Solving such an equation consists of determining a set $S \subseteq \mathbb{R}$ such that

$$x \in S \Leftrightarrow f(x) \in g(x).$$

3.2. Fundamental Theorems

Theorem 1 (Set-Arithmetic Preservation).

If $a \in A$ and $b \in B$ then

$$\begin{aligned} a + b &\in A + B, & a - b &\in A - B, \\ ab &\in A \cdot B, & a/b &\in A/B \ (b \neq 0), \\ a^n &\in A^n, & \sqrt[n]{a} &\in \sqrt[n]{A}. \end{aligned}$$

Theorem 2 (Scalar Multiplication).

If $a \in A$ and $\beta \in \mathbb{R}$ then

$$\beta a \in \beta A.$$

Both theorems follow directly from the definitions of the set-operations above.

3.3 Solving Procedure

- **Reduce the right-hand side** to an explicit interval (or set) using set-arithmetic.
- **Translate** the membership relation $f(x) \in (g\text{-interval})$ into a pair of ordinary inequalities.
- **Solve** the inequalities for x; the solution set is the maximal interval (or union of intervals) satisfying the original appurtenance condition.

3.4 Example

Solve

$$4 - 5x \ \in \ 1 + 2 \cdot (0.5, 0.8).$$

Step 1:

$$2 \cdot (0.5, 0.8) = (1.0, 1.6);\text{ adding 1 yields the interval } (2.0, 2.6).$$

Step 2:

$$4 - 5x > 2.0, 4 - 5x < 2.6.$$

Step 3:

$$-5x > -2.0 \Rightarrow x < 0.40,$$
$$-5x < -1.4 \Rightarrow x > 0.28.$$

Hence

$$x \in (0.28, 0.40).$$

4. Inclusion Equations

4.1 Definition

An **Inclusion Equation** asserts that one set-valued expression is (strictly) contained in another:

$$f(X) \subseteq g(Y) \text{or} f(X) \subset g(Y),$$

where $X, Y \subseteq \mathbb{R}$. In the neutrosophic context the typical form is

$$a + bV \subseteq a + bI,$$

with $V \subseteq I$ denoting a *true-value* set and I the indeterminacy set.

4.2 Fundamental Theorems

Theorem 3 (Preservation of Inclusion under Arithmetic).

If $A \subseteq B$ and $C \subseteq D$ then

$$A + C \subseteq B + D, \quad A - C \subseteq B - D,$$
$$A \cdot C \subseteq B \cdot D, \quad A/C \subseteq B/D \ (0 \notin C),$$
$$A^n \subseteq B^n.$$

Theorem 4 (Scalar Inclusion).

If $A \subseteq B$ and $\beta > 0$ then

$$\beta A \subseteq \beta B.$$

These results guarantee that algebraic manipulation of inclusion statements remains valid.

4.3 Solving Procedure

- **Express** each side as an explicit interval (or union of intervals).
- **Impose** the inclusion constraints: the lower bound of the left side must be **greater than or equal to** the lower bound of the right side, and the upper bound must be **less than or equal to** the upper bound of the right side.
- **Derive** inequalities for the unknown(s) and solve them.
- **Combine** feasible ranges (if multiple cases arise) to obtain the maximal solution set.

4.4 Example

Solve

$$1 + x \cdot (1,2) \subseteq (0,5).$$

Step 1:

$$x \cdot (1,2) = \begin{cases} (x, 2x), & x > 0, \\ (2x, x), & x < 0. \end{cases}$$

Adding 1 gives

$$\begin{cases} (1 + x, 1 + 2x), & x > 0, \\ (1 + 2x, 1 + x), & x < 0. \end{cases}$$

Step 2: Enforce inclusion in $(0, 5)$.

Case $x > 0$:

$$1 + x > 0, 1 + 2x < 5 \;\Rightarrow\; x < 2.$$

Thus $x \in (0,2)$.

Case $x < 0$:

$$1 + 2x > 0 \;\Rightarrow\; x > -0.5, 1 + x < 5 \text{ (always true)}.$$

Thus $x \in (-0.5,0)$.

Step 3: Union of the two admissible intervals gives

$$x \in (-0.5,0) \cup (0,2).$$

5. Practical Applications

The Appurtenance and Inclusion frameworks have been employed in a variety of domains where data are intrinsically imprecise.

Table 1. Representative Applications of the Appurtenance and Inclusion Frameworks in Domains with Intrinsically Imprecise Data.

Domain	*Problem Setting*	*Equation Type*	*Outcome*
Quality-Control (Manufacturing)	Drill depth $D = 10 + 2T$ must lie in $[99.5, 100.5]$ mm	Appurtenance	Acceptable drilling time $T \in [44.75,45.25]$ s
Financial Planning	Profit $P = 5U - [1800, 2000]$must be in $[5000, 7000]$	Appurtenance (via interval subtraction)	Required sales units $U \in [1360,1800]$
Electrical Engineering	Voltage $V = I \cdot R$ with $I \in [4.5,5.5]$ mA, target $V \in [1.15,1.25]$ V	Inclusion (ensuring whole interval of possible voltages fits)	Feasible resistance $R \in [209.1,277.8]\ \Omega$
Neutrosophic Regression	Model $y \in a + bx$ with interval-valued a, b	Both Appurtenance (solve for x) and Inclusion (check prediction set)	Provides interval predictions for future observations
Hypothesis Testing	Test statistic $T \in (t_1, t_2)$ versus rejection region R	Inclusion	Determines three-way decision (accept, reject, indeterminate)
Sensor Fusion	Two sensors give $x \in (10,12)$ and $x \in (11,14)$	Appurtenance (intersection)	Combined estimate $x \in (11,12)$
Reliability Engineering	Measured dimension $d \in (9.7,10.3)$ vs specification $(9.8, 10.2)$	Inclusion	Pass/fail decision based on set containment

These examples illustrate how the equations translate vague specifications into mathematically tractable constraints, preserving the full information content of the indeterminate data.

6. Discussion

The introduction of Appurtenance and Inclusion equations resolves a central obstacle in neutrosophic mathematics: **the lack of a coherent algebraic language for set-valued quantities**. By grounding operations in well-defined set-arithmetic, the framework guarantees consistency across addition, subtraction, multiplication, division, and exponentiation.

Moreover, the dual nature of the two equation families mirrors the classical distinction between *element-wise* and *set-wise* reasoning, thereby facilitating a smooth conceptual transition for researchers familiar with traditional statistics.

Potential extensions include:

- **Algorithmic implementation** of the solution procedures within symbolic computation systems.
- **Generalization to multivariate neutrosophic vectors**, where inclusion must be verified component-wise or via convex hulls.
- **Integration with probabilistic uncertainty models**, yielding hybrid frameworks that combine stochastic and neutrosophic descriptions.

7. Conclusion

Appurtenance and Inclusion equations provide a rigorous, yet intuitive, toolkit for performing algebraic manipulations on real neutrosophic numbers. Their theoretical foundations—captured in Theorems 1–4—ensure that the usual arithmetic properties survive the passage from crisp numbers to interval-valued entities. Through worked examples and a suite of practical applications, we have demonstrated that these equations enable precise reasoning in fields ranging from manufacturing tolerancing to financial risk assessment, thereby broadening the applicability of neutrosophic statistics to real-world problems characterized by indeterminacy. Future work will focus on computational libraries, multivariate extensions, and empirical validation of neutrosophic models in experimental settings.

References

1. Kandasamy, Vasantha W.B.; K. Ilanthenral, Florentin Smarandache (2015). *Natural neutrosophic numbers and MOD neutrosophic numbers*. Bruxelles, Belgium.
2. Smarandache, F. (2021) "Probabilistic statistics and biostatistics are generalizations of probabilistic and multivariate statistics." *Neutrosophic Sets and Systems*, 43, 280-289.
3. Smarandache, F. (2022). "Neutrosophic Statistics is an extension of Interval Statistics, while Plithogenic Statistics is the most general form of statistics (second version)." *International Journal of Neutrosophic Science*, 2(1), 148–165. https://fs.unm.edu/NS/AppurtenanceInclusionEquations.pdf
4. Smarandache, F. (2024) "Foundation of Appurtenance and Inclusion Equations for Constructing the Operations of Neutrosophic Numbers Needed in Neutrosophic Statistics," *Neutrosophic Systems with Applications* 15(1), Art. 2. https://doi.org/10.61356/j.nswa.2024.1513856
5. Smarandache, F. (2023). "Foundation of Appurtenance and Inclusion Equations for Constructing the Operations of Neutrosophic Numbers Needed in Neutrosophic Statistics (revised)," *Prospects for Applied Mathematics and Data Analysis* (PAMDA) 3(1), 29-48, https://fs.unm.edu/NS/AppurtenanceInclusionEquations-revised.pdf

Neutrosophic Knowledge, Volume 9, 2026

University of New Mexico

Fuzzy Off-SuperHyperGraphs: Extending Uncertainty Modeling Beyond Classical Boundaries

Takaaki Fujita[1] *, *Ajoy Kanti Das* [2], *Suman Das* [3], *Sankar Prasad Mondal* [4]

[1] Independent Researcher, Tokyo, Japan. (Takaaki.fujita060@gmail.com)

[2] Associate Professor, Department of Mathematics, Tripura University, Agartala-799022, Tripura, India. (ajoykantidas@gmail.com)

[3] Assistant Professor (Mathematics), Department of Education (ITEP), NIT Agartala, Jirania, 799046, Tripura, India. (dr.sumandas1995@gmail.com)

[4] Department of Applied Mathematics, Maulana Abul Kalam Azad University of Technology, West Bengal, Haringhata-741249, West Bengal, India. (sankar.mondal02@gmail.com)

*Correspondence: Takaaki.fujita060@gmail.com

Received*: 01/02/2026;* Accepted*: 01/21/2026*

Abstract. Graph theory provides a mathematical framework for representing relationships and connectivity through vertices and edges. Hypergraphs extend this classical notion by introducing *hyperedges* that may connect more than two vertices at once. Superhypergraphs further enrich the model by employing iterated powerset constructions, thereby capturing hierarchical and self-referential structures among hyperedges. A fuzzy n-SuperHyperGraph advances this approach by assigning membership degrees to both supervertices and superedges, offering a flexible tool for modeling uncertainty in complex systems. In this paper, we propose an extension of this framework, termed the *Fuzzy Off-SuperHyperGraph*, which integrates the offgraph paradigm into fuzzy n-SuperHyperGraphs. We establish its formal definition, investigate its structural properties, and discuss its potential applications in uncertainty modeling and hierarchical network analysis.

Keywords: Superhypergraph, Hypergraph, Fuzzy OffGraph, Fuzzy Offset, Fuzzy Set

1. **Preliminaries**

We record basic notions and notation used throughout. Unless stated otherwise, all graphs are finite, undirected, and loopless (multiple edges are allowed only when explicitly declared).

1.1. *SuperHyperGraphs*

Classical hypergraphs enrich ordinary graphs by allowing an edge to join any finite number of vertices; this makes them apt for modeling multiway relations [1–3]. A *SuperHyperGraph* pushes this idea further by building vertices and edges from iterated powersets of a ground set; this perspective has recently attracted attention in several settings [4–8]. Applications have appeared in, e.g., molecular modeling, network analysis, and signal processing [9–12]. Throughout, the *level* parameter n is a fixed nonnegative integer.

Definition 1.1 (Base set)**.** [13–15] A *base set* (or ground set) is a fixed finite set S from which higher-level objects are formed:

$$S = \{ x \mid x \text{ lies in the chosen domain} \}.$$

All constructions below ultimately draw their elements from S.

Definition 1.2 (Powerset)**.** [16] For a set X, its powerset is

$$\mathcal{P}(X) = \{ A \mid A \subseteq X \}.$$

We also use the nonempty powerset $\mathcal{P}^*(X) := \mathcal{P}(X) \setminus \{\varnothing\}$.

Definition 1.3 (Iterated powerset)**.** [17, 18] For $k \in \mathbb{N}_0$ define

$$\mathcal{P}^0(X) := X, \qquad \mathcal{P}^{k+1}(X) := \mathcal{P}\big(\mathcal{P}^k(X)\big).$$

Similarly, with nonempty levels,

$$\big(\mathcal{P}^*\big)^0(X) := X, \qquad \big(\mathcal{P}^*\big)^{k+1}(X) := \mathcal{P}^*\big((\mathcal{P}^*)^k(X)\big).$$

Proposition 1.4 (Cardinality recursion)**.** *Let* $m := |X|$*. Then*

$$\big|\mathcal{P}^1(X)\big| = 2^m, \qquad \big|\mathcal{P}^{k+1}(X)\big| = 2^{|\mathcal{P}^k(X)|} \quad (k \ge 0).$$

In particular, if $m \ge 1$ *then* $|(\mathcal{P}^*)^1(X)| = 2^m - 1$ *and* $|(\mathcal{P}^*)^{k+1}(X)| = 2^{|(\mathcal{P}^*)^k(X)|} - 1$.

Proof. The identity $|\mathcal{P}(Y)| = 2^{|Y|}$ is standard. Applying it with $Y = \mathcal{P}^k(X)$ gives $|\mathcal{P}^{k+1}(X)| = 2^{|\mathcal{P}^k(X)|}$. For the nonempty versions, subtract 1 (removing $\varnothing$) at each step. □

Definition 1.5 (Hypergraph [2, 19])**.** A *hypergraph* is a pair $H = (V(H), E(H))$ where $V(H) \neq \varnothing$ and $E(H) \subseteq \mathcal{P}^*(V(H))$. In this paper we work with finite $V(H)$ and finite $E(H)$.

Example 1.6 (Real-world hypergraph: project teams)**.** *Interpretation.* Vertices are students; each hyperedge is a project team (a team may have more than two members).
Construction. Let

$$V = \{S_1, S_2, S_3, S_4\}, \qquad E = \big\{\{S_1, S_2, S_3\},\ \{S_2, S_4\}\big\}.$$

Then $H = (V, E)$ is a finite hypergraph since $E \subseteq \mathcal{P}^*(V)$. The 3-way relation "work together on Project A" is encoded by the hyperedge $\{S_1, S_2, S_3\}$, while Project B uses $\{S_2, S_4\}$.

Definition 1.7 (n-SuperHyperGraph)**.** [20, 21] Fix a finite base set V_0. Define iterated powersets by

$$\mathcal{P}^0(V_0) := V_0, \qquad \mathcal{P}^{n+1}(V_0) := \mathcal{P}\big(\mathcal{P}^n(V_0)\big) \quad (n \in \mathbb{N}_0).$$

For a level $n \in \mathbb{N}_0$, an *n-SuperHyperGraph* is a pair

$$\mathrm{SHG}^{(n)} = (V, E), \qquad V \subseteq \mathcal{P}^n(V_0), \quad E \subseteq \mathcal{P}(V),$$

whose elements are called *n-supervertices* (elements of V) and *n-superedges* (elements of E), i.e., collections of n-supervertices. When desired, one may require $E \subseteq \mathcal{P}^*(V)$ to forbid empty superedges. If one also wishes to forbid emptiness at every nesting level of supervertices, one may impose $V \subseteq (\mathcal{P}^*)^n(V_0)$.

Example 1.8 (Real-world n-SuperHyperGraph ($n = 1$): meal planning)**.** *Interpretation.* Base items are dishes; supervertices are bundles of dishes; superedges specify bundles served together.
Construction. Let the base set be $V_0 = \{D, S, M\}$ (drink, salad, main). Take

$$V = \big\{\{D\},\ \{S\},\ \{M\},\ \{D, S\}\big\} \subseteq \mathcal{P}(V_0).$$

Define superedges as nonempty subsets of V:

$$e_1 = \big\{\{D\}, \{S\}\big\}, \qquad e_2 = \big\{\{D, S\}, \{M\}\big\}, \qquad E = \{e_1, e_2\} \subseteq \mathcal{P}^*(V).$$

Then $\mathrm{SHG}^{(1)} = (V, E)$ is a 1-SuperHyperGraph: $V \subseteq \mathcal{P}^1(V_0)$ and $E \subseteq \mathcal{P}(V) \subseteq \mathcal{P}^2(V_0)$.
In Fig. 1, we briefly summarize the structure of the graph for this illustrative example.

1.2. *Fuzzy n-SuperHyperGraphs*

A fuzzy set assigns a membership degree in $[0, 1]$ to each element of a universe [22, 23]. Fuzzy graphs and fuzzy hypergraphs endow vertices and (hyper)edges with such degrees [24–28]. A fuzzy n-SuperHyperGraph is a higher-level network structure assigning membership degrees to supervertices and superedges for modeling complex relations (cf. [21, 29]).

Meal planning as a 1-SuperHyperGraph

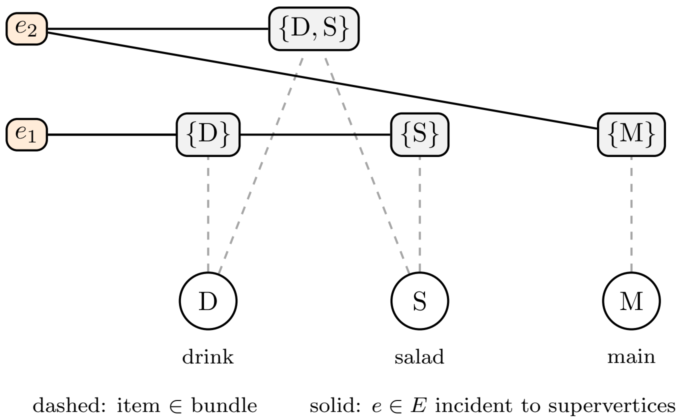

FIGURE 1. Real-world 1-SuperHyperGraph for meal planning. Supervertices are bundles of dishes; superedges encode bundles served together.

Definition 1.9 (Fuzzy n-SuperHyperGraph)**.** (cf. [30, 31]) Let $\mathrm{SHG}^{(n)} = (V, E)$ be an n-SuperHyperGraph. A *fuzzy n-SuperHyperGraph* is a quadruple

$$\big(V, E, \sigma, \mu\big),$$

where $\sigma : V \to [0, 1]$ and $\mu : E \to [0, 1]$ satisfy the *appurtenance constraint*

$$\mu(e) \ \leq \ \min_{v \in e} \sigma(v) \qquad \text{for every } e \in E.$$

Example 1.10 (Real-world fuzzy n-SuperHyperGraph ($n = 1$): sensor fusion)**.** *Interpretation.* Base sensors: temperature (T), humidity (H), pressure (P). Supervertices are singletons/pairs of sensors; memberships model detection reliability in $[0, 1]$. Superedges connect bundles that co-trigger an alert.

Construction. Let $V_0 = \{\mathrm{T}, \mathrm{H}, \mathrm{P}\}$ and

$$V = \big\{\{\mathrm{T}\},\ \{\mathrm{H}\},\ \{\mathrm{P}\},\ \{\mathrm{T}, \mathrm{H}\}\big\} \subseteq \mathcal{P}(V_0), \qquad \begin{aligned} e_1 &= \big\{\{\mathrm{T}\}, \{\mathrm{H}\}\big\}, \\ e_2 &= \big\{\{\mathrm{T}, \mathrm{H}\}, \{\mathrm{P}\}\big\}, \end{aligned} \qquad E = \{e_1, e_2\}.$$

Define vertex-memberships $\sigma : V \to [0, 1]$ and edge-memberships $\mu : E \to [0, 1]$ by

$$\sigma(\{\mathrm{T}\}) = 0.85, \quad \sigma(\{\mathrm{H}\}) = 0.65, \quad \sigma(\{\mathrm{P}\}) = 0.40, \quad \sigma(\{\mathrm{T}, \mathrm{H}\}) = 0.70.$$

Then the admissible maxima are

$$\mu_{\max}(e_1) = \min\{0.85, 0.65\} = 0.65, \qquad \mu_{\max}(e_2) = \min\{0.70, 0.40\} = 0.40.$$

Choose

$$\mu(e_1) = 0.60 \leq 0.65, \qquad \mu(e_2) = 0.38 \leq 0.40.$$

Verification. For each edge $e \in E$,

$$\mu(e) \;\le\; \min_{v \in e} \sigma(v)$$

holds numerically by the computations above; hence (V, E, σ, μ) is a valid fuzzy 1-SuperHyperGraph.

1.3. *Fuzzy Offgraph*

A fuzzy offgraph is a variant of the offset/offgraph model in which membership values may exceed the classical unit interval, inspired by studies on neutrosophic offsets and over/under offgraphs(cf. [13, 32–34]).

Definition 1.11 (Admissible fuzzy offgraph)**.** Let $G = (V, E)$ be a finite, loopless, undirected simple graph, so $E \subseteq \binom{V}{2}$. Fix real bounds $\Psi < 0 < 1 < \Omega$. An *admissible fuzzy offgraph* on G is a quadruple (V, E, ℓ_V, ℓ_E) such that

$$\ell_V : V \to [\Psi, \Omega], \qquad \ell_E : E \to [\Psi, \Omega],$$

and

$$\ell_E(\{u, v\}) \;\le\; \min\{\ell_V(u), \ell_V(v)\} \qquad (\forall \{u, v\} \in E),$$

together with the offness requirement that there exist $v_0 \in V$ and $e_0 \in E$ with $\ell_V(v_0) \notin [0, 1]$ and $\ell_E(e_0) \notin [0, 1]$.

Example 1.12 (Admissible fuzzy offgraph: overloaded/blocked road segment)**.** *Interpretation.* Vertices represent intersections and edges represent road segments. Vertex-memberships quantify intersection stress relative to nominal operation: values in $[0, 1]$ are normal-to-saturated, values > 1 indicate overload, and values < 0 indicate a closed or invalid state. Edge-memberships quantify segment condition and must not exceed the weaker (minimum) condition of its endpoints.

Construction. Let $G = (V, E)$ be the path on three vertices

$$V = \{a, b, c\}, \qquad E = \big\{\{a, b\}, \{b, c\}\big\} \subseteq \binom{V}{2}.$$

Fix bounds $\Psi = -0.6$ and $\Omega = 1.4$. Define the vertex-membership map $\ell_V : V \to [\Psi, \Omega]$ by

$$\ell_V(a) = 1.20, \qquad \ell_V(b) = 0.70, \qquad \ell_V(c) = 0.40,$$

and define the edge-membership map $\ell_E : E \to [\Psi, \Omega]$ by

$$\ell_E(\{a, b\}) = 1.10, \qquad \ell_E(\{b, c\}) = -0.20.$$

Verification (admissibility). We check the inequality in Definition 1.11 edgewise:

$$\min\{\ell_V(a), \ell_V(b)\} = \min\{1.20, 0.70\} = 0.70, \qquad \ell_E(\{a, b\}) = 1.10 \;\not\le\; 0.70.$$

Thus the choice $\ell_E(\{a,b\}) = 1.10$ would violate admissibility. To obtain an *admissible* fuzzy offgraph, redefine

$$\ell_E(\{a,b\}) = 0.65 \le 0.70, \qquad \ell_E(\{b,c\}) = -0.20 \le \min\{0.70, 0.40\} = 0.40.$$

Hence the admissibility condition holds for all edges.

Verification (offness). Since $\ell_V(a) = 1.20 > 1$, we have $\ell_V(a) \notin [0,1]$. Also $\ell_E(\{b,c\}) = -0.20 < 0$, so $\ell_E(\{b,c\}) \notin [0,1]$. Therefore the offness requirement is satisfied.

Consequently, (V, E, ℓ_V, ℓ_E) is an admissible fuzzy offgraph on G with bounds $\Psi = -0.6$ and $\Omega = 1.4$.

2. Result: Fuzzy Off SuperHyperGraph

An admissible (Ψ, Ω)-fuzzy n-SuperHyperGraph is an n-SuperHyperGraph (V, E), with $\Psi < 0 < 1 < \Omega$, $\sigma : V \to [\Psi, \Omega]$, $\mu : E \to [\Psi, \Omega]$, and $\mu(e) \le \min_{v \in e} \sigma(v)$, ensuring superedge membership never exceeds the weakest incident supervertex, possibly outside $[0,1]$ under the admissibility inequality.

Definition 2.1 (Admissible (Ψ, Ω)-fuzzy n-SuperHyperGraph and fuzzy off n-SuperHyperGraph)**.** Fix real bounds $\Psi < 0 < 1 < \Omega$ and let $\mathrm{SHG}^{(n)} = (V, E)$ be an n-SuperHyperGraph with $E \subseteq \mathcal{P}^*(V)$ (i.e., each $e \in E$ is a nonempty subset of V). An *admissible* (Ψ, Ω)*-fuzzy n-SuperHyperGraph* is a quadruple

$$(V, E, \sigma, \mu),$$

where $\sigma : V \to [\Psi, \Omega]$ and $\mu : E \to [\Psi, \Omega]$ satisfy the admissibility inequality

$$\mu(e) \ \le \ \min_{v \in e} \sigma(v) \qquad (\forall e \in E). \tag{1}$$

Define the *off-vertex set* and *off-edge set* by

$$V_{\text{off}} := \{\, v \in V : \ \sigma(v) \notin [0,1] \,\}, \qquad E_{\text{off}} := \{\, e \in E : \ \mu(e) \notin [0,1] \,\}.$$

A *fuzzy off n-SuperHyperGraph (FOSH)* is an admissible (Ψ, Ω)-fuzzy n-SuperHyperGraph that satisfies the *vertex-and-edge offness condition*

$$V_{\text{off}} \neq \varnothing \quad \text{and} \quad E_{\text{off}} \neq \varnothing, \tag{2}$$

equivalently, there exist $v_0 \in V$ and $e_0 \in E$ such that $\sigma(v_0) \notin [0,1]$ and $\mu(e_0) \notin [0,1]$.

Example 2.2 (Admissible (Ψ, Ω)-fuzzy n-SuperHyperGraph ($n = 1$): sensor bundles, and when it becomes off)**.** *Interpretation.* Base items are sensors. A level-1 supervertex is a bundle of sensors, and a 1-superedge is a nonempty collection of such bundles that are assessed jointly (e.g., a fused decision rule). Memberships σ and μ measure reliability/activation on an extended scale $[\Psi, \Omega]$: values > 1 represent exceptional reliability (bounded overshoot), while values < 0 represent invalid or penalized states.

Construction (admissible). Let $V_0 = \{\mathrm{T}, \mathrm{H}, \mathrm{P}\}$ (temperature, humidity, pressure) and $n = 1$. Take

$$V = \big\{\{\mathrm{T}\},\ \{\mathrm{H}\},\ \{\mathrm{P}\},\ \{\mathrm{T}, \mathrm{H}\}\big\} \subseteq \mathcal{P}(V_0).$$

Define two 1-superedges (nonempty subsets of V):

$$e_1 = \big\{\{\mathrm{T}\}, \{\mathrm{H}\}\big\}, \qquad e_2 = \big\{\{\mathrm{T}, \mathrm{H}\}, \{\mathrm{P}\}\big\}, \qquad E = \{e_1, e_2\} \subseteq \mathcal{P}^*(V).$$

Fix bounds $\Psi = -0.4$ and $\Omega = 1.3$. Define $\sigma : V \to [\Psi, \Omega]$ by

$$\sigma(\{\mathrm{T}\}) = 1.10, \quad \sigma(\{\mathrm{H}\}) = 0.70, \quad \sigma(\{\mathrm{P}\}) = 0.35, \quad \sigma(\{\mathrm{T}, \mathrm{H}\}) = 0.80.$$

Compute the admissible maxima (edgewise minima of σ):

$$\min_{v \in e_1} \sigma(v) = \min\{1.10, 0.70\} = 0.70, \qquad \min_{v \in e_2} \sigma(v) = \min\{0.80, 0.35\} = 0.35.$$

Define $\mu : E \to [\Psi, \Omega]$ by

$$\mu(e_1) = 0.65 \le 0.70, \qquad \mu(e_2) = 0.30 \le 0.35.$$

Verification (admissibility). The displayed computations give $\mu(e) \le \min_{v \in e} \sigma(v)$ for $e = e_1, e_2$, hence (V, E, σ, μ) is admissible.

Offness check (this instance is not a FOSH). Define

$$V_{\text{off}} = \{v \in V : \sigma(v) \notin [0, 1]\}, \qquad E_{\text{off}} = \{e \in E : \mu(e) \notin [0, 1]\}.$$

Here $\sigma(\{\mathrm{T}\}) = 1.10 \notin [0, 1]$, so $V_{\text{off}} = \{\{\mathrm{T}\}\} \neq \varnothing$. However, $\mu(e_1) = 0.65$ and $\mu(e_2) = 0.30$ both lie in $[0, 1]$, so $E_{\text{off}} = \varnothing$. Thus the *vertex-and-edge* offness condition fails, and this admissible example is *not* a FOSH.

How to make it a FOSH (minimal modification). Increase the bundle reliability of $\{\mathrm{T}, \mathrm{H}\}$ and add one joint assessment edge supported on vertices with overshoot: set

$$\sigma^+(\{\mathrm{T}\}) = 1.10, \quad \sigma^+(\{\mathrm{H}\}) = 0.70, \quad \sigma^+(\{\mathrm{P}\}) = 0.35, \quad \sigma^+(\{\mathrm{T}, \mathrm{H}\}) = 1.20,$$

and define an additional 1-superedge

$$e_3 = \big\{\{\mathrm{T}\}, \{\mathrm{T}, \mathrm{H}\}\big\}, \qquad E^+ = \{e_1, e_2, e_3\}.$$

Then

$$\min_{v \in e_3} \sigma^+(v) = \min\{1.10, 1.20\} = 1.10,$$

so we may choose (still within $[\Psi, \Omega] = [-0.4, 1.3]$)

$$\mu^+(e_1) = 0.65, \qquad \mu^+(e_2) = 0.30, \qquad \mu^+(e_3) = 1.05 \le 1.10.$$

Hence $(V, E^+, \sigma^+, \mu^+)$ is admissible, and now

$$V^+_{\text{off}} \neq \varnothing \quad (\text{since } \sigma^+(\{\text{T}\}) = 1.10,\ \sigma^+(\{\text{T}, \text{H}\}) = 1.20), \qquad E^+_{\text{off}} \neq \varnothing \quad (\text{since } \mu^+(e_3) = 1.05 \notin [0, 1]),$$

so the vertex-and-edge offness condition holds and $(V, E^+, \sigma^+, \mu^+)$ is a *FOSH*.

Example 2.3 (Admissible (Ψ, Ω)-fuzzy n-SuperHyperGraph ($n = 2$): hierarchical product–group collections (and it is off))**.** *Interpretation.* Base items are products. A level-2 supervertex is a collection of subsets of products, capturing a two-level grouping ("families of product bundles"). Memberships on $[\Psi, \Omega]$ allow penalization (< 0) or exceptional priority (> 1), while the admissibility inequality still constrains each superedge membership by its incident supervertices.

Construction. Let $V_0 = \{x, y\}$ and $n = 2$, so $\mathcal{P}(V_0) = \{\varnothing, \{x\}, \{y\}, \{x, y\}\}$. Define three level-2 supervertices (elements of $\mathcal{P}^2(V_0) = \mathcal{P}(\mathcal{P}(V_0))$):

$$v_1 = \big\{\{x\}, \{y\}\big\}, \qquad v_2 = \big\{\{x, y\}\big\}, \qquad v_3 = \big\{\varnothing, \{x\}\big\},$$

and set

$$V = \{v_1, v_2, v_3\} \subseteq \mathcal{P}^2(V_0).$$

Define two 2-superedges as nonempty subsets of V:

$$e_1 = \{v_1, v_2\}, \qquad e_2 = \{v_2, v_3\}, \qquad E = \{e_1, e_2\} \subseteq \mathcal{P}^*(V).$$

Fix bounds $\Psi = -0.8$ and $\Omega = 1.5$. Define $\sigma : V \to [\Psi, \Omega]$ by

$$\sigma(v_1) = 0.90, \qquad \sigma(v_2) = 0.60, \qquad \sigma(v_3) = -0.20.$$

Then the admissible maxima are

$$\min_{v \in e_1} \sigma(v) = \min\{0.90, 0.60\} = 0.60, \qquad \min_{v \in e_2} \sigma(v) = \min\{0.60, -0.20\} = -0.20.$$

Choose $\mu : E \to [\Psi, \Omega]$ by

$$\mu(e_1) = 0.55 \leq 0.60, \qquad \mu(e_2) = -0.35 \leq -0.20.$$

Verification (admissibility). The displayed inequalities show that $\mu(e) \leq \min_{v \in e} \sigma(v)$ for each $e \in E$. Therefore (V, E, σ, μ) is an admissible (Ψ, Ω)-fuzzy 2-SuperHyperGraph.

Offness check (this instance <u>is</u> a FOSH). With

$$V_{\text{off}} = \{v \in V : \sigma(v) \notin [0, 1]\}, \qquad E_{\text{off}} = \{e \in E : \mu(e) \notin [0, 1]\},$$

we have $\sigma(v_3) = -0.20 \notin [0, 1]$, hence $V_{\text{off}} \neq \varnothing$, and $\mu(e_2) = -0.35 \notin [0, 1]$, hence $E_{\text{off}} \neq \varnothing$. Thus the vertex-and-edge offness condition holds, and this admissible example is also a *FOSH*.

In Fig. 2, we present a brief incidence-view overview of this example.

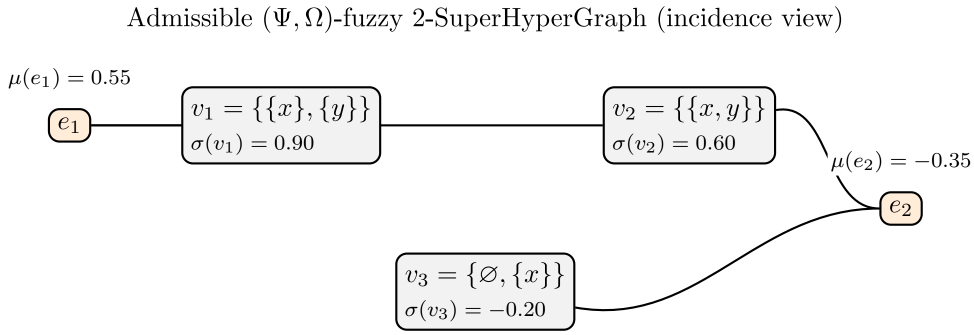

FIGURE 2. A diagram of Example 2.3: supervertices v_1, v_2, v_3 (with σ) and superedges e_1, e_2 (with μ).

Theorem 2.4 (Reduction to fuzzy n-SuperHyperGraphs)**.** *Assume $\Psi = 0$ and $\Omega = 1$.*

(a) Every admissible $(0,1)$-fuzzy n-SuperHyperGraph (V, E, σ, μ) (in the sense of Definition 2.1) is exactly a fuzzy n-SuperHyperGraph.

(b) No FOSH exists with bounds $(\Psi, \Omega) = (0, 1)$.

Proof. (a) If $\Psi = 0$ and $\Omega = 1$, then $\sigma : V \to [0,1]$ and $\mu : E \to [0,1]$. The admissibility inequality is precisely the usual appurtenance constraint for fuzzy n-SuperHyperGraphs, hence (V, E, σ, μ) is a fuzzy n-SuperHyperGraph.
(b) If $\sigma(V) \subseteq [0,1]$ and $\mu(E) \subseteq [0,1]$, then no value can lie outside $[0,1]$. Therefore the offness requirement cannot be satisfied. □

Theorem 2.5 (Reduction to admissible fuzzy offgraphs)**.** *Let $n = 0$ and assume $E \subseteq \binom{V}{2}$ (loopless simple case). Then a FOSH $\big(V, E, \sigma, \mu; \Psi, \Omega\big)$ induces an admissible fuzzy offgraph on $G = (V, E)$ in the sense of Definition 1.11, by setting $\ell_V = \sigma$ and $\ell_E = \mu$. Conversely, any admissible fuzzy offgraph (V, E, ℓ_V, ℓ_E) yields a FOSH at level $n = 0$ (with $\sigma = \ell_V$ and $\mu = \ell_E$).*

Proof. When $n = 0$, we have $V \subseteq \mathcal{P}^0(V_0) = V_0$ and (by the incidence convention) $E \subseteq \mathcal{P}^*(V)$. Imposing $E \subseteq \binom{V}{2}$ identifies (V, E) with a loopless simple graph.
If $\big(V, E, \sigma, \mu; \Psi, \Omega\big)$ is a FOSH, then $\sigma : V \to [\Psi, \Omega]$ and $\mu : E \to [\Psi, \Omega]$, and the admissibility inequality reads

$$\mu(\{u, v\}) \;\le\; \min\{\sigma(u), \sigma(v)\} \qquad (\forall \{u, v\} \in E),$$

which is exactly the admissibility condition in Definition 1.11. The offness condition supplies both a vertex and an edge whose memberships lie outside $[0,1]$. Hence (V, E, σ, μ) is an admissible fuzzy offgraph.
Conversely, given an admissible fuzzy offgraph (V, E, ℓ_V, ℓ_E), define $\sigma = \ell_V$ and $\mu = \ell_E$. Then the assumed offness gives the required vertex-and-edge offness. Thus we obtain a FOSH. □

Proposition 2.6 (Maximal admissible edge map). *Fix $\Psi < 0 < 1 < \Omega$ and let $\sigma : V \to [\Psi, \Omega]$ be given. Define*

$$\mu^{\max}(e) := \min_{v \in e} \sigma(v) \qquad (e \in E).$$

Then a map $\mu : E \to [\Psi, \Omega]$ satisfies the admissibility inequality if and only if $\mu \le \mu^{\max}$ pointwise. In particular, $\mu^{\max}$ is the largest admissible edge-membership map among all $\mu : E \to [\Psi, \Omega]$ for the fixed σ.

Proof. The admissibility is exactly the pointwise condition $\mu(e) \le \min_{v \in e} \sigma(v) = \mu^{\max}(e)$ for every $e \in E$, i.e., $\mu \le \mu^{\max}$. The maximality is immediate. □

Proposition 2.7 (Monotonicity in vertex memberships). *Let $\sigma_1, \sigma_2 : V \to [\Psi, \Omega]$ satisfy $\sigma_1 \le \sigma_2$ pointwise. Then for every $e \in E$,*

$$\mu^{\max}_{\sigma_1}(e) = \min_{v \in e} \sigma_1(v) \ \le \ \min_{v \in e} \sigma_2(v) = \mu^{\max}_{\sigma_2}(e).$$

Consequently, the feasible set $\{\mu : E \to [\Psi, \Omega] \mid \mu \le \mu^{\max}_{\sigma}\}$ expands monotonically with σ.

Proof. The minimum of finitely many real numbers is nondecreasing in each argument, hence the displayed inequality holds. The monotonicity of feasible sets follows directly from Proposition 2.6. □

Proposition 2.8 (Propagation of under-offness (negative memberships)). *Fix real bounds $\Psi < 0 < 1 < \Omega$ and let (V, E, σ, μ) be an admissible (Ψ, Ω)-fuzzy n-SuperHyperGraph, so that $\sigma : V \to [\Psi, \Omega]$ and $\mu : E \to [\Psi, \Omega]$ satisfy*

$$\mu(e) \le \min_{v \in e} \sigma(v) \qquad (\forall e \in E).$$

Define the edgewise admissible maximum

$$\mu^{\max}(e) := \min_{v \in e} \sigma(v) \qquad (e \in E),$$

and the under-off *vertex/edge sets*

$$V^{-}_{\text{off}} := \{\, v \in V : \sigma(v) < 0 \,\}, \qquad E^{-}_{\text{off}} := \{\, e \in E : \mu(e) < 0 \,\}.$$

If $v^- \in V^{-}_{\text{off}}$ (i.e., $\sigma(v^-) < 0$), then every edge $e \in E$ incident to v^- satisfies

$$\mu^{\max}(e) = \min_{v \in e} \sigma(v) \ \le \ \sigma(v^-) \ < \ 0.$$

Consequently, for every admissible μ one has $\mu(e) < 0$ for each $e \in E$ with $v^- \in e$, hence

$$\{\, e \in E : \ v^- \in e \,\} \subseteq E^{-}_{\text{off}}.$$

Proof. Let $e \in E$ with $v^- \in e$. Then by the definition of $\mu^{\max}$,

$$\mu^{\max}(e) = \min_{v \in e} \sigma(v) \le \sigma(v^-) < 0,$$

which proves the first claim.

Now let μ be any admissible edge membership function. By admissibility,

$$\mu(e) \le \min_{v \in e} \sigma(v) = \mu^{\max}(e) < 0,$$

so $\mu(e) < 0$ for every e incident to v^-. Therefore each such e lies in E^-_{off}. □

Remark 2.9. If $\sigma(v) > 1$ for all $v \in e$, then $\mu^{\max}(e) > 1$. However, admissibility only requires $\mu(e) \le \mu^{\max}(e)$, so one may still have $\mu(e) \in [0, 1]$. Thus overshoot of all incident vertices does not force an edge to be off.

Theorem 2.10 (Clipping to a fuzzy n-SuperHyperGraph)**.** *Let* $\text{clip}(x) := \min\{1, \max\{0, x\}\}$. *If* (V, E, σ, μ) *is an admissible* (Ψ, Ω)*-fuzzy* n*-SuperHyperGraph (in particular, if it is a FOSH), then*

$$\big(V, E,\ \text{clip}\circ\sigma,\ \text{clip}\circ\mu\big)$$

is a fuzzy n*-SuperHyperGraph (codomain* $[0, 1]$*) and satisfies*

$$\text{clip}\big(\mu(e)\big)\ \le\ \min_{v \in e} \text{clip}\big(\sigma(v)\big) \qquad (\forall e \in E).$$

Proof. The function clip is nondecreasing on $\mathbb{R}$. For each $e \in E$, admissibility gives $\mu(e) \le \min_{v \in e} \sigma(v)$. Applying clip and using monotonicity,

$$\text{clip}\big(\mu(e)\big)\ \le\ \text{clip}\Big(\min_{v \in e} \sigma(v)\Big).$$

Since clip is nondecreasing and min is taken over finitely many values,

$$\text{clip}\Big(\min_{v \in e} \sigma(v)\Big) = \min_{v \in e} \text{clip}\big(\sigma(v)\big).$$

Finally, $\text{clip} \circ \sigma$ and $\text{clip} \circ \mu$ take values in $[0, 1]$ by definition of clip, so we obtain a fuzzy n-SuperHyperGraph. □

Theorem 2.11 (Affine normalization)**.** *Define the increasing affine map* $T : [\Psi, \Omega] \to [0, 1]$ *by*

$$T(x) := \frac{x - \Psi}{\Omega - \Psi}.$$

If (V, E, σ, μ) *is an admissible* (Ψ, Ω)*-fuzzy* n*-SuperHyperGraph (in particular, if it is a FOSH), then*

$$\big(V, E,\ T \circ \sigma,\ T \circ \mu\big)$$

is a fuzzy n*-SuperHyperGraph, and*

$$T\big(\mu(e)\big)\ \le\ \min_{v \in e} T\big(\sigma(v)\big) \qquad (\forall e \in E)$$

holds.

Proof. The map T is increasing on $[\Psi, \Omega]$. Hence, for each $e \in E$, admissibility yields

$$T\big(\mu(e)\big) \;\leq\; T\Big(\min_{v\in e} \sigma(v)\Big) \;=\; \min_{v\in e} T\big(\sigma(v)\big),$$

where the last equality follows because T is increasing and min is taken over finitely many reals. Moreover, $T \circ \sigma$ and $T \circ \mu$ map into $[0, 1]$ by construction, so the result is a fuzzy n-SuperHyperGraph. □

Proposition 2.12 (Induced substructures)**.** *Let $W \subseteq V$ and define $E|_W := \{e \in E : \; e \subseteq W\}$. Restrict σ and μ to W and $E|_W$, respectively.*

(a) If (V, E, σ, μ) is an admissible (Ψ, Ω)-fuzzy n-SuperHyperGraph, then $\big(W, E|_W, \sigma|_W, \mu|_{E|_W}\big)$ is also an admissible (Ψ, Ω)-fuzzy n-SuperHyperGraph.

(b) If $\big(V, E, \sigma, \mu; \Psi, \Omega\big)$ is a FOSH, then the induced structure $\big(W, E|_W, \sigma|_W, \mu|_{E|_W}; \Psi, \Omega\big)$ is a FOSH if and only if both

$$\exists\, v \in W : \; \sigma(v) \notin [0, 1] \quad \text{and} \quad \exists\, e \in E|_W : \; \mu(e) \notin [0, 1].$$

Proof. (a) For any $e \in E|_W$, we have $e \in E$ and $e \subseteq W$, hence

$$\mu|_{E|_W}(e) = \mu(e) \;\leq\; \min_{v\in e} \sigma(v) \;=\; \min_{v\in e} \sigma|_W(v),$$

so admissibility is preserved under restriction.
(b) The induced structure is a FOSH precisely when it satisfies admissibility (which holds by (a)) and it still has both a vertex and an edge with membership outside $[0, 1]$, which is exactly the displayed condition. □

Lemma 2.13 (Edge feasibility is downward closed)**.** *Fix $\sigma : V \to [\Psi, \Omega]$ and let $\mu^{\max}$ be as in Proposition 2.6. If $\mu_1, \mu_2 : E \to [\Psi, \Omega]$ satisfy $\mu_1 \leq \mu_2 \leq \mu^{\max}$, then every convex combination $\lambda\mu_1 + (1 - \lambda)\mu_2$ with $\lambda \in [0, 1]$ is admissible.*

Proof. Since $[\Psi, \Omega]$ is convex, $\lambda\mu_1 + (1-\lambda)\mu_2$ takes values in $[\Psi, \Omega]$. Moreover, for each $e \in E$,

$$\lambda\mu_1(e) + (1 - \lambda)\mu_2(e) \;\leq\; \lambda\mu^{\max}(e) + (1 - \lambda)\mu^{\max}(e) \;=\; \mu^{\max}(e),$$

so admissibility follows from Proposition 2.6. □

Lemma 2.14 (Tightness on incident under-off vertices)**.** *Let $\sigma : V \to [\Psi, \Omega]$ and $\mu^{\max}$ be as above. If $e \in E$ has a vertex $v^- \in e$ with $\sigma(v^-) = \min_{u\in e} \sigma(u)$, then $\mu^{\max}(e) = \sigma(v^-)$. In particular, if $\sigma(v^-) < 0$ and is the unique minimum on e, then every admissible μ satisfies*

$$\mu(e) \in [\Psi, \sigma(v^-)] \subset (-\infty, 0).$$

Proof. The identity $\mu^{\max}(e) = \min_{u \in e} \sigma(u) = \sigma(v^-)$ is immediate from the hypothesis. If $\sigma(v^-) < 0$, then admissibility gives $\mu(e) \le \mu^{\max}(e) = \sigma(v^-) < 0$, while $\mu(e) \ge \Psi$ by codomain. □

Lemma 2.15 (Restriction of off sets). *Let $W \subseteq V$ and $E|_W := \{e \in E : \ e \subseteq W\}$. Define off-sets for the restricted maps by*

$$V_{\text{off}}^{\pm}(W) := \{v \in W : \ \sigma(v) \gtrless 1 \text{ or } \sigma(v) \lesseqgtr 0\}, \qquad E_{\text{off}}^{\pm}(W) := \{e \in E|_W : \ \mu(e) \gtrless 1 \text{ or } \mu(e) \lesseqgtr 0\},$$

i.e., the elements whose memberships lie outside $[0,1]$. Then

$$V_{\text{off}}^{+}(W) = V_{\text{off}}^{+} \cap W, \qquad V_{\text{off}}^{-}(W) = V_{\text{off}}^{-} \cap W,$$

and

$$E_{\text{off}}^{+}(W) = E_{\text{off}}^{+} \cap E|_W, \qquad E_{\text{off}}^{-}(W) = E_{\text{off}}^{-} \cap E|_W.$$

In particular, if the induced structure on W is a FOSH (cf. Proposition 2.12(b)), then these are exactly its vertex and edge off sets.

Proof. All equalities are immediate from the definitions: restricting the domain to W (respectively $E|_W$) simply intersects the original off-sets with W (respectively with $E|_W$). □

3. Conclusion

In this paper, we proposed an extension of the existing framework, termed the *Fuzzy Off-SuperHyperGraph*, which incorporates the offgraph paradigm into fuzzy n-SuperHyperGraphs. This novel structure broadens the scope of uncertainty modeling by allowing vertex and edge memberships to extend beyond the classical unit interval.

For future work, we plan to further develop the theory of Fuzzy Off-SuperHyperGraphs by exploring their integration with several advanced set-theoretic models, including Neutrosophic Sets [35,36], Hesitant Fuzzy Sets [37], Soft Sets [38], QuadriPartitioned Neutrosophic Sets [39,40], Uncertain Sets [13], and Plithogenic Sets [41,42]. Such extensions are expected to provide richer tools for modeling complex, uncertain, and multi-dimensional systems, and open new directions for applications in decision-making, data analysis, and hierarchical network structures.

Funding

This study did not receive any financial or external support from organizations or individuals.

Acknowledgments

We extend our sincere gratitude to everyone who provided insights, inspiration, and assistance throughout this research. We particularly thank our readers for their interest and acknowledge the authors of the cited works for laying the foundation that made our study possible. We also appreciate the support from individuals and institutions that provided the resources and infrastructure needed to produce and share this paper. Finally, we are grateful to all those who supported us in various ways during this project.

Data Availability

This research is purely theoretical, involving no data collection or analysis. We encourage future researchers to pursue empirical investigations to further develop and validate the concepts introduced here.

Ethical Approval

As this research is entirely theoretical in nature and does not involve human participants or animal subjects, no ethical approval is required.

Conflicts of Interest

The authors confirm that there are no conflicts of interest related to the research or its publication.

Use of Generative AI and AI-Assisted Tools

We use generative AI and AI-assisted tools for tasks such as English grammar checking, and we do not employ them in any way that violates ethical standards.

Supplementary Information

No supplementary materials accompany this paper.

References

[1] Muhammad Akram, A Nagoor Gani, and A Borumand Saeid. Vague hypergraphs. *Journal of Intelligent & Fuzzy Systems*, 26(2):647–653, 2014.

[2] Claude Berge. *Hypergraphs: combinatorics of finite sets*, volume 45. Elsevier, 1984.

[3] Yue Gao, Zizhao Zhang, Haojie Lin, Xibin Zhao, Shaoyi Du, and Changqing Zou. Hypergraph learning: Methods and practices. *IEEE Transactions on Pattern Analysis and Machine Intelligence*, 44(5):2548–2566, 2020.

[4] Eduardo Martín Campoverde Valencia, Jessica Paola Chuisaca Vásquez, and Francisco Ángel Becerra Lois. Multineutrosophic analysis of the relationship between survival and business growth in the manufacturing sector of azuay province, 2020–2023, using plithogenic n-superhypergraphs. *Neutrosophic Sets and Systems*, 84:341–355, 2025.

[5] Takaaki Fujita and Florentin Smarandache. *HyperGraph and SuperHyperGraph Theory with Applications (IV): Uncertain Graph Theory*, volume IV of *HyperGraph and SuperHyperGraph Theory with Applications*. Neutrosophic Science International Association (NSIA) Publishing House, 1.0 edition, 2026.

[6] Takaaki Fujita and Florentin Smarandache. *HyperGraph and SuperHyperGraph Theory with Applications (III): Intersection Graph and Graph Labeling*, volume III of *HyperGraph and SuperHyperGraph Theory with Applications*. Neutrosophic Science International Association (NSIA) Publishing House, 2026.

[7] Takaaki Fujita and Florentin Smarandache. *HyperGraph and SuperHyperGraph Theory with Applications (II): Graph Property and Parameter*, volume II of *HyperGraph and SuperHyperGraph Theory with Applications*. Neutrosophic Science International Association (NSIA) Publishing House, 1.0 edition, 2026.

[8] Takaaki Fujita and Florentin Smarandache. *HyperGraph and SuperHyperGraph Theory with Applications*. Neutrosophic Science International Association (NSIA) Publishing House, 2026.

[9] Takaaki Fujita. An introduction and reexamination of molecular hypergraph and molecular n-superhypergraph. *Asian Journal of Physical and Chemical Sciences*, 13(3):1–38, 2025.

[10] Berrocal Villegas Salomón Marcos, Montalvo Fritas Willner, Berrocal Villegas Carmen Rosa, Flores Fuentes Rivera María Yissel, Espejo Rivera Roberto, Laura Daysi Bautista Puma, and Dante Manuel Macazana Fernández. Using plithogenic n-superhypergraphs to assess the degree of relationship between information skills and digital competencies. *Neutrosophic Sets and Systems*, 84:513–524, 2025.

[11] Shouxian Zhu. Neutrosophic n-superhypernetwork: A new approach for evaluating short video communication effectiveness in media convergence. *Neutrosophic Sets and Systems*, 85:1004–1017, 2025.

[12] Takaaki Fujita and Arif Mehmood. Actor hypernetworks and urban road hypernetworks with real-life applications. *Neutrosophic Computing and Machine Learning*, 41:143–171, 2025.

[13] Takaaki Fujita and Florentin Smarandache. A unified framework for u-structures and functorial structure: Managing super, hyper, superhyper, tree, and forest uncertain over/under/off models. *Neutrosophic Sets and Systems*, 91:337–380, 2025.

[14] Takaaki Fujita, Atiqe Ur Rahman, Arkan A. Ghaib, Talal Ali Al-Hawary, and Arif Mehmood. On the properties and illustrative examples of soft superhypergraphs and rough superhypergraphs. *Prospects for Applied Mathematics and Data Analysis*, 5(1):12–31, 2025.

[15] Takaaki Fujita. Unifying grain boundary networks and crystal graphs: A hypergraph and superhypergraph perspective in material sciences. *Asian Journal of Advanced Research and Reports*, 19(5):344–379, 2025.

[16] Thomas Jech. *Set theory: The third millennium edition, revised and expanded*. Springer, 2003.

[17] Florentin Smarandache. The cardinal of the m-powerset of a set of n elements used in the superhyperstructures and neutrosophic superhyperstructures. *Systems Assessment and Engineering Management*, 2:19–22, 2024.

[18] Ajoy Kanti Das, Rajat Das, Suman Das, Bijoy Krishna Debnath, Carlos Granados, Bimal Shil, and Rakhal Das. A comprehensive study of neutrosophic superhyper bci-semigroups and their algebraic significance. *Transactions on Fuzzy Sets and Systems*, 8(2):80, 2025.

[19] Alain Bretto. Hypergraph theory. *An introduction. Mathematical Engineering. Cham: Springer*, 1, 2013.

[20] Min Huang, Fenghua Li, et al. Modeling cross-cultural competence in vocational education internationalization using neutrosophic superhyperfunctions and big data driven cultural clusters. *Neutrosophic Sets and Systems*, 88:362–373, 2025.

[21] Florentin Smarandache. *Extension of HyperGraph to n-SuperHyperGraph and to Plithogenic n-SuperHyperGraph, and Extension of HyperAlgebra to n-ary (Classical-/Neutro-/Anti-) HyperAlgebra*. Infinite Study, 2020.

[22] Lotfi A Zadeh. Fuzzy sets. *Information and control*, 8(3):338–353, 1965.

[23] Lotfi A Zadeh. Fuzzy logic, neural networks, and soft computing. In *Fuzzy sets, fuzzy logic, and fuzzy systems: selected papers by Lotfi A Zadeh*, pages 775–782. World Scientific, 1996.

[24] TM Nishad, Talal Ali Al-Hawary, and B Mohamed Harif. General fuzzy graphs. *Ratio Mathematica*, 47, 2023.

[25] Azriel Rosenfeld. Fuzzy graphs. In *Fuzzy sets and their applications to cognitive and decision processes*, pages 77–95. Elsevier, 1975.

[26] Takaaki Fujita and Florentin Smarandache. A review of the hierarchy of plithogenic, neutrosophic, and fuzzy graphs: Survey and applications. In *Advancing Uncertain Combinatorics through Graphization, Hyperization, and Uncertainization: Fuzzy, Neutrosophic, Soft, Rough, and Beyond (Second Volume)*. Biblio Publishing, 2024.

[27] Talal Al-Hawary. Complete fuzzy graphs. *International Journal of Mathematical Combinatorics*, 4:26, 2011.

[28] Mahdi Farshi and Bijan Davvaz. Generalized fuzzy hypergraphs and hypergroupoids. *Filomat*, 30(9):2375–2387, 2016.

[29] Mohammed Alqahtani. Intuitionistic fuzzy quasi-supergraph integration for social network decision making. *International Journal of Analysis and Applications*, 23:137–137, 2025.

[30] Takaaki Fujita. Extensions of multidirected graphs: Fuzzy, neutrosophic, plithogenic, rough, soft, hypergraph, and superhypergraph variants. *International Journal of Topology*, 2(3):11, 2025.

[31] Takaaki Fujita and Florentin Smarandache. Directed n-superhypergraphs incorporating bipolar fuzzy information: A multi-tier framework for modeling bipolar uncertainty in complex networks. *Neutrosophic Sets and Systems*, 88:164–183, 2025.

[32] Takaaki Fujita. A review of fuzzy and neutrosophic offsets: Connections to some set concepts and normalization function. *Advancing Uncertain Combinatorics through Graphization, Hyperization, and Uncertainization: Fuzzy, Neutrosophic, Soft, Rough, and Beyond*, page 74, 2024.

[33] Florentin Smarandache, Miguel A. Quiroz-Martínez, Jesús Estupiñán, Noel Batista Hernández, and Maikel Yelandi Leyva Vazquez. Application of neutrosophic offsets for digital image processing. *Investigacion Operacional*, 2020.

[34] Florentin Smarandache. *Practical Applications of the Independent Neutrosophic Components and of the Neutrosophic Offset Components*. Infinite Study, 2021.

[35] Said Broumi, Mohamed Talea, Assia Bakali, and Florentin Smarandache. Single valued neutrosophic graphs. *Journal of New theory*, 10:86–101, 2016.

[36] Florentin Smarandache and Maissam Jdid. An overview of neutrosophic and plithogenic theories and applications. 2023.

[37] Vicenç Torra and Yasuo Narukawa. On hesitant fuzzy sets and decision. In *2009 IEEE international conference on fuzzy systems*, pages 1378–1382. IEEE, 2009.

[38] Dmitriy Molodtsov. Soft set theory-first results. *Computers & mathematics with applications*, 37(4-5):19–31, 1999.

[39] R Radha, A Stanis Arul Mary, and Florentin Smarandache. Quadripartitioned neutrosophic pythagorean soft set. *International Journal of Neutrosophic Science (IJNS) Volume 14, 2021*, page 11, 2021.

[40] Satham Hussain, Jahir Hussain, Isnaini Rosyida, and Said Broumi. Quadripartitioned neutrosophic soft graphs. In *Handbook of Research on Advances and Applications of Fuzzy Sets and Logic*, pages 771–795. IGI Global, 2022.

[41] Muhammad Azeem, Humera Rashid, Muhammad Kamran Jamil, Selma Gütmen, and Erfan Babaee Tirkolaee. Plithogenic fuzzy graph: A study of fundamental properties and potential applications. *Journal of Dynamics and Games*, pages 0–0, 2024.

[42] Takaaki Fujita and Florentin Smarandache. *A Dynamic Survey of Fuzzy, Intuitionistic Fuzzy, Neutrosophic, , and Extensional Sets*. Neutrosophic Science International Association (NSIA), 2025.

Neutrosophic Knowledge, Volume 9, 2026

University of New Mexico

Molecular Line HyperGraphs and SuperHyperGraphs

Takaaki Fujita[1] *, *Ajoy Kanti Das* [2], *Suman Das* [3]

[1] Independent Researcher, Tokyo, Japan. (Takaaki.fujita060@gmail.com)

[2] Associate Professor, Department of Mathematics, Tripura University, Agartala-799022, Tripura, India. (ajoykantidas@gmail.com)

[3] Assistant Professor (Mathematics), Department of Education (ITEP), NIT Agartala, Jirania, 799046, Tripura, India. (dr.sumandas1995@gmail.com)

*Correspondence: Takaaki.fujita060@gmail.com

Received*: 01/02/2026;* Accepted*: 01/21/2026*

Abstract. Hypergraphs extend classical graphs by allowing *hyperedges* to connect any nonempty subset of vertices, thereby capturing complex group-level relationships. Superhypergraphs advance this framework by introducing recursively nested powerset layers, which represent hierarchical and self-referential connections among hyperedges. A *line graph* encodes edge adjacencies of a given graph by turning each edge into a vertex and joining two such vertices when the corresponding edges share an endpoint. An *iterated line graph* applies this construction repeatedly, each time to the result of the previous step. Within chemistry, molecular and chemical graphs are well established, and hypergraphs, line graphs, and superhypergraphs have also been explored in this setting. In this paper, we introduce *Molecular Line SuperHyperGraphs* and *Molecular Iterated Line SuperHyperGraphs*, provide formal definitions, and discuss potential applications. We expect that these frameworks will enable clearer and more faithful representations of hierarchical molecular structure in chemistry.

Keywords: SuperHyperGraph, HyperGraph, Line Graph, Molecular Graph, Iterated Line Graph

---

1. **Preliminaries**

This section outlines the fundamental notions and notation adopted in the present work. Throughout, all graphs and hypergraphs under consideration are assumed to be finite.

1.1. *Hypergraphs and Superhypergraphs*

A *hypergraph* extends the standard graph model by permitting each edge, termed a *hyperedge*, to link any nonempty subset of the vertex set, thereby enabling the modeling of interactions among more than two vertices [1–4]. A *superhypergraph* builds upon this concept by repeatedly applying powerset operations to the hypergraph structure, producing hierarchically nested layers of hyperedge connections [5–7]. This enhanced structural model has been the focus of several recent studies [8–10]. Given its high descriptive capacity for hierarchical modeling, the superhypergraph framework is anticipated to support a broadening scope of applications [11–14], and it is expected to assume an even more prominent role in the future.

Definition 1.1 (Base Set)**.** Let S be a nonempty set, called the *base set.* All higher-order objects, such as powersets and supervertices, are constructed from S:

$$S = \{\, x \mid x \text{ is an element of the domain} \,\}.$$

Definition 1.2 (Powerset)**.** [15] For any set S, its *powerset* $\mathrm{POWS}(S)$ is the collection of all subsets of S, including $\emptyset$ and S itself:

$$\mathrm{POWS}(S) = \{\, A \mid A \subseteq S \,\}.$$

Definition 1.3 (n-th Powerset)**.** [16]. Let H be a set. The *n-th powerset* $\mathrm{POWS}^n(H)$ is defined recursively by

$$\mathrm{POWS}^0(H) = H, \qquad \mathrm{POWS}^{k+1}(H) = \mathrm{POWS}\big(\mathrm{POWS}^k(H)\big), \quad k \geq 0.$$

The *nonempty n-th powerset* $\mathrm{POWS}^{*n}(H)$ is defined similarly but removes the empty set at each stage:

$$\mathrm{POWS}^{*0}(H) = H, \qquad \mathrm{POWS}^{*(k+1)}(H) = \mathrm{POWS}^*\big(\mathrm{POWS}^{*k}(H)\big),$$

where $\mathrm{POWS}^*(X) = \mathrm{POWS}(X) \setminus \{\emptyset\}$

Example 1.4 (n-th powerset in biochemistry: amino-acid subsets and collections of subsets (with concrete uses))**.** Let $H = \{\mathrm{Ala}, \mathrm{Gly}, \mathrm{Ser}\}$ be a set of three amino acids ($|H| = 3$). Then

$$\mathrm{POWS}^1(H) = \mathrm{POWS}(H) = \big\{\emptyset,\ \{\mathrm{Ala}\},\ \{\mathrm{Gly}\},\ \{\mathrm{Ser}\},\ \{\mathrm{Ala}, \mathrm{Gly}\},\ \{\mathrm{Ala}, \mathrm{Ser}\},\ \{\mathrm{Gly}, \mathrm{Ser}\},\ H\big\},$$

so $|\mathrm{POWS}^1(H)| = 2^3 = 8$. The second powerset $\mathrm{POWS}^2(H) = \mathrm{POWS}(\mathrm{POWS}(H))$ consists of *collections of amino-acid subsets.* For instance,

$$\big\{\emptyset, \{\mathrm{Ala}\}\big\}, \qquad \big\{\{\mathrm{Ala}, \mathrm{Gly}\}, \{\mathrm{Ser}\}\big\}, \qquad \mathrm{POWS}^1(H) \ \in\ \mathrm{POWS}^2(H).$$

Since $|\mathrm{POWS}^1(H)| = 8$, we have $|\mathrm{POWS}^2(H)| = 2^8 = 256$. Likewise, the nonempty versions $\mathrm{POWS}^{*1}(H) = \mathrm{POWS}(H) \setminus \{\emptyset\}$ and $\mathrm{POWS}^{*2}(H) = \mathrm{POWS}\big(\mathrm{POWS}^{*1}(H)\big) \setminus \{\emptyset\}$ remove $\emptyset$ at each level.

Concrete biochemical uses.

(a) *Alternative binding-site compositions across conditions.* Suppose three experimentally observed microstates of a pocket have residue sets

$$S_1 = \{\mathrm{Ala}, \mathrm{Gly}\}, \quad S_2 = \{\mathrm{Gly}, \mathrm{Ser}\}, \quad S_3 = \{\mathrm{Ala}, \mathrm{Ser}\},$$

occurring with frequencies $p_1 = 0.5$, $p_2 = 0.3$, $p_3 = 0.2$ (with $p_1+p_2+p_3 = 1$). The *ensemble of observed compositions* is $X = \{S_1, S_2, S_3\} \in \mathrm{POWS}^2(H)$. From X and $\mathbf{p}$, we obtain explicit, decision-relevant quantities:

$$\mathbb{P}(\text{Ala present}) = p_1 + p_3 = 0.7, \qquad \mathbb{P}(\text{Gly present}) = p_1 + p_2 = 0.8,$$

$$\mathbb{P}(\text{Ser present}) = p_2 + p_3 = 0.5, \qquad \mathbb{E}[|S|] = \sum_{i=1}^{3} p_i\,|S_i| = 2.0.$$

Conservation and variability are summarized by

$$\text{consensus core } = \bigcap X = \emptyset, \qquad \text{coverage } = \bigcup X = H, \qquad s(X) := \frac{|\cap X|}{|\cup X|} = \frac{0}{3} = 0,$$

while focusing on the "Gly-including" subensemble $X' = \{S_1, S_2\}$ yields $\cap X' = \{\mathrm{Gly}\}$, $\cup X' = \{\mathrm{Ala}, \mathrm{Gly}, \mathrm{Ser}\}$, and $s(X') = 1/3$. Thus $\mathrm{POWS}^2(H)$ encodes concrete microstate ensembles supporting probabilistic pocket design (e.g., prioritizing Gly-compatible ligands).

(b) *Peptide-motif library specification.* A position-tolerant motif can be declared as a *set of allowed residue sets.* For example, the repertoire

$$\mathcal{R} = \big\{\{\mathrm{Ala}\},\ \{\mathrm{Gly}\},\ \{\mathrm{Ala}, \mathrm{Gly}\}\big\} \in \mathrm{POWS}^2(H)$$

precisely states which single-residue choices (and their allowable variability) the library will synthesize at that position. Quantities such as the minimum/maximum diversity and a consensus choice are computed directly:

$$\cap\mathcal{R} = \emptyset, \qquad \cup\mathcal{R} = \{\mathrm{Ala}, \mathrm{Gly}\}, \qquad \text{effective alphabet size } = |\cup\mathcal{R}| = 2.$$

Definition 1.5 (HyperGraph)**.** [17] A finite *HyperGraph* $H = (V, E)$ is specified by:

- A nonempty vertex set V.
- A collection E of hyperedges, where each $e \in E$ is a nonempty subset of V.

HyperGraphs generalize ordinary graphs by permitting edges to join any number of vertices, making them ideal for modeling higher-order relationships. In this work, we assume both V and E are finite.

Example 1.6 (Biochemical HyperGraph: a small metabolic fragment)**.** (cf. [18]) Let the vertex set list metabolites

$$V = \{\mathrm{Glc}, \mathrm{ATP}, \mathrm{G6P}, \mathrm{ADP}, \mathrm{F6P}, \mathrm{Pi}\}.$$

Define three hyperedges representing (undirected) participation sets of reactions:

$$e_1 = \{\text{Glc}, \text{ATP}, \text{G6P}, \text{ADP}\} \qquad \text{(hexokinase step)},$$
$$e_2 = \{\text{G6P}, \text{F6P}\} \qquad \text{(phosphoglucose isomerase)},$$
$$e_3 = \{\text{ATP}, \text{ADP}, \text{Pi}\} \qquad \text{(ATP hydrolysis / phosphate transfer pool)}.$$

Then $\mathcal{H} = (V, E)$ with $E = \{e_1, e_2, e_3\}$ is a molecular hypergraph capturing multi-metabolite participation. With row order $(\text{Glc}, \text{ATP}, \text{G6P}, \text{ADP}, \text{F6P}, \text{Pi})$ and column order (e_1, e_2, e_3), the incidence matrix is

$$\mathbf{H} = \begin{bmatrix} 1 & 0 & 0 \\ 1 & 0 & 1 \\ 1 & 1 & 0 \\ 1 & 0 & 1 \\ 0 & 1 & 0 \\ 0 & 0 & 1 \end{bmatrix},$$

where $H_{v,e} = 1$ iff metabolite v participates in reaction-hyperedge e. This representation natively accommodates multi-substrate/multi-product chemistry.

Definition 1.7 (Level-n SuperHyperGraph (incidence form))**.** (cf. [19]) Fix a finite base set V_0 and an integer $n \geq 0$. Let $V_n \subseteq \text{POWS}^n(V_0)$ be a finite set, whose elements are called *n-supervertices*. A *level-n SuperHyperGraph* is a pair

$$\mathcal{H}^{(n)} = \big(V_n, \mathcal{E}\big), \quad \text{with} \quad \emptyset \neq \mathcal{E} \subseteq \text{POWS}(V_n) \setminus \{\emptyset\}.$$

Thus each *n-superedge* $E \in \mathcal{E}$ is a nonempty subset of the vertex set V_n. (When $n = 0$, this is an ordinary finite hypergraph; when, additionally, every $E \in \mathcal{E}$ has size 2, it is an ordinary graph.)

Notation 1 (Stars)**.** *For $\mathcal{H}^{(n)} = (V_n, \mathcal{E})$ and $v \in V_n$, the* star *of v is*

$$\mathsf{Star}_{\mathcal{H}}(v) := \{\, E \in \mathcal{E} \,:\, v \in E \,\} \subseteq \mathcal{E}.$$

We also write $\mathcal{E}^{\neq\emptyset}(v) := \mathsf{Star}_{\mathcal{H}}(v)$ and $\mathcal{E}^{(\geq 2)}(v) := \{\, E \in \mathcal{E} : v \in E \text{ and } |E| \geq 2 \,\}$ when we wish to exclude size-1 edges in the star.

Example 1.8 (Level-1 Molecular SuperHyperGraph: signaling modules along EGFR–MAPK)**.** (cf. [20]) Let the base set V_0 collect reaction/bond identifiers

$$V_0 = \big\{\, r_{\text{EGF:EGFR}},\ r_{\text{EGFR}\to\text{RAS}},\ r_{\text{RAF}\to\text{MEK}},\ r_{\text{MEK}\to\text{ERK}} \,\big\}.$$

Form three 1-supervertices (subsets of V_0) corresponding to functional modules:

$$M_{\text{EGFR}} = \{\, r_{\text{EGF:EGFR}},\ r_{\text{EGFR}\to\text{RAS}} \,\},$$
$$M_{\text{Bridge}} = \{\, r_{\text{EGFR}\to\text{RAS}},\ r_{\text{RAF}\to\text{MEK}} \,\},$$
$$M_{\text{MAPK}} = \{\, r_{\text{RAF}\to\text{MEK}},\ r_{\text{MEK}\to\text{ERK}} \,\}.$$

Set $V_1 = \{M_{\text{EGFR}}, M_{\text{Bridge}}, M_{\text{MAPK}}\} \subseteq \text{POWS}^1(V_0)$. Define 1-superedges (nonempty subsets of V_1) to encode immediate module couplings:

$$E_A = \{M_{\text{EGFR}}, M_{\text{Bridge}}\}, \qquad E_B = \{M_{\text{Bridge}}, M_{\text{MAPK}}\}.$$

Then the level-1 SuperHyperGraph is

$$\mathcal{H}^{(1)} = \big(V_1,\ \mathcal{E}\big), \qquad \mathcal{E} = \{E_A, E_B\} \subseteq \text{POWS}(V_1) \setminus \{\emptyset\}.$$

Concrete "lift" from reactions to modules. Order the reactions as $(r_{\text{EGF:EGFR}},\ r_{\text{EGFR}\to\text{RAS}},\ r_{\text{RAF}\to\text{MEK}},\ r_{\text{MEK}\to\text{ERK}})$ and the modules as $(M_{\text{EGFR}},\ M_{\text{Bridge}},\ M_{\text{MAPK}})$. The *module-membership incidence matrix* $B \in \{0,1\}^{4\times 3}$, with $B_{r,M} = 1 \iff r \in M$, is

$$B = \begin{array}{c} \begin{matrix} M_{\text{EGFR}} & M_{\text{Bridge}} & M_{\text{MAPK}} \end{matrix} \\ \begin{bmatrix} 1 & 0 & 0 \\ 1 & 1 & 0 \\ 0 & 1 & 1 \\ 0 & 0 & 1 \end{bmatrix} \end{array} \qquad \text{(rows in the reaction order above).}$$

From B we obtain the *module-overlap matrix*

$$O \;:=\; B^{\top} B \;=\; \begin{bmatrix} 2 & 1 & 0 \\ 1 & 2 & 1 \\ 0 & 1 & 2 \end{bmatrix}, \qquad O_{ij} = |\, M_i \cap M_j \,|.$$

The "lift" is now explicit: we place a 1-superedge between modules M_i and M_j *iff* they share at least one reaction, i.e. $O_{ij} \geq 1$ for $i \neq j$. Thus the superedge set $\mathcal{E} = \{E_A, E_B\}$ is precisely the set of pairs with $O_{ij} \geq 1$:

$$E_A = \{M_{\text{EGFR}}, M_{\text{Bridge}}\} \ \ (\text{since } O_{12} = 1), \qquad E_B = \{M_{\text{Bridge}}, M_{\text{MAPK}}\} \ \ (\text{since } O_{23} = 1),$$

and there is no superedge between M_{EGFR} and M_{MAPK} because $O_{13} = 0$.
Equivalently, the *module-coupling adjacency* is the thresholded matrix

$$A_{\text{mod}} \;=\; \mathbf{1}\{\, O_{ij} \geq 1,\ i \neq j \,\} \;=\; \begin{bmatrix} 0 & 1 & 0 \\ 1 & 0 & 1 \\ 0 & 1 & 0 \end{bmatrix},$$

which encodes exactly the two superedges above. The 1-superedge incidence (rows M, columns E_A, E_B) is

$$S = \begin{bmatrix} 1 & 0 \\ 1 & 1 \\ 0 & 1 \end{bmatrix}, \qquad \deg_{\mathcal{H}^{(1)}}(M_{\text{EGFR}}) = 1, \quad \deg_{\mathcal{H}^{(1)}}(M_{\text{Bridge}}) = 2, \quad \deg_{\mathcal{H}^{(1)}}(M_{\text{MAPK}}) = 1.$$

Hence, (i) embed modules as subsets $V_1 \subseteq \text{POWS}(V_0)$; (ii) compute overlaps $O = B^\top B$ to obtain a *deterministic* coupling rule $(M_i, M_j) \in \mathcal{E} \iff O_{ij} \geq 1$; and (iii) represent the resulting module–module couplings by A_{mod} or S. This makes the passage from reaction-level incidence to module-level connectivity explicit, algorithmic, and checkable, and it extends verbatim to deeper levels $n > 1$ by replacing B with the corresponding level-n membership matrix.

Figure 1 illustrates the graph for this concrete example.

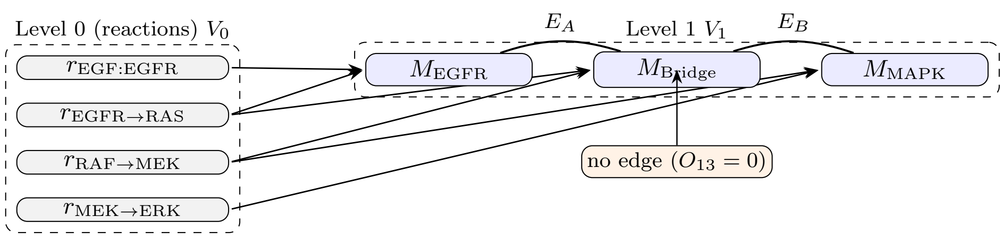

FIGURE 1. Level-1 Molecular SuperHyperGraph (EGFR–MAPK): reactions (level 0) lift to modules (level 1), and module couplings form 1-superedges E_A, E_B.

Example 1.9 (Biochemical 2-SuperHyperGraph: EGFR–MAPK signaling programs)**.** (cf. [21]) We build a concrete level-2 SuperHyperGraph that organizes biochemical reactions → modules → programs.

Level 0 (base set of reactions). Let the base set V_0 collect reaction/interaction identifiers

$$V_0 = \{r_{\text{EGF:EGFR}},\ r_{\text{EGFR}\to\text{RAS}},\ r_{\text{RAF}\to\text{MEK}},\ r_{\text{MEK}\to\text{ERK}}\}.$$

Level 1 (modules as subsets of V_0). Define three 1-supervertices (functional modules)

$$M_{\text{EGFR}} := \{\, r_{\text{EGF:EGFR}},\ r_{\text{EGFR}\to\text{RAS}} \,\},$$
$$M_{\text{Bridge}} := \{\, r_{\text{EGFR}\to\text{RAS}},\ r_{\text{RAF}\to\text{MEK}} \,\},$$
$$M_{\text{MAPK}} := \{\, r_{\text{RAF}\to\text{MEK}},\ r_{\text{MEK}\to\text{ERK}} \,\},$$

and set $V_1 := \{M_{\text{EGFR}}, M_{\text{Bridge}}, M_{\text{MAPK}}\} \subseteq \text{POWS}^1(V_0)$.

Level 2 (programs as subsets of modules). Form 2-supervertices (programs) by grouping modules:

$$P_1 := \{ M_{\mathrm{EGFR}}, M_{\mathrm{Bridge}} \}, \qquad P_2 := \{ M_{\mathrm{Bridge}}, M_{\mathrm{MAPK}} \}, \qquad P_3 := \{ M_{\mathrm{EGFR}}, M_{\mathrm{Bridge}}, M_{\mathrm{MAPK}} \}.$$

Each P_i is a subset of V_1, hence an element of $\mathrm{POWS}(V_1) = \mathrm{POWS}^2(V_0)$. Set the level-2 vertex set

$$V_2 := \{P_1, P_2, P_3\} \subseteq \mathrm{POWS}^2(V_0).$$

Level 2 superedges (coupled programs). Define nonempty 2-superedges as subsets of V_2 that capture jointly active programs:

$$F_1 := \{P_1, P_2\}, \qquad F_2 := \{P_2, P_3\}.$$

Let $\mathcal{E}_2 := \{F_1, F_2\} \subseteq \mathrm{POWS}(V_2) \setminus \{\emptyset\}$.
Resulting 2-SuperHyperGraph. The biochemical level-2 SuperHyperGraph is

$$\mathcal{H}^{(2)} := \big(V_2,\ \mathcal{E}_2\big),$$

where:

- V_2 consists of 2-supervertices P_i, each a *set of modules* (i.e., a set of sets of reactions).
- $\mathcal{E}_2$ consists of 2-superedges F_j, each a nonempty set of such programs indicating co-activation/coupling.

By construction $V_2 \subseteq \mathrm{POWS}^2(V_0)$ (each $P_i \subseteq V_1 \subseteq \mathrm{POWS}^1(V_0)$), and $\mathcal{E}_2 \subseteq \mathrm{POWS}(V_2) \setminus \{\emptyset\}$. Hence $\mathcal{H}^{(2)}$ satisfies the definition of a finite level-2 SuperHyperGraph.

1.2. *Line Graph*

A line graph represents edges of a graph as vertices, linking them if the original edges share a common endpoint (cf. [22–24]).

Definition 1.10 (Line graph)**.** (cf. [22–24]) Let $G = (V(G), E(G))$ be a (loopless) undirected simple graph. The *line graph* $L(G)$ is the (simple) graph defined by

$$V\big(L(G)\big) = E(G), \qquad \{e, f\} \in E\big(L(G)\big) \iff e \cap f \neq \emptyset,$$

i.e., two vertices of $L(G)$ are adjacent exactly when the corresponding two edges of G share an endpoint.

Example 1.11 (Line Graph in chemical physics: linear triatomic O=C=O)**.** Model the molecule by the simple graph $G = (V, E)$ with

$$V = \{\mathrm{O_L}, \mathrm{C}, \mathrm{O_R}\}, \qquad E = \{e_{\mathrm{C\text{–}O_L}} = \{\mathrm{C}, \mathrm{O_L}\},\ e_{\mathrm{C\text{–}O_R}} = \{\mathrm{C}, \mathrm{O_R}\}\}.$$

The line graph $L(G)$ has vertex set $V' := E = \{e_{\mathrm{C–O_L}}, e_{\mathrm{C–O_R}}\}$. Since the two bonds share the common atom C, they are adjacent in $L(G)$:

$$E' = \{\ \{e_{\mathrm{C–O_L}},\ e_{\mathrm{C–O_R}}\}\ \}.$$

Thus $L(G) \cong K_2$. Physically, $L(G)$ encodes bond–bond adjacency (useful for building bond-coupling models in vibrational or electronic Hamiltonians).

A line hypergraph transforms each hyperedge into a vertex and encodes how these vertices (interaction terms) meet at original vertices; it is thus a higher-order analogue of the line graph (cf. [25–29]).

Definition 1.12 (Clique of rank r)**.** Let X be a finite set and let r be an integer with $0 \le r \le |X|$. The *clique of rank* r on X is the (simple) r-uniform hypergraph

$$\mathsf{K}^{(r)}(X) := \big(X, \binom{X}{r}\big).$$

In particular, rank 2 yields the complete graph on X; rank 1 yields the hypergraph with singleton hyperedges; rank 0 yields the hypergraph with empty hyperedge family (all vertices isolated).

Definition 1.13 (Line hypergraph (multi-valued))**.** (cf. [25–28]) Let $H = (V, \mathcal{E})$ be a hypergraph without isolated vertices, and list $V = \{v_1, \ldots, v_n\}$. For each $v \in V$, write

$$\mathcal{E}_H(v) := \{\, e \in \mathcal{E} :\ v \in e \,\} \qquad \text{and} \qquad \deg_H(v) := |\mathcal{E}_H(v)|.$$

Define two integer vectors

$$\mathbf{1}_H = (\deg_H(v_1), \ldots, \deg_H(v_n)), \qquad \mathbf{0}_H = (\, 0_{v_i}\,)_{i=1}^{n} \ \text{ with } \ 0_{v_i} = \begin{cases} 0, & \deg_H(v_i) = 1, \\ 2, & \deg_H(v_i) \ge 2. \end{cases}$$

Let $\mathcal{D}_H := \{D = (d_{v_i})_{i=1}^{n} :\ \mathbf{0}_H \le D \le \mathbf{1}_H \text{ componentwise}\}$. For any $D \in \mathcal{D}_H$, define the (single-valued) line hypergraph

$$L_D(H) := \Big(\ \mathcal{E},\ \bigcup_{v \in V} \binom{\mathcal{E}_H(v)}{d_v}\ \Big),$$

i.e., the vertex set is $\mathcal{E}$ (original hyperedges), and for each $v \in V$ we add the rank-d_v clique on $\mathcal{E}_H(v)$. The (multi-valued) *line hypergraph* of H is the set

$$L(H) := \{\, L_D(H) : D \in \mathcal{D}_H \,\}.$$

Remark 1.14 (Two standard specializations)**.** Within the family $L(H)$, two choices are particularly common:

(i) (Pairwise adjacency / line graph analogue) Choosing $d_v = 2$ for all v with $\deg_H(v) \geq 2$ produces a 2-uniform line hypergraph (a simple graph) that connects two hyperedges whenever they share at least one original vertex.

(ii) (Star hyperedges) Choosing $d_v = \deg_H(v)$ produces one hyperedge $\mathcal{E}_H(v)$ per v, i.e., the "star" of v. This yields a natural higher-order grouping of interaction terms.

Example 1.15 (Line hypergraph in chemical physics: four-atom cluster with two three-body terms)**.** Let the atom set be $V = \{A, B, C, D\}$. Include three pair interactions and two three-body (angular) interactions:

$$\mathcal{E} = \big\{e_{AB} = \{A, B\},\ e_{BC} = \{B, C\},\ e_{CD} = \{C, D\},\ e_{ABC} = \{A, B, C\},\ e_{BCD} = \{B, C, D\}\big\}.$$

Set $\mathcal{H} := (V, \mathcal{E})$. For each atom $v \in V$, the incident-hyperedge set (star) is

$$\mathcal{E}_{\mathcal{H}}(v) := \{\, e \in \mathcal{E} :\ v \in e \,\}.$$

Concretely,

$$\begin{aligned}
\mathcal{E}_{\mathcal{H}}(A) &= \{e_{AB}, e_{ABC}\},\\
\mathcal{E}_{\mathcal{H}}(B) &= \{e_{AB}, e_{BC}, e_{ABC}, e_{BCD}\},\\
\mathcal{E}_{\mathcal{H}}(C) &= \{e_{BC}, e_{CD}, e_{ABC}, e_{BCD}\},\\
\mathcal{E}_{\mathcal{H}}(D) &= \{e_{CD}, e_{BCD}\}.
\end{aligned}$$

Now choose the maximal parameter vector $D^{\max} \in \mathcal{D}_{\mathcal{H}}$ defined by $d_v := \deg_{\mathcal{H}}(v) = |\mathcal{E}_{\mathcal{H}}(v)|$ for all $v \in V$. Then $\binom{\mathcal{E}_{\mathcal{H}}(v)}{d_v} = \{\mathcal{E}_{\mathcal{H}}(v)\}$, hence

$$L_{D^{\max}}(\mathcal{H}) = \Big(\ \mathcal{E},\ \{\mathcal{E}_{\mathcal{H}}(A), \mathcal{E}_{\mathcal{H}}(B), \mathcal{E}_{\mathcal{H}}(C), \mathcal{E}_{\mathcal{H}}(D)\}\ \Big).$$

Interpretation: each vertex represents an interaction term (pair or three-body), and each hyperedge groups all interaction terms that meet at a common atom—an organization useful for many-body potential assembly in chemical-physics simulations.

A line superhypergraph maps each superedge to a vertex, linking them through superedges containing a common supervertex in the original structure [30].

Definition 1.16 (Line SuperHyperGraph)**.** [30] Let $\mathcal{H}^{(n)} = (V_n, \mathcal{E})$ be a level-n SuperHyperGraph. Its *line SuperHyperGraph* is the pair

$$\mathsf{L}^{(n)}(\mathcal{H}) \ =\ \big(V'_{n+1},\ \mathcal{E}'_{n+1}\big)$$

defined by

$$V'_{n+1} \ :=\ \mathcal{E} \qquad \text{and} \qquad \mathcal{E}'_{n+1} \ :=\ \big\{\, \mathsf{Star}_{\mathcal{H}}(v) \subseteq \mathcal{E}\ :\ v \in V_n,\ \mathsf{Star}_{\mathcal{H}}(v) \neq \emptyset \,\big\}.$$

Intuitively, $\mathsf{L}^{(n)}(\mathcal{H})$ has one vertex for each superedge of $\mathcal{H}$; for every supervertex $v \in V_n$, we add a (hyper)edge collecting *all* superedges that contain v.

Example 1.17 (Line SuperHyperGraph in chemical physics: conjugated fragment couplings)**.** Let $V_0 = \{b_{12}, b_{23}, b_{34}\}$ denote bond identifiers along a short conjugated chain $C_1{-}C_2{-}C_3{-}C_4$. Form a level-1 molecular SuperHyperGraph $\mathcal{H}^{(1)} = (V_1, \mathcal{E})$ by grouping bonds into chemically meaningful fragments (supervertices):

$$T_{\text{left}} = \{b_{12}, b_{23}\}, \quad T_{\text{right}} = \{b_{23}, b_{34}\}, \quad T_{\text{cap}} = \{b_{12}\}.$$

Set

$$V_1 = \{T_{\text{left}}, T_{\text{right}}, T_{\text{cap}}\}, \qquad \mathcal{E} = \left\{ E_1 = \{T_{\text{left}}, T_{\text{right}}\},\ \ E_2 = \{T_{\text{left}}, T_{\text{cap}}\} \right\},$$

where E_1 encodes π-conjugation across the central region and E_2 encodes local coupling at the chain end. The *line SuperHyperGraph* $\mathbf{L}(\mathcal{H}^{(1)}) = (V_2', \mathcal{E}_2')$ has

$$V_2' := \mathcal{E} = \{E_1, E_2\},$$

and, for each $T \in V_1$, the hyperedge $\mathsf{Star}_{\mathcal{H}^{(1)}}(T) = \{E \in \mathcal{E} : T \in E\}$. Explicitly,

$$\mathsf{Star}(T_{\text{left}}) = \{E_1, E_2\}, \qquad \mathsf{Star}(T_{\text{right}}) = \{E_1\}, \qquad \mathsf{Star}(T_{\text{cap}}) = \{E_2\}.$$

Therefore

$$\mathcal{E}_2' = \left\{ \ \{E_1, E_2\},\ \{E_1\},\ \{E_2\} \ \right\}.$$

Here, vertices of $\mathbf{L}(\mathcal{H}^{(1)})$ represent fragment–fragment coupling channels (E_1, E_2), while its hyperedges record which channels meet at the same fragment—an arrangement aligning with fragment-based Hamiltonian partitioning and energy-transfer analyses in chemical physics.

1.3. *Iterated line graphs*

An iterated line graph is formed by repeatedly applying the line graph transformation to a graph, using each result as the next input [31–36].

Definition 1.18 (Iterated line graphs)**.** (cf. [31–36]) Define $L^0(G) := G$. For each integer $n \geq 1$, the *n-th iterated line graph* of G is defined recursively by

$$L^n(G) \ := \ L\big(L^{n-1}(G)\big).$$

Equivalently, many authors write $L_1(G) = L(G)$ and $L_n(G) = L\big(L_{n-1}(G)\big)$ for $n \geq 2$.

Example 1.19 (Iterated Line Graph: a peptide backbone fragment)**.** Consider a linear four–residue peptide fragment with C_α atoms

$$V = \{R_1, R_2, R_3, R_4\}, \qquad E = \{e_{12} = \{R_1, R_2\},\ e_{23} = \{R_2, R_3\},\ e_{34} = \{R_3, R_4\}\}.$$

This graph models covalent backbone connectivity (edges = peptide bonds). The line graph $L(G)$ has

$$V' = E = \{e_{12}, e_{23}, e_{34}\}, \qquad E' = \big\{\{e_{12}, e_{23}\},\ \{e_{23}, e_{34}\}\big\},$$

so $L(G) \cong P_3$ (a path on three vertices), encoding *bond–bond adjacency*. Iterating once more,

$$L^2(G) = L(P_3) = P_2,$$

and then $L^3(G) = L(P_2) = P_1$ (a single vertex). In general for a chain P_n (e.g., an unbranched peptide segment),

$$L(P_n) = P_{n-1} \quad (n \geq 2), \qquad L^k(P_n) = P_{n-k} \text{ while defined.}$$

This illustrates how repeated line transforms propagate from atom–atom bonds to adjacency between bonds, then to adjacency between those adjacencies, and so on.

An iterated line hypergraph applies the line hypergraph construction repeatedly to a hypergraph, capturing higher-order adjacency of hyperedges over iterations [30].

Definition 1.20 (Iterated line hypergraphs)**.** [30] Define $L^0(H) := H$ and, for each $n \geq 1$, set

$$L^n(H) \;:=\; L\big(L^{n-1}(H)\big).$$

Example 1.21 (Iterated line hypergraph: a phosphate–transfer micro-network)**.** (cf. [37]) Let metabolites be

$$V = \{\text{ATP}, \ \text{ADP}, \ \text{Pi}\},$$

and define a hypergraph $\mathcal{H} = (V, \mathcal{E})$ whose hyperedges encode participation sets of elementary processes:

$$e_0 = \{\text{ATP}, \text{ADP}, \text{Pi}\} \text{ (triad pool)}, \quad e_1 = \{\text{ATP}, \text{ADP}\},$$

$$e_2 = \{\text{ATP}, \text{Pi}\}, \quad e_3 = \{\text{ADP}, \text{Pi}\},$$

$$\mathcal{E} = \{e_0, e_1, e_2, e_3\}.$$

First iteration (star specialization). We take the *star* specialization of the multi-valued line hypergraph (cf. Remark 1.14(ii)), namely $\mathsf{L}_H(\mathcal{H}) := L_{D^{\max}}(\mathcal{H})$, where $D^{\max}$ is given by $d_x = \deg_{\mathcal{H}}(x)$. Thus $\mathsf{L}_H(\mathcal{H}) = (\mathcal{E}, \mathcal{F})$ has vertex set $\mathcal{E}$ and hyperedge family $\mathcal{F} = \{\mathcal{E}_{\mathcal{H}}(x) : x \in V\}$, where

$$\mathcal{E}_{\mathcal{H}}(x) := \{\, e \in \mathcal{E} : x \in e \,\}.$$

Explicitly,

$$\mathcal{E}_{\mathcal{H}}(\text{ATP}) = \{e_0, e_1, e_2\},$$

$$\mathcal{E}_{\mathcal{H}}(\text{ADP}) = \{e_0, e_1, e_3\},$$

$$\mathcal{E}_{\mathcal{H}}(\text{Pi}) = \{e_0, e_2, e_3\}.$$

Hence

$$\mathcal{F} = \big\{\{e_0, e_1, e_2\}, \ \{e_0, e_1, e_3\}, \ \{e_0, e_2, e_3\}\big\}.$$

Second iteration. Define the second iterated line hypergraph (still under the same star specialization) by

$$\mathsf{L}_H^{(2)}(\mathcal{H}) := \mathsf{L}_H\big(\mathsf{L}_H(\mathcal{H})\big) = \mathsf{L}_H(\mathcal{E}, \mathcal{F}).$$

Its vertex set is $\mathcal{F}$. For each old vertex $e \in \mathcal{E}$, form the star in $\mathsf{L}_H(\mathcal{H})$:

$$\mathcal{F}_{\mathsf{L}_H(\mathcal{H})}(e) := \{\, F \in \mathcal{F} : e \in F \,\}.$$

Concretely, writing

$$F_{\mathrm{ATP}} := \{e_0, e_1, e_2\}, \quad F_{\mathrm{ADP}} := \{e_0, e_1, e_3\}, \quad F_{\mathrm{Pi}} := \{e_0, e_2, e_3\},$$

we obtain

$$\mathcal{F}_{\mathsf{L}_H(\mathcal{H})}(e_0) = \{F_{\mathrm{ATP}}, F_{\mathrm{ADP}}, F_{\mathrm{Pi}}\},$$
$$\mathcal{F}_{\mathsf{L}_H(\mathcal{H})}(e_1) = \{F_{\mathrm{ATP}}, F_{\mathrm{ADP}}\},$$
$$\mathcal{F}_{\mathsf{L}_H(\mathcal{H})}(e_2) = \{F_{\mathrm{ATP}}, F_{\mathrm{Pi}}\},$$
$$\mathcal{F}_{\mathsf{L}_H(\mathcal{H})}(e_3) = \{F_{\mathrm{ADP}}, F_{\mathrm{Pi}}\}.$$

Thus $\mathsf{L}_H^{(2)}(\mathcal{H})$ has three vertices $F_{\mathrm{ATP}}, F_{\mathrm{ADP}}, F_{\mathrm{Pi}}$ and four hyperedges given by the above stars.

Interpretation. This construction moves from *metabolite–process incidence* (the original $\mathcal{H}$) to *process–process co-participation* (the first line hypergraph $\mathsf{L}_H(\mathcal{H})$), and then to *co-participation-of-co-participations* (the second iterate $\mathsf{L}_H^{(2)}(\mathcal{H})$).

An iterated line superhypergraph repeatedly applies the line superhypergraph transformation to a superhypergraph, modeling evolving hierarchical incidence patterns across multiple levels.

Definition 1.22 (Iterated line superhypergraphs)**.** [30] For an initial level-n superhypergraph $\mathcal{H}^{(n)}$, define

$$\mathbf{L}^{0}(\mathcal{H}^{(n)}) := \mathcal{H}^{(n)}, \qquad \mathbf{L}^{t+1}(\mathcal{H}^{(n)}) := \mathbf{L}\big(\mathbf{L}^{t}(\mathcal{H}^{(n)})\big) \quad (t \geq 0).$$

$\mathbf{L}^{t}(\mathcal{H}^{(n)})$ is level $n+t$.

Example 1.23 (Iterated Line SuperHyperGraph: pathway modules $\to$ coupling channels $\to$ couplings of channels)**.** Let the base set V_0 list reaction identifiers along a short signaling/glycolytic segment:

$$V_0 = \{r_1,\ r_2,\ r_3,\ r_4\}.$$

Form three level-1 supervertices (modules) as subsets of V_0:

$$M_1 = \{r_1, r_2\}, \qquad M_2 = \{r_2, r_3\}, \qquad M_3 = \{r_3, r_4\},$$

and set $V_1 = \{M_1, M_2, M_3\}$. Define level-1 superedges (module couplings)

$$E_1 = \{M_1, M_2\}, \qquad E_2 = \{M_2, M_3\},$$

so $\mathcal{H}^{(1)} = (V_1, \mathcal{E}^{(1)})$ with $\mathcal{E}^{(1)} = \{E_1, E_2\}$. Apply the line SuperHyperGraph operator to obtain

$$\mathbf{L}\big(\mathcal{H}^{(1)}\big) = (V_2', \mathcal{E}_2'), \qquad V_2' = \mathcal{E}^{(1)} = \{E_1, E_2\},$$

and (nonempty) stars in $\mathcal{H}^{(1)}$:

$$\mathrm{Star}_{\mathcal{H}^{(1)}}(M_1) = \{E_1\}, \quad \mathrm{Star}_{\mathcal{H}^{(1)}}(M_2) = \{E_1, E_2\}, \quad \mathrm{Star}_{\mathcal{H}^{(1)}}(M_3) = \{E_2\}.$$

Thus

$$\mathcal{E}_2' = \{ \ \{E_1\}, \ \{E_1, E_2\}, \ \{E_2\} \ \}.$$

Iterate once more to get the *Iterated Line SuperHyperGraph*

$$\mathbf{L}^2\big(\mathcal{H}^{(1)}\big) = \mathbf{L}\Big(\mathbf{L}\big(\mathcal{H}^{(1)}\big)\Big) = (V_3', \mathcal{E}_3'),$$

with

$$V_3' = \mathcal{E}_2' = \{ \ \{E_1\}, \ \{E_1, E_2\}, \ \{E_2\} \ \},$$

and stars in $\mathbf{L}(\mathcal{H}^{(1)})$:

$$\mathrm{Star}_{\mathbf{L}(\mathcal{H}^{(1)})}(E_1) = \{ \ \{E_1\}, \ \{E_1, E_2\} \ \},$$
$$\mathrm{Star}_{\mathbf{L}(\mathcal{H}^{(1)})}(E_2) = \{ \ \{E_1, E_2\}, \ \{E_2\} \ \}.$$

Hence

$$\mathcal{E}_3' = \{ \ \{\{E_1\}, \{E_1, E_2\}\}, \ \{\{E_1, E_2\}, \{E_2\}\} \ \}.$$

Chemically, level 1 groups reactions into modules, level 2 turns module couplings into "channel vertices" and records which channels meet at a module, and level 3 records how those channels themselves co-occur via shared channel–vertices.

1.4. *Molecular Line Graph and Iterated Line Graph*

Molecular Graph models a molecule with atoms as vertices and bonds as edges, representing its structural connectivity [38–43]. Related concepts to the molecular graph include the chemical graph [44–48]. Molecular graphs have been extensively studied in a wide variety of research works [49–52].

Molecular Line Graph represents each bond of a molecular graph as a vertex, connecting them if the bonds share an atom (cf. [53, 54]). Molecular Iterated Line Graph repeatedly applies the line-graph transformation to reveal successive higher-order bond adjacency relationships [55–57].

Definition 1.24 (Molecular Graph)**.** [38, 39] A *molecular graph* is a finite, simple, undirected graph $G = (V, E)$ in which each vertex $v \in V$ represents an atom and each edge $e = \{u, v\} \in E$ represents a chemical bond between atoms u and v. (Optionally, vertex/edge labels may encode atom types and bond types or orders.)

Example 1.25 (Methane CH_4)**.** (cf. [58]) Consider methane, which consists of one carbon atom bonded to four hydrogen atoms. The molecular graph is

$$G = (V, E), \qquad V = \{C, H_1, H_2, H_3, H_4\}, \quad E = \{\{C, H_1\}, \{C, H_2\}, \{C, H_3\}, \{C, H_4\}\}.$$

Here the single carbon vertex C is connected to each hydrogen vertex, forming a star graph $K_{1,4}$. This representation captures the tetrahedral bonding pattern of methane in a simplified graph-theoretic form.

Definition 1.26 (Molecular Line Graph)**.** (cf. [53,54]). Let $G = (V, E)$ be a molecular graph. The *molecular line graph* $L(G) = (V', E')$ is the (simple, undirected) line graph of G defined by:

- $V' := E$ (each vertex of $L(G)$ corresponds to a bond of G);
- for distinct $e, e' \in V' = E$, $\{e, e'\} \in E'$ iff the two bonds e and e' share a common atom in G (i.e., are incident in G).

Equivalently, two vertices of $L(G)$ are adjacent precisely when their corresponding edges of G are incident.

Example 1.27 (Linear chain on four atoms: $G = P_4$)**.** (cf. [59]) Let $V = \{1, 2, 3, 4\}$ and $E = \{e_{12}, e_{23}, e_{34}\}$ with $e_{ij} := \{i, j\}$. Then the molecular line graph $L(G) = (V', E')$ has

$$V' := E = \{e_{12}, e_{23}, e_{34}\}, \qquad E' := \big\{\{e_{12}, e_{23}\},\ \{e_{23}, e_{34}\}\big\},$$

so $L(G)$ is the path P_3. With vertex order (e_{12}, e_{23}, e_{34}), its adjacency matrix is

$$A\big(L(G)\big) = \begin{bmatrix} 0 & 1 & 0 \\ 1 & 0 & 1 \\ 0 & 1 & 0 \end{bmatrix}.$$

Iterating once,

$$L^2(G) = L\big(P_3\big) = P_2 \quad \text{with} \quad V'' = \big\{\{e_{12}, e_{23}\}, \{e_{23}, e_{34}\}\big\},\ E'' = \big\{\{\{e_{12}, e_{23}\}, \{e_{23}, e_{34}\}\}\big\}.$$

Iterating again, $L^3(G) = L(P_2) = P_1$ (a single vertex). In general, $L(P_n) = P_{n-1}$ for $n \geq 2$, so $L^k(P_n) = P_{n-k}$ while defined.

Definition 1.28 (Molecular Iterated Line Graph)**.** For a molecular graph G, define the sequence $\{L^k(G)\}_{k\geq 0}$ recursively by

$$L^0(G) := G, \qquad L^{k+1}(G) := L\big(L^k(G)\big) \ \text{ for } k \geq 0.$$

The graph $L^k(G)$ is called the *k-th molecular iterated line graph* of G.

Example 1.29 (Linear alkane backbone: $G = P_5$ (e.g., a pentane fragment))**.** (cf. [60]) Model a five-carbon chain by the simple molecular graph

$$V = \{C_1, C_2, C_3, C_4, C_5\}, \qquad E = \{e_{12} = \{C_1, C_2\},\ e_{23} = \{C_2, C_3\},\ e_{34} = \{C_3, C_4\},\ e_{45} = \{C_4, C_5\}\}.$$

Thus G is the path P_5. By definition of the line graph, the first iterate has

$$V\big(L(G)\big) = E = \{e_{12}, e_{23}, e_{34}, e_{45}\}, \quad E\big(L(G)\big) = \big\{\{e_{12}, e_{23}\},\ \{e_{23}, e_{34}\},\ \{e_{34}, e_{45}\}\big\},$$

so $L(G) \cong P_4$. With vertex order $(e_{12}, e_{23}, e_{34}, e_{45})$, the adjacency matrix is

$$A\big(L(G)\big) = \begin{bmatrix} 0 & 1 & 0 & 0 \\ 1 & 0 & 1 & 0 \\ 0 & 1 & 0 & 1 \\ 0 & 0 & 1 & 0 \end{bmatrix}.$$

Iterating again,

$$L^2(G) = L\big(P_4\big) = P_3, \qquad A\big(L^2(G)\big) = \begin{bmatrix} 0 & 1 & 0 \\ 1 & 0 & 1 \\ 0 & 1 & 0 \end{bmatrix}.$$

Continuing,

$$L^3(G) = L(P_3) = P_2, \qquad L^4(G) = L(P_2) = P_1 \ \text{(single vertex)}, \qquad L^5(G) = L(P_1) = P_0 \ \text{(empty)}.$$

In general, for a path P_n (an unbranched alkane backbone with n carbon atoms),

$$L(P_n) = P_{n-1} \ \ (n \geq 2), \qquad L^k(P_n) = P_{n-k} \ \text{ while } n - k \geq 1.$$

Size evolution. If $|V(G)| = n$ and $|E(G)| = n - 1$ (a path), then

$$|V(L^k(G))| = n - k - 1, \qquad |E(L^k(G))| = n - k - 2 \quad (k = 0, 1, \ldots, n - 2).$$

This explicitly tracks how bond–bond adjacencies (and higher) shrink along iterations.

Example 1.30 (Aromatic ring: $G = C_6$ (benzene))**.** (cf. [61]) Let G be the 6-cycle with vertices $V = \{C_1, \ldots, C_6\}$ and edges $E = \{\{C_1, C_2\}, \{C_2, C_3\}, \ldots, \{C_6, C_1\}\}$. Every edge in G meets exactly two others, and the edge–adjacency pattern is itself a 6-cycle. Hence

$$L(G) \cong C_6, \qquad L^k(G) \cong C_6 \ \text{ for all } k \geq 1.$$

Thus benzene is a fixed point of the line-graph operator, reflecting the uniform bond–bond adjacency around the ring.

Example 1.31 (Linear alkane backbone: n-pentane fragment $C_1{-}C_2{-}C_3{-}C_4{-}C_5$)**.** We model an unbranched five–carbon backbone (as appears in n-pentane) by the simple molecular graph

$$G = (V, E), \qquad V = \{C_1, C_2, C_3, C_4, C_5\}, \quad E = \{e_{12}, e_{23}, e_{34}, e_{45}\},$$

where $e_{ij} = \{C_i, C_j\}$ represents the covalent C–C bond.

Adjacency matrix of G. In the vertex order $(C_1, C_2, C_3, C_4, C_5)$, G is the path P_5 with

$$A(G) = \begin{bmatrix} 0 & 1 & 0 & 0 & 0 \\ 1 & 0 & 1 & 0 & 0 \\ 0 & 1 & 0 & 1 & 0 \\ 0 & 0 & 1 & 0 & 1 \\ 0 & 0 & 0 & 1 & 0 \end{bmatrix}.$$

First iterate $L(G)$: bond–bond adjacency. By definition of the line graph, the vertices of $L(G)$ are the bonds of G:

$$V\big(L(G)\big) = E = \{e_{12}, e_{23}, e_{34}, e_{45}\}.$$

Two vertices of $L(G)$ are adjacent iff the corresponding bonds share a carbon in G. Thus $L(G) \cong P_4$ with edges

$$\{\{e_{12}, e_{23}\},\ \{e_{23}, e_{34}\},\ \{e_{34}, e_{45}\}\}.$$

In the order $(e_{12}, e_{23}, e_{34}, e_{45})$,

$$A\big(L(G)\big) = \begin{bmatrix} 0 & 1 & 0 & 0 \\ 1 & 0 & 1 & 0 \\ 0 & 1 & 0 & 1 \\ 0 & 0 & 1 & 0 \end{bmatrix}.$$

Counts: $|V(L(G))| = 4$, $|E(L(G))| = 3$.

Second iterate $L^2(G) = L(L(G))$. Applying the line-graph operator to P_4 yields P_3. Its vertices correspond to the three edges of $L(G)$:

$$V\big(L^2(G)\big) = \big\{\{e_{12}, e_{23}\},\ \{e_{23}, e_{34}\},\ \{e_{34}, e_{45}\}\big\},$$

and the edges of $L^2(G)$ reflect shared adjacency:

$$E\big(L^2(G)\big) = \big\{\{\{e_{12}, e_{23}\}, \{e_{23}, e_{34}\}\},\ \{\{e_{23}, e_{34}\}, \{e_{34}, e_{45}\}\}\big\}.$$

In the order $(\{e_{12}, e_{23}\}, \{e_{23}, e_{34}\}, \{e_{34}, e_{45}\})$,

$$A\big(L^2(G)\big) = \begin{bmatrix} 0 & 1 & 0 \\ 1 & 0 & 1 \\ 0 & 1 & 0 \end{bmatrix}.$$

Counts: $|V(L^2(G))| = 3$, $|E(L^2(G))| = 2$.

Higher iterates and general pattern. Continuing,

$$L^3(G) = L(P_3) = P_2, \qquad L^4(G) = L(P_2) = P_1 \ \ \text{(single vertex)},$$

$$L^5(G) = L(P_1) = P_0 \ \ \text{(empty)}.$$

In general for an unbranched n-carbon chain $G = P_n$,

$$L(P_n) = P_{n-1} \ (n \geq 2), \qquad L^k(P_n) = P_{n-k} \quad \text{while } n-k \geq 1.$$

G encodes atom–atom connectivity (C–C bonds). $L(G)$ turns bonds into vertices and records which bonds are *adjacent* at a common carbon—useful, e.g., for constructing bond–bond coupling terms in vibrational or NMR coupling models along an alkane backbone. Iterating to $L^2(G)$ captures adjacency among *bond–adjacency relations* themselves, which can organize higher-order constraints (e.g., sequential coupling pathways or coarse-grained segment interactions) in linear hydrocarbons such as n-pentane.

2. Molecular Line HyperGraph and Iterated Line HyperGraph

Molecular Hypergraph represents atoms as vertices and chemical bonds as hyperedges, capturing multi-atom interactions in a molecular structure [62–64]. Molecular hypergraphs have been the subject of various studies in recent years [65,66]. Molecular Line HyperGraph transforms a molecular hypergraph by representing bonds as vertices and connecting them when sharing common atoms. Iterated Line HyperGraph repeatedly applies the line-hypergraph transformation, revealing higher-order adjacency relationships between bonds in successive levels.

Definition 2.1 (Molecular Hypergraph)**.** [62,63] A *molecular hypergraph* is a finite, simple, undirected hypergraph $\mathcal{H} = (V, E)$, where V is the set of atoms and $E \subseteq 2^V \setminus \{\emptyset\}$ is the family of *bonds/interaction groups*. We allow $|e| \geq 2$ to encode multi-center interactions; multiple identical hyperedges are not allowed and loops are excluded. For $v \in V$, the (hypergraph) degree is $\deg_{\mathcal{H}}(v) := |\{\, e \in E : v \in e \,\}|$.

Example 2.2 (Molecular HyperGraph: Diborane B_2H_6 with three-center bonds)**.** Consider diborane with atoms

$$V = \{\, B_1, B_2,\ H_{b1}, H_{b2},\ H_{t1}, H_{t2}, H_{t3}, H_{t4} \,\},$$

where H_{b1}, H_{b2} are bridging hydrogens and $H_{t1}, \ldots, H_{t4}$ are terminal hydrogens. Model two-center B–H bonds as size-2 hyperedges and each three-center two-electron bridge $\mathrm{B{-}H{-}B}$ as a size-3 hyperedge:

$$\begin{aligned} E \;=\; & \underbrace{\big\{\{B_1, H_{t1}\}, \{B_1, H_{t2}\}, \{B_2, H_{t3}\}, \{B_2, H_{t4}\}\big\}}_{\text{terminal two-center bonds}} \\ & \cup\; \underbrace{\big\{\{B_1, H_{b1}, B_2\}, \{B_1, H_{b2}, B_2\}\big\}}_{\text{bridging three-center bonds}}. \end{aligned}$$

The molecular hypergraph is $\mathcal{H} = (V, E)$. This representation captures both ordinary two-center bonds and multi-center $\mathrm{B{-}H{-}B}$ interactions within the same hypergraph formalism.

Example 2.3 (Molecular Hypergraph)**.** We encode ordinary B–H *two-center* bonds and *three-center* B–H–B bridges in a single molecular hypergraph $\mathcal{H} = (V, E)$.

Atom (vertex) set.

$$V = \{\, B_1, B_2,\ H_{b1}, H_{b2},\ H_{t1}, H_{t2}, H_{t3}, H_{t4}\,\}.$$

Bond/interaction family (hyperedges). Two-center terminals and three-center bridges:

$$E = \{e_{t1} = \{B_1, H_{t1}\},\ e_{t2} = \{B_1, H_{t2}\},\ e_{t3} = \{B_2, H_{t3}\},\ e_{t4} = \{B_2, H_{t4}\},$$
$$e_{b1} = \{B_1, H_{b1}, B_2\},\ e_{b2} = \{B_1, H_{b2}, B_2\}\ \}.$$

Incidence matrix (rows: $B_1, B_2, H_{b1}, H_{b2}, H_{t1}, H_{t2}, H_{t3}, H_{t4}$; columns: $e_{t1}, e_{t2}, e_{t3}, e_{t4}, e_{b1}, e_{b2}$).

$$\mathbf{H} = \begin{array}{c} \\ B_1 \\ B_2 \\ H_{b1} \\ H_{b2} \\ H_{t1} \\ H_{t2} \\ H_{t3} \\ H_{t4} \end{array} \begin{array}{c} \begin{matrix} e_{t1} & e_{t2} & e_{t3} & e_{t4} & e_{b1} & e_{b2} \end{matrix} \\ \begin{bmatrix} 1 & 1 & 0 & 0 & 1 & 1 \\ 0 & 0 & 1 & 1 & 1 & 1 \\ 0 & 0 & 0 & 0 & 1 & 0 \\ 0 & 0 & 0 & 0 & 0 & 1 \\ 1 & 0 & 0 & 0 & 0 & 0 \\ 0 & 1 & 0 & 0 & 0 & 0 \\ 0 & 0 & 1 & 0 & 0 & 0 \\ 0 & 0 & 0 & 1 & 0 & 0 \end{bmatrix} \end{array}$$

Degrees and sanity check.

$$\deg(B_1) = 4,\ \deg(B_2) = 4,\ \deg(H_{b1}) = \deg(H_{b2}) = \deg(H_{t1}) = \cdots = \deg(H_{t4}) = 1.$$

The total incidence count equals both the sum of vertex degrees and the sum of hyperedge sizes:

$$\sum_{v \in V} \deg(v) = 4 + 4 + 1 + 1 + 1 + 1 + 1 + 1 = 14$$
$$\sum_{e \in E} |e| = 2 + 2 + 2 + 2 + 3 + 3 = 14,$$

verifying consistency. This hypergraph cleanly unifies two-center and three-center bonding motifs in a single combinatorial object.

Definition 2.4 (2-section (primal) of a Hypergraph)**.** For a hypergraph $\mathcal{F} = (\mathsf{V}, \mathsf{E})$, its *2-section* $\mathrm{Sec}_2(\mathcal{F})$ is the simple graph on vertex set V with an edge $\{x, y\}$ for distinct $x, y \in \mathsf{V}$ iff there exists $f \in \mathsf{E}$ such that $\{x, y\} \subseteq f$.

Definition 2.5 (Line Hypergraph Operator)**.** Let $\mathcal{H} = (V, E)$ be any finite hypergraph. The *line hypergraph* (also called incidence-dual expansion) of $\mathcal{H}$ is

$$\mathsf{L}_H(\mathcal{H}) \;:=\; \big(E,\ \mathsf{E}\big) \quad \text{with} \quad \mathsf{E} \;:=\; \big\{\, N_{\mathcal{H}}(v) \subseteq E :\ v \in V,\ N_{\mathcal{H}}(v) \neq \emptyset \,\big\},$$

where

$$N_{\mathcal{H}}(v) \;:=\; \{\, e \in E : \; v \in e \,\}$$

collects all hyperedges of $\mathcal{H}$ incident to v. Thus vertices of $\mathsf{L}_H(\mathcal{H})$ are the bonds E of $\mathcal{H}$, and each atom v induces a hyperedge consisting of all bonds meeting v.

Definition 2.6 (Molecular Line HyperGraph)**.** For a molecular hypergraph $\mathcal{H} = (V, E)$, its *Molecular Line HyperGraph* is $\mathrm{MLH}(\mathcal{H}) := \mathsf{L}_H(\mathcal{H})$.

Example 2.7 (Molecular Line HyperGraph of B_2H_6)**.** Let $\mathcal{H} = (V, E)$ be as above and name the hyperedges

$$e_{t1} = \{B_1, H_{t1}\}, \quad e_{t2} = \{B_1, H_{t2}\}, \quad e_{t3} = \{B_2, H_{t3}\}, \quad e_{t4} = \{B_2, H_{t4}\},$$
$$e_{b1} = \{B_1, H_{b1}, B_2\}, \quad e_{b2} = \{B_1, H_{b2}, B_2\}.$$

The Molecular Line HyperGraph $\mathrm{MLH}(\mathcal{H}) = \mathsf{L}_H(\mathcal{H})$ has

$$V' := E = \{e_{t1}, e_{t2}, e_{t3}, e_{t4}, e_{b1}, e_{b2}\},$$

and for each atom $v \in V$ we add the hyperedge $\mathrm{Star}_{\mathcal{H}}(v) = \{\, e \in E : \; v \in e \,\}$. Concretely,

$$\mathrm{Star}(B_1) = \{e_{t1}, e_{t2}, e_{b1}, e_{b2}\}, \qquad \mathrm{Star}(B_2) = \{e_{t3}, e_{t4}, e_{b1}, e_{b2}\},$$
$$\mathrm{Star}(H_{t1}) = \{e_{t1}\}, \; \mathrm{Star}(H_{t2}) = \{e_{t2}\}, \; \mathrm{Star}(H_{t3}) = \{e_{t3}\}, \; \mathrm{Star}(H_{t4}) = \{e_{t4}\},$$
$$\mathrm{Star}(H_{b1}) = \{e_{b1}\}, \; \mathrm{Star}(H_{b2}) = \{e_{b2}\}.$$

Thus the hyperedge set of $\mathrm{MLH}(\mathcal{H})$ is

$$E' = \big\{\mathrm{Star}(v) : v \in V, \; \mathrm{Star}(v) \neq \emptyset\big\}.$$

Intuitively, each vertex of $\mathrm{MLH}(\mathcal{H})$ represents an original bond or multi-center interaction, and hyperedges group all such interactions incident to a common atom.

Example 2.8 (Molecular Line HyperGraph: Cyclopropane C_3H_6 (C–C skeleton))**.** Consider the carbon triangle $(C_1C_2C_3)$ as a molecular hypergraph with only C–C bonds (each a size-2 hyperedge). Let

$$V = \{C_1, C_2, C_3\}, \qquad E = \{e_{12} = \{C_1, C_2\}, \; e_{23} = \{C_2, C_3\}, \; e_{31} = \{C_3, C_1\}\}.$$

The Molecular Line HyperGraph is $\mathrm{MLH}(\mathcal{H}) = \mathsf{L}_H(\mathcal{H}) = (E, E')$, where each atom C_i contributes the (nonempty) star $N_{\mathcal{H}}(C_i) \subseteq E$:

$$N_{\mathcal{H}}(C_1) = \{e_{12}, e_{31}\},$$
$$N_{\mathcal{H}}(C_2) = \{e_{12}, e_{23}\},$$
$$N_{\mathcal{H}}(C_3) = \{e_{23}, e_{31}\}.$$

Hence

$$V\big(\mathrm{MLH}(\mathcal{H})\big) = E = \{e_{12}, e_{23}, e_{31}\}, \qquad E' = \big\{\{e_{12}, e_{31}\}, \; \{e_{12}, e_{23}\}, \; \{e_{23}, e_{31}\}\big\}.$$

2-section and adjacency (numerical form). The 2-section $\mathrm{Sec}_2\big(\mathrm{MLH}(\mathcal{H})\big)$ is a simple graph on vertices (e_{12}, e_{23}, e_{31}) with edge set

$$\{\{e_{12}, e_{23}\},\ \{e_{23}, e_{31}\},\ \{e_{31}, e_{12}\}\},$$

i.e. a 3-cycle. Its adjacency matrix (in the order e_{12}, e_{23}, e_{31}) is

$$A = \begin{bmatrix} 0 & 1 & 1 \\ 1 & 0 & 1 \\ 1 & 1 & 0 \end{bmatrix}.$$

This matches the classical line graph $L(C_3) \cong C_3$, confirming $\mathrm{Sec}_2\big(\mathrm{MLH}(\mathcal{H})\big) = L(\mathcal{H})$ in this instance. Chemically, vertices of MLH are the C–C bonds, and each hyperedge groups the two bonds that meet at a carbon, capturing bond–bond adjacencies around the strained three-membered ring.

Theorem 2.9 (Molecular Line HyperGraph is a Line HyperGraph)**.** *For every molecular hypergraph $\mathcal{H}$,* MLH$(\mathcal{H})$ *is, by construction, a line hypergraph of $\mathcal{H}$; i.e.*

$$\mathrm{MLH}(\mathcal{H}) \ = \ \mathsf{L}_H(\mathcal{H}).$$

Proof. By definition, MLH$(\mathcal{H})$ has vertex set E and hyperedge set $\{\, N_{\mathcal{H}}(v) : v \in V,\ N_{\mathcal{H}}(v) \neq \emptyset \,\}$. This equals the line-hypergraph construction $\mathsf{L}_H(\mathcal{H})$ word for word. □

Theorem 2.10 (Generalizes the Molecular Line Graph)**.** *Let $G = (V, E)$ be a molecular* graph *(every $e \in E$ has $|e| = 2$). Then the 2-section of the Molecular Line HyperGraph recovers the ordinary line graph:*

$$\mathrm{Sec}_2\big(\mathrm{MLH}(G)\big) \ = \ L(G).$$

Proof. Vertices on both sides are E (bonds of G). For distinct $e, e' \in E$, adjacency in $\mathrm{Sec}_2(\mathrm{MLH}(G))$ holds iff there exists a hyperedge $N_G(v)$ of MLH(G) with $\{e, e'\} \subseteq N_G(v)$. By definition of $N_G(v)$, this is equivalent to $v \in e \cap e'$, i.e. the two bonds meet at atom v. Thus $\{e, e'\}$ is an edge of $\mathrm{Sec}_2(\mathrm{MLH}(G))$ iff $e \cap e' \neq \emptyset$ in G, which is precisely the adjacency condition in $L(G)$. Hence $\mathrm{Sec}_2(\mathrm{MLH}(G)) = L(G)$. □

Definition 2.11 (Molecular Iterated Line HyperGraph)**.** For a molecular hypergraph $\mathcal{H}$, its *Molecular Iterated Line HyperGraph of order k* is

$$\mathrm{MILH}^{(k)}(\mathcal{H}) \ := \ \mathsf{L}_H^{k}(\mathcal{H}) \qquad (k \in \mathbb{N}_0).$$

Example 2.12 (Molecular Iterated Line HyperGraph: a linear C–C–C–C fragment)**.** Consider a four-carbon chain fragment (e.g., a butane skeleton segment) with atoms

$$V = \{C_1, C_2, C_3, C_4\}, \qquad E = \{e_{12} = \{C_1, C_2\},\ e_{23} = \{C_2, C_3\},\ e_{34} = \{C_3, C_4\}\}.$$

The molecular hypergraph $\mathcal{H} = (V, E)$ is an ordinary graph (all hyperedges have size 2). Its Molecular Line HyperGraph $\mathrm{MLH}(\mathcal{H}) = \mathsf{L}_H(\mathcal{H})$ has

$$V^{(1)} := E = \{e_{12}, e_{23}, e_{34}\},$$

and hyperedges given by the stars of the atoms:

$$\mathrm{Star}(C_1) = \{e_{12}\}, \quad \mathrm{Star}(C_2) = \{e_{12}, e_{23}\}, \quad \mathrm{Star}(C_3) = \{e_{23}, e_{34}\}, \quad \mathrm{Star}(C_4) = \{e_{34}\}.$$

Now iterate once more to form the Molecular *Iterated* Line HyperGraph $\mathrm{MILH}^{(1)}(\mathrm{MLH}(\mathcal{H})) = \mathsf{L}_H(\mathrm{MLH}(\mathcal{H}))$. The new vertex set is the hyperedge set from the previous step,

$$V^{(2)} := \{\ \{e_{12}\},\ \{e_{12}, e_{23}\},\ \{e_{23}, e_{34}\},\ \{e_{34}\}\ \},$$

and for each $x \in V^{(1)} = \{e_{12}, e_{23}, e_{34}\}$ we add the star in $\mathrm{MLH}(\mathcal{H})$:

$$\begin{aligned}
\mathrm{Star}_{\mathrm{MLH}}(e_{12}) &= \{\ \{e_{12}\},\ \{e_{12}, e_{23}\}\ \},\\
\mathrm{Star}_{\mathrm{MLH}}(e_{23}) &= \{\ \{e_{12}, e_{23}\},\ \{e_{23}, e_{34}\}\ \},\\
\mathrm{Star}_{\mathrm{MLH}}(e_{34}) &= \{\ \{e_{23}, e_{34}\},\ \{e_{34}\}\ \}.
\end{aligned}$$

Hence the hyperedges of $\mathrm{MILH}^{(1)}$ are precisely these three sets. This concretely exhibits the iteration: vertices become "groups of adjacent bonds," and new hyperedges record which of those groups share a bond-vertex in the previous layer.

Example 2.13 (Diborane B_2H_6: two-center and three-center bonding)**.** We build $\mathrm{MILH}^{(2)}(\mathcal{H})$ starting from a molecular hypergraph that encodes both ordinary two-center B–H bonds and three-center two-electron $\mathrm{B-H-B}$ bridges.

Level 0 (molecular hypergraph). Let the atom set be

$$V = \{B_1, B_2,\ H_{b1}, H_{b2},\ H_{t1}, H_{t2}, H_{t3}, H_{t4}\}.$$

Define the hyperedge family (two-center terminal bonds and three-center bridges)

$$\begin{aligned}
E = \{e_{t1} = \{B_1, H_{t1}\},\ e_{t2} = \{B_1, H_{t2}\},\ e_{t3} = \{B_2, H_{t3}\},\ e_{t4} = \{B_2, H_{t4}\},\\
e_{b1} = \{B_1, H_{b1}, B_2\},\ e_{b2} = \{B_1, H_{b2}, B_2\}\ \}.
\end{aligned}$$

Thus $\mathcal{H} = (V, E)$ has $|V| = 8$ and $|E| = 6$.

First iteration $L(H)$ (line hypergraph). By definition, $L(H) = (E, \mathsf{E})$, where for each $v \in V$, $\mathrm{Star}_H(v) := \{\, e \in E : v \in e \,\}$ contributes a (nonempty) hyperedge. Explicitly,

$$\mathrm{Star}(B_1) = \{e_{t1}, e_{t2}, e_{b1}, e_{b2}\}, \quad \mathrm{Star}(B_2) = \{e_{t3}, e_{t4}, e_{b1}, e_{b2}\},$$
$$\mathrm{Star}(H_{t1}) = \{e_{t1}\},\ \mathrm{Star}(H_{t2}) = \{e_{t2}\},\ \mathrm{Star}(H_{t3}) = \{e_{t3}\},\ \mathrm{Star}(H_{t4}) = \{e_{t4}\},$$
$$\mathrm{Star}(H_{b1}) = \{e_{b1}\},\ \mathrm{Star}(H_{b2}) = \{e_{b2}\}.$$

Hence $|V(L(H))| = |E| = 6$ and $|\mathsf{E}| = 8$.

Second iteration $L^2(H)$. Vertices of $L^2(H)$ are the hyperedges of $L(H)$:

$$V\big(L^2(H)\big) = \Big\{\, \mathrm{Star}(x) \ :\ x \in V \,\Big\}.$$

For each $e \in E$, the star in $L(H)$ is the set of *previous* stars that contain e:

$$\mathrm{Star}_{L(H)}(e) := \{\, F \in \mathsf{E} \ :\ e \in F \,\}.$$

Enumerating,

$$\mathrm{Star}_{L(H)}(e_{t1}) = \{\mathrm{Star}(B_1), \mathrm{Star}(H_{t1})\},$$
$$\mathrm{Star}_{L(H)}(e_{t2}) = \{\mathrm{Star}(B_1), \mathrm{Star}(H_{t2})\},$$
$$\mathrm{Star}_{L(H)}(e_{t3}) = \{\mathrm{Star}(B_2), \mathrm{Star}(H_{t3})\},$$
$$\mathrm{Star}_{L(H)}(e_{t4}) = \{\mathrm{Star}(B_2), \mathrm{Star}(H_{t4})\},$$
$$\mathrm{Star}_{L(H)}(e_{b1}) = \{\mathrm{Star}(B_1), \mathrm{Star}(B_2), \mathrm{Star}(H_{b1})\},$$
$$\mathrm{Star}_{L(H)}(e_{b2}) = \{\mathrm{Star}(B_1), \mathrm{Star}(B_2), \mathrm{Star}(H_{b2})\}.$$

Thus $|\mathsf{E}(L^2(H))| = 6$ with four size-2 hyperedges (from terminals) and two size-3 hyperedges (from bridges).

Chemical interpretation. $L(H)$ reorganizes "interaction terms" (bonds) by common atoms; $L^2(H)$ captures how those *groupings* co-occur via shared interaction terms. The larger size-3 hyperedges in $L^2(H)$ reflect the cooperativity introduced by three-center B–H–B bonding.

Example 2.14 (Benzene C_6H_6: σ bonds plus a delocalized π sextet)**.** We include the six two-center σ C–C bonds and a six-center π hyperedge to reflect aromatic delocalization, then compute $\mathrm{MILH}^{(2)}$.

Level 0 (molecular hypergraph). Let the carbon ring be $V = \{C_1, \ldots, C_6\}$ (indices mod 6). Define the hyperedge family

$$E = \big\{\, e_{12}, e_{23}, e_{34}, e_{45}, e_{56}, e_{61},\ p \,\big\},$$

where $e_{i\,i+1} := \{C_i, C_{i+1}\}$ are the six σ bonds and $p := \{C_1, C_2, C_3, C_4, C_5, C_6\}$ encodes the delocalized π sextet. Hence $|V| = 6$, $|E| = 7$.

First iteration $L(H)$. Vertices are E. For each C_i,

$$\mathrm{Star}_H(C_i) = \{\, e_{i-1\,i},\ e_{i\,i+1},\ p\,\}.$$

Therefore

$$V\big(L(H)\big) = E, \qquad \mathsf{E} = \Big\{\, \{e_{12}, e_{61}, p\},\ \{e_{12}, e_{23}, p\},\ \dots,\ \{e_{56}, e_{45}, p\}\Big\},$$

six (size-3) hyperedges total, one per carbon.

Second iteration $L^2(H)$. Vertices are the six triples above. For any σ edge $e_{i\,i+1}$,

$$\mathrm{Star}_{L(H)}(e_{i\,i+1}) = \big\{\, \mathrm{Star}(C_i),\ \mathrm{Star}(C_{i+1})\,\big\} \quad \text{(size 2)}.$$

For the π sextet p,

$$\mathrm{Star}_{L(H)}(p) = \big\{\, \mathrm{Star}(C_1), \mathrm{Star}(C_2), \dots, \mathrm{Star}(C_6)\,\big\} \quad \text{(size 6)}.$$

Hence $L^2(H)$ has 6 vertices and 7 hyperedges: six size-2 hyperedges (one per σ bond) and one size-6 hyperedge (from p).

Chemical interpretation. $L(H)$ records, for each carbon, the pair of adjacent σ bonds together with the global π channel. $L^2(H)$ then captures how "bond groups at carbons" co-occur via a shared σ bond (yielding size-2 hyperedges) and how all such groups co-occur via the delocalized π system (yielding a size-6 hyperedge), reflecting ring-wide aromatic coupling.

Theorem 2.15 (Molecular Iterated Line HyperGraph is an Iterated Line HyperGraph)**.** *For every $k \geq 0$ and molecular hypergraph $\mathcal{H}$,*

$$\mathrm{MILH}^{(k)}(\mathcal{H}) \;=\; \mathsf{L}_H^k(\mathcal{H}).$$

Proof. By definition of $\mathrm{MILH}^{(k)}$ as L_H^k, the identity is immediate. □

Definition 2.16 (Molecular iterated line hypergraph with 2-section normalization)**.** Let G be a molecular (simple) graph. Define recursively

$$\mathrm{MILH}^{(0)}(G) \;:=\; G, \qquad \mathrm{MILH}^{(k+1)}(G) \;:=\; \mathsf{L}_H\Big(\mathrm{Sec}_2\big(\mathrm{MILH}^{(k)}(G)\big)\Big) \quad (k \geq 0),$$

where $\mathsf{L}_H(\cdot)$ denotes the molecular line hypergraph operator.

Theorem 2.17 (Generalizes the Molecular Iterated Line Graph)**.** *Let G be a molecular* graph. *For all $k \geq 0$,*

$$\mathrm{Sec}_2\big(\mathrm{MILH}^{(k)}(G)\big) \;=\; L^k(G),$$

where $L^0(G) := G$ and $L^{k+1}(G) := L\big(L^k(G)\big)$.

Proof. We argue by induction on k.

Base $k = 0$*:* $\mathrm{Sec}_2(\mathrm{MILH}^{(0)}(G)) = \mathrm{Sec}_2(G) = G = L^0(G)$, since G is a simple graph.

Inductive step: Assume $\mathrm{Sec}_2(\mathrm{MILH}^{(k)}(G)) = L^k(G)$. Set

$$X := \mathrm{Sec}_2\big(\mathrm{MILH}^{(k)}(G)\big).$$

Then X is a (molecular) simple graph, hence Theorem 2.10 applies to X. Using Definition 2.16, we obtain

$$\mathrm{Sec}_2\big(\mathrm{MILH}^{(k+1)}(G)\big) = \mathrm{Sec}_2\Big(\mathsf{L}_H(X)\Big) = L(X) = L\big(\mathrm{Sec}_2(\mathrm{MILH}^{(k)}(G))\big) = L\big(L^k(G)\big) = L^{k+1}(G).$$

This completes the induction. □

3. Molecular Line SuperHypergraph and Iterated Line SuperHypergraph

A Molecular n-SuperHypergraph models hierarchical molecular structures using nested sets of atoms or interactions up to depth n (cf. [67–69]). A molecular line superhypergraph maps molecular superedges to vertices, linking them via shared atoms, enabling higher-order chemical connectivity analysis. A molecular iterated line superhypergraph repeatedly transforms molecular superedges into vertices, uncovering multi-level hierarchical connectivity in complex chemical structures.

Definition 3.1 (Level-n Molecular SuperHyperGraph)**.** Fix a finite base set V_0 of bond identifiers and an integer $n \geq 0$. Let $\mathcal{P}^0(V_0) = V_0$ and $\mathcal{P}^{k+1}(V_0) = \mathcal{P}\big(\mathcal{P}^k(V_0)\big)$. A *level-n molecular SuperHyperGraph* is a pair

$$\mathcal{H}^{(n)} = \big(V_n, \mathcal{E}\big) \quad \text{with} \quad V_n \subseteq \mathcal{P}^n(V_0), \qquad \emptyset \neq \mathcal{E} \subseteq \mathcal{P}(V_n) \setminus \{\emptyset\}.$$

Elements of V_n are *n-supernodes*; elements of $\mathcal{E}$ are *n-superedges*. Incidence is the usual membership $v \in E$ for $v \in V_n$, $E \in \mathcal{E}$.

Notation 2 (Stars)**.** *For* $\mathcal{H}^{(n)} = (V_n, \mathcal{E})$ *and* $v \in V_n$*, define the (nonempty-or-empty) star*

$$\mathrm{Star}_{\mathcal{H}}(v) := \{\, E \in \mathcal{E} \;:\; v \in E \,\} \subseteq \mathcal{E}.$$

When forming hyperedges below we will use only the nonempty stars $\mathrm{Star}_{\mathcal{H}}(v) \neq \emptyset$*.*

Example 3.2 (Molecular SuperHyperGraph for ethanol C_2H_5OH; level $n = 1$)**.** Let the base set V_0 collect bond identifiers

$$V_0 := \{b_{\mathrm{CC}},\ b_{\mathrm{CO}},\ b_{\mathrm{OH}},\ b_{C_1H_1},\ b_{C_1H_2},\ b_{C_1H_3},\ b_{C_2H_1},\ b_{C_2H_2}\}.$$

We form three 1-supervertices (subsets of V_0) corresponding to chemically meaningful groups:

$$T_{\text{methyl}} := \{ b_{C_1H_1}, b_{C_1H_2}, b_{C_1H_3} \},$$
$$T_{\text{methylene}} := \{ b_{\text{CC}}, b_{C_2H_1}, b_{C_2H_2} \},$$
$$T_{\text{hydroxyl}} := \{ b_{\text{CO}}, b_{\text{OH}} \}.$$

Set the level-1 vertex set $V_1 := \{T_{\text{methyl}}, T_{\text{methylene}}, T_{\text{hydroxyl}}\} \subseteq \mathcal{P}(V_0)$. Define two 1-superedges (nonempty subsets of V_1) reflecting adjacency of functional parts:

$$E_1 := \{T_{\text{methyl}}, T_{\text{methylene}}\}, \qquad E_2 := \{T_{\text{methylene}}, T_{\text{hydroxyl}}\}.$$

Then the level-1 Molecular SuperHyperGraph is

$$\mathcal{H}^{(1)} := \big(V_1, \mathcal{E}^{(1)}\big), \qquad \mathcal{E}^{(1)} := \{ E_1, E_2 \} \subseteq \mathcal{P}(V_1) \setminus \{\emptyset\}.$$

Here each 1-supervertex is a collection of bonds (a functional group), and each 1-superedge bundles the groups that are directly connected in the molecular framework.

Definition 3.3 (Line SuperHyperGraph operator)**.** Given $\mathcal{H}^{(n)} = (V_n, \mathcal{E})$, its *line SuperHyperGraph* is

$$\mathbf{L}\big(\mathcal{H}^{(n)}\big) := \big(V'_{n+1}, \mathcal{E}'_{n+1}\big)$$

with

$$V'_{n+1} := \mathcal{E} \qquad \text{and} \qquad \mathcal{E}'_{n+1} := \Big\{ \operatorname{Star}_{\mathcal{H}}(v) \subseteq \mathcal{E} \;:\; v \in V_n,\ \operatorname{Star}_{\mathcal{H}}(v) \neq \emptyset \Big\}.$$

Thus each original superedge becomes a vertex; for every supernode v, we add a (hyper)edge consisting of all superedges incident with v.

Definition 3.4 (Molecular Line SuperHyperGraph)**.** Let $\mathcal{H}^{(n)}$ be a level-n molecular SuperHyperGraph. Its *Molecular Line SuperHyperGraph* is the line SuperHyperGraph

$$\operatorname{MLSH}\big(\mathcal{H}^{(n)}\big) := \mathbf{L}\big(\mathcal{H}^{(n)}\big).$$

Example 3.5 (Molecular Line SuperHyperGraph of the ethanol example)**.** Apply the line SuperHyperGraph operator to $\mathcal{H}^{(1)} = (V_1, \mathcal{E}^{(1)})$. By definition, the vertex set of $\mathbf{L}(\mathcal{H}^{(1)})$ is the previous superedge set:

$$V'_2 := \mathcal{E}^{(1)} = \{E_1, E_2\}.$$

For each $v \in V_1$, form the (nonempty) star $\operatorname{Star}_{\mathcal{H}^{(1)}}(v) := \{ E \in \mathcal{E}^{(1)} : v \in E \}$. Explicitly,

$$\operatorname{Star}_{\mathcal{H}^{(1)}}(T_{\text{methyl}}) = \{E_1\},$$
$$\operatorname{Star}_{\mathcal{H}^{(1)}}(T_{\text{methylene}}) = \{E_1, E_2\},$$
$$\operatorname{Star}_{\mathcal{H}^{(1)}}(T_{\text{hydroxyl}}) = \{E_2\}.$$

The hyperedge set of the Molecular Line SuperHyperGraph is the collection of these nonempty stars:

$$\mathcal{E}_2' := \{ \{E_1\},\ \{E_1, E_2\},\ \{E_2\} \} \ \subseteq\ \mathcal{P}(V_2') \setminus \{\emptyset\}.$$

Therefore

$$\mathrm{MLSH}(\mathcal{H}^{(1)}) \ :=\ \mathbf{L}(\mathcal{H}^{(1)}) \ =\ (V_2',\ \mathcal{E}_2'),$$

where vertices represent the original superedges (E_1, E_2), and hyperedges record which of them meet at a common 1-supervertex in $\mathcal{H}^{(1)}$.

Definition 3.6 (Molecular Iterated Line SuperHyperGraph)**.** For $k \in \mathbb{N}_0$, the *Molecular Iterated Line SuperHyperGraph of order k* is

$$\mathrm{MILSH}^{(k)}(\mathcal{H}^{(n)}) \ :=\ \mathbf{L}^{k}(\mathcal{H}^{(n)}).$$

Example 3.7 (Molecular Iterated Line SuperHyperGraph (second layer on ethanol))**.** Iterate the line construction once more:

$$\mathrm{MILSH}^{(2)}(\mathcal{H}^{(1)}) \ :=\ \mathbf{L}\Big(\mathrm{MLSH}(\mathcal{H}^{(1)})\Big) \ =\ \mathbf{L}(V_2', \mathcal{E}_2').$$

Its vertex set is the previous hyperedge set,

$$V_3' \ :=\ \mathcal{E}_2' \ =\ \{\ \{E_1\},\ \{E_1, E_2\},\ \{E_2\}\ \}.$$

For each $x \in V_2' = \{E_1, E_2\}$, compute the star in $\mathrm{MLSH}(\mathcal{H}^{(1)})$:

$$\mathrm{Star}_{\mathrm{MLSH}}(E_1) = \{\ \{E_1\},\ \{E_1, E_2\}\ \},$$

$$\mathrm{Star}_{\mathrm{MLSH}}(E_2) = \{\ \{E_1, E_2\},\ \{E_2\}\ \}.$$

Thus the hyperedge set at the second iteration is

$$\mathcal{E}_3' \ :=\ \{\ \{\{E_1\}, \{E_1, E_2\}\},\ \{\{E_1, E_2\}, \{E_2\}\}\ \} \ \subseteq\ \mathcal{P}(V_3') \setminus \{\emptyset\}.$$

Hence

$$\mathrm{MILSH}^{(2)}(\mathcal{H}^{(1)}) \ =\ (V_3',\ \mathcal{E}_3'),$$

which concretely illustrates how vertices (interaction groups) at one iteration become the "units" that are grouped into hyperedges at the next, thereby encoding higher-order incidence among functional parts through repeated line–superhypergraph lifting.

Example 3.8 (Conjugated aromatic fragment (para–disubstituted benzene))**.** We construct a level 1 molecular SuperHyperGraph from bond identifiers of a benzene ring and compute its Molecular *Iterated* Line SuperHyperGraph up to the second iteration.

Level 0 (base set of bonds). Let

$$V_0 = \{ b_{12}, b_{23}, b_{34}, b_{45}, b_{56}, b_{61} \}$$

denote the six C–C bonds of the cycle C_6 labeled in order.

Level 1 (supervertices = fragments). Define three chemically meaningful fragments (supervertices)

$$T_{\text{left}} := \{\, b_{12}, b_{23}, b_{34} \,\},$$

$$T_{\text{bridge}} := \{\, b_{23}, b_{34}, b_{45} \,\},$$

$$T_{\text{right}} := \{\, b_{45}, b_{56}, b_{61} \,\},$$

and set $V_1 := \{T_{\text{left}}, T_{\text{bridge}}, T_{\text{right}}\} \subseteq \mathcal{P}(V_0)$.

Level 1 superedges (adjacent fragments). Let

$$E_1 := \{T_{\text{left}}, T_{\text{bridge}}\}, \qquad E_2 := \{T_{\text{bridge}}, T_{\text{right}}\},$$

and $\mathcal{E}^{(1)} := \{E_1, E_2\} \subseteq \mathcal{P}(V_1) \setminus \{\emptyset\}$. Thus $\mathcal{H}^{(1)} = (V_1, \mathcal{E}^{(1)})$ is a level 1 molecular SuperHyperGraph.

First line lift (Molecular Line SuperHyperGraph). By Definition 3.3,

$$\text{MLSH}\big(\mathcal{H}^{(1)}\big) = \mathbf{L}\big(\mathcal{H}^{(1)}\big) = (V_2', \mathcal{E}_2'), \quad V_2' = \mathcal{E}^{(1)} = \{E_1, E_2\}.$$

For each $T \in V_1$ the nonempty star is

$$\text{Star}(T_{\text{left}}) = \{E_1\}, \quad \text{Star}(T_{\text{bridge}}) = \{E_1, E_2\}, \quad \text{Star}(T_{\text{right}}) = \{E_2\}.$$

Hence

$$\mathcal{E}_2' = \{\ \{E_1\},\ \{E_1, E_2\},\ \{E_2\}\ \} \subseteq \mathcal{P}(V_2') \setminus \{\emptyset\}.$$

Second line lift (Molecular Iterated Line SuperHyperGraph). The order-2 MILSH is

$$\text{MILSH}^{(2)}\big(\mathcal{H}^{(1)}\big) = \mathbf{L}^2\big(\mathcal{H}^{(1)}\big) = (V_3', \mathcal{E}_3'), \quad V_3' = \mathcal{E}_2' = \big\{\{E_1\}, \{E_1, E_2\}, \{E_2\}\big\}.$$

Stars in $\mathbf{L}(\mathcal{H}^{(1)})$ (taken at the vertices E_1, E_2) are

$$\text{Star}_{\mathbf{L}}(E_1) = \big\{\{E_1\}, \{E_1, E_2\}\big\}, \qquad \text{Star}_{\mathbf{L}}(E_2) = \big\{\{E_1, E_2\}, \{E_2\}\big\},$$

thus

$$\mathcal{E}_3' = \{\ \{\{E_1\}, \{E_1, E_2\}\},\ \{\{E_1, E_2\}, \{E_2\}\}\ \}.$$

Verification and interpretation. All inclusions are explicit: $V_1 \subseteq \mathcal{P}(V_0)$, $\mathcal{E}^{(1)} \subseteq \mathcal{P}(V_1) \setminus \{\emptyset\}$, $V_2' = \mathcal{E}^{(1)} \subseteq \mathcal{P}^2(V_0)$, $\mathcal{E}_2' \subseteq \mathcal{P}(V_2') \setminus \{\emptyset\}$, etc. Chemically, level 1 groups contiguous π-segments; the first line lift turns their pairwise couplings into vertices and records which couplings meet at a fragment; the second lift captures *co-occurrence of coupling channels*, useful for modeling conjugation pathways in para–disubstituted benzenes.

Example 3.9 (Hydrogen-bonded water trimer $(H_2O)_3$)**.** We model the cyclic H-bond network and compute the order-2 Molecular Iterated Line SuperHyperGraph.

Level 0 (base set of H-bonds). Let $V_0 = \{h_{12}, h_{23}, h_{31}\}$, where h_{ij} denotes the hydrogen bond from monomer i (donor) to monomer j (acceptor) in the cyclic trimer.

Level 1 (motif supervertices). Define three donor/acceptor motifs (each a subset of bonds)

$$D_1 := \{h_{12}, h_{31}\}, \qquad D_2 := \{h_{23}, h_{12}\}, \qquad D_3 := \{h_{31}, h_{23}\},$$

and set $V_1 := \{D_1, D_2, D_3\} \subseteq \mathcal{P}(V_0)$.

Level 1 superedges (adjacent motifs along the ring). Let

$$E_1 := \{D_1, D_2\}, \qquad E_2 := \{D_2, D_3\}, \qquad E_3 := \{D_3, D_1\},$$

and $\mathcal{E}^{(1)} := \{E_1, E_2, E_3\} \subseteq \mathcal{P}(V_1) \setminus \{\emptyset\}$. Then $\mathcal{H}^{(1)} = (V_1, \mathcal{E}^{(1)})$ is a level 1 molecular SuperHyperGraph.

First line lift (Molecular Line SuperHyperGraph).

$$\mathrm{MLSH}\big(\mathcal{H}^{(1)}\big) = \mathbf{L}\big(\mathcal{H}^{(1)}\big) = (V_2', \mathcal{E}_2'), \qquad V_2' = \{E_1, E_2, E_3\}.$$

Nonempty stars at level 1 are

$$\mathrm{Star}(D_1) = \{E_1, E_3\}, \quad \mathrm{Star}(D_2) = \{E_1, E_2\}, \quad \mathrm{Star}(D_3) = \{E_2, E_3\},$$

hence

$$\mathcal{E}_2' = \{ \ \{E_1, E_3\}, \ \{E_1, E_2\}, \ \{E_2, E_3\} \ \}.$$

Second line lift (Molecular Iterated Line SuperHyperGraph).

$$\mathrm{MILSH}^{(2)}\big(\mathcal{H}^{(1)}\big) = \mathbf{L}^2\big(\mathcal{H}^{(1)}\big) = (V_3', \mathcal{E}_3'), \quad V_3' = \mathcal{E}_2'.$$

Stars in $\mathbf{L}(\mathcal{H}^{(1)})$ (taken at the vertices E_1, E_2, E_3) are

$$\begin{aligned}
\mathrm{Star}_{\mathbf{L}}(E_1) &= \big\{\{E_1, E_3\}, \{E_1, E_2\}\big\},\\
\mathrm{Star}_{\mathbf{L}}(E_2) &= \big\{\{E_1, E_2\}, \{E_2, E_3\}\big\},\\
\mathrm{Star}_{\mathbf{L}}(E_3) &= \big\{\{E_1, E_3\}, \{E_2, E_3\}\big\},
\end{aligned}$$

so

$$\mathcal{E}_3' = \{ \ \{\{E_1, E_3\}, \{E_1, E_2\}\}, \ \{\{E_1, E_2\}, \{E_2, E_3\}\}, \ \{\{E_1, E_3\}, \{E_2, E_3\}\} \ \}.$$

Verification and interpretation. All sets are explicitly contained in the required powersets: $V_1 \subseteq \mathcal{P}(V_0)$, $\mathcal{E}^{(1)} \subseteq \mathcal{P}(V_1)\setminus\{\emptyset\}$, $V_2' = \mathcal{E}^{(1)} \subseteq \mathcal{P}^2(V_0)$, and so on. Physically, level 1 motifs encode each monomer's donor/acceptor participation; the first line lift turns motif–motif couplings into vertices and records which couplings meet at a motif; the second lift captures *cooperativity of coupling channels*, relevant to collective effects in cyclic H-bond networks.

Theorem 3.10 (Well-definedness and level shift)**.** *If $\mathcal{H}^{(n)} = (V_n, \mathcal{E})$ is a level-n molecular SuperHyperGraph, then $\mathbf{L}\big(\mathcal{H}^{(n)}\big)$ is a level-$(n+1)$ molecular SuperHyperGraph. More generally, for every $k \geq 0$, $\mathbf{L}^k\big(\mathcal{H}^{(n)}\big)$ is level $n+k$.*

Proof. Since each superedge $E \in \mathcal{E}$ is a nonempty subset of $V_n \subseteq \mathcal{P}^n(V_0)$, we have $E \in \mathcal{P}(V_n) \subseteq \mathcal{P}\big(\mathcal{P}^n(V_0)\big) = \mathcal{P}^{n+1}(V_0)$. Thus $V'_{n+1} = \mathcal{E} \subseteq \mathcal{P}^{n+1}(V_0)$. Every hyperedge $\mathrm{Star}_{\mathcal{H}}(v)$ is a nonempty subset of V'_{n+1} by construction, hence $\mathcal{E}'_{n+1} \subseteq \mathcal{P}(V'_{n+1}) \setminus \{\emptyset\}$. Therefore $\mathbf{L}(\mathcal{H}^{(n)})$ satisfies the definition at level $n+1$. The iterated statement follows by induction on k. □

Theorem 3.11 (Molecular Line SuperHyperGraph is a Line SuperHyperGraph)**.** *For any level-n molecular SuperHyperGraph $\mathcal{H}^{(n)}$, $\mathrm{MLSH}\big(\mathcal{H}^{(n)}\big)$ coincides with the line SuperHyperGraph $\mathbf{L}\big(\mathcal{H}^{(n)}\big)$ of Definition.*

Proof. By definition we set $\mathrm{MLSH}(\mathcal{H}^{(n)}) := \mathbf{L}(\mathcal{H}^{(n)})$, so the two objects are identical in vertex set and hyperedge set. □

Theorem 3.12 (Generalizes Molecular Line HyperGraph)**.** *Let $n = 0$ and regard a molecular hypergraph $H = (V, E)$ as $\mathcal{H}^{(0)} = (V, \mathcal{E})$ with $\mathcal{E} = E$. Then $\mathrm{MLSH}\big(\mathcal{H}^{(0)}\big)$ equals the usual Molecular Line HyperGraph: its vertex set is E and each atom $v \in V$ contributes the hyperedge $\mathrm{Star}_{\mathcal{H}}(v) = \{\, e \in E : \ v \in e \,\}$.*

Proof. When $n = 0$, supernodes are atoms and superedges are ordinary hyperedges. Definition 3.3 produces vertices E and, for each $v \in V$, the hyperedge consisting of all $e \in E$ incident to v. This is precisely the line-hypergraph construction in the molecular hypergraph setting. □

Theorem 3.13 (Generalizes Molecular SuperHyperGraph)**.** *For any $n \geq 0$, $\mathrm{MLSH}\big(\mathcal{H}^{(n)}\big)$ is itself a (level-$n+1$) molecular SuperHyperGraph. Hence the Molecular Line SuperHyperGraph generalizes the Molecular SuperHyperGraph by producing a valid superhypergraph one level higher.*

Proof. Immediate from Theorem 3.10. □

Theorem 3.14 (Molecular Iterated Line SuperHyperGraph is an Iterated Line SuperHyperGraph)**.** *For any $k \geq 0$ and level-n molecular SuperHyperGraph $\mathcal{H}^{(n)}$,*

$$\mathrm{MILSH}^{(k)}\big(\mathcal{H}^{(n)}\big) \;=\; \mathbf{L}^{k}\big(\mathcal{H}^{(n)}\big),$$

i.e. it is the k-fold iterated line SuperHyperGraph of $\mathcal{H}^{(n)}$. Moreover, it is level $n+k$.

Proof. The equality is by definition of $\mathrm{MILSH}^{(k)}$. The level statement follows from Theorem 3.10 by induction on k. □

Theorem 3.15 (Generalizes Molecular Iterated Line HyperGraph)**.** *Let $n = 0$ and let $H = (V, E)$ be a molecular hypergraph. For all $k \geq 0$,*

$$\mathrm{MILSH}^{(k)}(\mathcal{H}^{(0)}) \quad \textit{equals the } k\textit{-fold iterated Molecular Line HyperGraph of } H,$$

obtained by repeatedly applying the line-hypergraph construction.

Proof. For $n = 0$, $\mathbf{L}$ reduces to the molecular line-hypergraph operator by Theorem 3.12. Iteration preserves this identification, so $\mathbf{L}^k(\mathcal{H}^{(0)})$ is exactly the k-fold line-hypergraph iteration on H. □

Theorem 3.16 (Generalizes Molecular SuperHyperGraph under iteration)**.** *For any $n \geq 0$ and $k \geq 0$, $\mathrm{MILSH}^{(k)}(\mathcal{H}^{(n)})$ is a (level-$n+k$) molecular SuperHyperGraph.*

Proof. Combine Theorems 3.10 and 3.14. □

4. Conclusion

In this paper, we introduced the notions of *Molecular Line SuperHyperGraphs* and *Molecular Iterated Line SuperHyperGraphs*, providing formal definitions and examining their potential applications. Looking ahead, we expect future work to extend these concepts using frameworks such as Fuzzy Graphs [70], Intuitionistic Fuzzy Graphs [71], Neutrosophic Graphs [72–75], Neutrosophic HyperGraphs [76,77], Uncertain Graphs [78,79], and Plithogenic Graphs [80–82]. We also anticipate developments in programming tools and libraries, as well as quantitative analyses carried out through computer-based machine learning and experimental investigations.

Funding

This study did not receive any financial or external support from organizations or individuals.

Acknowledgments

We extend our sincere gratitude to everyone who provided insights, inspiration, and assistance throughout this research. We particularly thank our readers for their interest and acknowledge the authors of the cited works for laying the foundation that made our study possible. We also appreciate the support from individuals and institutions that provided the resources and infrastructure needed to produce and share this paper. Finally, we are grateful to all those who supported us in various ways during this project.

Data Availability

This research is purely theoretical, involving no data collection or analysis. We encourage future researchers to pursue empirical investigations to further develop and validate the concepts introduced here.

Ethical Approval

As this research is entirely theoretical in nature and does not involve human participants or animal subjects, no ethical approval is required.

Conflicts of Interest

The authors confirm that there are no conflicts of interest related to the research or its publication.

Use of Generative AI and AI-Assisted Tools

We use generative AI and AI-assisted tools for tasks such as English grammar checking, and we do not employ them in any way that violates ethical standards.

Supplementary Information

No supplementary materials accompany this paper.

References

[1] M Amin Bahmanian and Mateja Šajna. Hypergraphs: connection and separation. *arXiv preprint arXiv:1504.04274*, 2015.

[2] Mohammad A Bahmanian and Mateja Sajna. Connection and separation in hypergraphs. *Theory and Applications of Graphs*, 2(2):5, 2015.

[3] Yifan Feng, Haoxuan You, Zizhao Zhang, Rongrong Ji, and Yue Gao. Hypergraph neural networks. In *Proceedings of the AAAI conference on artificial intelligence*, volume 33, pages 3558–3565, 2019.

[4] Yuxin Wang, Quan Gan, Xipeng Qiu, Xuanjing Huang, and David Wipf. From hypergraph energy functions to hypergraph neural networks. In *International Conference on Machine Learning*, pages 35605–35623. PMLR, 2023.

[5] Florentin Smarandache. *Introduction to the n-SuperHyperGraph-the most general form of graph today*. Infinite Study, 2022.

[6] Yan Cao. Integrating treesoft and hypersoft paradigms into urban elderly care evaluation: A comprehensive n-superhypergraph approach. *Neutrosophic Sets and Systems*, 85:852–873, 2025.

[7] Takaaki Fujita and Florentin Smarandache. Topological generalizations of graphs: Integrating hypergraph and superhypergraph perspectives. *Turkish Journal of Mathematics and Computer Science*, 17(2):322–337, 2025.

[8] Takaaki Fujita and Florentin Smarandache. *HyperGraph and SuperHyperGraph Theory with Applications (IV): Uncertain Graph Theory*, volume IV of *HyperGraph and SuperHyperGraph Theory with Applications*. Neutrosophic Science International Association (NSIA) Publishing House, 1.0 edition, 2026.

[9] Mohammad Hamidi, Florentin Smarandache, and Elham Davneshvar. Spectrum of superhypergraphs via flows. *Journal of Mathematics*, 2022(1):9158912, 2022.

[10] Takaaki Fujita and Florentin Smarandache. *HyperGraph and SuperHyperGraph Theory with Applications.* Neutrosophic Science International Association (NSIA) Publishing House, 2026.

[11] Takaaki Fujita and Florentin Smarandache. *HyperGraph and SuperHyperGraph Theory with Applications (II): Graph Property and Parameter*, volume II of *HyperGraph and SuperHyperGraph Theory with Applications*. Neutrosophic Science International Association (NSIA) Publishing House, 1.0 edition, 2026.

[12] Takaaki Fujita and Florentin Smarandache. *HyperGraph and SuperHyperGraph Theory with Applications (III): Intersection Graph and Graph Labeling*, volume III of *HyperGraph and SuperHyperGraph Theory with Applications*. Neutrosophic Science International Association (NSIA) Publishing House, 2026.

[13] Takaaki Fujita. Metahypergraphs, metasuperhypergraphs, and iterated metagraphs: Modeling graphs of graphs, hypergraphs of hypergraphs, superhypergraphs of superhypergraphs, and beyond. *Current Research in Interdisciplinary Studies*, 4(5):1–23, 2025.

[14] Takaaki Fujita and Arif Mehmood. Actor hypernetworks and urban road hypernetworks withreal-life applications. *Neutrosophic Computing and Machine Learning. ISSN 2574-1101*, 41:143–171, 2026.

[15] Thomas Jech. *Set theory: The third millennium edition, revised and expanded.* Springer, 2003.

[16] Florentin Smarandache. Foundation of superhyperstructure & neutrosophic superhyperstructure. *Neutrosophic Sets and Systems*, 63(1):21, 2024.

[17] Alain Bretto. Hypergraph theory. *An introduction. Mathematical Engineering. Cham: Springer*, 1, 2013.

[18] Ronan MT Fleming, Hulda S Haraldsdottir, German Preciat, Luojiao Huang, Ines Thiele, Amy Harms, and Thomas Hankemeier. Conserved moiety fluxomics. *bioRxiv*, pages 2024–11, 2024.

[19] Takaaki Fujita. Exploration of graph classes and concepts for superhypergraphs and n-th power mathematical structures. *Advancing Uncertain Combinatorics through Graphization, Hyperization, and Uncertainization: Fuzzy, Neutrosophic, Soft, Rough, and Beyond*, 2025.

[20] Weihua Jiang, Xiaowen Wang, Chenguang Zhang, Laiti Xue, and Liang Yang. Expression and clinical significance of mapk and egfr in triple-negative breast cancer. *Oncology letters*, 19(3):1842–1848, 2020.

[21] Lan K Nguyen, Walter Kolch, and Boris N Kholodenko. When ubiquitination meets phosphorylation: a systems biology perspective of egfr/mapk signalling. *Cell Communication and Signaling*, 11(1):52, 2013.

[22] Chen Yan. Properties of spectra of graphs and line graphs. *Applied Mathematics-A Journal of Chinese Universities*, 17(3):371–376, 2002.

[23] Robert Kincaid and Heidi Lam. Line graph explorer: scalable display of line graphs using focus+ context. In *Proceedings of the working conference on Advanced visual interfaces*, pages 404–411, 2006.

[24] Gary Chartrand. On hamiltonian line-graphs. *Transactions of the American Mathematical Society*, 134(3):559–566, 1968.

[25] RI Tyshkevich and Vadim E Zverovich. Line hypergraphs. *Discrete Mathematics*, 161(1-3):265–283, 1996.

[26] Regina I Tyshkevich and Vadim E Zverovich. Line hypergraphs: A survey. *Acta Applicandae Mathematica*, 52(1-3):209–222, 1998.

[27] V Zverovich, Yu Metelsky, and P Skums. Line graphs and hypergraphs. *Methods of Graph Decompositions*, page 169, 2024.

[28] AG Levin and RI Tyshkevich. Line hypergraphs. *Discrete Mathematics and Applications*, 3(4):407–428, 1993.

[29] Jean-Claude Bermond, Fahir Ergincan, and Michel Syska. Line directed hypergraphs. In *Cryptography and Security: From Theory to Applications: Essays Dedicated to Jean-Jacques Quisquater on the Occasion of His 65th Birthday*, pages 25–34. Springer, 2012.

[30] Takaaki Fujita. Note for line and total superhypergraphs: Connecting vertices, edges, edges of edges, edges of edges of edges in hierarchical systems. EngrXiv, 2025.

[31] Martin Knor and Ludovit Niepel. Connectivity of iterated line graphs. *Discrete applied mathematics*, 125(2-3):255–266, 2003.

[32] Harishchandra S Ramane, Hanumappa B Walikar, Siddani Bhaskara Rao, B Devadas Acharya, Prabhakar Ramrao Hampiholi, Sudhir R Jog, and Ivan Gutman. Spectra and energies of iterated line graphs of regular graphs. *Applied mathematics letters*, 18(6):679–682, 2005.

[33] Liming Xiong and Zhanhong Liu. Hamiltonian iterated line graphs. *Discrete mathematics*, 256(1-2):407–422, 2002.

[34] Yehong Shao. A bound on connectivity of iterated line graphs. *Electronic Journal of Graph Theory & Applications*, 10(2), 2022.

[35] Martin Knor and L'udovít Niepel. Iterated line graphs are maximally ordered. *Journal of Graph Theory*, 52(2):171–180, 2006.

[36] Harishchandra Ramane, Ivan Gutman, and Mahadevappa Gundloor. Seidel energy of iterated line graphs of regular graphs. 2015.

[37] Zupeng Yan, Hao Zheng, Jianfang Chen, and Ying Ye. The micro network of polyacrylonitrile (pan)-polyaniline (pani)-graphene (gra) hybrid nanocomposites for effective electrochemical detection of glucose and improved stability. *International Journal of Electrochemical Science*, 14(3):3011–3023, 2019.

[38] Steven Kearnes, Kevin McCloskey, Marc Berndl, Vijay Pande, and Patrick Riley. Molecular graph convolutions: moving beyond fingerprints. *Journal of computer-aided molecular design*, 30:595–608, 2016.

[39] Ivan Gutman and Ernesto Estrada. Topological indices based on the line graph of the molecular graph. *Journal of chemical information and computer sciences*, 36(3):541–543, 1996.

[40] Jiaxuan You, Bowen Liu, Zhitao Ying, Vijay Pande, and Jure Leskovec. Graph convolutional policy network for goal-directed molecular graph generation. *Advances in neural information processing systems*, 31, 2018.

[41] Johannes Gasteiger, Janek Gro, and Stephan Günnemann. Directional message passing for molecular graphs. *arXiv preprint arXiv:2003.03123*, 2020.

[42] Wengong Jin, Regina Barzilay, and Tommi Jaakkola. Hierarchical generation of molecular graphs using structural motifs. In *International conference on machine learning*, pages 4839–4848. PMLR, 2020.

[43] Wengong Jin, Regina Barzilay, and Tommi Jaakkola. Junction tree variational autoencoder for molecular graph generation. In *International conference on machine learning*, pages 2323–2332. PMLR, 2018.

[44] Nenad Trinajstic. *Chemical graph theory*. CRC press, 2018.

[45] Takaaki Fujita and Florentin Smarandache. A reconsideration of advanced concepts in neutrosophic graphs: Smart, zero divisor, layered, weak, semi, and chemical graphs. *Advancing Uncertain Combinatorics through Graphization, Hyperization, and Uncertainization: Fuzzy, Neutrosophic, Soft, Rough, and Beyond*, page 308, 2025.

[46] Ramón García-Domenech, Jorge Gálvez, Jesus V de Julián-Ortiz, and Lionello Pogliani. Some new trends in chemical graph theory. *Chemical Reviews*, 108(3):1127–1169, 2008.

[47] Stephan Wagner and Hua Wang. *Introduction to chemical graph theory*. Chapman and Hall/CRC, 2018.

[48] Milan Randić. On history of the randić index and emerging hostility toward chemical graph theory. *MATCH Commun. Math. Comput. Chem*, 59(1):5–124, 2008.

[49] Benoıt Goupil, Antonin Joly, Niccoló Pancino, Pietro Bongini, Franco Scarselli, and Monica Bianchini. Molgmp: A markov approach for molecular graph generation with gnns. *Neurocomputing*, page 131066, 2025.

[50] Linh Nguyen Thi My and Tham Vo. Anti-symmetric molecular graph learning approach with residual adaptive network based fuzzy inference system for lethal dose forecasting problem. *Journal of Computational Chemistry*, 46(19):e70176, 2025.

[51] Chaoyi Li, Hongxin Xiang, Wenjie Du, Tengfei Ma, Haowen Chen, Xiangxiang Zeng, and Lei Xu. Graphgim: rethinking molecular graph contrastive learning via geometry image modeling. *BMC biology*, 23(1):189, 2025.

[52] Shuo Liu, Mengyun Chen, Xiaojun Yao, and Huanxiang Liu. Fingerprint-enhanced hierarchical molecular graph neural networks for property prediction. *Journal of Pharmaceutical Analysis*, page 101242, 2025.

[53] Robert Penfold and Peter J Wilde. Enumerating and indexing many-body intramolecular interactions: a graph theoretic approach. *Journal of mathematical chemistry*, 53(7):1634–1648, 2015.

[54] Zahra Samiei and Fateme Movahedi. Investigating graph invariants for predicting properties of chemical structures of antiviral drugs. *Polycyclic Aromatic Compounds*, 44(10):6696–6713, 2024.

[55] DANIEL B Dix. An application of iterated line graphs to biomolecular conformation. *preprint*, 2000.

[56] Željko Tomović and Ivan Gutman. Modeling boiling points of cycloalkanes by means of iterated line graph sequences. *Journal of chemical information and computer sciences*, 41(4):1041–1045, 2001.

[57] Steven H Bertz. Branching in graphs and molecules. *Discrete applied mathematics*, 19(1-3):65–83, 1988.

[58] Sung-Hyuk Cha, Edgar G DuCasse, Louis V Quintas, Kyle Kravette, and David M Mendoza. A graph model related to chemistry: Conversion of methane to higher alkanes. *International Journal of Chemical Modeling*, 7(1):17, 2015.

[59] Joseph Delhalle and Frank E Harris. Fourier representation method for electronic structures of linear polymers: Ii. linear chain of hydrogen atoms. *Theoretica chimica acta*, 48(2):127–141, 1978.

[60] Maurizio Mondello and Gary S Grest. Molecular dynamics of linear and branched alkanes. *The Journal of chemical physics*, 103(16):7156–7165, 1995.

[61] Norman L Allinger and Jenn-Huei Lii. Benzene, aromatic rings, van der waals molecules, and crystals of aromatic molecules in molecular mechanics (mm3). *Journal of computational chemistry*, 8(8):1146–1153, 1987.

[62] Ahsanur Rahman, Christopher L Poirel, David J Badger, and TM Murali. Reverse engineering molecular hypergraphs. In *Proceedings of the ACM Conference on Bioinformatics, Computational Biology and Biomedicine*, pages 68–75, 2012.

[63] Hiroshi Kajino. Molecular hypergraph grammar with its application to molecular optimization. In *International Conference on Machine Learning*, pages 3183–3191. PMLR, 2019.

[64] Junyoung Park, Fangying Chen, and Jinkyoo Park. A molecular hypergraph convolutional network with functional group information. 2021.

[65] Junwu Chen and Philippe Schwaller. Molecular hypergraph neural networks. *The Journal of Chemical Physics*, 160(14), 2024.

[66] Nicholas Casetti, Pragnay Nevatia, Junwu Chen, Philippe Schwaller, and Connor W Coley. Comment on "molecular hypergraph neural networks"[j. chem. phys. 160, 144307 (2024)]. *The Journal of Chemical Physics*, 161(20), 2024.

[67] Takaaki Fujita. An introduction and reexamination of molecular hypergraph and molecular n-superhypergraph. *Asian Journal of Physical and Chemical Sciences*, 13(3):1–38, 2025.

[68] Takaaki Fujita. Molecular fuzzy graphs, hypergraphs, and superhypergraphs. *Journal of Intelligent Decision and Computational Modelling*, 1(3):158–171, 2025.

[69] Takaaki Fujita, Muhammad Gulistan, and A Ghaib Arkan. Modeling molecular interactions with hypernetworks and super-hypernetworks. *Advances in Research*, 26(4):294–326, 2025.

[70] Azriel Rosenfeld. Fuzzy graphs. In *Fuzzy sets and their applications to cognitive and decision processes*, pages 77–95. Elsevier, 1975.

[71] N Vinoth Kumar and G Geetha Ramani. Product intuitionistic fuzzy graph. *International Journal of Computer Applications*, 28(1):31–33, 2011.

[72] Said Broumi, Mohamed Talea, Assia Bakali, and Florentin Smarandache. Single valued neutrosophic graphs. *Journal of New theory*, (10):86–101, 2016.

[73] Takaaki Fujita and Florentin Smarandache. *Neutrosophy Revisited: Formalizing Core Concepts from Nidus idearum (Book Series) and Related Research*. Neutrosophic Science International Association (NSIA), 2025.

[74] Haibin Wang, Florentin Smarandache, Yanqing Zhang, and Rajshekhar Sunderraman. *Single valued neutrosophic sets*. Infinite study, 2010.

[75] Muhammad Akram, Hafsa M Malik, Sundas Shahzadi, and Florentin Smarandache. Neutrosophic soft rough graphs with application. *Axioms*, 7(1):14, 2018.

[76] Muhammad Aslam Malik, Ali Hassan, Said Broumi, Assia Bakali, Mohamed Talea, and Florentin Smarandache. Isomorphism of bipolar single valued neutrosophic hypergraphs. *Collected Papers. Volume IX: On Neutrosophic Theory and Its Applications in Algebra*, page 72, 2022.

[77] Muhammad Akram and Anam Luqman. Intuitionistic single-valued neutrosophic hypergraphs. *Opsearch*, 54:799–815, 2017.

[78] Takaaki Fujita and Florentin Smarandache. *A Dynamic Survey of Fuzzy, Intuitionistic Fuzzy, Neutrosophic, and Extensional Sets*. Neutrosophic Science International Association (NSIA), 2025.

[79] Takaaki Fujita and Florentin Smarandache. A unified framework for u-structures and functorial structure: Managing super, hyper, superhyper, tree, and forest uncertain over/under/off models. *Neutrosophic Sets and Systems*, 91:337–380, 2025.

[80] WB Vasantha Kandasamy, K Ilanthenral, and Florentin Smarandache. *Plithogenic Graphs*. Infinite Study, 2020.

[81] Fazeelat Sultana, Muhammad Gulistan, Mumtaz Ali, Naveed Yaqoob, Muhammad Khan, Tabasam Rashid, and Tauseef Ahmed. A study of plithogenic graphs: applications in spreading coronavirus disease (covid-19) globally. *Journal of ambient intelligence and humanized computing*, 14(10):13139–13159, 2023.

[82] Takaaki Fujita and Florentin Smarandache. A review of the hierarchy of plithogenic, neutrosophic, and fuzzy graphs: Survey and applications. In *Advancing Uncertain Combinatorics through Graphization, Hyperization, and Uncertainization: Fuzzy, Neutrosophic, Soft, Rough, and Beyond (Second Volume)*. Biblio Publishing, 2024.

Neutrosophic Knowledge, Volume 9, 2026

University of New Mexico

Bipolar Treesoft Sets, Bipolar Treefuzzy Sets, and Their Extensions

Takaaki Fujita[1] *, *Ajoy Kanti Das* [2], *Suman Das* [3], *Volkan Duran* [4], *Sankar Prasad Mondal* [5], *Mithun Datta* [6]

[1] Independent Researcher, Tokyo, Japan. (Takaaki.fujita060@gmail.com)

[2] Associate Professor, Department of Mathematics, Tripura University, Agartala-799022, Tripura, India. (ajoykantidas@gmail.com)

[3] Assistant Professor (Mathematics), Department of Education (ITEP), NIT Agartala, Jirania, 799046, Tripura, India. (dr.sumandas1995@gmail.com)

[4] Department of Computer Engineering Igdır University. Turkey. (volkan.duran@igdir.edu.tr)

[5] Department of Applied Mathematics, Maulana Abul Kalam Azad University of Technology, West Bengal, Haringhata-741249, West Bengal, India. (sankar.mondal02@gmail.com)

[6] Department of Mathematics, The ICFAI University Tripura, India. (mithunagt007@gmail.com)

*Correspondence: Takaaki.fujita060@gmail.com

Received: *01/02/2026;* Accepted: *01/21/2026*

Abstract. Concepts such as Fuzzy Sets, Neutrosophic Sets, Soft sets, HyperSoft Sets, Rough Sets, and Plithogenic Sets have been extensively studied to address uncertainty, with diverse applications across various fields. As extensions of Fuzzy Sets, Neutrosophic Sets, and Soft Sets, concepts such as Bipolar Fuzzy Sets, Bipolar Neutrosophic Sets, and Bipolar Soft Sets have been introduced. In this paper, we further extend these notions and explore Bipolar Treesoft Sets, Bipolar Treefuzzy Sets, Multipolar Treefuzzy Sets, and Bipolar Treeneutrosophic Sets.

Keywords: Soft Set, Fuzzy Set, Neutrosophic Set, Treesoft set, Treefuzzy set, Bipolar Treesoft set, Multipolar Fuzzy Set

1. Preliminaries

This section recalls the basic notions and notation used throughout the paper.

1.1. *Fuzzy Sets, Bipolar Fuzzy Sets, and Multipolar Fuzzy Sets*

Fuzzy sets provide a standard set-theoretic framework for modeling graded membership and uncertainty. We recall the classical definition of a fuzzy set due to Zadeh [1], and then summarize two widely used extensions: bipolar fuzzy sets and multipolar (or m-polar) fuzzy sets [2,3].

Definition 1.1 (Fuzzy set and induced fuzzy relation [1])**.** Let Y be a nonempty set. A *fuzzy set* on Y is a function $\tau : Y \to [0,1]$. A *fuzzy relation* on Y is a fuzzy set on $Y \times Y$, i.e., a function $\delta : Y \times Y \to [0,1]$. If τ is a fuzzy set on Y, then a fuzzy relation δ on Y is said to be *compatible with* τ (or a *fuzzy relation on* τ) if

$$\delta(y,z) \ \leq \ \min\{\tau(y),\tau(z)\} \qquad (\forall\, y,z \in Y).$$

Definition 1.2 (Bipolar fuzzy set [3,4])**.** Let X be a nonempty set. A *bipolar fuzzy set* on X is an ordered pair

$$B = (\mu_B^+, \mu_B^-),$$

where

$$\mu_B^+ : X \to [0,1] \quad \text{and} \quad \mu_B^- : X \to [-1,0].$$

For $x \in X$, the value $\mu_B^+(x)$ represents the *positive* degree of membership (or satisfaction) of x, whereas $\mu_B^-(x)$ represents the *negative* degree of membership (or degree of counter-satisfaction). The family of all bipolar fuzzy sets on X is denoted by $BF(X)$.

Definition 1.3 (m-polar (multipolar) fuzzy set [3])**.** Let X be a nonempty set and let $m \in \mathbb{N}$. An *m-polar fuzzy set* on X is a mapping

$$M : X \to [0,1]^m,$$

so that each $x \in X$ is assigned an m-tuple

$$M(x) = \big(\mu_1(x), \mu_2(x), \dots, \mu_m(x)\big),$$

where $\mu_i(x) \in [0,1]$ is interpreted as the membership degree of x with respect to the i-th perspective, attribute, or agent.

Tree-based variants of fuzzy sets incorporate hierarchical attribute structures represented by a rooted tree.

Definition 1.4 (TreeFuzzy set [5])**.** Let Tree(A) be a fixed rooted tree whose nodes/leaves encode attributes, and let U be a nonempty universe. Write $P(\text{Tree}(A))$ for the power set of the set of all nodes and leaves of Tree(A). A *TreeFuzzy set* is a mapping

$$F : P(\text{Tree}(A)) \longrightarrow [0,1]^U,$$

where $[0,1]^U$ denotes the set of all membership functions $\mu : U \to [0,1]$. Thus, for each $S \in P(\mathrm{Tree}(A))$, the value $F(S)$ is a fuzzy set on U; we write

$$F(S) = \mu_S \quad \text{with} \quad \mu_S : U \to [0,1].$$

For $x \in U$, the number $\mu_S(x)$ is interpreted as the degree to which x satisfies the attribute combination S.

Example 1.5 (TreeFuzzy set: hierarchical product attributes)**.** Let $U = \{p_1, p_2, p_3\}$ be a set of products. Consider the rooted attribute tree

$$\mathrm{Tree}(A) = \{\mathrm{Quality},\ \mathrm{HighQuality},\ \mathrm{LowQuality},\ \mathrm{Durability},\ \mathrm{HighDurability}\},$$

where Quality and Durability are internal nodes, and HighQuality, LowQuality, HighDurability are leaves. Then $P(\mathrm{Tree}(A))$ denotes the power set of these nodes/leaves.
Define a mapping

$$F : P(\mathrm{Tree}(A)) \longrightarrow [0,1]^U$$

by specifying, for several attribute-combinations $S \subseteq \mathrm{Tree}(A)$, the membership functions $\mu_S := F(S) : U \to [0,1]$ as follows:

$$\mu_{\{\mathrm{HighQuality}\}}(p_1) = 0.90,$$

$$\mu_{\{\mathrm{HighQuality}\}}(p_2) = 0.50,$$

$$\mu_{\{\mathrm{HighQuality}\}}(p_3) = 0.20,$$

$$\mu_{\{\mathrm{HighDurability}\}}(p_1) = 0.60,$$

$$\mu_{\{\mathrm{HighDurability}\}}(p_2) = 0.85,$$

$$\mu_{\{\mathrm{HighDurability}\}}(p_3) = 0.40,$$

$$\mu_{\{\mathrm{HighQuality},\mathrm{HighDurability}\}}(p_1) = 0.70,$$

$$\mu_{\{\mathrm{HighQuality},\mathrm{HighDurability}\}}(p_2) = 0.55,$$

$$\mu_{\{\mathrm{HighQuality},\mathrm{HighDurability}\}}(p_3) = 0.10,$$

and set $\mu_\varnothing(p_i) = 0$ for $i = 1, 2, 3$. For all other $S \subseteq \mathrm{Tree}(A)$ not listed explicitly, define μ_S arbitrarily in $[0,1]^U$ (e.g., $\mu_S \equiv 0$).
Then F is a TreeFuzzy set (i.e., each S is assigned a fuzzy set μ_S on U). The value $\mu_{\{\mathrm{HighQuality},\mathrm{HighDurability}\}}(p_1) = 0.70$, for instance, means that p_1 satisfies the combined attribute "high quality and high durability" to degree 0.70.

1.2. *Neutrosophic Sets and Bipolar Neutrosophic Sets*

Neutrosophic sets extend fuzzy sets by explicitly incorporating an *indeterminacy* component, and thus enable one to describe truth, indeterminacy, and falsity degrees simultaneously (cf. [6–8]). Several notable refinements and generalizations have also been proposed, including double-valued neutrosophic sets [9,10], quadripartitioned neutrosophic sets [11], refined neutrosophic sets [12,13], and plithogenic sets [14].

Definition 1.6 (Neutrosophic set [6,15])**.** Let X be a nonempty set. A *neutrosophic set* A on X is specified by three functions

$$T_A : X \to [0,1], \qquad I_A : X \to [0,1], \qquad F_A : X \to [0,1],$$

where, for each $x \in X$, the numbers $T_A(x)$, $I_A(x)$, and $F_A(x)$ represent the degrees of truth-membership, indeterminacy-membership, and falsity-membership of x, respectively. These values satisfy

$$0 \ \le\ T_A(x) + I_A(x) + F_A(x) \ \le\ 3 \qquad (\forall\, x \in X).$$

Definition 1.7 (Bipolar neutrosophic set [16–18])**.** Let X be a nonempty set. A *bipolar neutrosophic set* A on X is given by six membership functions

$$T_A^+, I_A^+, F_A^+ : X \to [0,1], \qquad T_A^-, I_A^-, F_A^- : X \to [-1,0].$$

Equivalently, one may write

$$A = \Big\{ \big\langle x,\ T_A^+(x), I_A^+(x), F_A^+(x),\ T_A^-(x), I_A^-(x), F_A^-(x) \big\rangle :\ x \in X \Big\}.$$

For each $x \in X$, the triple $(T_A^+(x), I_A^+(x), F_A^+(x))$ describes the positive degrees of truth, indeterminacy, and falsity, while $(T_A^-(x), I_A^-(x), F_A^-(x))$ describes the corresponding negative degrees.

Tree-based variants of neutrosophic sets similarly organize attributes through a rooted tree (see, e.g., [19,20]).

Definition 1.8 (TreeNeutrosophic set [5])**.** Let $\mathrm{Tree}(A)$ be a fixed rooted tree of attributes and let U be a nonempty universe. A *TreeNeutrosophic set* is a mapping

$$F : P(\mathrm{Tree}(A)) \longrightarrow \big([0,1] \times [0,1] \times [0,1]\big)^U.$$

Hence, for each $S \in P(\mathrm{Tree}(A))$ and each $x \in U$, the value $F(S)(x)$ is a triple

$$F(S)(x) = \big(T_S(x), I_S(x), F_S(x)\big) \in [0,1]^3,$$

interpreted as the degrees of truth-membership, indeterminacy-membership, and falsity-membership of x with respect to the attribute combination S. These values satisfy

$$0 \ \le\ T_S(x) + I_S(x) + F_S(x) \ \le\ 3 \qquad (\forall\, x \in U,\ \forall\, S \in P(\mathrm{Tree}(A))).$$

1.3. *Soft Sets, Bipolar Soft Sets, and Treesoft Sets*

Soft set theory provides a parameterized framework for representing uncertainty: each parameter is associated with a subset of a universe, yielding a family of approximations of the underlying objects [21–23]. Among several generalizations, *bipolar soft sets* incorporate both positive and negative information and have been widely studied [24–26]. We next recall these notions, and then present the tree-structured extension known as a *Treesoft set* [27,28].

Definition 1.9 (Soft set [23])**.** Let U be a nonempty universe and let E be a nonempty set of parameters. A *soft set* over U is an ordered pair (F, E), where

$$F : E \longrightarrow \mathcal{P}(U)$$

is a mapping to the power set of U. For each parameter $e \in E$, the set $F(e) \subseteq U$ is interpreted as the collection of *e-approximate* (or e-admissible) elements of U. Thus, (F, E) represents a parameterized family of subsets of U.

Definition 1.10 (Bipolar soft set [24–26])**.** Let U be a nonempty universe and let E be a nonempty set of parameters. Fix a nonempty subset $A \subseteq E$ (the set of *positive* parameters), and let

$$\neg A := E \setminus A$$

denote the corresponding set of *negative* parameters. A *bipolar soft set* over U is a triple (F, G, A), where

$$F : A \to \mathcal{P}(U) \quad \text{and} \quad G : \neg A \to \mathcal{P}(U)$$

are mappings, called the *positive* and *negative* approximate mappings, respectively, and they satisfy the *consistency condition*

$$F(e) \cap G(\neg e) = \varnothing \qquad (\forall\, e \in A).$$

Equivalently, one may represent (F, G, A) as the family

$$(F, G, A) = \big\{ \big(e,\, F(e),\, G(\neg e)\big) : e \in A \big\},$$

together with the understanding that $F(e) \cap G(\neg e) = \varnothing$ for each $e \in A$.

Tree-structured variants of soft sets model hierarchical attributes by organizing parameters into a rooted tree.

Definition 1.11 (Treesoft set [29])**.** Let U be a universe of discourse and let $H \subseteq U$ be a nonempty subset. Let $A = \{A_1, A_2, \ldots, A_n\}$ be a set of (first-level) attributes with $n \geq 1$. Assume that each attribute may be refined into lower-level sub-attributes, thereby forming a rooted, finite tree of attributes, denoted by $\mathrm{Tree}(A)$, whose root is A (level 0) and whose nodes/leaves are the attributes appearing at levels $1, 2, \ldots, m$ for some depth $m \geq 1$. The terminal nodes (nodes without descendants) are called the *leaves* of Tree(A).

Write $\mathcal{P}(\mathrm{Tree}(A))$ for the power set of the set of all nodes and leaves of Tree(A), and write $\mathcal{P}(H)$ for the power set of H. A *Treesoft set* is a mapping

$$F : \mathcal{P}(\mathrm{Tree}(A)) \longrightarrow \mathcal{P}(H).$$

For each $S \subseteq \mathrm{Tree}(A)$, the set $F(S) \subseteq H$ is interpreted as the collection of elements of H that satisfy (or are approximated by) the attribute combination encoded by S.

2. Results in This Paper

In this section we collect the main definitions introduced in this paper and present several inclusion results. After defining bipolar Treesoft sets, bipolar Treefuzzy sets, multipolar Treefuzzy sets, and bipolar Treeneutrosophic sets, we show that a number of existing set-theoretic models arise as special cases.

First, we present the definition of a bipolar Treesoft set below.

Definition 2.1 (Bipolar Treesoft set)**.** Let U be a nonempty universe, let $H \subseteq U$ be a nonempty subset, and let Tree(A) be a fixed attribute tree. Assume that Tree(A) is equipped with an *attribute negation* map

$$\neg : \mathrm{Tree}(A) \to \mathrm{Tree}(A),$$

such that $\neg(\neg a) = a$ for all $a \in \mathrm{Tree}(A)$ (involution). Extend $\neg$ to subsets by $\neg S := \{\neg a : a \in S\}$.

A *bipolar Treesoft set* on U (with respect to Tree(A)) is a pair of mappings

$$F : \mathcal{P}(\mathrm{Tree}(A)) \to \mathcal{P}(H) \qquad \text{and} \qquad G : \mathcal{P}(\mathrm{Tree}(A)) \to \mathcal{P}(H)$$

satisfying the *consistency condition*

$$F(S) \cap G(\neg S) = \varnothing \qquad (\forall\, S \subseteq \mathrm{Tree}(A)).$$

For each $S \subseteq \mathrm{Tree}(A)$, the set $F(S)$ is interpreted as the *positive approximation* associated with the attribute combination S, while $G(\neg S)$ is interpreted as the corresponding *negative approximation* (refutation) for S.

Remark 2.2 (Admissible attribute combinations)**.** In applications, one may wish to restrict $\mathcal{P}(\mathrm{Tree}(A))$ to a family of *admissible* attribute combinations (e.g., consistent selections along the tree). For simplicity, Definition 2.1 is stated on the full powerset.

Example 2.3 (Bipolar Treesoft set)**.** Let $U = \{1, 2, 3, 4\}$ and $H = U$. Consider the attribute tree

$$\mathrm{Tree}(A) = \{\mathrm{High}, \mathrm{Low}\}, \qquad \neg(\mathrm{High}) = \mathrm{Low},\ \neg(\mathrm{Low}) = \mathrm{High}.$$

Then $\mathcal{P}(\text{Tree}(A)) = \{\varnothing, \{\text{High}\}, \{\text{Low}\}, \{\text{High}, \text{Low}\}\}$. Define $F, G : \mathcal{P}(\text{Tree}(A)) \to \mathcal{P}(H)$ by

$$F(\varnothing) = \varnothing, \quad G(\varnothing) = \varnothing,$$

$$F(\{\text{High}\}) = \{1, 2\}, \quad G(\{\text{High}\}) = \{1\},$$

$$F(\{\text{Low}\}) = \{3, 4\}, \quad G(\{\text{Low}\}) = \{3\},$$

$$F(\{\text{High}, \text{Low}\}) = \{1, 2, 3\}, \quad G(\{\text{High}, \text{Low}\}) = \{4\}.$$

A direct check shows that $F(S) \cap G(\neg S) = \varnothing$ for every $S \subseteq \text{Tree}(A)$. Hence (F, G) is a bipolar Treesoft set on U.

We present the definition of a bipolar Treefuzzy set below.

Definition 2.4 (Bipolar Treefuzzy set)**.** Let U be a nonempty universe and let $\text{Tree}(A)$ be a fixed tree of attributes. A *bipolar Treefuzzy set* on U is a pair of functions

$$\tau^+ : \mathcal{P}(\text{Tree}(A)) \times U \to [0, 1], \qquad \tau^- : \mathcal{P}(\text{Tree}(A)) \times U \to [-1, 0].$$

For each $S \subseteq \text{Tree}(A)$ and $x \in U$, the values $\tau^+(S, x)$ and $\tau^-(S, x)$ represent, respectively, the positive and negative degrees of membership of x with respect to the attribute combination S.

Example 2.5 (Bipolar Treefuzzy set)**.** Let $U = \{\text{Taro}, \text{Ayako}\}$ and let $\text{Tree}(A) = \{\text{Tall}, \text{Short}\}$. Define τ^+ and τ^- as follows. For $S = \varnothing$, set $\tau^+(\varnothing, x) = 0$ and $\tau^-(\varnothing, x) = 0$ for all $x \in U$. For $S = \{\text{Tall}\}$ set

$$\tau^+(\{\text{Tall}\}, \text{Taro}) = 0.8, \quad \tau^-(\{\text{Tall}\}, \text{Taro}) = -0.1,$$

$$\tau^+(\{\text{Tall}\}, \text{Ayako}) = 0.3, \quad \tau^-(\{\text{Tall}\}, \text{Ayako}) = -0.2.$$

For $S = \{\text{Short}\}$ set

$$\tau^+(\{\text{Short}\}, \text{Taro}) = 0.2, \quad \tau^-(\{\text{Short}\}, \text{Taro}) = -0.3,$$

$$\tau^+(\{\text{Short}\}, \text{Ayako}) = 0.9, \quad \tau^-(\{\text{Short}\}, \text{Ayako}) = -0.05.$$

For $S = \{\text{Tall}, \text{Short}\}$ set

$$\tau^+(\{\text{Tall}, \text{Short}\}, \text{Taro}) = 0.5, \quad \tau^-(\{\text{Tall}, \text{Short}\}, \text{Taro}) = -0.2,$$

$$\tau^+(\{\text{Tall}, \text{Short}\}, \text{Ayako}) = 0.6, \quad \tau^-(\{\text{Tall}, \text{Short}\}, \text{Ayako}) = -0.3.$$

Then (τ^+, τ^-) is a bipolar Treefuzzy set on U.

We present the definition of a m-polar (multipolar) Treefuzzy set below.

Definition 2.6 (m-polar (multipolar) Treefuzzy set)**.** Let U be a nonempty universe, let $\mathrm{Tree}(A)$ be a fixed tree of attributes, and let $m \in \mathbb{N}$. An *m-polar Treefuzzy set* on U is a mapping

$$\mu : \mathcal{P}(\mathrm{Tree}(A)) \times U \to [0,1]^m,$$

so that for each $S \subseteq \mathrm{Tree}(A)$ and $x \in U$,

$$\mu(S,x) = \big(\mu_1(S,x), \mu_2(S,x), \ldots, \mu_m(S,x)\big),$$

where $\mu_i(S,x) \in [0,1]$ is interpreted as the membership degree from the i-th perspective, attribute, or agent.

Example 2.7 (m-polar Treefuzzy set with $m = 2$)**.** Let $U = \{\mathrm{Item1}, \mathrm{Item2}\}$ and let $\mathrm{Tree}(A) = \{\mathrm{Quality}, \mathrm{Durability}\}$. Define $\mu : \mathcal{P}(\mathrm{Tree}(A)) \times U \to [0,1]^2$ by

$$\mu(\varnothing, x) = (0,0) \qquad (\forall\, x \in U),$$

$$\mu(\{\mathrm{Quality}\}, \mathrm{Item1}) = (0.9, 0.8), \quad \mu(\{\mathrm{Quality}\}, \mathrm{Item2}) = (0.7, 0.6),$$

$$\mu(\{\mathrm{Durability}\}, \mathrm{Item1}) = (0.5, 0.4), \quad \mu(\{\mathrm{Durability}\}, \mathrm{Item2}) = (0.8, 0.9),$$

$$\mu(\{\mathrm{Quality}, \mathrm{Durability}\}, \mathrm{Item1}) = (0.85, 0.75),$$

$$\mu(\{\mathrm{Quality}, \mathrm{Durability}\}, \mathrm{Item2}) = (0.65, 0.55).$$

Then μ is a 2-polar Treefuzzy set on U.

We present the definition of a Bipolar Treeneutrosophic set below.

Definition 2.8 (Bipolar Treeneutrosophic set)**.** Let U be a nonempty universe and let $\mathrm{Tree}(A)$ be a fixed tree of attributes. A *bipolar Treeneutrosophic set* on U is a pair of mappings

$$\Phi^+ : \mathcal{P}(\mathrm{Tree}(A)) \times U \to [0,1]^3, \qquad \Phi^- : \mathcal{P}(\mathrm{Tree}(A)) \times U \to [-1,0]^3.$$

For each $S \subseteq \mathrm{Tree}(A)$ and $x \in U$ we write

$$\Phi^+(S,x) = \big(T^+(S,x),\, I^+(S,x),\, F^+(S,x)\big), \qquad \Phi^-(S,x) = \big(T^-(S,x),\, I^-(S,x),\, F^-(S,x)\big),$$

where $T^+, I^+, F^+ \in [0,1]$ represent, respectively, the positive degrees of truth, indeterminacy, and falsity, and $T^-, I^-, F^- \in [-1,0]$ represent the corresponding negative degrees.

Example 2.9 (Bipolar Treeneutrosophic set)**.** Let $U = \{\mathrm{X}, \mathrm{Y}\}$ and $\mathrm{Tree}(A) = \{\mathrm{Efficiency}, \mathrm{Reliability}\}$. Define Φ^+ and Φ^- by setting, for all $x \in U$,

$$\Phi^+(\varnothing, x) = (0,0,0), \qquad \Phi^-(\varnothing, x) = (0,0,0),$$

and by specifying the following values on singletons and their union:

$$\Phi^+(\{\mathrm{Efficiency}\}, \mathrm{X}) = (0.8, 0.1, 0.1), \quad \Phi^-(\{\mathrm{Efficiency}\}, \mathrm{X}) = (-0.3, -0.2, -0.5),$$

$$\Phi^+(\{\mathrm{Efficiency}\}, \mathrm{Y}) = (0.7, 0.2, 0.1), \quad \Phi^-(\{\mathrm{Efficiency}\}, \mathrm{Y}) = (-0.2, -0.1, -0.3),$$

$$\Phi^+(\{\text{Reliability}\}, \text{X}) = (0.9, 0.05, 0.05), \quad \Phi^-(\{\text{Reliability}\}, \text{X}) = (-0.4, -0.1, -0.1),$$

$$\Phi^+(\{\text{Reliability}\}, \text{Y}) = (0.6, 0.3, 0.1),$$

$$\Phi^-(\{\text{Reliability}\}, \text{Y}) = (-0.1, -0.2, -0.3),$$

$$\Phi^+(\{\text{Efficiency}, \text{Reliability}\}, \text{X}) = (0.85, 0.15, 0.0),$$

$$\Phi^-(\{\text{Efficiency}, \text{Reliability}\}, \text{X}) = (-0.35, -0.25, -0.4),$$

$$\Phi^+(\{\text{Efficiency}, \text{Reliability}\}, \text{Y}) = (0.65, 0.25, 0.1),$$

$$\Phi^-(\{\text{Efficiency}, \text{Reliability}\}, \text{Y}) = (-0.15, -0.15, -0.35).$$

Then (Φ^+, Φ^-) is a bipolar Treeneutrosophic set on U.

Theorem 2.10. *Every Treesoft set and every bipolar soft set can be viewed as a special case of a bipolar Treesoft set.*

Proof. (1) Treesoft sets. Let $F : \mathcal{P}(\text{Tree}(A)) \to \mathcal{P}(H)$ be a Treesoft set. Define $G : \mathcal{P}(\text{Tree}(A)) \to \mathcal{P}(H)$ by $G(S) = \varnothing$ for all $S \subseteq \text{Tree}(A)$. Then for every $S \subseteq \text{Tree}(A)$ we have $F(S) \cap G(\neg S) = \varnothing$, hence (F, G) is a bipolar Treesoft set. The original Treesoft set is recovered by ignoring G.

(2) Bipolar soft sets. Let (F', G', A) be a bipolar soft set in the usual sense, where $F' : A \to \mathcal{P}(U)$ and $G' : \neg A \to \mathcal{P}(U)$ satisfy $F'(e) \cap G'(\neg e) = \varnothing$ for all $e \in A$. Let $E := A \cup \neg A$ and consider the trivial attribute tree with node set $\text{Tree}(A) = E$. Assume $\neg : E \to E$ is an involution with $\neg(\neg e) = e$ and $\neg(A) = \neg A$.
Define $F, G : \mathcal{P}(E) \to \mathcal{P}(U)$ by

$$F(S) = \begin{cases} F'(e), & \text{if } S = \{e\} \text{ with } e \in A, \\ \varnothing, & \text{otherwise,} \end{cases} \qquad G(S) = \begin{cases} G'(e), & \text{if } S = \{e\} \text{ with } e \in \neg A, \\ \varnothing, & \text{otherwise.} \end{cases}$$

Then for any $S \subseteq E$ we have $F(S) \cap G(\neg S) = \varnothing$: if $|S| \neq 1$, then $F(S) = \varnothing$; if $S = \{e\}$ with $e \in A$, then $\neg S = \{\neg e\}$ and

$$F(S) \cap G(\neg S) = F'(e) \cap G'(\neg e) = \varnothing;$$

if $S = \{\neg e\}$ with $e \in A$, then $F(S) = \varnothing$. Hence (F, G) is a bipolar Treesoft set. Restricting to singleton positive sets $\{e\}$ $(e \in A)$ recovers (F', G', A). □

Theorem 2.11. *Every bipolar fuzzy set and every Treefuzzy set can be viewed as a special case of a bipolar Treefuzzy set.*

Proof. (1) Bipolar fuzzy sets. Let (μ^+, μ^-) be a bipolar fuzzy set on U, i.e., $\mu^+ : U \to [0,1]$ and $\mu^- : U \to [-1,0]$. Choose a trivial attribute tree with $\mathrm{Tree}(A) = \{a\}$. Define

$$\tau^+(\{a\}, x) = \mu^+(x), \qquad \tau^-(\{a\}, x) = \mu^-(x) \qquad (\forall\, x \in U),$$

and set $\tau^+(\varnothing, x) = \tau^-(\varnothing, x) = 0$. Then (τ^+, τ^-) is a bipolar Treefuzzy set that restricts to (μ^+, μ^-) on $\{a\}$.

(2) Treefuzzy sets. Let $\tilde{\tau} : \mathcal{P}(\mathrm{Tree}(A)) \times U \to [0,1]$ be a Treefuzzy set. Define $\tau^+ = \tilde{\tau}$ and set $\tau^-(S, x) = 0$ for all (S, x). Then (τ^+, τ^-) is a bipolar Treefuzzy set and reduces to $\tilde{\tau}$ when the negative part is ignored. □

Theorem 2.12. *Every m-polar fuzzy set and every Treefuzzy set can be viewed as a special case of an m-polar Treefuzzy set.*

Proof. (1) m-polar fuzzy sets. Let $M : U \to [0,1]^m$ be an m-polar fuzzy set. Choose a trivial attribute tree with $\mathrm{Tree}(A) = \{a\}$. Define $\mu(\{a\}, x) = M(x)$ for all $x \in U$ (and, e.g., $\mu(\varnothing, x) = (0, \ldots, 0)$). Then μ is an m-polar Treefuzzy set that restricts to M on $\{a\}$.

(2) Treefuzzy sets. If $m = 1$, then $[0,1]^m = [0,1]$ and an m-polar Treefuzzy set is exactly a Treefuzzy set by definition. □

Theorem 2.13. *Every TreeNeutrosophic set and every bipolar neutrosophic set can be viewed as a special case of a bipolar Treeneutrosophic set.*

Proof. (1) TreeNeutrosophic sets. Let $\tilde{\Phi} : \mathcal{P}(\mathrm{Tree}(A)) \times U \to [0,1]^3$ be a TreeNeutrosophic set, where $\tilde{\Phi}(S, x) = (T(S, x), I(S, x), F(S, x))$. Define $\Phi^+ = \tilde{\Phi}$ and set $\Phi^-(S, x) = (0, 0, 0)$ for all (S, x). Then (Φ^+, Φ^-) is a bipolar Treeneutrosophic set that reduces to $\tilde{\Phi}$ when the negative part is ignored.

(2) Bipolar neutrosophic sets. Let A be a bipolar neutrosophic set on U given by

$$(T^+, I^+, F^+) : U \to [0,1]^3 \quad \text{and} \quad (T^-, I^-, F^-) : U \to [-1,0]^3.$$

Choose a trivial attribute tree with $\mathrm{Tree}(A) = \{a\}$ and define

$$\Phi^+(\{a\}, x) = \big(T^+(x), I^+(x), F^+(x)\big), \qquad \Phi^-(\{a\}, x) = \big(T^-(x), I^-(x), F^-(x)\big)$$

for all $x \in U$ (and, e.g., $\Phi^\pm(\varnothing, x) = (0, 0, 0)$). Then (Φ^+, Φ^-) is a bipolar Treeneutrosophic set that restricts to the given bipolar neutrosophic set on $\{a\}$. □

3. Conclusion

In this paper, we further extended these notions and explored Bipolar Treesoft Sets, Bipolar Treefuzzy Sets, Multipolar Treefuzzy Sets, and Bipolar Treeneutrosophic Sets. In future work, we hope that research will advance on extensions of the concepts introduced here and on their applications, using frameworks such as graphs [30], hypergraphs [31], SuperHyperGraphs [32, 33], hyperalgebras [34], uncertain sets [35], and hyperstructures [36, 37]. Since the present paper is devoted to theoretical investigation, we hope that future work by domain experts will conduct computational experiments and other quantitative analyses.

Funding

This research received no external funding.

Acknowledgments

The authors thank the reviewers and readers for their constructive comments and interest. We also acknowledge the authors of the cited works, whose contributions provided important foundations for this study.

Data Availability

No data were generated or analyzed in this theoretical study. We hope that future work will include computational experiments and other quantitative analyses to further assess the proposed concepts.

Ethical Approval

Ethical approval was not required for this study because it is purely theoretical and involves no human participants or animal subjects.

Conflicts of Interest

The authors declare no conflicts of interest.

Use of Generative AI and AI-Assisted Tools

Generative AI and AI-assisted tools were used only for English proofreading (e.g., grammar and style checks). They were not used to generate scientific content, results, or conclusions, and were used in accordance with applicable ethical standards.

Supplementary Information

No supplementary materials are provided.

References

[1] Lotfi A Zadeh. Fuzzy sets. *Information and control*, 8(3):338–353, 1965.

[2] Muhammad Riaz and Syeda Tayyba Tehrim. Cubic bipolar fuzzy set with application to multi-criteria group decision making using geometric aggregation operators. *Soft Computing*, 24:16111 – 16133, 2020.

[3] Juanjuan Chen, Shenggang Li, Shengquan Ma, and Xueping Wang. m-polar fuzzy sets: an extension of bipolar fuzzy sets. *The scientific world journal*, 2014(1):416530, 2014.

[4] Muhammad Gulistan, Naveed Yaqoob, Ahmed Elmoasry, and Jawdat Alebraheem. Complex bipolar fuzzy sets: An application in a transport's company. *J. Intell. Fuzzy Syst.*, 40:3981–3997, 2021.

[5] Takaaki Fujita. *Advancing Uncertain Combinatorics through Graphization, Hyperization, and Uncertainization: Fuzzy, Neutrosophic, Soft, Rough, and Beyond*. Biblio Publishing, 2025.

[6] Florentin Smarandache. A unifying field in logics: Neutrosophic logic. In *Philosophy*, pages 1–141. American Research Press, 1999.

[7] Said Broumi, Mohamed Talea, Assia Bakali, and Florentin Smarandache. Single valued neutrosophic graphs. *Journal of New theory*, 10:86–101, 2016.

[8] M Kaviyarasu, Muhammad Aslam, Farkhanda Afzal, Maha Mohammed Saeed, Arif Mehmood, and Saeed Gul. The connectivity indices concept of neutrosophic graph and their application of computer network, highway system and transport network flow. *Scientific Reports*, 14(1):4891, 2024.

[9] Lin Wei. An integrated decision-making framework for blended teaching quality evaluation in college english courses based on the double-valued neutrosophic sets. *J. Intell. Fuzzy Syst.*, 45:3259–3266, 2023.

[10] Qaisar Khan, Peide Liu, and Tahir Mahmood. Some generalized dice measures for double-valued neutrosophic sets and their applications. *Mathematics*, 6(7):121, 2018.

[11] Takaaki Fujita. Advanced partitioned neutrosophic sets: Formalization of hexa-, hepta-, octa-, nona-, and deca-partitioned structures. *Abhath Journal of Basic and Applied Sciences*, 4(2):40–60, 2025.

[12] Florentin Smarandache. Ambiguous set is a subclass of the double refined indeterminacy neutrosophic set, and of the refined neutrosophic set in general. *Neutrosophic Sets & Systems*, 58, 2023.

[13] Florentin Smarandache. n-valued refined neutrosophic logic and its applications to physics. *Infinite study*, 4:143–146, 2013.

[14] Takaaki Fujita and Florentin Smarandache. *A Dynamic Survey of Fuzzy, Intuitionistic Fuzzy, Neutrosophic, and Extensional Sets*. Neutrosophic Science International Association (NSIA), 2025.

[15] Florentin Smarandache. Neutrosophy: neutrosophic probability, set, and logic: analytic synthesis & synthetic analysis. 1998.

[16] Vakkas Ulucay, Irfan Deli, and Mehmet Sahin. Similarity measures of bipolar neutrosophic sets and their application to multiple criteria decision making. *Neural Computing and Applications*, 29:739–748, 2018.

[17] Irfan Deli, S Yusuf, Florentin Smarandache, and Mumtaz Ali. Interval valued bipolar neutrosophic sets and their application in pattern recognition. In *IEEE world congress on computational intelligence*, 2016.

[18] Muhammad Akram and Musavarah Sarwar. Novel multiple criteria decision making methods based on bipolar neutrosophic sets and bipolar neutrosophic graphs. *viXra*, 2017.

[19] Takaaki Fujita and Florentin Smarandache. *Forestfuzzy, forestneutrosophic, forestplithogenic, and forestrough set*. Infinite Study, 2025.

[20] Takaaki Fujita and Florentin Smarandache. Some types of hyperneutrosophic set (5): Support, paraconsistent, faillibilist, and others. *Advancing Uncertain Combinatorics through Graphization, Hyperization, and Uncertainization: Fuzzy, Neutrosophic, Soft, Rough, and Beyond*, 2025.

[21] Jinta Jose, Bobin George, and Rajesh K Thumbakara. Soft graphs: A comprehensive survey. *New Mathematics and Natural Computation*, pages 1–52, 2024.

[22] Dmitriy Molodtsov. Soft set theory-first results. *Computers & mathematics with applications*, 37(4-5):19–31, 1999.

[23] Pradip Kumar Maji, Ranjit Biswas, and A Ranjan Roy. Soft set theory. *Computers & mathematics with applications*, 45(4-5):555–562, 2003.

[24] Orhan Dalkılıç. A decision-making approach to reduce the margin of error of decision makers for bipolar soft set theory. *International Journal of Systems Science*, 53:265 – 274, 2021.

[25] Orhan Dalkılıç and Naime Demirtaş. Decision analysis review on the concept of class for bipolar soft set theory. *Computational and Applied Mathematics*, 41, 2022.

[26] Orhan DALKILIÇ and Naime Demirtaş. Combination of the bipolar soft set and soft expert set with an application in decision making. *Gazi University Journal of Science*, pages 1–1, 2022.

[27] Takaaki Fujita. Double-framed superhypersoft set and double-framed treesoft set. *Advancing Uncertain Combinatorics through Graphization, Hyperization, and Uncertainization: Fuzzy, Neutrosophic, Soft, Rough, and Beyond*, page 71, 2025.

[28] G Dhanalakshmi, S Sandhiya, and Florentin Smarandache. Stock price predictions with lstm-arima hybrid model under neutrosophic treesoft sets with mcdm interaction. *Neutrosophic Sets and Systems*, 80:674–699, 2025.

[29] Florentin Smarandache. New types of soft sets: Hypersoft set, indetermsoft set, indetermhypersoft set, and treesoft set. *International Journal of Neutrosophic Science*, 2023.

[30] Reinhard Diestel. *Graph theory*. Springer (print edition); Reinhard Diestel (eBooks), 2024.

[31] Yifan Feng, Haoxuan You, Zizhao Zhang, Rongrong Ji, and Yue Gao. Hypergraph neural networks. In *Proceedings of the AAAI conference on artificial intelligence*, volume 33, pages 3558–3565, 2019.

[32] Florentin Smarandache. *Extension of HyperGraph to n-SuperHyperGraph and to Plithogenic n-SuperHyperGraph, and Extension of HyperAlgebra to n-ary (Classical-/Neutro-/Anti-) HyperAlgebra*. Infinite Study, 2020.

[33] Takaaki Fujita and Florentin Smarandache. *HyperGraph and SuperHyperGraph Theory with Applications*. Neutrosophic Science International Association (NSIA) Publishing House, 2026.

[34] JE Humphreys. On the hyperalgebra of a semisimple algebraic group. In *Contributions to Algebra*, pages 203–210. Elsevier, 1977.

[35] Takaaki Fujita and Florentin Smarandache. A unified framework for u-structures and functorial structure: Managing super, hyper, superhyper, tree, and forest uncertain over/under/off models. *Neutrosophic Sets and Systems*, 91:337–380, 2025.

[36] Florentin Smarandache. Foundation of superhyperstructure & neutrosophic superhyperstructure. *Neutrosophic Sets and Systems*, 63(1):21, 2024.

[37] M Al Tahan and Bijan Davvaz. Weak chemical hyperstructures associated to electrochemical cells. *Iranian Journal of Mathematical Chemistry*, 9(1):65–75, 2018.

NeutrosophicKnowledge, Vol. 09, 2026
University of New Mexico

Article

Neutrosophic Quadratic Equations

Nirmal Sarkar [1] *

[1] Department of Mathematics, Dakshin Dinajpur University; nrmlsrkr@gmail.com

* Correspondence: nrmlsrkr@gmail.com

Received: 01-28-2026; *Accepted:* 02-06-2026.

Abstract: This study develops a comprehensive framework for solving neutrosophic quadratic equation (NQE). These equations are classified into three distinct types based on the coefficients of the x^2 term, with systematic solution methods derived for each type. For NQE Type 1, we establish conditions for the existence of distinct real solutions by analyzing the discriminants of the real and indeterminate components. Explicit solution formulations are derived, and the algebraic properties of their summation and product are rigorously examined. The methodologies are extended to solve NQE Types 2 and 3. To validate the theoretical findings, illustrative examples are provided for each equation type, demonstrating the practical implementation of the proposed methods.

Keywords: Neutrosophic real number; Neutrosophic complex number; Neutrosophic limit; Neutrosophic algebraic equation

---

1. Introduction

Neutrosophic Logic, introduced by Smarandache, serves as a modern alternative to classical logical frameworks, offering a mathematical model to handle uncertainty, vagueness, and inconsistency in data. Rooted in his philosophical concept of neutrosophy, this approach reconceptualizes the mathematical representation of indeterminate information [1, 2, 3, 4]. Subsequent advancements have further enriched this framework. For instance, Al-Tahan extended neutrosophic logic to single-valued neutrosophic (weak) polygroups, broadening its algebraic applications [23]. Additionally, Edalatpanah introduced an algorithm for neutrosophic linear programming utilizing triangular neutrosophic numbers for variables and constraints [24], and Chakraborty applied pentagonal neutrosophic numbers to network optimization, addressing shortest-path problems [25, 26]. Further, Abdel-Basset leveraged neutrosophic numbers in group decision-making using the TOPSIS technique for supplier selection [27], and Alvaracín Jarrín et al. applied neutrosophic statistics to model ambiguity in social science data [19].

In foundational work on Neutrosophic Real Numbers (NRNs), Smarandache established conditions for division and root-taking of both real and complex neutrosophic numbers, defining a standard form for Neutrosophic Complex Numbers (NCNs) [6, 7, 18]. His contributions further extend to Neutrosophic Probability, Statistics, and a unique neutrosophic calculus encompassing concepts such as the mereo-limit, mereo-derivative, and mereo-integral [5, 8].

Recent studies have increasingly explored the applications of neutrosophic numbers in advanced mathematical contexts. Alhasan's contributions to neutrosophic complex numbers in exponential form [9, 10] and his development of neutrosophic integrals [17, 14] have provided a foundation for further research in this area. Neutrosophic mathematics has demonstrated its relevance across diverse domains. For instance, Abobala and Hatip (2021) introduced neutrosophic Euclidean geometry as a generalization of classical Euclidean geometry [11]. Similarly, Çeven and Sekmen (2023) proposed the concept of neutrosophic square matrices and developed methods for solving systems of neutrosophic linear equations [21].

Alhasan's extensive work has established a robust framework for neutrosophic differential calculus, linear equations, and integration, providing valuable tools for analyzing uncertainty in mathematical settings [17, 16]. His studies on neutrosophic straight lines and circles (2023) have enhanced the visualization of uncertain data in two-dimensional spaces [15], while his formulation of double neutrosophic integrals has enabled multidimensional analyses [20]. Additionally, Alhasan and Musa (2023) introduced the concept of neutrosophic limits [12]. More recently, Narzary and Basumatary (2025) investigated the n-th derivative of neutrosophic functions, advancing the theory of differential calculus under uncertainty [13].

Quadratic equations are foundational to numerous areas of mathematics. Abobala (2020) examined linear and quadratic equations in neutrosophic fields [22]. However, his work does not provide a systematic method for determining the roots of neutrosophic quadratic equations, nor does it address the behavior of their solutions. This paper aims to fill this gap by developing a structured approach to solving neutrosophic quadratic equations of the form: $(p_1 + p_2I)x^2 + (q_1 + q_2I)x + (r_1 + r_2I) = 0_I$, where I is a neutrosophic indeterminate unit satisfying $I^2 = I$.

2. Preliminaries

Definition 2.1 *[7] Let N be a neutrosophic real number, which takes the standard form $N = a + bI$, where $a, b \in \mathbb{R}$ and I represents an indeterminate unit such that $I \cdot 0 = 0$ and $I^n = I$ for all $n \in \mathbb{Z}$.*

Definition 2.2 *[7] Let $N_1 = a_1 + b_1I$ and $N_2 = a_2 + b_2I$ be two neutrosophic numbers, The operations between these neutrosophic numbers are defined as follows:*

1. *Addition:*

$$N_1 + N_2 = (a_1 + a_2) + (b_1 + b_2)I$$

2. Subtraction:

$$N_1 - N_2 = (a_1 - a_2) + (b_1 - b_2)I$$

3. Multiplication:

$$N_1 \times N_2 = a_1a_2 + (a_1b_2 + b_1a_2 + b_1b_2)I$$

4. Division:

$$\frac{N_1}{N_2} = \frac{a_1}{a_2} + \frac{b_1a_2 - a_1b_2}{a_2(a_2 + b_2)}I \quad a_2 \neq 0 \quad and \quad a_2 \neq -b_2.$$

We denote neutrosophic zero as $0_I = 0 + 0I$.

3. General Neutrosophic Quadratic Equation

Consider the general form of the neutrosophic quadratic equation:

$$(p_1 + p_2 I)x^2 + (q_1 + q_2 I)x + (r_1 + r_2 I) = 0_I, \quad (1)$$

where p_1, p_2, q_1, q_2, r_1, and r_2 are real numbers. Here, we note that there are six parameters involved. To simplify the problem, we divide the entire equation by $p_1 + p_2 I$. This division leads to three distinct cases, with each case corresponding to a specific type of neutrosophic quadratic equation (NQE). The following are the cases:

Case 1: $p_1 \neq 0$ and $p_1 \neq -p_2$

If $p_1 \neq 0$ and $p_1 \neq -p_2$, the original equation can be normalized as follows:

$$x^2 + \left(\frac{q_1+q_2 I}{p_1+p_2 I}\right)x + \left(\frac{r_1+r_2 I}{p_1+p_2 I}\right) = 0_I.$$

Introducing simplified coefficients, we write:

$$\boldsymbol{x^2 + (\bar{q}_1 + \bar{q}_2 I)x + (\bar{r}_1 + \bar{r}_2 I) = 0_I,}$$

where

$$\bar{q}_1 + \bar{q}_2 I = \frac{q_1+q_2 I}{p_1+p_2 I}, \qquad \bar{r}_1 + \bar{r}_2 I = \frac{r_1+r_2 I}{p_1+p_2 I}.$$

This form is referred to as a Neutrosophic Quadratic Equation Type 1 (NQE Type 1).

Case 2: $p_1 = 0$

If $p_1 = 0$, the equation reduces to:

$$\boldsymbol{p_2 I x^2 + (q_1 + q_2 I)x + (r_1 + r_2 I) = 0_I.}$$

This form is identified as a Neutrosophic Quadratic Equation Type 2 (NQE Type 2).

Case 3: $p_1 = -p_2$

If $p_1 = -p_2$, the equation transforms into:

$$\boldsymbol{p_2(-1 + I)x^2 + (q_1 + q_2 I)x + (r_1 + r_2 I) = 0_I.}$$

This variation is termed a Neutrosophic Quadratic Equation Type 3 (NQE Type 3).

In the following three sections, we will find the solution for each of the cases outlined above, providing an example for each case to illustrate the approach.

4. Solution of NQE Type 1

In this section, we develop a method to solve a NQE Type 1 of the form:

$$x^2 + (q_1 + q_2 I)x + (r_1 + r_2 I) = 0_I \tag{2}$$

To determine the solution, we substitute $x = a + bI$ into equation (2):

$$(a + bI)^2 + (q_1 + q_2 I)(a + bI) + (r_1 + r_2 I) = 0_I. \tag{3}$$

Expanding $(a + bI)^2$:

$$(a + bI)^2 = a^2 + 2abI + b^2 I^2 = a^2 + (2ab + b^2)I, \text{ since } I^2 = I.$$

Next, we expand $(q_1 + q_2 I)(a + bI)$:

$$(q_1 + q_2 I)(a + bI) = q_1 a + q_1 bI + q_2 aI + q_2 bI^2 = q_1 a + (q_1 b + q_2 a + q_2 b)I.$$

Substituting these expanded expressions into equation (3) yields:

$$a^2 + (2ab + b^2)I + q_1 a + (q_1 b + q_2 a + q_2 b)I + r_1 + r_2 I = 0_I.$$

Separating the real and indeterminate parts, we obtain:

$$a^2 + q_1 a + r_1 + (2ab + b^2 + q_1 b + q_2 a + q_2 b + r_2)I = 0_I.$$

Equating the real and indeterminate parts separately, we have:

$$a^2 + q_1 a + r_1 = 0. \tag{4}$$

$$2ab + b^2 + q_1 b + q_2 a + q_2 b + r_2 = 0,$$

which can be rearranged as:

$$b^2 + (2a + q_1 + q_2)b + (q_2 a + r_2) = 0. \tag{5}$$

To solve for a, consider the quadratic equation (4): $a^2 + q_1 a + r_1 = 0$.

The discriminant of this equation is $\Delta_1 = q_1^2 - 4r_1$, yielding the solutions for a:

$$a_1 = \frac{-q_1 + \sqrt{\Delta_1}}{2}, \quad a_2 = \frac{-q_1 - \sqrt{\Delta_1}}{2}.$$

Solution for b, For each $a = a_1$, Equation (5) becomes:

$$b^2 + (2a_1 + q_1 + q_2)b + (q_2 a_1 + r_2) = 0.$$

Using the quadratic formula, the solutions for b are:

$$b_1 = \frac{-(2a_1 + q_1 + q_2) + \sqrt{(2a_1 + q_1 + q_2)^2 - 4(q_2 a_1 + r_2)}}{2},$$

$$b_2 = \frac{-(2a_1 + q_1 + q_2) - \sqrt{(2a_1 + q_1 + q_2)^2 - 4(q_2 a_1 + r_2)}}{2}.$$

For $a = a_2$, Equation (5) becomes:

$$b^2 + (2a_2 + q_1 + q_2)b + (q_2a_2 + r_2) = 0.$$

The solutions for b are:

$$b_3 = \frac{-(2a_2 + q_1 + q_2) + \sqrt{(2a_2 + q_1 + q_2)^2 - 4(q_2a_2 + r_2)}}{2},$$

$$b_4 = \frac{-(2a_2 + q_1 + q_2) - \sqrt{(2a_2 + q_1 + q_2)^2 - 4(q_2a_2 + r_2)}}{2}.$$

Thus, the solutions for a and b are obtained from the two quadratic equations (4) and (5). Using these values, we have the following four solutions:

$$x_1 = a_1 + b_1I, x_2 = a_1 + b_2I, x_3 = a_2 + b_3I, x_4 = a_2 + b_4I.$$

Substituting $2a_1 + q_1 = \sqrt{\Delta_1}$ and $2a_2 + q_1 = -\sqrt{\Delta_1}$, we obtain:

$$x_1 = a_1 + b_1I = \frac{-q_1 + \sqrt{\Delta_1}}{2} + \left(\frac{-(\sqrt{\Delta_1} + q_2) + \sqrt{(\sqrt{\Delta_1} + q_2)^2 - 4(q_2a_1 + r_2)}}{2}\right)I.$$

$$x_2 = a_1 + b_2I = \frac{-q_1 + \sqrt{\Delta_1}}{2} + \left(\frac{-(\sqrt{\Delta_1} + q_2) - \sqrt{(\sqrt{\Delta_1} + q_2)^2 - 4(q_2a_1 + r_2)}}{2}\right)I.$$

$$x_3 = a_2 + b_3I = \frac{-q_1 - \sqrt{\Delta_1}}{2} + \left(\frac{-(-\sqrt{\Delta_1} + q_2) + \sqrt{(-\sqrt{\Delta_1} + q_2)^2 - 4(q_2a_2 + r_2)}}{2}\right)I.$$

$$x_4 = a_2 + b_4I = \frac{-q_1 - \sqrt{\Delta_1}}{2} + \left(\frac{-(-\sqrt{\Delta_1} + q_2) - \sqrt{(-\sqrt{\Delta_1} + q_2)^2 - 4(q_2a_2 + r_2)}}{2}\right)I.$$

Theorem 4.2 *Let $x^2 + (q_1 + q_2I)x + (r_1 + r_2I) = 0_I$ be a NQE of Type 1, where $x = a + bI$ and a satisfies the real part equation $a^2 + q_1a + r_1 = 0$. If $\Delta_1 = q_1^2 - 4r_1 > 0$, yielding two distinct real solutions a_1 and a_2, then the discriminants Δ_{a_1} and Δ_{a_2} of the equations*

$$b^2 + (2a_1 + q_1 + q_2)b + (q_2a_1 + r_2) = 0$$

and

$$b^2 + (2a_2 + q_1 + q_2)b + (q_2a_2 + r_2) = 0$$

are equal, i.e., $\Delta_{a_1} = \Delta_{a_2}$.

Proof. Since $\Delta_1 = q_1^2 - 4r_1 > 0$, the equation $a^2 + q_1a + r_1 = 0$ has two distinct real solutions, given by

$$a_1 = \frac{-q_1 + \sqrt{\Delta_1}}{2}, a_2 = \frac{-q_1 - \sqrt{\Delta_1}}{2}.$$

Now, the discriminant Δ_{a_1} of the quadratic equation: $b^2 + (2a_1 + q_1 + q_2)b + (q_2a_1 + r_2) = 0$ is given by

$$\begin{aligned}
\Delta_{a_1} &= (2a_1 + q_1 + q_2)^2 - 4(q_2 a_1 + r_2) \\
&= \left(2 \cdot \tfrac{-q_1+\sqrt{\Delta_1}}{2} + q_1 + q_2\right)^2 - 4\left(q_2 \cdot \tfrac{-q_1+\sqrt{\Delta_1}}{2} + r_2\right) \\
&= (\sqrt{\Delta_1} + q_2)^2 - 4\left(\tfrac{-q_1 q_2 + q_2\sqrt{\Delta_1}}{2} + r_2\right) \\
&= \Delta_1 + q_2^2 + 2q_1 q_2 - 4r_2 \\
&= (q_1 + q_2)^2 - 4(r_1 + r_2), \qquad since\ \ \Delta_1 = q_1^2 - 4r_1.
\end{aligned}$$

Similarly, the discriminant Δ_{a_2} of the quadratic equation $b^2 + (2a_2 + q_1 + q_2)b + (q_2 a_2 + r_2) = 0$ is given by

$$\begin{aligned}
\Delta_{a_2} &= (2a_2 + q_1 + q_2)^2 - 4(q_2 a_2 + r_2) \\
&= \left(2 \cdot \tfrac{-q_1-\sqrt{\Delta_1}}{2} + q_1 + q_2\right)^2 - 4\left(q_2 \cdot \tfrac{-q_1-\sqrt{\Delta_1}}{2} + r_2\right) \\
&= (-\sqrt{\Delta_1} + q_2)^2 - 4\left(\tfrac{-q_1 q_2 - q_2\sqrt{\Delta_1}}{2} + r_2\right) \\
&= \Delta_1 + q_2^2 + 2q_1 q_2 - 4r_2 \\
&= (q_1 + q_2)^2 - 4(r_1 + r_2), \qquad since\ \ \Delta_1 = q_1^2 - 4r_1.
\end{aligned}$$

Thus, $\Delta_{a_1} = \Delta_{a_2}$ as required.

4.3 Solutions Formula for NQE Type 1

Using the above theorem, we can simplify the solutions for the NQE Type 1. The roots of this equation are derived as follows:

$$\begin{aligned}
x_1 = a_1 + b_1 I &= \frac{-q_1 + \sqrt{\Delta_1}}{2} + \frac{-q_2 - (\sqrt{\Delta_1} - \sqrt{\Delta_2})}{2} I, \\
x_2 = a_1 + b_2 I &= \frac{-q_1 + \sqrt{\Delta_1}}{2} + \frac{-q_2 - (\sqrt{\Delta_1} + \sqrt{\Delta_2})}{2} I, \\
x_3 = a_2 + b_3 I &= \frac{-q_1 - \sqrt{\Delta_1}}{2} + \frac{-q_2 + (\sqrt{\Delta_1} + \sqrt{\Delta_2})}{2} I, \\
x_4 = a_2 + b_4 I &= \frac{-q_1 - \sqrt{\Delta_1}}{2} + \frac{-q_2 + (\sqrt{\Delta_1} - \sqrt{\Delta_2})}{2} I,
\end{aligned}$$

where the discriminants are defined as $\Delta_1 = q_1^2 - 4r_1$ and $\Delta_2 = (q_1 + q_2)^2 - 4(r_1 + r_2)$.

4.4 Count Number of Distinct Real Solutions for NQE Type 1

To determine the conditions under which the NQE Type 1 has distinct real solutions, we expand and separate the equation into real and indeterminate components. This yields the following equations:

1. **Real Part:** $a^2 + q_1 a + r_1 = 0$.
2. **Indeterminate Part:** $b^2 + (2a + q_1 + q_2)b + (q_2 a + r_2) = 0$.

The discriminant for the real part is given by $\Delta_1 = q_1^2 - 4r_1$.
The number of real solutions for a depends on the value of Δ_1:

If $\Delta_1 > 0$: There are two distinct real solutions for a, denoted by a_1 and a_2. For each a_i, the discriminant of the indeterminate part, given by $\Delta_2 = (q_1 + q_2)^2 - 4(r_1 + r_2)$,
determines the number of real solutions for x:

- If $\Delta_2 > 0$, there are four distinct real solutions for x.
- If $\Delta_2 = 0$, there are two distinct real solutions for x.
- If $\Delta_2 < 0$, there are no real solutions for x.

If $\Delta_1 = 0$: There is a single (repeated) real solution for a. In this case, the discriminant

$$\Delta_2 = (q_1 + q_2)^2 - 4(r_1 + r_2)$$

dictates the number of solutions for x:

- If $\Delta_2 > 0$, there are two distinct real solutions for x.
- If $\Delta_2 = 0$, there is one distinct real solution for x.
- If $\Delta_2 < 0$, there are no real solutions for x.

If $\Delta_1 < 0$: There are no real solutions for a, hence there are no real solutions for x.

Condition on Δ_1	**Condition on Δ_2**	**Number of Distinct Real Solutions for x**
$\Delta_1 > 0$	$\Delta_2 > 0$	4
$\Delta_1 > 0$	$\Delta_2 = 0$	2
$\Delta_1 > 0$	$\Delta_2 < 0$	0
$\Delta_1 = 0$	$\Delta_2 > 0$	2
$\Delta_1 = 0$	$\Delta_2 = 0$	1
$\Delta_1 = 0$	$\Delta_2 < 0$	0
$\Delta_1 < 0$	-	0

Table 1: Count of Distinct Real Solutions of NQE Type 1

From the above discussion we conclude next theorem as

Theorem 4.5 *The NQE Type 1 has all solutions are neutrosophic real numbers if and only if $\Delta_1 \geq 0$ and $\Delta_2 \geq 0$.*

Theorem 4.6 *Let $x_1 = a_1 + b_1 I$, $x_2 = a_1 + b_2 I$, $x_3 = a_2 + b_3 I$, and $x_4 = a_2 + b_4 I$ be the four solutions of the neutrosophic quadratic equation $x^2 + (q_1 + q_2 I)x + (r_1 + r_2 I) = 0_I$. Then the following holds:*

a) $x_1 + x_4 = x_2 + x_3 = -q_1 - q_2 I$
b) $x_1 + x_2 + x_3 + x_4 = -2q_1 - 2q_2 I$.

c) $x_1x_4 = x_2x_3 = r_1 + r_2I$

d) $x_1x_2x_3x_4 = (r_1 + r_2I)^2$.

Proof. (a) From section 4.3 adding x_1 and x_4, we get:

$$x_1 + x_4 = \frac{-q_1 + \sqrt{\Delta_1} - q_1 - \sqrt{\Delta_1}}{2} + \frac{-q_2 - (\sqrt{\Delta_1} - \sqrt{\Delta_2}) - q_2 + (\sqrt{\Delta_1} - \sqrt{\Delta_2})}{2}I = -q_1 - q_2I.$$

Similarly, adding x_2 and x_3:

$$x_2 + x_3 = \frac{-q_1 + \sqrt{\Delta_1} - q_1 - \sqrt{\Delta_1}}{2} + \frac{-q_2 - (\sqrt{\Delta_1} + \sqrt{\Delta_2}) - q_2 + (\sqrt{\Delta_1} + \sqrt{\Delta_2})}{2}I = -q_1 - q_2I.$$

Thus,

$$x_1 + x_4 = x_2 + x_3 = -q_1 - q_2I.$$

(b) Summing all four roots:

$$\begin{aligned} x_1 + x_2 + x_3 + x_4 &= (x_1 + x_4) + (x_2 + x_3) \\ &= -q_1 - q_2I + -q_1 - q_2I \\ &= -2q_1 - 2q_2I. \end{aligned}$$

Thus,

$$x_1 + x_2 + x_3 + x_4 = -2q_1 - 2q_2I.$$

(c) Let's calculate the product of x_2 and x_3. We are given:

$$x_2 = a_1 + b_2I, x_3 = a_2 + b_3I,$$

where

$$a_1 = \frac{-q_1 + \sqrt{\Delta_1}}{2}, b_2 = \frac{-q_2 - (\sqrt{\Delta_1} + \sqrt{\Delta_2})}{2},$$

$$a_2 = \frac{-q_1 - \sqrt{\Delta_1}}{2}, b_3 = \frac{-q_2 + (\sqrt{\Delta_1} + \sqrt{\Delta_2})}{2}.$$

Thus, $x_2x_3 = a_1a_2 + (a_1b_3 + b_2a_2 + b_2b_3)I$.

Calculate the expressions for $a_1a_2a_1b_3$, b_2a_2, and b_2b_3:

$$a_1a_2 = \left(\frac{-q_1+\sqrt{\Delta_1}}{2}\right)\left(\frac{-q_1-\sqrt{\Delta_1}}{2}\right) = \frac{q_1^2-(\sqrt{\Delta_1})^2}{4} = \frac{q_1^2-\Delta_1}{4} = \frac{4r_1}{4} = r_1.$$

$$a_1b_3 = \left(\frac{-q_1+\sqrt{\Delta_1}}{2}\right)\left(\frac{-q_2+\sqrt{\Delta_1}+\sqrt{\Delta_2}}{2}\right) = \frac{q_1q_2-q_1(\sqrt{\Delta_1}+\sqrt{\Delta_2})-q_2\sqrt{\Delta_1}+\Delta_1+\sqrt{\Delta_1}\sqrt{\Delta_2}}{4}$$

$$b_2a_2 = \left(\frac{-q_2-\sqrt{\Delta_1}-\sqrt{\Delta_2}}{2}\right)\left(\frac{-q_1-\sqrt{\Delta_1}}{2}\right) = \frac{q_1q_2+q_1(\sqrt{\Delta_1}+\sqrt{\Delta_2})+q_2\sqrt{\Delta_1}+\Delta_1+\sqrt{\Delta_1}\sqrt{\Delta_2}}{4}$$

$$b_2b_3 = \left(\frac{-q_2-\sqrt{\Delta_1}-\sqrt{\Delta_2}}{2}\right)\left(\frac{-q_2+\sqrt{\Delta_1}+\sqrt{\Delta_2}}{2}\right) = \frac{q_2^2-(\sqrt{\Delta_1}+\sqrt{\Delta_2})^2}{4} = \frac{q_2^2-(\Delta_1+\Delta_2+2\sqrt{\Delta_1}\sqrt{\Delta_2})}{4}$$

Now, we add the expressions for a_1b_3, b_2a_2, and b_2b_3:

$$a_1b_3 + b_2a_2 + b_2b_3 = \frac{q_1q_2 - q_1(\sqrt{\Delta_1} + \sqrt{\Delta_2}) - q_2\sqrt{\Delta_1} + \Delta_1 + \sqrt{\Delta_1}\sqrt{\Delta_2}}{4}$$

$$+\frac{q_1q_2 + q_1(\sqrt{\Delta_1} + \sqrt{\Delta_2}) + q_2\sqrt{\Delta_1} + \Delta_1 + \sqrt{\Delta_1}\sqrt{\Delta_2}}{4} + \frac{q_2^2 - (\Delta_1 + \Delta_2 + 2\sqrt{\Delta_1}\sqrt{\Delta_2})}{4}.$$

After combining like terms, we get:

$$a_1b_3 + b_2a_2 + b_2b_3 = \frac{2q_1q_2 + q_2^2 + \Delta_1 - \Delta_2}{4}$$

$$= \frac{2q_1q_2 + q_2^2 + (q_1^2 - 4r_1) - [(q_1 + q_2)^2 - 4(r_1 + r_2)]}{4}$$

$$= \frac{2q_1q_2 + q_2^2 + q_1^2 - 4r_1 - (q_1^2 + 2q_1q_2 + q_2^2) + 4r_1 + 4r_2}{4} = \frac{4r_2}{4} = r_2.$$

Thus, we have shown that:

$$a_1b_3 + b_2a_2 + b_2b_3 = r_2.$$

After performing all the calculations and simplifying, we conclude:

$$x_2x_3 = a_1a_2 + (a_1b_3 + b_2a_2 + b_2b_3)I = r_1 + r_2I.$$

Similarly we can prove that

$$x_1x_4 = a_2a_2 + (a_1b_4 + b_1a_2 + b_1b_4)I = r_1 + r_2I.$$

(d) Now product of all solutions

$$\begin{aligned} x_1x_2x_3x_4 &= (x_1x_4)(x_2x_3) \\ &= (r_1 + r_2I)(r_1 + r_2I) \\ &= (r_1 + r_2I)^2. \end{aligned}$$

This completes the proof.

Example 4.7 *Consider the neutrosophic quadratic equation Type 1*

$$x^2 + (4 + 2I)x + (3 + 2I) = 0_I.$$

Here, we identify the coefficients $q_1 = 4$, $q_2 = 2$, $r_1 = 3$, and $r_2 = 2$. The roots are determined as follows. The discriminants are given by: $\Delta_1 = q_1^2 - 4r_1 = 4^2 - 4 \cdot 3 = 16 - 12 = 4$,

$$\Delta_2 = (q_1 + q_2)^2 - 4(r_1 + r_2) = (4 + 2)^2 - 4(3 + 2) = 6^2 - 4 \cdot 5 = 36 - 20 = 16.$$

The square roots of the discriminants are:

$$\sqrt{\Delta_1} = \sqrt{4} = 2, \qquad \sqrt{\Delta_2} = \sqrt{16} = 4.$$

Using the formulas for the roots, we substitute $q_1 = 4$, $\sqrt{\Delta_1} = 2$, $q_2 = 2$, and $\sqrt{\Delta_2} = 4$. The roots x_1, x_2, x_3, x_4 are computed as follows:

$$x_1 = \frac{-q_1 + \sqrt{\Delta_1}}{2} + \frac{-q_2 - (\sqrt{\Delta_1} - \sqrt{\Delta_2})}{2}I = \frac{-4 + 2}{2} + \frac{-2 - (2 - 4)}{2}I = -1$$

$$x_2 = \frac{-q_1 + \sqrt{\Delta_1}}{2} + \frac{-q_2 - (\sqrt{\Delta_1} + \sqrt{\Delta_2})}{2} I == \frac{-4+2}{2} + \frac{-2-(2+4)}{2} I = -1 - 4I$$

$$x_3 = \frac{-q_1 - \sqrt{\Delta_1}}{2} + \frac{-q_2 + (\sqrt{\Delta_1} + \sqrt{\Delta_2})}{2} I == \frac{-4-2}{2} + \frac{-2+(2+4)}{2} I = -3 + 2I$$

$$x_4 = \frac{-q_1 - \sqrt{\Delta_1}}{2} + \frac{-q_2 + (\sqrt{\Delta_1} - \sqrt{\Delta_2})}{2} I == \frac{-4-2}{2} + \frac{-2+(2-4)}{2} I == -3 - 2I.$$

The roots of the equation $x^2 + (4 + 2I)x + (3 + 2I) = 0_I$ are:

$$x_1 = -1,\ x_2 = -1 - 4I, x_3 = -3 + 2I,\ x_4 = -3 - 2I.$$

5. Solution of NQE Type 2

The neutrosophic quadratic equation of Type 2 is expressed as:

$$pIx^2 + (q_1 + q_2 I)x + (r_1 + r_2 I) = 0_I, \tag{6}$$

where p, q_1, q_2, r_1, r_2 are real constants, and I denotes the indeterminate unit.

To solve this equation, we substitute $x = a + bI$ into Equation (6):

$$pI(a + bI)^2 + (q_1 + q_2 I)(a + bI) + (r_1 + r_2 I) = 0_I. \tag{7}$$

First, expand $pI(a + bI)^2$:

$$pI(a + bI)^2 = pI(a^2 + 2abI + b^2 I^2) = (pa^2 + 2pab + pb^2)I, \text{(since } \mathrm{I}^2 = \mathrm{I}).$$

Next, expand $(q_1 + q_2 I)(a + bI)$:

$$(q_1 + q_2 I)(a + bI) = q_1 a + q_1 bI + q_2 aI + q_2 bI^2 = q_1 a + (q_1 b + q_2 a + q_2 b)I, \text{(since } \mathrm{I}^2 = \mathrm{I}).$$

Substitute these expansions back into Equation (7):

$$(pa^2 + 2pab + pb^2)I + q_1 a + (q_1 b + q_2 a + q_2 b)I + (r_1 + r_2 I) = 0_I.$$

Separate the real and indeterminate components:

$$(q_1 a + r_1) + (pa^2 + 2pab + pb^2 + q_1 b + q_2 a + q_2 b + r_2)I = 0_I.$$

Equating the coefficients of the real and indeterminate parts to zero gives:

$$q_1 a + r_1 = 0, \tag{8}$$

$$pb^2 + (2pa + q_1 + q_2)b + (pa^2 + q_2 a + r_2) = 0. \tag{9}$$

Solving for a and b From Equation (8), solve for a:

$$a = -\frac{r_1}{q_1}, \text{where } q_1 \neq 0.$$

Substitute $a = -\frac{r_1}{q_1}$ into Equation (9). The resulting quadratic equation in b has solutions b_1 and b_2. Therefore, the complete solution to the neutrosophic quadratic equation of Type 2 is:

$$x = a + b_1 I \quad \text{and} \quad x = a + b_2 I.$$

Example 5.1 *Consider the NQE of Type 2:*

$$2Ix^2 + (3 + 4I)x + (-6 + 8I) = 0_I.$$

Comparing this equation with Equation (6), we identify:

$$p = 2, q_1 = 3, q_2 = 4, r_1 = -6, r_2 = 8.$$

From Equation (8):

$$q_1 a + r_1 = 03a - 6 = 0 \qquad a = \frac{6}{3} = 2.$$

Next, substitute $a = 2$ into Equation (9):

$$pb^2 + (2pa + q_1 + q_2)b + (pa^2 + q_2 a + r_2) = 0.$$

Substituting the known values:

$$2b^2 + 15b + 24 = 0.$$

Solve this quadratic equation using the quadratic formula:

$$b_{1,2} = \frac{-15 \pm \sqrt{15^2 - 4 \cdot 2 \cdot 24}}{2 \cdot 2} = \frac{-15 \pm \sqrt{33}}{4}.$$

Thus, the two possible solutions for b are:

$$b_1 = \frac{-15 + \sqrt{33}}{4}, b_2 = \frac{-15 - \sqrt{33}}{4}.$$

Final Solutions The solutions for x are:

$$x_1 = 2 + \frac{-15 + \sqrt{33}}{4} I, \qquad x_2 = 2 + \frac{-15 - \sqrt{33}}{4} I.$$

6. Solution of NQE Type 3

The neutrosophic quadratic equation of Type 3 is expressed as:

$$p(-1 + I)x^2 + (q_1 + q_2 I)x + (r_1 + r_2 I) = 0_I. \tag{10}$$

To solve this equation, substitute $x = a + bI$ into Equation (10):

$$p(-1 + I)(a + bI)^2 + (q_1 + q_2 I)(a + bI) + (r_1 + r_2 I) = 0_I.$$

Expand the first term:

$$\begin{aligned} p(-1 + I)(a + bI)^2 &= p(-1 + I)(a^2 + (b^2 + 2ab)I) \\ &= -pa^2 + pa^2 I - p(b^2 + 2ab)I + p(b^2 + 2ab)I \\ &= -pa^2 + pa^2 I. \end{aligned}$$

Expand the second term:

$$(q_1 + q_2 I)(a + bI) = q_1 a + q_1 bI + q_2 aI + q_2 bI^2$$
$$= q_1 a + (q_1 b + q_2 a + q_2 b)I, \text{ (since } I^2 = I).$$

Substituting the expansions into the equation:

$$(-pa^2 + pa^2 I) + (q_1 a + (q_1 b + q_2 a + q_2 b)I) + (r_1 + r_2 I) = 0_I.$$

Separation of Components Group the real and I-components:

$$-pa^2 + q_1 a + r_1 + (pa^2 + q_1 b + q_2 a + q_2 b + r_2)I = 0_I.$$

Equating the coefficients of the real and indeterminate (I) parts to zero:

$$-pa^2 + q_1 a + r_1 = 0, \tag{11}$$

$$pa^2 + q_1 b + q_2 a + q_2 b + r_2 = 0. \tag{12}$$

Equation (11) is a quadratic equation in a. Solving using the quadratic formula:

$$a = \frac{-q_1 \pm \sqrt{q_1^2 - 4(-p)(r_1)}}{2(-p)}.$$

Simplifying further:

$$a_1 = \frac{q_1 + \sqrt{q_1^2 + 4pr_1}}{2p}, a_2 = \frac{q_1 - \sqrt{q_1^2 + 4pr_1}}{2p}.$$

Solving for b Substitute $a = a_1$ and $a = a_2$ into Equation (12):

$$pa^2 + q_1 b + q_2 a + q_2 b + r_2 = 0.$$

Grouping terms for b:

$$(q_1 + q_2)b = -pa^2 - q_2 a - r_2.$$

Solve for b:

$$b_1 = \frac{-pa_1^2 - q_2 a_1 - r_2}{q_1 + q_2}, b_2 = \frac{-pa_2^2 - q_2 a_2 - r_2}{q_1 + q_2}.$$

The complete solutions to the neutrosophic quadratic equation are:

$$x_1 = a_1 + b_1 I = a_1 + \frac{-pa_1^2 - q_2 a_1 - r_2}{q_1 + q_2} I,$$

$$x_2 = a_2 + b_2 I = a_2 + \frac{-pa_2^2 - q_2 a_2 - r_2}{q_1 + q_2} I.$$

Example 6.1 *Consider the neutrosophic quadratic equation of Type 3:*

$$-(-1 + I)x^2 + (-5 + 1I)x + (6 + 2I) = 0_I.$$

Here:

$$p = -1, q_1 = -5, q_2 = 1, r_1 = 6, r_2 = 2.$$

Solving for a From Equation (11):

$$-pa^2 + q_1 a + r_1 = 0.$$

Substitute the values:

$$a^2 - 5a + 6 = 0.$$

Using the quadratic formula:

$$a = \frac{5 \pm \sqrt{25 - 24}}{2} = \frac{5 \pm \sqrt{1}}{2}.$$

This gives:

$$a_1 = \frac{5 + 1}{2} = 3, a_2 = \frac{5 - 1}{2} = 2.$$

Solving for b Using Equation (12):

$$pa^2 + q_1 b + q_2 a + q_2 b + r_2 = 0.$$

Substitute the values:

$$b = \frac{-pa^2 - q_2 a - r_2}{q_1 + q_2} = \frac{a^2 - a - 2}{-4}.$$

For $a_1 = 3$:

$$b_1 = \frac{3^2 - 3 - 2}{-4} = -1.$$

For $a_2 = 2$:

$$b_2 = \frac{2^2 - 2 - 2}{-4} = 0.$$

The solutions for x are:

$$x_1 = 3 - I,\ x_2 = 2.$$

7. Conclusions

This work advances the study of neutrosophic quadratic equations by addressing key gaps in the literature, particularly the determination of roots and their behavior under uncertainty. The proposed framework enables systematic analysis and classification, contributing to the broader understanding of neutrosophic mathematics. Further research may extend this approach to higher-order neutrosophic polynomials. Additionally, applications of neutrosophic solutions in complex systems modeling, uncertain decision-making processes, and artificial intelligence are promising avenues for investigation. Studying the stability and behavior of these solutions in dynamic and probabilistic contexts could also reveal new properties and potential applications in systems with inherent indeterminacy.

Funding: This research received no external funding.

Acknowledgments: The author gratefully acknowledges the valuable suggestions of the editors and anonymous reviewers, which helped improve the quality of this manuscript.

Conflicts of Interest: The authors declare no conflict of interest.

References

1. Smarandache, F. Neutrosophy: Neutrosophic Probability, Set, and Logic. Am. Res. Press 1998.
2. Smarandache, F. A Unifying Field in Logics: Neutrosophic Logic. Am. Res. Press 1999.
3. Smarandache, F. Proceedings of the First International Conference on Neutrosophy: Neutrosophic Set, Neutrosophic Probability, and Statistics. Univ. New Mexico Press 2001.
4. Smarandache, F. Neutrosophy and Neutrosophic Logic: First International Conference on Neutrosophy. Univ. New Mexico 2002.

5. Smarandache, F. Introduction to Neutrosophic Measure, Neutrosophic Integral, and Neutrosophic Probability. Sitech-Educ. Publ. 2013.
6. Smarandache, F. Finite Neutrosophic Complex Numbers (by W. B. V. Kandasamy). Zip Publ. 2011, 1–16.
7. Smarandache, F. Introduction to Neutrosophic Statistics. Sitech-Educ. Publ. 2014, 34–44.
8. Smarandache, F. Neutrosophic Precalculus and Neutrosophic Calculus. Book 2015.
9. Alhasan, Y. Concepts of Neutrosophic Complex Numbers. Int. J. Neutrosophic Sci. 2020, 8(1), 9–18.
10. Alhasan, Y. The General Exponential Form of a Neutrosophic Complex Number. Int. J. Neutrosophic Sci. 2020, 11(2), 100–107.
11. Abobala, M.; Hatip, A. An Algebraic Approach to Neutrosophic Euclidean Geometry. Neutrosophic Sets Syst. 2021, 43(1), 10.
12. Alhasan, Y.A.; Musa, I.A. The Neutrosophic Limits. Neutrosophic Sets Syst. 2023, 53(1), 23.
13. Narzary, G.; Basumatary, B. A Study on n-th Derivative of Neutrosophic Function and Neutrosophic Differential Equation. Neutrosophic Sets Syst. 2025, 75, 29–49.
14. Alhasan, Y.A. The Neutrosophic Differentials Calculus. Neutrosophic Sets Syst. 2022, 49, 357–374.
15. Alhasan, Y.A. The Equations of Neutrosophic Straight Line and Neutrosophic Circle. Neutrosophic Sets Syst. 2023, 53(1), 20.
16. Alhasan, Y.A. The Neutrosophic Linear Differential Equations. NeuroQuantology 2022, 20(14), 988.
17. Alhasan, Y. The Neutrosophic Integrals and Integration Methods. Neutrosophic Sets Syst. 2021, 43, 290–301.
18. Alhasan, Y.A.; Musa, I.A.; Sheen, S. Convert Between Neutrosophic Complex Numbers Forms. Neutrosophic Sets Syst. 2023, 56(1), 3.
19. Alvaracín Jarrín, A.A.; Proaño Tamayo, D.S.; Montecé Giler, S.A.; Arandia Zambrano, J.C.; Macazana, D.M. Neutrosophic Statistics Applied in Social Science. Neutrosophic Sets Syst. 2021, 44(1), 1.
20. Alhasan, Y.A.; Sheen, S.; Abdulfatah, R.A. Double Neutrosophic Integrals. Neutrosophic Sets Syst. 2023, 58(1), 5.
21. Çeven, Y.; Sekmen, A.İ. On Neutrosophic Square Matrices and Solutions of Systems of Linear Equations. SDU J. Sci. 2023, 18(3), 203–212.
22. Abobala, M. On Some Neutrosophic Algebraic Equations. J. New Theory 2020, 33, 26–32.
23. Al-Tahan, M. Some Results on Single Valued Neutrosophic (Weak) Polygroups. Int. J. Neutrosophic Sci. 2020, 2(1), 38–46.
24. Edalatpanah, S. A Direct Model for Triangular Neutrosophic Linear Programming. Int. J. Neutrosophic Sci. 2020, 1(1), 19–28.
25. Chakraborty, A. A New Score Function of Pentagonal Neutrosophic Number and Its Application in Networking Problem. Int. J. Neutrosophic Sci. 2020, 1(1), 40–51.
26. Chakraborty, A. Application of Pentagonal Neutrosophic Number in Shortest Path Problem. Int. J. Neutrosophic Sci. 2020, 3(1), 21–28.
27. Abdel-Basset, M. An Approach of TOPSIS Technique for Developing Supplier Selection with Group Decision Making under Type-2 Neutrosophic Number. Appl. Soft Comput. 2019, 83, 438–452.

Neutrosophic Knowledge, Vol. 09, 2026
University of New Mexico

Article

Neutrosophic Split Quaternions and Their Matrix Forms

Ceremnur Tetik [1,*] and Abdullah Dertli [2]

1 Department of Mathematics, Ondokuz Mayıs University, Türkiye; ceremnurtetik@gmail.com
2 Department of Mathematics, Ondokuz Mayıs University, Türkiye; abdullah.dertli@omu.edu.tr

* Correspondence: ceremnurtetik@gmail.com

Received: 01-28-2026; *Accepted:* 02-20-2026.

Abstract: In this study, we developed a new approach to split quaternions using neutrosophic sets, which have recently gained attention in mathematics, and examined some properties of neutrosophic split quaternions. We also provided the matrix form of these new quaternions.

Keywords: neutrosophic numbers; neutrosophic split quaternions; neutrosophic split quaternion matrices.

1. Introduction

Quaternions were introduced by the Irish mathematician Sir William Rowan Hamilton in 1843 and hold a significant place in mathematics, [1]. Quaternions, also known as four-dimensional hypercomplex numbers, are widely utilized in various mathematical fields such as commutative ring theory, number theory, group theory, geometric topology, spectral theory of Riemannian manifolds, algebraic geometry, as well as in physics and engineering.

After the work of Hamilton, in 1849, James Cockle introduced the set of split quaternions, [2]. Later, Alagöz, Oral and Yüce gave the matrix form of split quaternions and studied their properties, [3]. Split quaternions can be represented as

$$H_S = \{q \mid q = a_0 + a_1 i + a_2 j + a_3 k, a_n \in \mathbb{R}, n = 0,1,2,3\},$$

where the split quaternion bases i, j and k satisfy the following identities are known as

$$i^2 = -1, j^2 = k^2 = 1, ijk = 1.$$

For any $q = a_0 + a_1 i + a_2 j + a_3 k \in H_S$, the real part of q defined by $Re(q) = a_0$ and the imaginary part of q defined by $Im(q) = a_1 i + a_2 j + a_3 k$. The conjugate of a split quaternion number is defined as $\bar{q} = a_0 - a_1 i - a_2 j - a_3 k$. The split quaternion multiplication is not commutative.

Neutrosophic numbers, a concept with roots in neutrosophy, were first introduced by Florentin Smarandache in the early 21st century, [4]. The set of real neutrosophic real numbers is defined as

$$N(\mathbb{R}) = \{q_I = a + bI \mid a, b \in \mathbb{R}\},$$

where $I^n = I,\ 0.I = 0,\ I$ represents indeterminacy.

More detailed information about neutrosophic numbers can be found in [4]. Also, using this definition, Alhasan defined the general exponential form of a neutrosophic complex number, [5]. A neutrosophic complex number is represented as

$$(x_1 + y_1 I) + (x_2 + y_2 I)i,$$

where $x_1, x_2, y_1, y_2 \in \mathbb{R}$, $i^2 = -1$ and I is the indeterminacy element.

Neutrosophic numbers provide an extended mathematical framework by incorporating indeterminacy into classical number systems. Within this framework, uncertain information can be modeled more effectively by taking into account the components of truth, indeterminacy and falsity together. This approach is particularly advantageous for the analysis of complex and uncertain data encountered in fields such as artificial intelligence, decision-making and quantum mechanics.

In recent years, Dertli and Tetik have combined the recently popular concepts of non-Newtonian calculus and neutrosophy to define and examine some of the properties of non-Newtonian neutrosophic numbers and non-Newtonian neutrosophic complex numbers, [6]. They also presented the non-Newtonian neutrosophic triangle inequality, frequently used in analysis and geometry and some properties of the non-Newtonian neutrosophic norm. This provides a broader perspective compared to existing studies, encompassing fields such as quantum mechanics, artificial intelligence, analysis, geometry and medicine.

Drawing on the works of Smarandache, Alhasan et al. introduced the notion of neutrosophic quaternion numbers in 2024, [7]. The set of neutrosophic quaternion numbers are defined as

$$H_N = \left\{ \begin{array}{c} q_I = a_0 + b_0 I + v_I \mid v_I = (a_1 + b_1 I)i + (a_2 + b_2 I)j + (a_3 + b_3 I)k, \\ a_s, b_s \in \mathbb{R}, s = 0,1,2,3 \end{array} \right\},$$

where $I^n = I,\ 0.I = 0,\ I$ represents the indeterminacy and the quaternion bases $i,\ j$ and k satisfy the following identities

$$i^2 = j^2 = k^2 = ijk = -1, ij = -ji = k, jk = -kj = i, ki = -ik = j.$$

The neutrosophic quaternion number $q_I = a_0 + b_0 I + v_I$ consist of two parts. The part $a_0 + b_0 I$ is called the neutrosophic real (scalar) part; the part $v_I = (a_1 + b_1 I)i + (a_2 + b_2 I)j + (a_3 + b_3 I)k$ is called the neutrosophic vector part. The conjugate of a neutrosophic quaternion number is defined as $\overline{q_I} = a_0 + b_0 I - v_I = a_0 + b_0 I - (a_1 + b_1 I)i - (a_2 + b_2 I)j - (a_3 + b_3 I)k$. The neutrosophic quaternion multiplication is not commutative.

Based on these definitions, in this study we define neutrosophic split quaternions and their matrix representations. Moreover, we examine some of their properties.

2. The Neutrosophic Split Quaternions

Definition 2.1. The set of neutrosophic split quaternion numbers is defined as

$$H_{S_N} = \left\{ \begin{matrix} q_N = a_0 + b_0 I + v_I \mid v_I = (a_1 + b_1 I)i + (a_2 + b_2 I)j + (a_3 + b_3 I)k, \\ a_s, b_s \in \mathbb{R}, s = 0,1,2,3 \end{matrix} \right\},$$

where $I^n = I,\ 0.I = 0,\ I$ represents the indeterminacy and the split quaternion bases $i,\ j$ and k satisfy the following identities

$$i^2 = -1, j^2 = k^2 = 1, ij = -ji = k, jk = -kj = -i, ki = -ik = j.$$

Definition 2.2. The operations of addition and multiplication for neutrosophic split quaternions are given by

$$\begin{aligned} +: H_{S_N} \times H_{S_N} &\rightarrow H_{S_N} \\ (q_N, p_N) &\rightarrow q_N + p_N = (a_0 + b_0 I + v_I) + (c_0 + d_0 I + u_I) \\ &\qquad = (a_0 + c_0) + (b_0 + d_0)I \\ &\qquad + \big((a_1 + c_1) + (b_1 + d_1)I\big)i \\ &\qquad + \big((a_2 + c_2) + (b_2 + d_2)I\big)j \\ &\qquad + \big((a_3 + c_3) + (b_3 + d_3)I\big)k \end{aligned}$$

and

$$\begin{aligned} \cdot : H_{S_N} \times H_{S_N} &\rightarrow H_{S_N} \\ (q_N, p_N) &\rightarrow q_N \cdot p_N = (a_0 + b_0 I)(c_0 + d_0 I) - (a_1 + b_1 I)(c_1 + d_1 I) \\ &\qquad + (a_2 + b_2 I)(c_2 + d_2 I) + (a_3 + b_3 I)(c_3 + d_3 I) \\ &\qquad + xi + yj + zk, \end{aligned}$$

where

$$\begin{aligned} x &= (a_0+b_0I)(c_1+d_1I)+(a_1+b_1I)(c_0+d_0I) \\ &\quad -(a_2+b_2I)(c_3+d_3I)+(a_3+b_3I)(c_2+d_2I), \\ y &= (a_0+b_0I)(c_2+d_2I)-(a_1+b_1I)(c_3+d_3I) \\ &\quad +(a_2+b_2I)(c_0+d_0I)+(a_3+b_3I)(c_1+d_1I), \\ z &= (a_0+b_0I)(c_3+d_3I)+(a_1+b_1I)(c_2+d_2I) \\ &\quad -(a_2+b_2I)(c_1+d_1I)+(a_3+b_3I)(c_0+d_0I). \end{aligned}$$

Example 2.3. Let $q_N = 1+2I+(3+5I)i+(1+4I)j+(2+3I)k$ and $p_N = 3+I+(2+2I)i+(1+I)j+(2+4I)k$. The addition and multiplication of $q_N, p_N \in H_{S_N}$ are

$$q_N + p_N = 4+3I+(5+7I)i+(2+5I)j+(4+7I)k$$

and

$$q_N \cdot p_N = 2+18I+(11+13I)i+(-12I)j+(9+25I)k,$$

respectively.

Definition 2.4. The conjugate of a neutrosophic split quaternion $q_N = a_0+b_0I+v_I$ is $\overline{q_N} = a_0+b_0I-v_I = a_0+b_0I-(a_1+b_1I)i-(a_2+b_2I)j-(a_3+b_3I)k$.

Remark 2.5. For $q_1, q_2 \in H_S$, neutrosophic split quaternions can be written as

$$\begin{aligned} q_N &= b_0+c_0I+(b_1+c_1I)i+(b_2+c_2I)j+(b_3+c_3I)k \\ &= (b_0+c_0I, b_1+c_1I, b_2+c_2I, b_3+c_3I) \\ &= (b_0,b_1,b_2,b_3)+(c_0,c_1,c_2,c_3)I \\ &= (b_0+b_1i+b_2j+b_3k)+(c_0+c_1i+c_2j+c_3k)I \\ &= q_1+q_2I. \end{aligned}$$

In addition, we can write the conjugate of a neutrosophic split quaternion as $\overline{q_N} = \overline{q_1}+\overline{q_2}I$.

Example 2.6. Let $q_N = 1+3I+(2+5I)i+(3+I)j+(1+2I)k \in H_{S_N}$. We can write

$$\begin{aligned} q_N &= (1+3I, 2+5I, 3+I, 1+2I) \\ &= (1,2,3,1)+(3,5,1,2)I \\ &= (1+2i+3j+k)+(3+5i+j+2k)I \\ &= q_1+q_2I. \end{aligned}$$

Furthermore, the conjugate of q_N is

$$\begin{aligned} \overline{q_N} &= \overline{q_1}+\overline{q_2}I \\ &= (1-2i-3j-k)+(3-5i-j-2k)I \\ &= 1+3I-(2+5I)i-(3+I)j-(1+2I)k. \end{aligned}$$

Definition 2.7. For a neutrosophic split quaternion $q_N = b_0+c_0I+v_I = b_0+c_0I+(b_1+c_1I)i+(b_2+c_2I)j+(b_3+c_3I)k$, b_0+c_0I is called the neutrosophic scalar part of q_N and $v_I = (b_1+c_1I)i+(b_2+c_2I)j+(b_3+c_3I)k$ is called the neutrosophic vector or imaginary part of q_N. Denoted by $S^*(q_N)$ and $V^*(q_N)$, respectively. Therefore, a neutrosophic split quaternion q_N can be written as $q_N = S^*(q_N) + V^*(q_N)$. Since $q_N + p_N = (b_0 + d_0) + (c_0 + e_0)I + \big((b_1 + d_1) + (c_1 + e_1)I\big)i + \big((b_2 + d_2) + (c_2 + e_2)I\big)j + \big((b_3 + d_3) + (c_3 + e_3)I\big)k$ neutrosophic split quaternions can be written as $S^*(q_N + p_N) = S^*(q_N) + S^*(p_N)$. Similarly, it can be easily seen that $V^*(q_N + p_N) = V^*(q_N) + V^*(p_N)$.

Using the above two definitions, the following corollary can be given:

Corollary 2.8. The neutrosophic real and neutrosophic imaginary parts of $q_N \in H_{S_N}$ are

$$S^*(q_N) = \frac{1}{2}(q_N + \overline{q_N})$$

and

$$V^*(q_N) = \frac{1}{2}(q_N - \overline{q_N}),$$

respectively.

Definition 2.9. The norm of a neutrosophic split quaternion is defined as

$$N_{q_N} = q_N \cdot \overline{q_N} = (b_0 + c_0 I)^2 + (b_1 + c_1 I)^2 - (b_2 + c_2 I)^2 - (b_3 + c_3 I)^2.$$

Definition 2.10. The inverse of a neutrosophic split quaternion is defined as

$$q_N^{-1} = \frac{\overline{q_N}}{N_{q_N}}.$$

Example 2.11. Let $q_N = 3 + I + (2 + 2I)i + (1 + I)j + (2 + 4I)k \in H_{S_N}$. The norm of q_N and inverse of q_N are

$$\begin{aligned} N_{q_N} &= (3 + I)^2 + (2 + 2I)^2 - (1 + I)^2 - (2 + 4I)^2 \\ &= 8 - 16I \end{aligned}$$

and

$$\begin{aligned} q_N^{-1} &= \frac{3 + I - (2 + 2I)i - (1 + I)j - (2 + 4I)k}{8 - 16I} \\ &= \frac{3 + I}{8 - 16I} - \left(\frac{2 + 2I}{8 - 16I}\right)i - \left(\frac{1 + I}{8 - 16I}\right)j - \left(\frac{2 + 4I}{8 - 16I}\right)k \\ &= \frac{1}{8}(3 - 14I - (2 - 12I)i - (1 + 6I)j - (2 - 16I)k), \end{aligned}$$

respectively.

Theorem 2.12. For any $q_N, p_N \in H_{S_N}$ and $\lambda \in \mathbb{R}$ we have,

1) $\overline{q_N \cdot p_N} = \overline{q_N} \cdot \overline{p_N}$,

2) $\overline{q_N + p_N} = \overline{q_N} + \overline{p_N}$, $\overline{q_N - p_N} = \overline{q_N} - \overline{p_N}$,

3) $\overline{\overline{q_N}} = q_N$,

4) $\overline{\overline{q_N} \cdot p_N} = \overline{p_N} \cdot q_N$,

5) $q_N \cdot \overline{q_N} = \overline{q_N} \cdot q_N = N_{q_N}$,

6) $\overline{\lambda q_N} = \lambda \overline{q_N}$,

Proof.

1) Let $q_N = (a_0 + b_0 I) + (a_1 + b_1 I)i + (a_2 + b_2 I)j + (a_3 + b_3 I)k$ and $p_N = (c_0 + d_0 I) + (c_1 + d_1 I)i + (c_2 + d_2 I)j + (c_3 + d_3 I)k$. Then $\overline{q_N} = (a_0 + b_0 I) - (a_1 + b_1 I)i - (a_2 + b_2 I)j - (a_3 + b_3 I)k$ and $\overline{p_N} = (c_0 + d_0 I) - (c_1 + d_1 I)i - (c_2 + d_2 I)j - (c_3 + d_3 I)k$. Using the multiplication of neutrosophic split quaternions and the definition of the conjugate of a neutrosophic split quaternion, we obtain

$$\begin{aligned} \overline{q_N \cdot p_N} = {} & (a_0 + b_0 I)(c_0 + d_0 I) - (a_1 + b_1 I)(c_1 + d_1 I) \\ & + (a_2 + b_2 I)(c_2 + d_2 I) + (a_3 + b_3 I)(c_3 + d_3 I) \\ & - [(a_0 + b_0 I)(c_1 + d_1 I) + (a_1 + b_1 I)(c_0 + d_0 I) \\ & - (a_2 + b_2 I)(c_3 + d_3 I) + (a_3 + b_3 I)(c_2 + d_2 I)]i \\ & - [(a_0 + b_0 I)(c_2 + d_2 I) - (a_1 + b_1 I)(c_3 + d_3 I) \\ & + (a_2 + b_2 I)(c_0 + d_0 I) + (a_3 + b_3 I)(c_1 + d_1 I)]j \\ & - [(a_0 + b_0 I)(c_3 + d_3 I) + (a_1 + b_1 I)(c_2 + d_2 I) \\ & - (a_2 + b_2 I)(c_1 + d_1 I) + (a_3 + b_3 I)(c_0 + d_0 I)]k \end{aligned}$$

and

$$\begin{aligned} \overline{q_N} \cdot \overline{p_N} = {} & (c_0 + d_0 I)(a_0 + b_0 I) - (c_1 + d_1 I)(a_1 + b_1 I) \\ & + (c_2 + d_2 I)(a_2 + b_2 I) + (c_3 + d_3 I)(a_3 + b_3 I) \\ & + [-(c_0 + d_0 I)(a_1 + b_1 I) - (c_1 + d_1 I)(a_0 + b_0 I) \\ & - (c_2 + d_2 I)(a_3 + b_3 I) + (c_3 + d_3 I)(a_2 + b_2 I)]i \\ & + [-(c_0 + d_0 I)(a_2 + b_2 I) - (c_1 + d_1 I)(a_3 + b_3 I) \\ & - (c_2 + d_2 I)(a_0 + b_0 I) + (c_3 + d_3 I)(a_1 + b_1 I)]j \\ & + [-(c_0 + d_0 I)(a_3 + b_3 I) + (c_1 + d_1 I)(a_2 + b_2 I) \\ & - (c_2 + d_2 I)(a_1 + b_1 I) - (c_3 + d_3 I)(a_0 + b_0 I)]k. \end{aligned}$$

Thus, it is easily seen that $\overline{q_N \cdot p_N} = \overline{q_N} \cdot \overline{p_N}$.

5) Let $q_N = (b_0 + c_0 I) + (b_1 + c_1 I)i + (b_2 + c_2 I)j + (b_3 + c_3 I)k$. Using the multiplication of neutrosophic split quaternions, the definition of the conjugate of a neutrosophic split quaternion and the norm of a neutrosophic split quaternion, we obtain

$$
\begin{aligned}
q_N \cdot \overline{q_N} &= (b_0+c_0I)^2+(b_1+c_1I)^2-(b_2+c_2I)^2-(b_3+c_3I)^2 \\
&\quad +[-(b_0+c_0I)(b_1+c_1I)+(b_1+c_1I)(b_0+c_0I) \\
&\quad +(b_2+c_2I)(b_3+c_3I)-(b_3+c_3I)(b_2+c_2I)]i \\
&\quad +[-(b_0+c_0I)(b_2+c_2I)+(b_1+c_1I)(b_3+c_3I) \\
&\quad +(b_2+c_2I)(b_0+c_0I)-(b_3+c_3I)(b_1+c_1I)]j \\
&\quad +[-(b_0+c_0I)(b_3+c_3I)-(b_1+c_1I)(b_2+c_2I) \\
&\quad +(b_2+c_2I)(b_1+c_1I)+(b_3+c_3I)(b_0+c_0I)]k \\
&= (b_0+c_0I)^2+(b_1+c_1I)^2-(b_2+c_2I)^2-(b_3+c_3I)^2 \\
&= N_{q_N}
\end{aligned}
$$

and

$$
\begin{aligned}
\overline{q_N} \cdot q_N &= (b_0+c_0I)^2+(b_1+c_1I)^2-(b_2+c_2I)^2-(b_3+c_3I)^2 \\
&\quad +[(b_0+c_0I)(b_1+c_1I)-(b_1+c_1I)(b_0+c_0I) \\
&\quad +(b_2+c_2I)(b_3+c_3I)-(b_3+c_3I)(b_2+c_2I)]i \\
&\quad +[(b_0+c_0I)(b_2+c_2I)+(b_1+c_1I)(b_3+c_3I) \\
&\quad -(b_2+c_2I)(b_0+c_0I)-(b_3+c_3I)(b_1+c_1I)]j \\
&\quad +[(b_0+c_0I)(b_3+c_3I)-(b_1+c_1I)(b_2+c_2I) \\
&\quad +(b_2+c_2I)(b_1+c_1I)-(b_3+c_3I)(b_0+c_0I)]k \\
&= (b_0+c_0I)^2+(b_1+c_1I)^2-(b_2+c_2I)^2-(b_3+c_3I)^2 \\
&= N_{q_N}.
\end{aligned}
$$

Thus, it is easily seen that $q_N \cdot \overline{q_N} = \overline{q_N} \cdot q_N = N_{q_N}$.

Other properties can be similarly proven.□

Let us now obtain the matrix representation of the neutrosophic split quaternion.

Theorem 2.13. Every neutrosophic split quaternion can be represented by a 2×2 neutrosophic complex matrix.

Proof.

Let $q_N \in H_{S_N}$, then there exist complex numbers q_1', q_1'', q_2', q_2'' such that $q = (q_1' + q_2'I) + (q_1'' + q_2''I)j$ by definition of neutrosophic complex numbers.

The linear map $\varphi_q: H_{S_N} \to H_{S_N}$ is defined by $\varphi_q(p_N) = p_N.q$ for all $p_N \in H_{S_N}$. This map is bijective and

$$\varphi_q(1) = 1\big((q_1' + q_2'I) + (q_1'' + q_2''I)j\big) = (q_1' + q_2'I) + (q_1'' + q_2''I)j,$$

$$\varphi_q(j) = j\big((q_1' + q_2'I) + (q_1'' + q_2''I)j\big) = \big(\overline{q_1'} + \overline{q_2'}I\big)j + \big(\overline{q_1''} + \overline{q_2''}I\big).$$

With this transformation neutrosophic split quaternions are defined as subset of the matrix ring $M_2\big(N(\mathbb{C})\big)$, the set of 2×2 neutrosophic complex matrices:

$$H'_{S_N} = \left\{ \begin{pmatrix} q'_1 + q'_2 I & q''_1 + q''_2 I \\ \overline{q''_1} + \overline{q''_2} I & \overline{q'_1} + \overline{q'_2} I \end{pmatrix} : q'_1, q''_1, q'_2, q''_2 \in \mathbb{C} \right\}.$$

H_{S_N} and H'_{S_N} are essentially the same. ▯

Note 2.14. $\mathcal{M}: q = (q'_1 + q'_2 I) + (q''_1 + q''_2 I)j \in H_{S_N} \longrightarrow q' = \begin{pmatrix} q'_1 + q'_2 I & q''_1 + q''_2 I \\ \overline{q''_1} + \overline{q''_2} I & \overline{q'_1} + \overline{q'_2} I \end{pmatrix} \in H'_{S_N}$

is bijective and preserves the operations.

Definition 2.15. Let $\mathcal{Q} = \begin{pmatrix} q'_1 + q'_2 I & q''_1 + q''_2 I \\ \overline{q''_1} + \overline{q''_2} I & \overline{q'_1} + \overline{q'_2} I \end{pmatrix}$ and $\mathcal{P} = \begin{pmatrix} p'_1 + p'_2 I & p''_1 + p''_2 I \\ \overline{p''_1} + \overline{p''_2} I & \overline{p'_1} + \overline{p'_2} I \end{pmatrix}$

be any two 2×2 neutrosophic complex matrices. The sum and product of $\mathcal{Q}$ and $\mathcal{P}$ are defined as

$$\mathcal{Q} \oplus \mathcal{P} = \begin{pmatrix} q'_1 + q'_2 I & q''_1 + q''_2 I \\ \overline{q''_1} + \overline{q''_2} I & \overline{q'_1} + \overline{q'_2} I \end{pmatrix} \oplus \begin{pmatrix} p'_1 + p'_2 I & p''_1 + p''_2 I \\ \overline{p''_1} + \overline{p''_2} I & \overline{p'_1} + \overline{p'_2} I \end{pmatrix}$$

$$= \begin{pmatrix} (q'_1 + p'_1) + (q'_2 + p'_2)I & (q''_1 + p''_1) + (q''_2 + p''_2)I \\ (\overline{q''_1} + \overline{p''_1}) + (\overline{q''_2} + \overline{p''_2})I & (\overline{q'_1} + \overline{p'_1}) + (\overline{q'_2} + \overline{p'_2})I \end{pmatrix}$$

and

$$\mathcal{Q} \otimes \mathcal{P} = \begin{pmatrix} \alpha_1 & \alpha_2 \\ \alpha_3 & \alpha_4 \end{pmatrix},$$

respectively, where

$$\alpha_1 = (q'_1 + q'_2 I)(p'_1 + p'_2 I) + (q''_1 + q''_2 I)(\overline{p''_1} + \overline{p''_2} I),$$

$$\alpha_2 = (q'_1 + q'_2 I)(p''_1 + p''_2 I) + (q''_1 + q''_2 I)(\overline{p'_1} + \overline{p'_2} I),$$

$$\alpha_3 = (\overline{q''_1} + \overline{q''_2} I)(p'_1 + p'_2 I) + (\overline{q'_1} + \overline{q'_2} I)(\overline{p''_1} + \overline{p''_2} I),$$

$$\alpha_4 = (\overline{q''_1} + \overline{q''_2} I)(p''_1 + p''_2 I) + (\overline{q'_1} + \overline{q'_2} I)(\overline{p'_1} + \overline{p'_2} I).$$

3. Conclusions

In this study, we re-examined split quaternions and split quaternion matrices using neutrosophic sets. Our findings offer new perspectives on quaternion theory and pave the way for future research on neutrosophic applications. In future studies, the properties of neutrosophic split quaternion matrices can be examined and neutrosophic split quaternions can be combined with number sequences.

Funding: This research received no external funding.

Conflicts of Interest: The authors declare no conflict of interest.

References

1. Van Der Waerden, B. L. (1976). Hamilton's discovery of quaternions. *Mathematics Magazine*, *49*(5), 227-234. https://doi.org/10.1080/0025570X.1976.11976586

2. Cockle, J. (1849). LII. On systems of algebra involving more than one imaginary; and on equations of the fifth degree. *The London, Edinburgh, and Dublin Philosophical Magazine and Journal of Science*, *35*(238), 434-437. https://doi.org/10.1080/14786444908646384

3. Alagöz, Y., Oral, K. H., & Yüce, S. (2012). Split quaternion matrices. *Miskolc Mathematical Notes*, *13*(2), 223-232. https://doi.org/10.18514/MMN.2012.364

4. Smarandache, F. (2002). Neutrosophy and neutrosophic logic, first international conference on neutrosophy, neutrosophic logic, set, probability, and statistics. *University of New Mexico, Gallup, NM*, *87301*.

5. Alhasan, Y. (2020). The general exponential form of a neutrosophic complex number. *International Journal of Neutrosophic Science*, *11*(2), 100-107. https://doi.org/10.5281/ZENODO.4165054

6. Dertli, A., & Tetik, C. (2025). New Approach to Neutrosophic Numbers and Neutrosophic Complex Numbers. *Axioms*, *14*(3), 212. https://doi.org/10.3390/axioms14030212

7. Alhasan, Y. A., Alarnous, B. H., & Musa, I. A. (2024). The neutrosophic quaternions numbers. *Neutrosophic Sets and Systems*, *64*, 46-56.

Neutrosophic Knowledge, Volume 9, 2026

University of New Mexico

Meta-Fuzzy Graph, Meta-Neutrosophic Graph, Meta-Digraph, and Meta-MultiGraph with some applications

Takaaki Fujita[1] *, *Ajoy Kanti Das* [2], *Suman Das* [3], *Sankar Prasad Mondal* [4]

[1] Independent Researcher, Tokyo, Japan. (Takaaki.fujita060@gmail.com)

[2] Associate Professor, Department of Mathematics, Tripura University, Agartala-799022, Tripura, India. (ajoykantidas@gmail.com)

[3] Assistant Professor (Mathematics), Department of Education (ITEP), NIT Agartala, Jirania, 799046, Tripura, India. (dr.sumandas1995@gmail.com)

[4] Department of Applied Mathematics, Maulana Abul Kalam Azad University of Technology, West Bengal, Haringhata-741249, West Bengal, India. (sankar.mondal02@gmail.com)

*Correspondence: Takaaki.fujita060@gmail.com

Received*: 02/04/2026;* Accepted*: 02/20/2026*

Abstract. Graph theory investigates mathematical structures consisting of vertices and edges to model relationships and connectivity. A *MetaGraph* is a higher-level graph whose vertices are themselves graphs, with edges representing specified relations among those graphs. An *Iterated MetaGraph* extends this idea recursively: its vertices are MetaGraphs, yielding a hierarchy of graph-of-graphs structures across multiple levels.

Fuzzy graphs incorporate fuzzy membership functions on vertices and edges, thereby capturing uncertainty and graded strength of connectivity. Neutrosophic graphs generalize this further by assigning to each vertex and edge three independent membership values—truth, indeterminacy, and falsity—providing a more comprehensive framework for uncertainty. A weighted graph is a graph in which each edge is assigned a numerical value (weight), typically representing cost, distance, or intensity. Multigraphs, which allow multiple parallel edges and loops, appear naturally when such multiplicities are required. Bidirected graphs (bidigraphs) assign local orientations to each vertex-edge incidence, allowing edges to point independently at both ends.

In this paper, we extend the frameworks of fuzzy graphs, neutrosophic graphs, multigraphs, weighted graphs, digraphs, and bidirected graphs by embedding them into the unified setting of MetaGraphs and Iterated MetaGraphs.

Keywords: Fuzzy Graph, Neutrosophic Graph, MultiGraph, Bidirected Graph, Weighted Graph, MetaGraph, Iterated MetaGraph

1. Preliminaries

This section presents the fundamental concepts and definitions that underpin the discussions in this paper. Unless otherwise noted, all graphs considered here are *undirected*, *finite*, and *simple*.

1.1. *MetaGraph (Graph of Graph)*

Graph theory investigates mathematical structures consisting of vertices and edges to model relationships and connectivity [1]. A MetaGraph is a graph whose vertices are themselves graphs, with edges representing specified relations between those graphs (cf. [2–4]).

Definition 1.1 (Metagraph (graph of graphs))**.** (cf. [5]) Fix a nonempty universe $\mathfrak{G}$ of finite graphs (undirected, loopless by default) and a nonempty family of binary relations

$$\mathcal{R} \subseteq \mathcal{P}\big(\mathfrak{G} \times \mathfrak{G}\big).$$

A *metagraph over* $(\mathfrak{G}, \mathcal{R})$ is a directed, labelled multigraph

$$M = (V, E, s, t, \lambda)$$

with

$$V \subseteq \mathfrak{G}, \qquad s, t : E \to V, \qquad \lambda : E \to \mathcal{R},$$

satisfying the incidence constraint

$$\forall e \in E : \big(s(e), t(e)\big) \in \lambda(e).$$

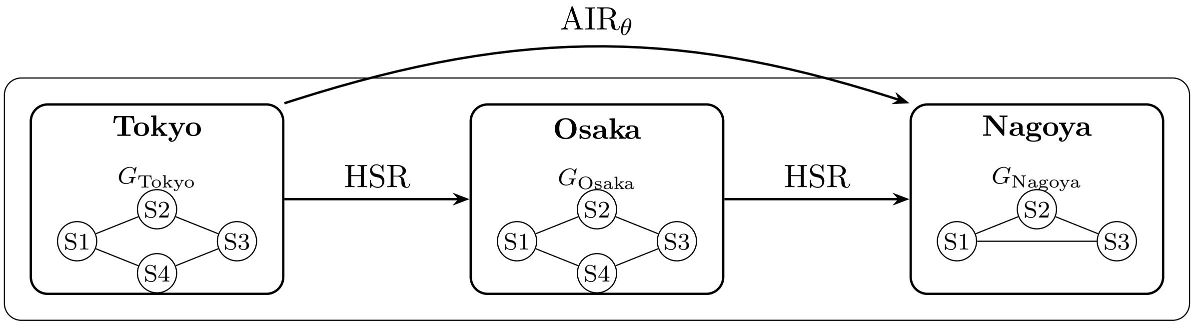

FIGURE 1. Urban mobility as a metagraph: each meta-vertex is a city-level transit graph, and meta-edges encode inter-city mobility relations (HSR, AIR$_\theta$).

Elements of V are *meta-vertices* (each is a graph $G \in \mathfrak{G}$). For $e \in E$ with $\lambda(e) = R$, we write $s(e) \xrightarrow{R} t(e)$ and call e a *meta-edge*. If $\mathcal{R} = \{R\}$ is a singleton, labels may be omitted. If every $R \in \mathcal{R}$ is symmetric, M can be viewed as an undirected labelled multigraph.

Example 1.2 (Urban Mobility as a Metagraph)**.** Let $\mathfrak{G}$ be the set of *city-level transit graphs* $G_c = (V_c, E_c)$, where V_c are stations in city c and E_c are intra-city rail/bus links. Define two binary relations on $\mathfrak{G}$:

$$\text{HSR} := \{(G_{c_1}, G_{c_2}) \mid \text{there exists a direct high-speed rail service between } c_1 \text{ and } c_2\},$$

$$\text{AIR}_\theta := \{(G_{c_1}, G_{c_2}) \mid \text{there exist } \geq \theta \text{ direct flights per week between } c_1 \text{ and } c_2\},$$

and set $\mathcal{R} := \{\text{HSR}, \text{AIR}_\theta\}$ for a fixed threshold $\theta \in \mathbb{N}$.
Consider the metagraph $M = (V, E, s, t, \lambda)$ with

$$V = \{G_{\text{Tokyo}},\, G_{\text{Osaka}},\, G_{\text{Nagoya}}\},$$

and meta-edges

$$e_1 :\; G_{\text{Tokyo}} \xrightarrow{\text{HSR}} G_{\text{Osaka}}, \qquad e_2 :\; G_{\text{Osaka}} \xrightarrow{\text{HSR}} G_{\text{Nagoya}}, \qquad e_3 :\; G_{\text{Tokyo}} \xrightarrow{\text{AIR}_\theta} G_{\text{Nagoya}}.$$

By construction, each e_i satisfies the incidence constraint $\big(s(e_i), t(e_i)\big) \in \lambda(e_i)$: there is high-speed rail between Tokyo–Osaka and Osaka–Nagoya (so $(G_{\text{Tokyo}}, G_{\text{Osaka}}) \in \text{HSR}$ and $(G_{\text{Osaka}}, G_{\text{Nagoya}}) \in \text{HSR}$), and the direct-flight relation AIR$_\theta$ holds for the chosen threshold on Tokyo–Nagoya. Thus M is a concrete *metagraph of cities*, where meta-vertices are city transit graphs and meta-edges encode inter-city mobility modes. A schematic illustration of this example is provided in Figure 1.

1.2. *Iterated MetaGraph (Graph of Graph of . . . of Graph)*

An *Iterated MetaGraph* is a graph whose vertices are themselves metagraphs, i.e., it recursively extends the *graph-of-graphs* paradigm across multiple hierarchical levels [3,6,7]. As a related notion, *MetaStructures* have also been studied [8].

Definition 1.3 (Unit metagraph embedding)**.** For $X \in \mathfrak{G}$ define the *unit metagraph*

$$\mathsf{U}(X) \;:=\; \big(\{X\},\, \emptyset,\, \_,\, \_,\, \_\big).$$

This gives an injective map $\mathsf{U} : \mathfrak{G} \hookrightarrow \mathrm{Obj}\big(\mathrm{Meta}(\mathfrak{G}, \mathcal{R})\big)$.

Definition 1.4 (Relation lifting)**.** Given $\mathcal{R}$ on $\mathfrak{G}$, define its *lift* $\mathcal{R}^{\uparrow}$ on finite metagraphs over $(\mathfrak{G}, \mathcal{R})$ by

$$\forall R \in \mathcal{R}, \quad (M_1, M_2) \in R^{\uparrow} \iff \exists x \in V(M_1),\, y \in V(M_2) :\; (x, y) \in R.$$

Set $\mathcal{R}^{\uparrow} := \{R^{\uparrow} : R \in \mathcal{R}\}$.

Definition 1.5 (Iterated object and relation universes)**.** Define recursively for $t \in \mathbb{N}_0$:

$$\mathfrak{G}^{(0)} := \mathfrak{G}, \qquad \mathcal{R}^{(0)} := \mathcal{R},$$

$$\mathfrak{G}^{(t+1)} := \Big\{ \text{finite metagraphs over } \big(\mathfrak{G}^{(t)}, \mathcal{R}^{(t)}\big) \Big\}, \qquad \mathcal{R}^{(t+1)} := \big(\mathcal{R}^{(t)}\big)^{\uparrow}.$$

Definition 1.6 (Iterated MetaGraph of depth t)**.** For $t \in \mathbb{N}_0$, an *iterated metagraph of depth* t is a metagraph

$$M^{(t)} = (V^{(t)}, E^{(t)}, s^{(t)}, t^{(t)}, \lambda^{(t)})$$

over $\big(\mathfrak{G}^{(t)}, \mathcal{R}^{(t)}\big)$, i.e., $V^{(t)} \subseteq \mathfrak{G}^{(t)}$, $\lambda^{(t)} : E^{(t)} \to \mathcal{R}^{(t)}$ and

$$\forall e \in E^{(t)} :\; \big(s^{(t)}(e),\, t^{(t)}(e)\big) \in \lambda^{(t)}(e).$$

Example 1.7 (Supply-Chain-of-Chains as an Iterated Metagraph)**.** Let $\mathfrak{G}^{(0)}$ be the set of *facility-level logistics graphs* $G = (V, E)$, where V are production/storage sites inside a firm and E are internal transport links. Fix a base relation family $\mathcal{R}^{(0)}$ containing

$$\mathrm{SHIP}_{\geq q} \;:=\; \{(G_1, G_2) \mid$$

$$\text{there exists a scheduled shipment from some site in } G_1 \text{ to some site in } G_2 \text{ at } \geq q \text{ trips/week}\},$$

for a chosen $q \in \mathbb{N}$.

Level 1 (metagraphs of firms). Firm A has two facilities with internal flows, modeled by $G_{A,1}, G_{A,2} \in \mathfrak{G}^{(0)}$; Firm B has one facility $G_{B,1} \in \mathfrak{G}^{(0)}$. Define metagraphs

$$M_A = (\{G_{A,1}, G_{A,2}\}, E_A, s_A, t_A, \lambda_A), \qquad M_B = (\{G_{B,1}\}, E_B, s_B, t_B, \lambda_B),$$

where edges of M_A record A's internal transfers (e.g. $G_{A,1} \xrightarrow{\mathrm{SHIP}_{\geq 5}} G_{A,2}$ if 5 trips/week are scheduled). Assume there is a *cross-firm* weekly shipment from A's facility $G_{A,2}$ to B's $G_{B,1}$ at rate 3/week. Then at base level,

$$(G_{A,2}, G_{B,1}) \in \mathrm{SHIP}_{\geq 1} \;\subseteq\; \mathcal{R}^{(0)}.$$

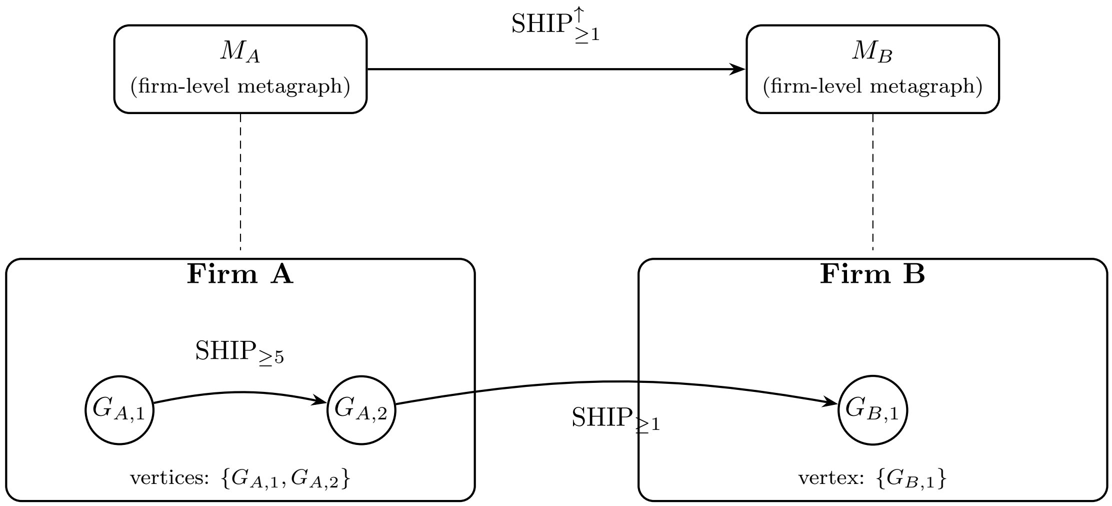

FIGURE 2. Supply-chain-of-chains as an iterated metagraph. Level 1: each firm is modeled as a metagraph whose vertices are facility-level logistics graphs. Level 2: the lifted relation induces a meta-edge $M_A \xrightarrow{\mathrm{SHIP}^{\uparrow}_{\geq 1}} M_B$.

Level 2 (iterated metagraph of firms). By relation lifting, the lifted relation $\mathrm{SHIP}^{\uparrow}_{\geq 1} \in \mathcal{R}^{(1)}$ satisfies

$$\big(M_A, M_B\big) \in \mathrm{SHIP}^{\uparrow}_{\geq 1} \quad \Longleftrightarrow \quad \exists\, X \in V(M_A),\, Y \in V(M_B) :\ (X, Y) \in \mathrm{SHIP}_{\geq 1}.$$

Since $(G_{A,2}, G_{B,1}) \in \mathrm{SHIP}_{\geq 1}$, we obtain a meta-edge

$$M_A \xrightarrow{\mathrm{SHIP}^{\uparrow}_{\geq 1}} M_B$$

in the *iterated metagraph* whose vertices are firm-level metagraphs. Thus, real shipments between specific facilities induce (via lifting) contractual/supply relationships between the firms at the meta-level. For reference, a schematic illustration of this example is shown in Figure 2.

1.3. *Fuzzy Graph*

A fuzzy set assigns each element a membership degree between 0 and 1, modeling partial belonging and uncertainty in classification [9,10]. A fuzzy graph combines fuzzy vertex and edge membership functions, representing relationships with uncertainty and graded connectivity among nodes [11–14].

Definition 1.8 (Fuzzy set)**.** [9] Let Y be a non-empty universe. A *fuzzy set* τ on Y is a function

$$\tau : Y \longrightarrow [0, 1],$$

assigning to each $y \in Y$ a membership value $\tau(y)$. A *fuzzy relation* on Y is a fuzzy subset δ of $Y \times Y$. Given a fuzzy set τ on Y, the relation δ is said to be a *fuzzy relation on* τ whenever

$$\delta(y, z) \ \leq \ \min\{\tau(y), \tau(z)\}, \quad \forall\, y, z \in Y.$$

Definition 1.9 (Fuzzy graph)**.** [12] A *fuzzy graph* on a vertex set V is a pair $G = (\sigma, \mu)$ consisting of:

- A vertex membership function $\sigma : V \to [0, 1]$, where $\sigma(x)$ gives the degree to which $x \in V$ belongs to the graph.
- An edge membership function $\mu : V \times V \to [0, 1]$, which is a fuzzy relation on σ, satisfying

$$\mu(x, y) \ \leq \ \sigma(x) \wedge \sigma(y), \quad \forall\, x, y \in V,$$

  where $\wedge$ denotes the minimum operator.

The associated *crisp graph* $G^* = (\sigma^*, \mu^*)$ is determined by

$$\sigma^* = \{\, x \in V \mid \sigma(x) > 0 \,\}, \qquad \mu^* = \{\, (x, y) \in V \times V \mid \mu(x, y) > 0 \,\}.$$

A *fuzzy subgraph* $H = (\sigma', \mu')$ of G is obtained by choosing a subset $X \subseteq V$ and defining

- a restricted vertex membership $\sigma' : X \to [0, 1]$,
- an edge membership $\mu' : X \times X \to [0, 1]$ such that

$$\mu'(x, y) \ \leq \ \sigma'(x) \wedge \sigma'(y), \quad \forall\, x, y \in X.$$

A neutrosophic set assigns to each element three independent membership degrees: truth, indeterminacy, and falsity, enabling richer uncertainty representation [15, 16]. A neutrosophic graph assigns each vertex and edge three membership values: truth, indeterminacy, and falsity, capturing uncertainty comprehensively [17–19].

Definition 1.10 (Neutrosophic Graph)**.** [17] Let V be a (finite) vertex set. A *neutrosophic graph* on V is a pair

$$G = (\sigma, \mu),$$

where

- $\sigma : V \to [0, 1]^3$, $v \mapsto \sigma(v) = \big(T_\sigma(v), I_\sigma(v), F_\sigma(v)\big)$ assigns to each vertex v its *truth*, *indeterminacy*, and *falsity* degrees, with $0 \leq T_\sigma(v), I_\sigma(v), F_\sigma(v) \leq 1$ and

$$0 \ \leq \ T_\sigma(v) + I_\sigma(v) + F_\sigma(v) \ \leq \ 3.$$

- $\mu : V \times V \to [0, 1]^3$, $(u, v) \mapsto \mu(u, v) = \big(T_\mu(u, v), I_\mu(u, v), F_\mu(u, v)\big)$ assigns neutrosophic degrees to (unordered) pairs $\{u, v\}$ (take $\mu(u, u)$ for loops if allowed), with $0 \leq T_\mu, I_\mu, F_\mu \leq 1$ and

$$0 \ \leq \ T_\mu(u, v) + I_\mu(u, v) + F_\mu(u, v) \ \leq \ 3.$$

These maps satisfy, for all distinct $u, v \in V$,

$$T_\mu(u,v) \le \min\{T_\sigma(u), T_\sigma(v)\}, \qquad I_\mu(u,v) \ge \max\{I_\sigma(u), I_\sigma(v)\}, \qquad F_\mu(u,v) \ge \max\{F_\sigma(u), F_\sigma(v)\}.$$

(For a nonedge one may set $\mu(u,v) = (0,0,0)$.) The *underlying crisp graph* $G^* = (V, E^*)$ is given by

$$E^* := \big\{\{u,v\} \subseteq V : \; T_\mu(u,v) > 0 \;\text{ or }\; I_\mu(u,v) > 0 \;\text{ or }\; F_\mu(u,v) > 0\big\}.$$

Unless stated otherwise, neutrosophic graphs are taken to be undirected and loopless.

Example 1.11 (News–Source Credibility as a Neutrosophic Graph)**.** Consider three online sources $V = \{\mathrm{A}, \mathrm{B}, \mathrm{C}\}$. Assign neutrosophic vertex-memberships (credibility T, uncertainty I, falsity risk F):

$$\sigma(\mathrm{A}) = (0.90,\, 0.10,\, 0.00), \quad \sigma(\mathrm{B}) = (0.60,\, 0.30,\, 0.10), \quad \sigma(\mathrm{C}) = (0.40,\, 0.50,\, 0.20).$$

Define neutrosophic edge-memberships (pairwise agreement/compatibility):

$$\mu(\mathrm{A},\mathrm{B}) = (0.55,\, 0.35,\, 0.15), \quad \mu(\mathrm{A},\mathrm{C}) = (0.25,\, 0.55,\, 0.25), \quad \mu(\mathrm{B},\mathrm{C}) = (0.35,\, 0.50,\, 0.20).$$

These values satisfy the neutrosophic constraints. For instance, for (A,B):

$$\min\{T_\sigma(\mathrm{A}), T_\sigma(\mathrm{B})\} = \min\{0.90, 0.60\} = 0.60 \;\ge\; T_\mu(\mathrm{A},\mathrm{B}) = 0.55,$$

$$\max\{I_\sigma(\mathrm{A}), I_\sigma(\mathrm{B})\} = \max\{0.10, 0.30\} = 0.30 \;\le\; I_\mu(\mathrm{A},\mathrm{B}) = 0.35,$$

$$\max\{F_\sigma(\mathrm{A}), F_\sigma(\mathrm{B})\} = \max\{0.00, 0.10\} = 0.10 \;\le\; F_\mu(\mathrm{A},\mathrm{B}) = 0.15,$$

and similarly for (A,C) and (B,C). Interpretation: A is highly credible, C is uncertain; their edge (A,C) has modest truth degree 0.25 with higher indeterminacy 0.55, reflecting inconsistent or incomplete cross-corroboration between those sources.

1.4. *Weighted Graph*

A weighted graph is a graph in which each edge is assigned a numerical value (weight), typically representing cost, distance, or intensity(cf. [20–25]).

Definition 1.12 (Weighted Graph)**.** (cf. [20, 21]) A *Weighted Graph* augments the structure of a graph by assigning a numerical weight to each edge. Formally, a weighted graph is defined as a triple $G = (V, E, w)$ where:

- V is a non-empty set of vertices.
- $E \subseteq \{\{u,v\} \mid u, v \in V,\; u \ne v\}$ is a set of edges.
- $w : E \to \mathbb{R}$ is a weight function that assigns a unique real number to each edge $e \in E$.

1.5. *Directed Graph and Bidirected Graph*

A directed graph consists of vertices connected by ordered edges, where each edge has a defined direction from source to target [26–28].

Definition 1.13 (Directed Graph)**.** [29] A *directed graph* (digraph) $G = (V, E)$ consists of:

- V: A finite set of vertices.
- $E \subseteq V \times V$: A set of directed edges, where each edge is an ordered pair (u, v) with $u, v \in V$.

The edge (u, v) indicates a directed connection from vertex u (source) to vertex v (target).

A Bidirected graph (Bidigraph) assigns local directions to each vertex-edge pair, enabling edges to point independently at both ends [30–33].

Definition 1.14 (Bidirected Graph (Bidigraph))**.** [31–33] A *bidirected graph* (also known as a *bigraph*) is a pair $B = (G, \tau)$, where:

- $G = (V, E)$ is a simple undirected graph, where V is a non-empty set of vertices and E is a set of edges (without parallel edges or loops).
- $\tau : V \times E \to \{-1, 0, 1\}$ is a function called the *bidirection function*, which assigns a *local orientation* to each vertex-edge pair (v, e) as follows:
  - $\tau(v, e) = 1$: Edge e is directed *towards* vertex v.
  - $\tau(v, e) = -1$: Edge e is directed *away from* vertex v.
  - $\tau(v, e) = 0$: Vertex v is not incident to edge e.

The graph G is referred to as the *underlying graph* of B, and the function τ provides the bidirected structure on G by assigning a direction at each endpoint of every edge in E.

Example 1.15 (Last-Mile Logistics Lane as a Bidirected Graph)**.** Let $G = (V, E)$ with facilities $V = \{\mathrm{F}, \mathrm{C}, \mathrm{R}\}$ for *Factory*, *Cross-dock*, and *Retail store*. Undirected transport links are

$$E = \{e_{\mathrm{FC}} = \{\mathrm{F}, \mathrm{C}\},\ e_{\mathrm{CR}} = \{\mathrm{C}, \mathrm{R}\},\ e_{\mathrm{FR}} = \{\mathrm{F}, \mathrm{R}\}\}.$$

Define a bidirection function $\tau : V \times E \to \{-1, 0, 1\}$ where $\tau(v, e) = +1$ means the lane is oriented *towards* v (arrivals at v), $\tau(v, e) = -1$ means *away from* v (departures from v), and $\tau(v, e) = 0$ if $v \notin e$. Set

$$(\tau(\mathrm{F}, e_{\mathrm{FC}}), \tau(\mathrm{C}, e_{\mathrm{FC}})) = (-1, +1) \quad \text{(factory ships to cross-dock)},$$

$$(\tau(\mathrm{C}, e_{\mathrm{CR}}), \tau(\mathrm{R}, e_{\mathrm{CR}})) = (-1, +1) \quad \text{(cross-dock dispatches to retail)},$$

$$(\tau(\mathrm{R}, e_{\mathrm{FR}}), \tau(\mathrm{F}, e_{\mathrm{FR}})) = (-1, +1) \quad \text{(empty containers return from retail to factory)}.$$

For completeness, non-incidences have value 0. A compact table is:

	e_{FC}	e_{CR}	e_{FR}
$\tau(\mathrm{F},\cdot)$	-1	0	$+1$
$\tau(\mathrm{C},\cdot)$	$+1$	-1	0
$\tau(\mathrm{R},\cdot)$	0	$+1$	-1

This bidirected model captures local endpoint behavior (depart/arrive) on each lane with a *single* undirected edge, which is natural for physical corridors where the admissible direction at one end can be specified independently of the other.

1.6. *MultiGraph*

A multigraph is a graph that allows multiple parallel edges between the same vertices and loops on vertices, used when necessary (cf. [34–38]). As a related concept, Iterative MultiStructure is also known [39].

Definition 1.16 (Multigraph)**.** A *multigraph* is a triple $G = (V, E, \varphi)$ where:

- V is a finite set of *vertices*.
- E is a finite *multiset* of *edges*.
- $\varphi : E \longrightarrow \{\{u, v\} \mid u, v \in V,\ u = v \text{ or } u \neq v\}$ is an *incidence function* that assigns to each edge $e \in E$ an unordered pair $\{u, v\}$ of one or two vertices. In particular:
  (1) If $\varphi(e) = \{u, v\}$ with $u \neq v$, then e is a *(simple) edge* connecting u and v.
  (2) If $\varphi(e) = \{v, v\}$ for some $v \in V$, then e is a *loop* at vertex v.
  (3) If there exist distinct edges $e_1, e_2 \in E$ such that $\varphi(e_1) = \varphi(e_2) = \{u, v\}$, then e_1 and e_2 are *parallel edges* between u and v.

2. **Reviews and Main Results**

In this section, we present the main results of this paper along with related discussions.

2.1. *Meta-Fuzzy Graph*

A Meta-Fuzzy Graph models relationships among fuzzy graphs, where vertices represent fuzzy graphs and edges encode higher-level fuzzy relations.

Definition 2.1 (Meta-Fuzzy Graph over $(\mathsf{FG}, \mathcal{R})$)**.** A *Meta-Fuzzy Graph* is a triple

$$\mathbb{M} \ := \ (\sigma_M,\, \mu_M,\, L_M)$$

consisting of:

- a *meta-vertex membership* $\sigma_M : \mathsf{FG} \to [0, 1]$;

- a *meta-edge membership* $\mu_M : \mathsf{FG} \times \mathsf{FG} \to [0,1]$ satisfying the fuzzy-graph constraint

$$\mu_M(F,G) \ \le \ \min\{\sigma_M(F), \sigma_M(G)\} \qquad (\forall F, G \in \mathsf{FG});$$

- a *label selector* $L_M : \mathsf{FG} \times \mathsf{FG} \to \mathcal{P}_{\text{fin}}(\mathcal{R})$ assigning to each ordered pair (F,G) a finite set $L_M(F,G)$ of labels from $\mathcal{R}$.

These data must satisfy the *witnessing (incidence) constraint*

$$\mu_M(F,G) \ \le \sup_{R \in L_M(F,G)} R(F,G) \qquad (\forall F, G \in \mathsf{FG}), \tag{1}$$

with the convention that $\sup \emptyset := 0$. The *support* (meta-vertex set) is $V(\mathbb{M}) = \{\, F \in \mathsf{FG} \mid \sigma_M(F) > 0 \,\}$, and the *crisp underlying meta-graph* is the directed graph with vertex set $V(\mathbb{M})$ and arc set $A(\mathbb{M}) = \{\, (F,G) \mid \mu_M(F,G) > 0 \,\}$, optionally decorated by $L_M(F,G)$.

Definition 2.2 (Crisp embedding of graphs into fuzzy graphs)**.** Given a (finite) simple graph $G = (V,E)$, define its *crisp fuzzy realization* $\iota(G) = (\sigma_G, \mu_G)$ by

$$\sigma_G(x) \ := \begin{cases} 1, & x \in V, \\ 0, & \text{otherwise}, \end{cases} \qquad \mu_G(x,y) \ := \begin{cases} 1, & \{x,y\} \in E, \\ 0, & \text{otherwise}. \end{cases}$$

Example 2.3 (Regional Retail Analytics as a Meta-Fuzzy Graph)**.** Let FG contain three fuzzy graphs representing *product co-purchase networks* for Tokyo (F_T), Osaka (F_O), and Nagoya (F_N). Each $F_\bullet$ has fuzzy vertex/edge memberships (omitted here), e.g. higher membership on products and pairs that appear frequently.

Set the meta-vertex membership (data quality / recency weight)

$$\sigma_M(F_T) = 0.90, \qquad \sigma_M(F_O) = 0.70, \qquad \sigma_M(F_N) = 0.50.$$

Label family $\mathcal{R}$. Define two fuzzy relations on $\mathsf{FG} \times \mathsf{FG}$:

$$R_{\text{overlap}}(F_i, F_j) = \text{normalized catalog overlap}, \qquad R_{\text{api}}(F_i, F_j) = \text{API interoperability score}.$$

Assume the following values (symmetric):

	F_T	F_O	F_N
$R_{\text{overlap}}(F_T, \cdot)$	–	0.65	0.35
$R_{\text{overlap}}(F_O, \cdot)$	0.65	–	0.45
$R_{\text{overlap}}(F_N, \cdot)$	0.35	0.45	–

	F_T	F_O	F_N
$R_{\text{api}}(F_T, \cdot)$	–	0.55	0.25
$R_{\text{api}}(F_O, \cdot)$	0.55	–	0.30
$R_{\text{api}}(F_N, \cdot)$	0.25	0.30	–

Choose the label set $L_M(F_i, F_j) = \{R_{\text{overlap}}, R_{\text{api}}\}$ for all $i \neq j$ and define

$$\mu_M(F_T, F_O) = 0.60, \qquad \mu_M(F_O, F_N) = 0.40, \qquad \mu_M(F_T, F_N) = 0.30.$$

(i) Fuzzy-graph constraint:

$$\mu_M(F_T, F_O) = 0.60 \le \min\{0.90, 0.70\} = 0.70, \quad \mu_M(F_O, F_N) = 0.40 \le \min\{0.70, 0.50\} = 0.50,$$

$$\mu_M(F_T, F_N) = 0.30 \le \min\{0.90, 0.50\} = 0.50.$$

(ii) Witnessing:

$$\sup_{R\in L_M(F_T,F_O)} R(F_T,F_O) = \max\{0.65, 0.55\} = 0.65 \ \geq \ 0.60,$$
$$\sup_{R\in L_M(F_O,F_N)} R(F_O,F_N) = \max\{0.45, 0.30\} = 0.45 \ \geq \ 0.40,$$
$$\sup_{R\in L_M(F_T,F_N)} R(F_T,F_N) = \max\{0.35, 0.25\} = 0.35 \ \geq \ 0.30.$$

Hence $\mathbb{M} = (\sigma_M, \mu_M, L_M)$ is a valid *Meta-Fuzzy Graph* modeling cross-regional analytics integration.

Definition 2.4 (Crisp-to-fuzzy lifting of labels)**.** Let $\mathfrak{G}$ be a universe of (finite) graphs and $\mathcal{R}_{\rm cr} \subseteq \mathcal{P}(\mathfrak{G}\times\mathfrak{G})$ a nonempty family of *crisp* binary relations (e.g. subgraph, homomorphism, minor, isomorphism). Define

$$\mathcal{R}^\flat \ := \ \{\, R^\flat \ \big|\ R\in\mathcal{R}_{\rm cr} \,\} \ \subseteq \ [0,1]^{\mathsf{FG}\times\mathsf{FG}}$$

by

$$R^\flat\big(\iota(G_1),\iota(G_2)\big) \ := \ \begin{cases} 1, & (G_1,G_2)\in R, \\ 0, & \text{otherwise,} \end{cases} \qquad R^\flat(F_1,F_2) := 0 \text{ if some } F_i \neq \iota(\,\cdot\,).$$

Theorem 2.5 (Meta-Fuzzy Graph generalizes MetaGraph)**.** *Let $M = (V,E,s,t,\lambda)$ be a (directed, labeled) MetaGraph over $(\mathfrak{G},\mathcal{R}_{\rm cr})$, i.e., $V\subseteq\mathfrak{G}$, $\lambda : E\to\mathcal{R}_{\rm cr}$, and*

$$\forall e\in E: \quad \big(s(e),\, t(e)\big)\in\lambda(e).$$

Define a Meta-Fuzzy Graph $\mathbb{M} = (\sigma_M,\mu_M,L_M)$ over $(\mathsf{FG},\mathcal{R}^\flat)$ by

$$\sigma_M(F) \ := \ \mathbf{1}_{\{\iota(v)\mid v\in V\}}(F),$$
$$\mu_M(F,G) \ := \ \max_{e\in E} \ \mathbf{1}_{\{\iota(s(e))\}}(F)\cdot\mathbf{1}_{\{\iota(t(e))\}}(G),$$
$$L_M(F,G) \ := \ \{\, \lambda(e) \ \big| \ e\in E,\ F=\iota\big(s(e)\big),\ G=\iota\big(t(e)\big) \,\}.$$

Then $\mathbb{M}$ is a Meta-Fuzzy Graph, and its underlying crisp meta-graph is (canonically) isomorphic to M.

Proof. (1) Fuzzy-graph constraint.) Fix $F,G\in\mathsf{FG}$. By definition, $\sigma_M(F)\in\{0,1\}$ and $\sigma_M(G)\in\{0,1\}$. If $\mu_M(F,G)=1$, then there exists $e\in E$ with $F=\iota\big(s(e)\big)$ and $G=\iota\big(t(e)\big)$. Hence $\sigma_M(F)=\sigma_M(G)=1$, so

$$\mu_M(F,G) = 1 \ \leq \ \min\{1,1\} = \min\{\sigma_M(F),\sigma_M(G)\}.$$

If $\mu_M(F,G)=0$, the inequality holds trivially. Thus the fuzzy-graph constraint is satisfied.

(2) Witnessing constraint.) Let $F,G\in\mathsf{FG}$. If $L_M(F,G)=\emptyset$, then by construction there is no $e\in E$ with $F=\iota(s(e))$, $G=\iota(t(e))$, hence $\mu_M(F,G)=0$, and (1) reads $0\leq\sup\emptyset=0$, which holds. If $L_M(F,G)\neq\emptyset$, then there exists $e\in E$ with $F=\iota(s(e))$, $G=\iota(t(e))$ and

$R := \lambda(e) \in L_M(F,G)$. By the MetaGraph incidence, $(s(e),t(e)) \in R$, hence by the definition of $R^\flat$,

$$R^\flat(F,G) \ = \ R^\flat\big(\iota(s(e)),\iota(t(e))\big) \ = \ 1.$$

Therefore

$$\sup_{Q\in L_M(F,G)} Q^\flat(F,G) \ \geq \ R^\flat(F,G) \ = \ 1 \ \geq \ \mu_M(F,G),$$

since $\mu_M(F,G) \in \{0,1\}$ and equals 1 exactly when such an e exists. Thus (1) holds.

(3) Underlying crisp meta-graph.) The support is $V(\mathbb{M}) = \{\iota(v) \mid v \in V\}$. The arc set is

$$A(\mathbb{M}) \ = \ \{\,(F,G) \mid \mu_M(F,G) > 0\,\} \ = \ \big\{\,(\iota(s(e)),\iota(t(e))) \mid e \in E\,\big\}.$$

Hence the map $\iota : V \to V(\mathbb{M})$, $v \mapsto \iota(v)$, is a bijection that extends to a digraph isomorphism from M to the underlying crisp meta-graph of $\mathbb{M}$, preserving labels via L_M. □

2.2. *Iterated Meta-Fuzzy Graph*

An Iterated Meta-Fuzzy Graph repeatedly applies meta-fuzzy construction across levels, producing hierarchical fuzzy graph networks capturing multi-scale relational uncertainty.

Definition 2.6 (Lifting of fuzzy relations to higher levels)**.** Suppose $\mathcal{U}$ is a class whose elements themselves carry fuzzy vertex-memberships (so each $X \in \mathcal{U}$ has a map $\Sigma_X : \cdot \to [0,1]$ on its own vertex-universe). Given $S : \mathcal{U} \times \mathcal{U} \to [0,1]$ and elements $X, Y \in \mathcal{U}$, define the *lifted* relation

$$S^\uparrow(X,Y) \ := \sup_{u\in\mathrm{Vert}(X),\, v\in\mathrm{Vert}(Y)} \min\big(\Sigma_X(u),\, \Sigma_Y(v),\, S(u,v)\big),$$

where $\mathrm{Vert}(X)$ denotes the level-below vertex-universe on which Σ_X lives.

Definition 2.7 (Iterated universes and lifted families)**.** Define recursively for $t \in \mathbb{N}_0$:

$$\mathsf{FG}^{(0)} := \mathsf{FG}, \qquad \mathcal{R}^{(0)} \ \text{ as fixed above},$$

$$\mathsf{FG}^{(t+1)} := \Big\{\text{all Meta-Fuzzy Graphs on } \mathsf{FG}^{(t)} \text{ with witnessing family } \mathcal{R}^{(t)}\Big\},$$

$$\mathcal{R}^{(t+1)} \ := \ \{\, R^\uparrow \mid R \in \mathcal{R}^{(t)}\,\}.$$

Definition 2.8 (Iterated Meta-Fuzzy Graph of depth t)**.** For $t \in \mathbb{N}_0$, an *Iterated Meta-Fuzzy Graph of depth t* is a Meta-Fuzzy Graph

$$\mathbb{M}^{(t)} = (\Sigma^{(t)}, \mathrm{M}^{(t)})$$

on the vertex universe $\mathsf{FG}^{(t)}$ with witnessing family $\mathcal{R}^{(t)}$, i.e., for all $X, Y \in \mathsf{FG}^{(t)}$:

$$\mathrm{M}^{(t)}(X,Y) \ \leq \ \min\{\Sigma^{(t)}(X), \Sigma^{(t)}(Y)\} \quad \text{and} \quad \mathrm{M}^{(t)}(X,Y) \ \leq \ \sup_{R\in\mathcal{R}^{(t)}} R(X,Y).$$

Example 2.9 (Division-Level Planning as an Iterated Meta-Fuzzy Graph)**.** Continue with $F_T, F_O, F_N \in \mathsf{FG}^{(0)}$ and the relations $R_{\text{overlap}}, R_{\text{api}} \in \mathcal{R}^{(0)}$ above. Construct two level-1 meta-fuzzy graphs (division views):

East division X on vertex set $\{F_T, F_N\}$ with internal meta-memberships

$$\Sigma_X(F_T) = 0.80, \qquad \Sigma_X(F_N) = 0.60,$$

and some internal meta-edges (omitted). *West division* Y on $\{F_O\}$ with

$$\Sigma_Y(F_O) = 0.90.$$

Lifted relations. By the lifting rule

$$R^{\uparrow}(X,Y) = \sup_{u \in V(X),\, v \in V(Y)} \min\bigl(\Sigma_X(u),\, \Sigma_Y(v),\, R(u,v)\bigr),$$

we compute

$$R^{\uparrow}_{\text{overlap}}(X,Y) = \max\bigl\{\min(0.80, 0.90, 0.65),\ \min(0.60, 0.90, 0.45)\bigr\} = \max\{0.65,\ 0.45\} = 0.65,$$

$$R^{\uparrow}_{\text{api}}(X,Y) = \max\bigl\{\min(0.80, 0.90, 0.55),\ \min(0.60, 0.90, 0.30)\bigr\} = \max\{0.55,\ 0.30\} = 0.55.$$

Thus in $\mathcal{R}^{(1)}$ we have two candidate labels between X and Y.

Level-1 meta-edge. Set the level-1 meta-vertex membership

$$\Sigma^{(1)}(X) = 0.85, \qquad \Sigma^{(1)}(Y) = 0.90,$$

and define a cross-division meta-edge

$$\mathrm{M}^{(1)}(X,Y) = 0.60, \qquad L^{(1)}(X,Y) = \{R^{\uparrow}_{\text{overlap}},\ R^{\uparrow}_{\text{api}}\}.$$

Verification. Fuzzy-graph bound at level 1:

$$\mathrm{M}^{(1)}(X,Y) = 0.60\ \le\ \min\{\Sigma^{(1)}(X), \Sigma^{(1)}(Y)\} = \min\{0.85, 0.90\} = 0.85.$$

Witnessing via lifted labels:

$$\sup_{R \in L^{(1)}(X,Y)} R(X,Y) = \max\{0.65, 0.55\} = 0.65\ \ge\ \mathrm{M}^{(1)}(X,Y) = 0.60.$$

Therefore $\mathbb{M}^{(1)} = (\Sigma^{(1)}, \mathrm{M}^{(1)})$ is a valid *Iterated Meta-Fuzzy Graph* whose vertices are the division-level meta-fuzzy graphs and whose inter-division linkage is witnessed by lifted overlap/API relations derived from facility-level data.

Theorem 2.10 (Depth 1 recovers Meta-Fuzzy Graph)**.** *The class of Iterated Meta-Fuzzy Graphs of depth* 1 *coincides with the class of Meta-Fuzzy Graphs over* $(\mathsf{FG}, \mathcal{R}^{(0)})$.

Proof. By definition, $\mathsf{FG}^{(1)}$ is precisely the class of Meta-Fuzzy Graphs on $\mathsf{FG}^{(0)} = \mathsf{FG}$ with witnessing family $\mathcal{R}^{(0)}$. Unfolding the definition of an Iterated Meta-Fuzzy Graph at $t = 1$ gives exactly the same constraints, hence the two classes are identical. □

Theorem 2.11 (Iterated Meta-Fuzzy Graphs generalize MetaGraph and Iterated Meta-Graph)**.** *Fix a universe* $\mathfrak{G}$ *of finite (crisp) graphs and a nonempty family* $\mathcal{R}_{\mathrm{cr}}^{(0)} \subseteq \mathcal{P}(\mathfrak{G} \times \mathfrak{G})$ *of crisp relations (e.g. subgraph, homomorphism, minor, isomorphism). Let* $\mathrm{IMeta}^{(t)}(\mathfrak{G}, \mathcal{R}_{\mathrm{cr}}^{(0)})$ *denote the class of iterated metagraphs of depth* t *(directed, labeled) built from* $(\mathfrak{G}, \mathcal{R}_{\mathrm{cr}}^{(0)})$ *using the usual existential lifting of relations. Then for every* $t \geq 0$ *there exists an injective map*

$$\mathsf{E}_t : \ \mathrm{IMeta}^{(t)}(\mathfrak{G}, \mathcal{R}_{\mathrm{cr}}^{(0)}) \ \hookrightarrow \ \mathsf{FG}^{(t)}$$

such that:

- *for* $t = 1$*,* E_1 *identifies each MetaGraph with a* crisp *Meta-Fuzzy Graph (all memberships in* $\{0, 1\}$*);*
- *for all* t*, the underlying crisp meta-structure (vertices with positive membership; edges with positive membership) of* $\mathsf{E}_t(\cdot)$ *is canonically isomorphic to the given iterated metagraph.*

Consequently, Iterated Meta-Fuzzy Graphs (allowing arbitrary $[0, 1]$*-memberships) strictly extend both Meta-Fuzzy Graphs (by Theorem 2.10) and Iterated MetaGraphs (by the embeddings* E_t*).*

Proof. We construct E_t by induction on t and verify the defining inequalities numerically via min/sup.

Step 0 (crisp embedding of graphs). For a simple graph $G = (V, E)$, define $\iota(G) = (\sigma_G, \mu_G) \in \mathsf{FG}$ by

$$\sigma_G(x) = \begin{cases} 1, & x \in V, \\ 0, & \text{else}, \end{cases} \qquad \mu_G(x, y) = \begin{cases} 1, & \{x, y\} \in E, \\ 0, & \text{else}. \end{cases}$$

This yields an injective map $\iota : \mathfrak{G} \hookrightarrow \mathsf{FG}^{(0)}$. For any crisp relation $R \in \mathcal{R}_{\mathrm{cr}}^{(0)}$ define the 0/1-valued fuzzy relation

$$R^\flat(F_1, F_2) := \begin{cases} 1, & \exists\, G_1, G_2 \in \mathfrak{G} : \ F_i = \iota(G_i) \text{ and } (G_1, G_2) \in R, \\ 0, & \text{otherwise}. \end{cases}$$

Set $\mathcal{R}^{(0)} := \{R^\flat : R \in \mathcal{R}_{\mathrm{cr}}^{(0)}\}$.

Inductive hypothesis. Assume for some $t \geq 0$ there is an injective map

$$\mathsf{E}_t : \ \mathrm{IMeta}^{(t)}(\mathfrak{G}, \mathcal{R}_{\mathrm{cr}}^{(0)}) \ \hookrightarrow \ \mathsf{FG}^{(t)},$$

and that for every crisp lifted relation $S \in \mathcal{R}_{\mathrm{cr}}^{(t)}$ (obtained by existential lifting at the crisp level), its fuzzy indicator $S^\flat$ belongs to $\mathcal{R}^{(t)}$ and satisfies

$$S^\flat\big(\mathsf{E}_t(X), \, \mathsf{E}_t(Y)\big) \ = \ \begin{cases} 1, & (X, Y) \in S, \\ 0, & \text{otherwise}. \end{cases}$$

Step $t \to t{+}1$. Let $M = (V_M, A_M, s, t, \lambda)$ be an iterated metagraph of depth $t{+}1$, i.e. a labeled digraph with $V_M \subseteq \mathrm{IMeta}^{(t)}$ and

$$\forall e \in A_M : \quad (\, s(e),\, t(e)\,) \;\in\; \lambda(e) \;\in\; \mathcal{R}^{(t)}_{\mathrm{cr}}.$$

Define $\mathsf{E}_{t+1}(M) = (\Sigma, \mathrm{M}) \in \mathsf{FG}^{(t+1)}$ by

$$\Sigma(X) \;:=\; \mathbf{1}_{\{\mathsf{E}_t(v) | v \in V_M\}}(X), \qquad \mathrm{M}(X,Y) \;:=\; \max_{e \in A_M} \; \mathbf{1}_{\{\mathsf{E}_t(s(e))\}}(X) \cdot \mathbf{1}_{\{\mathsf{E}_t(t(e))\}}(Y).$$

Then $\Sigma, \mathrm{M} \in \{0,1\}$ and for all X, Y one has the fuzzy-graph bound

$$\mathrm{M}(X,Y) \;\le\; \min\{\Sigma(X), \Sigma(Y)\},$$

since $\mathrm{M}(X,Y) = 1$ implies both indicators are 1. For the witnessing bound, fix $X = \mathsf{E}_t(s(e))$, $Y = \mathsf{E}_t(t(e))$ and $R := \lambda(e) \in \mathcal{R}^{(t)}_{\mathrm{cr}}$. By the inductive hypothesis,

$$R^{\flat}\big(X, Y\big) \;=\; 1.$$

Therefore

$$\sup_{Q \in \mathcal{R}^{(t)}} Q(X,Y) \;\ge\; R^{\flat}(X,Y) \;=\; 1 \;\ge\; \mathrm{M}(X,Y).$$

If no e connects X to Y, then $\mathrm{M}(X,Y) = 0$ and the inequality is trivial. Thus (Σ, M) satisfies both constraints and is a valid Meta-Fuzzy Graph on $\mathsf{FG}^{(t)}$, i.e. $\mathsf{E}_{t+1}(M) \in \mathsf{FG}^{(t+1)}$.

Injectivity and underlying crisp structure. By construction, the support

$$\{X : \Sigma(X) = 1\} \;=\; \{\mathsf{E}_t(v) \mid v \in V_M\}$$

is in bijection with V_M, and (X,Y) has $\mathrm{M}(X,Y) = 1$ iff there exists e with $s(e) = v$, $t(e) = w$ and $X = \mathsf{E}_t(v)$, $Y = \mathsf{E}_t(w)$. Hence the underlying crisp meta-digraph of $\mathsf{E}_{t+1}(M)$ is canonically isomorphic to M. Distinct M give distinct (Σ, M), so E_{t+1} is injective.

Base. For $t = 0$, take $\mathsf{E}_0 = \iota$ and note that all verifications above reduce to checking $0/1 \le \min(0/1, 0/1)$ and $0/1 \le \sup\{0,1\}$, which hold.

By induction, E_t exists for all t, proving the claim. □

2.3. *Meta-DiGraph*

Throughout, a (finite) *digraph* is a quadruple

$$D = (V_D, A_D, s_D, t_D),$$

where V_D is a finite vertex set, A_D is a finite arc set, and $s_D, t_D : A_D \to V_D$ give the source/target of each arc. Loops ($s_D(a) = t_D(a)$) and multiple arcs are allowed iff explicitly stated.

Definition 2.12 (Universe and relation family for digraphs)**.** Fix a nonempty universe $\mathfrak{D}$ of finite digraphs and a nonempty family of binary relations

$$\mathcal{R} \subseteq \mathcal{P}(\mathfrak{D} \times \mathfrak{D}).$$

Typical choices include:

- Sub: the (induced) subdigraph relation,
- Hom: the homomorphic reachability relation $(D_1, D_2) \in \mathrm{Hom}$ iff there exists a digraph homomorphism $D_1 \to D_2$,
- Min: the (directed) minor relation (when defined),
- Iso: isomorphism.

Definition 2.13 (Meta digraph over $(\mathfrak{D}, \mathcal{R})$)**.** A *meta digraph (digraph of digraphs)* over $(\mathfrak{D}, \mathcal{R})$ is a labeled digraph

$$M = (V_M, A_M, s_M, t_M, \lambda_M)$$

with

$$V_M \subseteq \mathfrak{D}, \qquad s_M, t_M : A_M \to V_M, \qquad \lambda_M : A_M \to \mathcal{R},$$

subject to the *incidence constraint*

$$\forall\, e \in A_M : \quad \big(s_M(e), t_M(e)\big) \in \lambda_M(e). \tag{2}$$

Each vertex of M is itself a (ground-level) digraph. For $e \in A_M$ with $\lambda_M(e) = R \in \mathcal{R}$, we write

$$s_M(e) \xrightarrow{R} t_M(e)$$

and call e a *meta-arc* (of type R).

Example 2.14 (Microservice Integration as a Meta Digraph)**.** Let $\mathfrak{D}$ contain the following ground-level *service call graphs* (digraphs):

$$D_{\mathrm{O}} = (V_{\mathrm{O}}, A_{\mathrm{O}}), \quad V_{\mathrm{O}} = \{\mathrm{web}, \mathrm{pay}\}, \quad A_{\mathrm{O}} = \{(\mathrm{web}, \mathrm{pay})\};$$

$$D_{\mathrm{P}} = (V_{\mathrm{P}}, A_{\mathrm{P}}), \quad V_{\mathrm{P}} = \{\mathrm{gw}, \mathrm{auth}\}, \quad A_{\mathrm{P}} = \{(\mathrm{gw}, \mathrm{auth})\};$$

$$D_{\mathrm{A}} = (V_{\mathrm{A}}, A_{\mathrm{A}}), \quad V_{\mathrm{A}} = \{\mathrm{etl}, \mathrm{db}\}, \quad A_{\mathrm{A}} = \{(\mathrm{etl}, \mathrm{db})\}.$$

Interpretation: Orders (D_{O}) calls Payments (D_{P}) which in turn feeds Analytics (D_{A}).
Let $\mathcal{R} := \{\mathrm{Hom}\}$, where $(D_1, D_2) \in \mathrm{Hom}$ iff there exists a digraph homomorphism $h : V(D_1) \to V(D_2)$ preserving arcs.
Witness homomorphisms. Define $h_1 : V_{\mathrm{O}} \to V_{\mathrm{P}}$ by $h_1(\mathrm{web}) = \mathrm{gw}$, $h_1(\mathrm{pay}) = \mathrm{auth}$. Then $(\mathrm{web}, \mathrm{pay}) \in A_{\mathrm{O}}$ maps to $(\mathrm{gw}, \mathrm{auth}) \in A_{\mathrm{P}}$, hence $(D_{\mathrm{O}}, D_{\mathrm{P}}) \in \mathrm{Hom}$. Define $h_2 : V_{\mathrm{P}} \to V_{\mathrm{A}}$ by $h_2(\mathrm{gw}) = \mathrm{etl}$, $h_2(\mathrm{auth}) = \mathrm{db}$. Then $(\mathrm{gw}, \mathrm{auth}) \in A_{\mathrm{P}}$ maps to $(\mathrm{etl}, \mathrm{db}) \in A_{\mathrm{A}}$, hence $(D_{\mathrm{P}}, D_{\mathrm{A}}) \in \mathrm{Hom}$.

Meta digraph. Let

$$M=(V_M,A_M,s_M,t_M,\lambda_M), \qquad V_M=\{D_{\mathrm{O}},D_{\mathrm{P}},D_{\mathrm{A}}\},$$

with meta-arcs

$$e_1:\ D_{\mathrm{O}}\xrightarrow{\mathrm{Hom}}D_{\mathrm{P}}, \qquad e_2:\ D_{\mathrm{P}}\xrightarrow{\mathrm{Hom}}D_{\mathrm{A}},$$

i.e. $s_M(e_1)=D_{\mathrm{O}}$, $t_M(e_1)=D_{\mathrm{P}}$, $\lambda_M(e_1)=\mathrm{Hom}$, and similarly for e_2. Each e_i satisfies the incidence constraint (2) by the witnessed h_1,h_2. (Composition $h_2\circ h_1$ also witnesses $(D_{\mathrm{O}},D_{\mathrm{A}})\in\mathrm{Hom}$, consistent with the meta-path $D_{\mathrm{O}}\to D_{\mathrm{P}}\to D_{\mathrm{A}}$.)

Proposition 2.15 (Symmetric relations induce undirected underlying meta structure)**.** *Suppose every $R\in\mathcal{R}$ is symmetric. Let M be a meta digraph over $(\mathfrak{D},\mathcal{R})$. Then the underlying unlabeled multigraph obtained by identifying each pair of opposite meta-arcs is well-defined. In particular, if $e\in A_M$ with $\lambda_M(e)=R$ and R is symmetric, then*

$$\big(t_M(e),s_M(e)\big)\in R,$$

so there exists a meta-arc e' (possibly equal to e) with $s_M(e')=t_M(e)$ and $t_M(e')=s_M(e)$.

Proof. Fix $e\in A_M$. By (2), $\big(s_M(e),t_M(e)\big)\in R$ with $R=\lambda_M(e)$. Symmetry gives $\big(t_M(e),s_M(e)\big)\in R$, hence a valid reverse meta-arc with the same label exists (in a simple meta digraph it must be identical, in a multidigraph it may be distinct). □

Proposition 2.16 (Compositional soundness along labeled meta-paths)**.** *Assume $\mathcal{R}$ is closed under (relational) composition: for any $R_1,\dots,R_k\in\mathcal{R}$ there exists $R\in\mathcal{R}$ with $R\supseteq R_k\circ\cdots\circ R_1$. If $x=v_0\xrightarrow{R_1}v_1\xrightarrow{R_2}\cdots\xrightarrow{R_k}v_k=y$ is a labeled meta-path in M, then*

$$(x,y)\ \in\ R_k\circ\cdots\circ R_1\ \subseteq\ R$$

for some $R\in\mathcal{R}$. In particular, reachability along meta-paths witnesses membership in (some) relation from $\mathcal{R}$ determined by composing the labels.

Proof. By (2), for each i one has $(v_{i-1},v_i)\in R_i$. Hence $(x,y)\in R_k\circ\cdots\circ R_1$ by definition of relational composition. Closure provides $R\in\mathcal{R}$ with $R\supseteq R_k\circ\cdots\circ R_1$. □

2.4. *Iterated Meta-DiGraph*

An Iterated Meta-DiGraph recursively builds meta-level digraphs over directed graphs, enabling layered representations of directional structures and their relational hierarchies.

Definition 2.17 (Relation lifting for digraphs)**.** Given $\mathcal{R}$ on $\mathfrak{D}$, define its *lift* $\mathcal{R}^{\uparrow}$ on the class of finite meta digraphs over $(\mathfrak{D},\mathcal{R})$ as

$$\mathcal{R}^{\uparrow}:=\{\,R^{\uparrow}\mid R\in\mathcal{R}\,\},\quad (M_1,M_2)\in R^{\uparrow}\iff\exists\,x\in V_{M_1},\,y\in V_{M_2}:\ (x,y)\in R.$$

Definition 2.18 (Iterated universes for digraphs)**.** Define recursively for $t \in \mathbb{N}_0$:

$$\mathfrak{D}^{(0)} := \mathfrak{D}, \qquad \mathcal{R}^{(0)} := \mathcal{R},$$

$$\mathfrak{D}^{(t+1)} := \Big\{ \text{all finite meta digraphs over } \big(\mathfrak{D}^{(t)}, \mathcal{R}^{(t)}\big) \Big\}, \qquad \mathcal{R}^{(t+1)} := \big(\mathcal{R}^{(t)}\big)^{\uparrow}.$$

Definition 2.19 (Iterated Meta Digraph of depth t)**.** For $t \in \mathbb{N}_0$, an *iterated meta digraph of depth t* is a labeled digraph

$$M^{(t)} = (V^{(t)}, A^{(t)}, s^{(t)}, t^{(t)}, \lambda^{(t)}),$$

with $V^{(t)} \subseteq \mathfrak{D}^{(t)}$, $\lambda^{(t)} : A^{(t)} \to \mathcal{R}^{(t)}$, and

$$\forall e \in A^{(t)} : \qquad \big(s^{(t)}(e),\, t^{(t)}(e)\big) \;\in\; \lambda^{(t)}(e). \tag{3}$$

Example 2.20 (Department-Level Adoption as an Iterated Meta Digraph)**.** Retain $\mathfrak{D}$ and $\mathcal{R} = \{\mathrm{Hom}\}$ as above. Form two level-1 *meta digraphs* representing departments:
Commerce M_{C} with vertex set $V(M_{\mathrm{C}}) = \{D_{\mathrm{O}}, D_{\mathrm{P}}\}$ and the meta-arc $D_{\mathrm{O}} \xrightarrow{\mathrm{Hom}} D_{\mathrm{P}}$ (witness h_1).
Data M_{D} with vertex set $V(M_{\mathrm{D}}) = \{D_{\mathrm{A}}\}$ (no internal meta-arc needed).
Define the lifted relation family $\mathcal{R}^{\uparrow}$ by

$$(M_1, M_2) \in \mathrm{Hom}^{\uparrow} \iff \exists\, x \in V(M_1),\, y \in V(M_2) :\; (x, y) \in \mathrm{Hom}.$$

Since $(D_{\mathrm{P}}, D_{\mathrm{A}}) \in \mathrm{Hom}$ (witness h_2) with $D_{\mathrm{P}} \in V(M_{\mathrm{C}})$ and $D_{\mathrm{A}} \in V(M_{\mathrm{D}})$, we have

$$(M_{\mathrm{C}}, M_{\mathrm{D}}) \in \mathrm{Hom}^{\uparrow}.$$

Iterated meta digraph (depth 1*).* Let

$$M^{(1)} = \big(V^{(1)}, A^{(1)}, s^{(1)}, t^{(1)}, \lambda^{(1)}\big), \qquad V^{(1)} = \{M_{\mathrm{C}}, M_{\mathrm{D}}\},$$

with the meta-arc

$$E :\; M_{\mathrm{C}} \xrightarrow{\mathrm{Hom}^{\uparrow}} M_{\mathrm{D}}.$$

By construction $\big(s^{(1)}(E), t^{(1)}(E)\big) = (M_{\mathrm{C}}, M_{\mathrm{D}}) \in \mathrm{Hom}^{\uparrow} = \lambda^{(1)}(E)$, so the incidence constraint (3) holds. Interpretation: because a concrete homomorphism maps Payments to Analytics at the service level, a *department-level* integration arrow exists from Commerce to Data at the iterated meta level.

Theorem 2.21 (Iterated Meta Digraph generalizes Meta Digraph)**.** *Depth* 1 *coincides with the meta level:*

$$\Big\{\textit{meta digraphs over } (\mathfrak{D}, \mathcal{R})\Big\} \;=\; \Big\{\textit{iterated meta digraphs of depth } 1\Big\}.$$

Hence the class of Iterated Meta Digraphs (depth $t \geq 1$) strictly extends the class of Meta Digraphs.

Proof. By Definition 2.18, $\mathfrak{D}^{(1)}$ is *by construction* the class of all finite meta digraphs over $(\mathfrak{D}, \mathcal{R})$, and $\mathcal{R}^{(1)} = \mathcal{R}^{\uparrow}$. Unfolding Definition 2.19 at $t = 1$ gives: an object

$$M^{(1)} = (V^{(1)}, A^{(1)}, s^{(1)}, t^{(1)}, \lambda^{(1)})$$

with $V^{(1)} \subseteq \mathfrak{D}^{(1)}$ and $\lambda^{(1)} : A^{(1)} \to \mathcal{R}^{(1)}$ satisfying (3). But this is *exactly* the definition of a meta digraph taken one level up (its vertices are digraphs-at-level 1, i.e., ordinary meta digraphs). Therefore "depth 1 iterated meta digraph" and "meta digraph" coincide after one expansion. Consequently, allowing $t \geq 1$ yields a hierarchy that contains the t=1 case as a special case, so Iterated Meta Digraphs generalize Meta Digraphs. □

2.5. *Meta-MultiGraph*

A Meta-MultiGraph treats multigraphs as vertices, with labeled meta-edges capturing relations like subgraph, isomorphism, or homomorphism among multigraphs.

Definition 2.22 (Universe and relation family for multigraphs)**.** Fix a nonempty universe $\mathfrak{M}$ of finite multigraphs and a nonempty family of binary relations

$$\mathcal{S} \subseteq \mathcal{P}\big(\mathfrak{M} \times \mathfrak{M}\big).$$

Typical relations include:

- $\mathrm{Sub}^{\times}$: multiplicity-respecting subgraph relation ($H \subseteq G$ and each edge multiplicity in H is $\leq$ that in G),
- $\mathrm{Hom}^{\times}$: existence of a multigraph homomorphism,
- $\mathrm{Iso}^{\times}$: multigraph isomorphism.

Definition 2.23 (Meta multigraph over $(\mathfrak{M}, \mathcal{S})$)**.** A *meta multigraph (multigraph of multigraphs)* over $(\mathfrak{M}, \mathcal{S})$ is a labeled multigraph

$$\mathbb{M} = (V_{\mathbb{M}}, E_{\mathbb{M}}, \varphi_{\mathbb{M}}, \lambda_{\mathbb{M}})$$

with

$$V_{\mathbb{M}} \subseteq \mathfrak{M}, \qquad \varphi_{\mathbb{M}} : E_{\mathbb{M}} \to \big\{\{X, Y\} \mid X, Y \in V_{\mathbb{M}}\big\}, \qquad \lambda_{\mathbb{M}} : E_{\mathbb{M}} \to \mathcal{S},$$

subject to the *incidence constraint*

$$\forall\, e \in E_{\mathbb{M}} : \quad \varphi_{\mathbb{M}}(e) = \{X, Y\} \;\Rightarrow\; (X, Y) \in \lambda_{\mathbb{M}}(e) \;\text{ and }\; (Y, X) \in \lambda_{\mathbb{M}}(e). \tag{4}$$

Thus each meta-edge e (possibly a loop when $X = Y$) connects two ground-level multigraphs $X, Y \in V_{\mathbb{M}}$ and is labeled by some $S = \lambda_{\mathbb{M}}(e) \in \mathcal{S}$ that relates X and Y. Parallel meta-edges $\{e_1, \ldots\}$ between the same pair $\{X, Y\}$ are permitted and may carry distinct labels from $\mathcal{S}$.

Example 2.24 (Airline Route Networks as a Meta-Multigraph)**.** Let $\mathfrak{M}$ be multigraphs whose vertices are airports and whose parallel edges encode the *number of daily direct flights* on a city pair. Consider three carriers on the airport set $\{\mathrm{HND}, \mathrm{KIX}, \mathrm{CTS}\}$:

Carrier J: G_J has 8 parallel edges on $\{\mathrm{HND}, \mathrm{CTS}\}$ and 6 on $\{\mathrm{HND}, \mathrm{KIX}\}$.
Carrier N: G_N has 5 on $\{\mathrm{HND}, \mathrm{KIX}\}$ and 3 on $\{\mathrm{KIX}, \mathrm{CTS}\}$.
Carrier F: G_F has 2 on $\{\mathrm{HND}, \mathrm{CTS}\}$.

Define two *symmetric* relations on $\mathfrak{M}$:

$$S^{\mathrm{Jacc}}_{\geq\theta}(X,Y) := \mathbf{1}\left\{\frac{|E^*_X \cap E^*_Y|}{|E^*_X \cup E^*_Y|} \geq \theta\right\},$$

$$S^{\mathrm{code}}(X,Y) := \mathbf{1}\{\text{codeshare agreement between the carriers of } X, Y\},$$

where E^* denotes the *underlying simple* edge set (multiplicities ignored). Fix $\theta = \frac{1}{3}$ and assume

$$S^{\mathrm{code}}(G_J, G_N) = 1, \qquad S^{\mathrm{code}}(G_J, G_F) = 0, \qquad S^{\mathrm{code}}(G_N, G_F) = 0.$$

Compute Jaccard indices:

$$E^*_{G_J} = \{\{\mathrm{HND}, \mathrm{KIX}\}, \{\mathrm{HND}, \mathrm{CTS}\}\}, \quad E^*_{G_N} = \{\{\mathrm{HND}, \mathrm{KIX}\}, \{\mathrm{KIX}, \mathrm{CTS}\}\}, \quad E^*_{G_F} = \{\{\mathrm{HND}, \mathrm{CTS}\}\}.$$

Hence

$$J(G_J, G_N) = \frac{1}{3}\ (\Rightarrow S^{\mathrm{Jacc}}_{\geq 1/3} = 1), \quad J(G_J, G_F) = \frac{1}{2}\ (\Rightarrow 1), \quad J(G_N, G_F) = 0\ (\Rightarrow 0).$$

Form the meta multigraph

$$\mathbb{M} = (V_{\mathbb{M}}, E_{\mathbb{M}}, \varphi_{\mathbb{M}}, \lambda_{\mathbb{M}}), \qquad V_{\mathbb{M}} = \{G_J, G_N, G_F\},$$

with (parallel) meta-edges over the same pair:

$$e_1 : \varphi_{\mathbb{M}}(e_1) = \{G_J, G_N\},\ \lambda_{\mathbb{M}}(e_1) = S^{\mathrm{Jacc}}_{\geq 1/3},$$
$$e_2 : \varphi_{\mathbb{M}}(e_2) = \{G_J, G_N\},\ \lambda_{\mathbb{M}}(e_2) = S^{\mathrm{code}},$$
$$e_3 : \varphi_{\mathbb{M}}(e_3) = \{G_J, G_F\},\ \lambda_{\mathbb{M}}(e_3) = S^{\mathrm{Jacc}}_{\geq 1/3}.$$

All labels are symmetric, so the incidence constraint (4) holds: for each e_i, $(X,Y) \in \lambda_{\mathbb{M}}(e_i)$ and $(Y,X) \in \lambda_{\mathbb{M}}(e_i)$. This concrete model exhibits the *multigraph* nature at the meta-level via the two parallel meta-edges e_1, e_2 between G_J and G_N, capturing distinct reasons (overlap vs. codeshare) for relating the two carriers.

Remark 2.25 (Directed variant)**.** A *directed* meta multigraph is obtained by replacing unordered pairs $\{X, Y\}$ with ordered pairs (X, Y) and dropping the symmetry requirement in (4).

Proposition 2.26 (Projection and forgetful functors)**.** *There is a natural forgetful projection*

$$\Pi:\ \mathbb{M} \longmapsto \big(V_{\mathbb{M}},\ \{\{X,Y\} \mid \exists e \in E_{\mathbb{M}} \text{ with } \varphi_{\mathbb{M}}(e) = \{X,Y\}\}\big),$$

which sends a meta multigraph to its unlabeled, underlying simple graph on meta-vertices. Moreover, the label map $\lambda_{\mathbb{M}}$ *factors through* Π *by aggregating labels on parallel meta-edges:*

$$\Lambda:\ \{X,Y\} \longmapsto \{\ \lambda_{\mathbb{M}}(e)\ :\ e \in E_{\mathbb{M}},\ \varphi_{\mathbb{M}}(e) = \{X,Y\}\ \} \ \subseteq\ \mathcal{S}.$$

Proof. By definition of $\varphi_{\mathbb{M}}$, each meta-edge determines an unordered pair $\{X,Y\}$, giving the edge set of $\Pi(\mathbb{M})$. Parallel meta-edges over the same pair are collapsed; collecting their labels defines Λ. □

2.6. *Iterated Meta-MultiGraph*

Fix a nonempty universe $\mathfrak{M}$ of finite multigraphs and a nonempty family $\mathcal{S}$ of *symmetric* binary relations on $\mathfrak{M}$ (e.g. multigraph isomorphism, "mutual" similarity, etc.).

Definition 2.27 (Relation lifting for multigraphs)**.** Given $\mathcal{S}$ on $\mathfrak{M}$, define its *lift* $\mathcal{S}^{\uparrow}$ on the class of finite meta multigraphs over $(\mathfrak{M},\mathcal{S})$ by

$$\mathcal{S}^{\uparrow} := \{\, S^{\uparrow} \mid S \in \mathcal{S}\,\}, \quad (\mathbb{M}_1,\mathbb{M}_2) \in S^{\uparrow} \iff \exists\, X \in V_{\mathbb{M}_1},\, Y \in V_{\mathbb{M}_2}:\ (X,Y) \in S.$$

If S is symmetric, then $S^{\uparrow}$ is symmetric as well.

Definition 2.28 (Iterated universes for multigraphs)**.** Define recursively for $t \in \mathbb{N}_0$:

$$\mathfrak{M}^{(0)} := \mathfrak{M}, \qquad \mathcal{S}^{(0)} := \mathcal{S},$$

$$\mathfrak{M}^{(t+1)} := \Big\{ \text{all finite meta multigraphs over } \big(\mathfrak{M}^{(t)},\mathcal{S}^{(t)}\big) \Big\}, \qquad \mathcal{S}^{(t+1)} := \big(\mathcal{S}^{(t)}\big)^{\uparrow}.$$

Definition 2.29 (Iterated Meta Multigraph of depth t)**.** For $t \in \mathbb{N}_0$, an *iterated meta multigraph of depth* t is a labeled multigraph

$$\mathbb{M}^{(t)} = (V^{(t)}, E^{(t)}, \varphi^{(t)}, \lambda^{(t)}),$$

with $V^{(t)} \subseteq \mathfrak{M}^{(t)}$, $\lambda^{(t)} : E^{(t)} \to \mathcal{S}^{(t)}$, and

$$\forall e \in E^{(t)}: \qquad \varphi^{(t)}(e) = \{X,Y\} \implies (X,Y) \in \lambda^{(t)}(e). \tag{5}$$

Example 2.30 (University Pathways as an Iterated Meta Digraph)**.** Let $\mathfrak{D}$ be *course-prerequisite digraphs.* Consider three curricula, each a single prerequisite arrow:

$$D_{\text{Calc}} = \big(\{C_1,C_2\},\{(C_1,C_2)\}\big), \quad D_{\text{Math}} = \big(\{M_1,M_2\},\{(M_1,M_2)\}\big),$$
$$D_{\text{Phys}} = \big(\{P_1,P_2\},\{(P_1,P_2)\}\big).$$

Let $\mathcal{R} = \{\text{Hom}\}$, where $(D_1, D_2) \in \text{Hom}$ iff there exists a digraph homomorphism $h : V(D_1) \to V(D_2)$ preserving arcs. Define

$$h_{CM}(C_1) = M_1,\ h_{CM}(C_2) = M_2 \quad \Rightarrow \quad (D_{\text{Calc}}, D_{\text{Math}}) \in \text{Hom},$$

$$h_{MP}(M_1) = P_1,\ h_{MP}(M_2) = P_2 \quad \Rightarrow \quad (D_{\text{Math}}, D_{\text{Phys}}) \in \text{Hom}.$$

Level 1 (Meta digraphs of departments). Let

$$M_{\text{Sci}} = (V_{\text{Sci}}, A_{\text{Sci}}, s, t, \lambda), \quad V_{\text{Sci}} = \{D_{\text{Calc}}, D_{\text{Math}}\}, \quad D_{\text{Calc}} \xrightarrow{\text{Hom}} D_{\text{Math}},$$

and

$$M_{\text{Eng}} = (V_{\text{Eng}}, A_{\text{Eng}}, s, t, \lambda), \quad V_{\text{Eng}} = \{D_{\text{Phys}}\} \text{ (no internal meta-arc)}.$$

Lifted relation. Define $\text{Hom}^{\uparrow}$ on level-1 meta objects by

$$(M_1, M_2) \in \text{Hom}^{\uparrow} \iff \exists\, x \in V_{M_1},\, y \in V_{M_2} :\ (x, y) \in \text{Hom}.$$

Because $(D_{\text{Math}}, D_{\text{Phys}}) \in \text{Hom}$ with $D_{\text{Math}} \in V_{\text{Sci}}$ and $D_{\text{Phys}} \in V_{\text{Eng}}$, we have

$$(M_{\text{Sci}}, M_{\text{Eng}}) \in \text{Hom}^{\uparrow}.$$

Iterated meta digraph (depth 1). Set

$$M^{(1)} = \big(\{M_{\text{Sci}}, M_{\text{Eng}}\}, \{E\}, s^{(1)}, t^{(1)}, \lambda^{(1)}\big), \qquad E :\ M_{\text{Sci}} \xrightarrow{\text{Hom}^{\uparrow}} M_{\text{Eng}}.$$

The incidence condition (3) holds since $\big(s^{(1)}(E), t^{(1)}(E)\big) = (M_{\text{Sci}}, M_{\text{Eng}}) \in \text{Hom}^{\uparrow}$. Interpretation: a concrete prerequisite mapping from Mathematics to Physics at the course level induces a *department-to-department* articulation arrow at the iterated meta level.

Theorem 2.31 (Iterated Meta Multigraph generalizes Meta Multigraph)**.** *Depth* 1 *coincides with the meta level:*

$$\Big\{\textit{meta multigraphs over } (\mathfrak{M}, \mathcal{S})\Big\} \;=\; \Big\{\textit{iterated meta multigraphs of depth } 1\Big\}.$$

Hence the class of Iterated Meta Multigraphs (depth $t \geq 1$) strictly extends the class of Meta Multigraphs.

Proof. By Definition 2.28, $\mathfrak{M}^{(1)}$ equals the class of all finite meta multigraphs over $(\mathfrak{M}, \mathcal{S})$, and $\mathcal{S}^{(1)} = \mathcal{S}^{\uparrow}$. Unfolding Definition 2.29 at $t = 1$ gives: an object

$$\mathbb{M}^{(1)} = (V^{(1)}, E^{(1)}, \varphi^{(1)}, \lambda^{(1)})$$

with $V^{(1)} \subseteq \mathfrak{M}^{(1)}$ and $\lambda^{(1)} : E^{(1)} \to \mathcal{S}^{(1)}$ satisfying (5). This is precisely the notion of a meta multigraph one level up (its vertices are multigraphs-at-level 1, i.e., ordinary meta multigraphs). Therefore depth 1 iterated meta multigraphs coincide (after one expansion) with meta multigraphs. Allowing $t \geq 1$ yields a hierarchy that contains the t=1 case, so iterated meta multigraphs generalize meta multigraphs. □

2.7. *Meta-Bidigraph*

A Meta-Bidigraph models relations among bidigraphs, with meta-edges labeled by corridor relations, ensuring endpoint orientations match operational requirements.

Definition 2.32 (Meta-Bidigraph over $(\mathfrak{B}, \mathcal{R})$)**.** Let $\mathcal{R} \subseteq \mathcal{P}(\mathfrak{B} \times \mathfrak{B})$ be a nonempty family of binary relations on $\mathfrak{B}$. A *Meta-Bidigraph* is a labeled bidigraph

$$\mathbb{M} \ := \ (V_{\mathbb{M}}, E_{\mathbb{M}}, \partial_{\mathbb{M}}, \tau_{\mathbb{M}}, \lambda_{\mathbb{M}})$$

consisting of:

- $V_{\mathbb{M}} \subseteq \mathfrak{B}$ (meta-vertices are bidigraphs),
- an incidence map $\partial_{\mathbb{M}} : E_{\mathbb{M}} \to \big\{\{X, Y\} \subseteq V_{\mathbb{M}} \mid X \neq Y\big\}$,
- a meta bidirection $\tau_{\mathbb{M}} : V_{\mathbb{M}} \times E_{\mathbb{M}} \to \{-1, 0, 1\}$ with $\tau_{\mathbb{M}}(v, e) = 0$ iff $v \notin \partial_{\mathbb{M}}(e)$ and otherwise $\tau_{\mathbb{M}}(v, e) \in \{-1, +1\}$,
- a label map $\lambda_{\mathbb{M}} : E_{\mathbb{M}} \to \mathcal{R}$,

subject to the *witnessing constraint*: for each $e \in E_{\mathbb{M}}$ with $\partial_{\mathbb{M}}(e) = \{X, Y\}$, define the *demand set*

$$\mathrm{Dem}(e) \ := \begin{cases} \{(X, Y)\}, & \text{if } \big(\tau_{\mathbb{M}}(X, e), \tau_{\mathbb{M}}(Y, e)\big) = (-1, +1), \\ \{(Y, X)\}, & \text{if } \big(\tau_{\mathbb{M}}(X, e), \tau_{\mathbb{M}}(Y, e)\big) = (+1, -1), \\ \{(X, Y), (Y, X)\}, & \text{if } \big(\tau_{\mathbb{M}}(X, e), \tau_{\mathbb{M}}(Y, e)\big) = (+1, +1), \\ \emptyset, & \text{if } \big(\tau_{\mathbb{M}}(X, e), \tau_{\mathbb{M}}(Y, e)\big) = (-1, -1). \end{cases}$$

Then one requires $\mathrm{Dem}(e) \subseteq \lambda_{\mathbb{M}}(e)$ (i.e. every oriented requirement encoded by the local signs is witnessed by the chosen relation label).

Example 2.33 (City Logistics Corridors as a Meta-Bidigraph)**. Ground level (bidigraphs).** Let $\mathfrak{B}$ contain district-level curbside logistics networks modeled as bidigraphs B_T, B_O, B_N for *Tokyo*, *Osaka*, *Nagoya*. Each $B = (G, \tau)$ has intersections as vertices and street segments as edges. At each incident pair (v, e), the local sign $\tau(v, e) \in \{-1, +1\}$ indicates whether the segment e is configured *away from* v (-1, dispatch/loading outflow) or *towards* v ($+1$, arrival/unloading inflow). (Non-incidences get 0.)

Assume there is a long-haul corridor between the two districts B_T and B_O realized by a street segment e_{TO} whose endpoints lie on the district boundaries (abstracted at the meta level). Operationally, freight travels from B_T to B_O, so we record at the meta level the local signs

$$\big(\tau_{\mathbb{M}}(B_T, e_{TO}),\ \tau_{\mathbb{M}}(B_O, e_{TO})\big) = (-1, +1).$$

Similarly, suppose B_O and B_N operate a *balanced exchange* corridor (temporary shuttle both ways), so for a meta edge e_{ON} we set

$$\big(\tau_{\mathbb{M}}(B_O, e_{ON}),\ \tau_{\mathbb{M}}(B_N, e_{ON})\big) = (+1, +1).$$

Relation family. Let $\mathcal{R} = \{\mathrm{Ship}, \mathrm{Sync}\}$, where

$$(X, Y) \in \mathrm{Ship} \iff \text{there exists at least one operational}$$

$$\text{outbound lane in } X \text{ and inbound lane in } Y \text{ along the corridor,}$$

$$(X, Y) \in \mathrm{Sync} \iff (X, Y) \in \mathrm{Ship} \text{ and}$$

$$(Y, X) \in \mathrm{Ship} \quad \text{(hence Sync is symmetric).}$$

Meta-Bidigraph. Define the Meta-Bidigraph

$$\mathbb{M} = \big(V_{\mathbb{M}}, E_{\mathbb{M}}, \partial_{\mathbb{M}}, \tau_{\mathbb{M}}, \lambda_{\mathbb{M}}\big), \qquad V_{\mathbb{M}} = \{B_T, B_O, B_N\},$$

with meta-edges and labels

$$\partial_{\mathbb{M}}(e_{TO}) = \{B_T, B_O\},\ \lambda_{\mathbb{M}}(e_{TO}) = \mathrm{Ship}, \qquad \partial_{\mathbb{M}}(e_{ON}) = \{B_O, B_N\},\ \lambda_{\mathbb{M}}(e_{ON}) = \mathrm{Sync}.$$

Witnessing holds:

$$\mathrm{Dem}(e_{TO}) = \{(B_T, B_O)\} \subseteq \mathrm{Ship} = \lambda_{\mathbb{M}}(e_{TO}), \qquad \mathrm{Dem}(e_{ON}) = \{(B_O, B_N), (B_N, B_O)\} \subseteq \mathrm{Sync} = \lambda_{\mathbb{M}}(e_{ON}).$$

Thus $\mathbb{M}$ is a concrete *Meta-Bidigraph* of district curb networks: meta-vertices are bidigraphs of local streets, and meta-edges encode corridor policies with endpoint-local orientations.

Remark 2.34 (Directed shadow)**.** Given a Meta-Bidigraph $\mathbb{M}$, its *directed shadow* is the labeled digraph

$$\overrightarrow{\mathbb{M}} = (V_{\mathbb{M}}, A, s, t, \Lambda), \quad A := \{\, e \in E_{\mathbb{M}} \mid \tau_{\mathbb{M}}(X, e) = -1,\ \tau_{\mathbb{M}}(Y, e) = +1 \,\},$$

with $s(e) = X$, $t(e) = Y$, and $\Lambda(e) := \lambda_{\mathbb{M}}(e)$. Thus $(-1, +1)$ at the endpoints realizes a directed meta-arc $X \to Y$.

Definition 2.35 (Simple digraph and Meta DiGraph (recall, restricted))**.** Let $\mathfrak{D}^{\circ}$ be the class of finite *simple* digraphs $D = (V_D, A_D)$: no loops; for distinct $u \neq v$ there is *at most one* of (u, v) or (v, u) in A_D (i.e. no 2-cycles and no parallel arcs). Let $\mathcal{Q} \subseteq \mathcal{P}(\mathfrak{D}^{\circ} \times \mathfrak{D}^{\circ})$ be a nonempty family of binary relations. A (labeled) *Meta DiGraph* over $(\mathfrak{D}^{\circ}, \mathcal{Q})$ is a quintuple

$$M = (V_M, A_M, s_M, t_M, \lambda_M),$$

with $V_M \subseteq \mathfrak{D}^{\circ}$, $s_M, t_M : A_M \to V_M$, $\lambda_M : A_M \to \mathcal{Q}$ and the incidence constraint

$$\forall a \in A_M : \quad (s_M(a), t_M(a)) \in \lambda_M(a).$$

Definition 2.36 (Embedding $\Phi : \mathfrak{D}^{\circ} \hookrightarrow \mathfrak{B}$)**.** For $D = (V_D, A_D) \in \mathfrak{D}^{\circ}$, define the bidigraph $\Phi(D) = (G, \tau)$ as follows:

$$G = (V_D, E), \qquad E = \big\{\{u, v\} \subseteq V_D \mid (u, v) \in A_D \text{ or } (v, u) \in A_D\big\}.$$

For $e = \{u, v\} \in E$ set

$$(\tau(u,e), \tau(v,e)) := \begin{cases} (-1,+1), & \text{if } (u,v) \in A_D, \\ (+1,-1), & \text{if } (v,u) \in A_D. \end{cases}$$

This is well-defined because $\mathfrak{D}^\circ$ forbids 2-cycles, so at most one of (u, v), (v, u) exists.

Definition 2.37 (Relation transfer $\mathcal{Q} \to \mathcal{R}$)**.** Given $\mathcal{Q} \subseteq \mathcal{P}(\mathfrak{D}^\circ \times \mathfrak{D}^\circ)$, define

$$\mathcal{R} := \left\{ R^\flat \subseteq \mathfrak{B} \times \mathfrak{B} \;\middle|\; R \in \mathcal{Q} \text{ and } R^\flat\big(\Phi(D_1), \Phi(D_2)\big) \iff (D_1, D_2) \in R \right\}.$$

Thus each crisp relation R on digraphs is transported to a relation $R^\flat$ on the image bidigraphs.

Theorem 2.38 (Meta-Bidigraph generalizes Meta DiGraph)**.** *Let $M = (V_M, A_M, s_M, t_M, \lambda_M)$ be a Meta DiGraph over $(\mathfrak{D}^\circ, \mathcal{Q})$. Define a Meta-Bidigraph*

$$\mathbb{M} := \big(V_{\mathbb{M}}, E_{\mathbb{M}}, \partial_{\mathbb{M}}, \tau_{\mathbb{M}}, \lambda_{\mathbb{M}}\big)$$

over $(\mathfrak{B}, \mathcal{R})$ by

$$V_{\mathbb{M}} := \{\Phi(D) \mid D \in V_M\}, \qquad E_{\mathbb{M}} := A_M, \qquad \partial_{\mathbb{M}}(a) := \big\{\Phi(s_M(a)), \Phi(t_M(a))\big\},$$

$$\tau_{\mathbb{M}}\big(\Phi(s_M(a)), a\big) = -1, \quad \tau_{\mathbb{M}}\big(\Phi(t_M(a)), a\big) = +1, \quad \lambda_{\mathbb{M}}(a) := \lambda_M(a)^\flat.$$

Then $\mathbb{M}$ is a Meta-Bidigraph, and its directed shadow $\overrightarrow{\mathbb{M}}$ is canonically isomorphic to M.

Proof. (1) *Well-defined bidirection.* For each $a \in A_M$, the edge a is incident exactly with the two meta-vertices $\Phi(s_M(a))$ and $\Phi(t_M(a))$. By definition $\tau_{\mathbb{M}}(\cdot, a) \in \{-1, +1\}$ on these two vertices and 0 elsewhere, hence it is a valid bidirection.

(2) *Witnessing constraint.* Let $a \in E_{\mathbb{M}}$ and write $X = \Phi(s_M(a))$, $Y = \Phi(t_M(a))$. Then $\big(\tau_{\mathbb{M}}(X, a), \tau_{\mathbb{M}}(Y, a)\big) = (-1, +1)$, so $\mathrm{Dem}(a) = \{(X, Y)\}$, which must be contained in $\lambda_{\mathbb{M}}(a)$. Since $\lambda_{\mathbb{M}}(a) = \lambda_M(a)^\flat$ and $(s_M(a), t_M(a)) \in \lambda_M(a)$ by the Meta DiGraph incidence, we get $(X, Y) \in \lambda_M(a)^\flat = \lambda_{\mathbb{M}}(a)$ by the definition of $R^\flat$. Thus the witnessing constraint holds for every a.

(3) *Directed shadow.* By construction, $a \in A$ (the shadow arcs) iff $\big(\tau_{\mathbb{M}}(X, a), \tau_{\mathbb{M}}(Y, a)\big) = (-1, +1)$, with $s(a) = X$ and $t(a) = Y$. The map

$$\varphi : V_M \to V_{\mathbb{M}}, \quad \varphi(D) := \Phi(D),$$

is a bijection (because Φ is injective); and $a \mapsto a$ identifies A_M with A preserving source, target, and labels ($\lambda_M(a)$ corresponds to $\lambda_{\mathbb{M}}(a) = \lambda_M(a)^\flat$). Hence $\overrightarrow{\mathbb{M}}$ is canonically isomorphic to M. Therefore $\mathbb{M}$ is a Meta-Bidigraph whose directed shadow recovers the given Meta DiGraph, proving that Meta-Bidigraphs generalize Meta DiGraphs (on the natural simple-digraph domain $\mathfrak{D}^\circ$). □

2.8. *Iterated Meta-Bidigraph*

An Iterated Meta-Bidigraph recursively builds meta-levels of bidigraphs, capturing hierarchical corridor structures where alliances of bidigraphs interact through lifted relations.

Definition 2.39 (Iterated universes and lifted relations)**.** Fix a nonempty universe $\mathfrak{B}$ of finite bidigraphs and a nonempty family $\mathcal{R}^{(0)} \subseteq \mathcal{P}(\mathfrak{B} \times \mathfrak{B})$ of binary relations on $\mathfrak{B}$. Define recursively for $t \in \mathbb{N}_0$:

$$\mathfrak{B}^{(0)} := \mathfrak{B}, \qquad \mathfrak{B}^{(t+1)} := \Big\{ \text{ all Meta-Bidigraphs over } \big(\mathfrak{B}^{(t)}, \mathcal{R}^{(t)}\big) \Big\},$$

$$\mathcal{R}^{(t+1)} := \{ R^{\uparrow} \mid R \in \mathcal{R}^{(t)} \}, \quad \text{where } (X,Y) \in R^{\uparrow} \iff \exists x \in V_X,\, y \in V_Y : (x,y) \in R.$$

(Here V_X denotes the meta-vertex set of $X \in \mathfrak{B}^{(t+1)}$.)

Definition 2.40 (Iterated Meta-Bidigraph of depth t)**.** For $t \in \mathbb{N}_0$, any object $\mathbb{M}^{(t)} \in \mathfrak{B}^{(t)}$ is called an *Iterated Meta-Bidigraph of depth* t. Equivalently, $\mathbb{M}^{(t+1)}$ is a Meta-Bidigraph whose meta-vertices are elements of $\mathfrak{B}^{(t)}$ and whose labels lie in $\mathcal{R}^{(t)}$, with the (previously fixed) Meta-Bidigraph witnessing constraint enforced at level $t+1$.

Example 2.41 (Regional Alliances as an Iterated Meta-Bidigraph)**. Level** 0 **(bidigraphs and relations).** Keep B_T, B_O, B_N and $\mathcal{R}^{(0)} = \{\mathrm{Ship}, \mathrm{Sync}\}$ as in the previous example, so that, in particular, $(B_T, B_O) \in \mathrm{Ship}$ and $(B_O, B_N), (B_N, B_O) \in \mathrm{Ship}$ (hence $(B_O, B_N) \in \mathrm{Sync}$). **Level** 1 **(Meta-Bidigraphs of alliances).** Form two *Meta-Bidigraph* alliances:

$$\mathbb{E} : V_{\mathbb{E}} = \{B_T, B_O\} \quad \text{(East Alliance)}, \qquad \mathbb{W} : V_{\mathbb{W}} = \{B_N\} \quad \text{(West Alliance)},$$

with their internal meta-edges inherited (e.g., $\{B_T, B_O\}$ labeled Ship, signs $(-1,+1)$ as above). **Lifted relations to level** 1**.** By the iterated construction, define

$$\mathcal{R}^{(1)} = \{R^{\uparrow} \mid R \in \mathcal{R}^{(0)}\}, \qquad (X,Y) \in R^{\uparrow} \iff \exists x \in V_X,\ y \in V_Y : (x,y) \in R.$$

Because $(B_O, B_N) \in \mathrm{Ship}$ with $B_O \in V_{\mathbb{E}}$ and $B_N \in V_{\mathbb{W}}$, we have

$$(\mathbb{E}, \mathbb{W}) \in \mathrm{Ship}^{\uparrow}.$$

Iterated Meta-Bidigraph (depth 1**).** Create a level-2 object whose meta-vertices are the *level-1 Meta-Bidigraphs* $\mathbb{E}$ and $\mathbb{W}$:

$$\mathbb{M}^{(1)} = \big(V^{(1)}, E^{(1)}, \partial^{(1)}, \tau^{(1)}, \lambda^{(1)}\big), \qquad V^{(1)} = \{\mathbb{E}, \mathbb{W}\}.$$

Add a meta-edge $e^{(1)}$ with

$$\partial^{(1)}(e^{(1)}) = \{\mathbb{E}, \mathbb{W}\}, \quad \big(\tau^{(1)}(\mathbb{E}, e^{(1)}), \tau^{(1)}(\mathbb{W}, e^{(1)})\big) = (-1,+1), \quad \lambda^{(1)}(e^{(1)}) = \mathrm{Ship}^{\uparrow}.$$

Witnessing at level 1 holds since

$$\mathrm{Dem}(e^{(1)}) = \{(\mathbb{E}, \mathbb{W})\} \subseteq \mathrm{Ship}^{\uparrow} = \lambda^{(1)}(e^{(1)}),$$

because it is witnessed by the base pair $(B_O, B_N) \in \mathrm{Ship}$. Interpretation: a concrete corridor from Osaka to Nagoya at the district level induces an *alliance-level* oriented supply relation from the East to the West, encoded as a meta-edge in the *Iterated Meta-Bidigraph.*

Theorem 2.42 (Depth 1 recovers Meta-Bidigraphs)**.** *$\mathfrak{B}^{(1)}$ is precisely the class of Meta-Bidigraphs over $(\mathfrak{B}^{(0)}, \mathcal{R}^{(0)})$. Hence Iterated Meta-Bidigraphs (with arbitrary depth $t \geq 1$) generalize Meta-Bidigraphs.*

Proof. By definition, $\mathfrak{B}^{(1)} := \{\text{all Meta-Bidigraphs over } (\mathfrak{B}^{(0)}, \mathcal{R}^{(0)})\}$. Thus the statement is immediate from the recursive construction. □

Theorem 2.43 (Iterated Meta-Bidigraphs generalize Iterated Meta DiGraphs)**.** *Let $\mathfrak{D}^{(0)}$ be a universe of finite simple digraphs and $\mathcal{Q}^{(0)} \subseteq \mathcal{P}\big(\mathfrak{D}^{(0)} \times \mathfrak{D}^{(0)}\big)$ a nonempty family of binary relations. Let $\mathrm{IMetaD}^{(t)}$ denote the class of Iterated Meta DiGraphs of depth t over $\big(\mathfrak{D}^{(0)}, \mathcal{Q}^{(0)}\big)$, with the same existential vertex-witness lifting used above to define $\mathcal{Q}^{(t+1)}$ from $\mathcal{Q}^{(t)}$. Assume $\mathcal{R}^{(0)}$ is chosen as the transport of $\mathcal{Q}^{(0)}$ along a fixed injective base embedding $\Phi : \mathfrak{D}^{(0)} \hookrightarrow \mathfrak{B}^{(0)}$ (the standard "arc $\leftrightarrow$ signed end" translation), i.e.*

$$R^{\flat}\big(\Phi(D_1), \Phi(D_2)\big) \iff (D_1, D_2) \in R \quad \textit{for } R \in \mathcal{Q}^{(0)},$$

and set $\mathcal{R}^{(0)} := \{R^{\flat} : R \in \mathcal{Q}^{(0)}\}$. Then, for every $t \geq 0$, there exists an injective map

$$\mathsf{E}_t : \ \mathrm{IMetaD}^{(t)} \ \hookrightarrow \ \mathfrak{B}^{(t)}$$

such that the directed shadow of $\mathsf{E}_t(M)$ is canonically isomorphic to M for all $M \in \mathrm{IMetaD}^{(t)}$. Consequently, Iterated Meta-Bidigraphs strictly extend Iterated Meta DiGraphs.

Proof. We proceed by induction on t.
Base case $t = 0$. Set $\mathsf{E}_0 := \Phi : \mathfrak{D}^{(0)} \hookrightarrow \mathfrak{B}^{(0)}$, which is injective by construction.
Inductive step $t \to t{+}1$. Assume $\mathsf{E}_t : \mathrm{IMetaD}^{(t)} \hookrightarrow \mathfrak{B}^{(t)}$ injective and that for every $S \in \mathcal{Q}^{(t)}$ its transport $S^{\flat} \in \mathcal{R}^{(t)}$ satisfies

$$S^{\flat}\big(\mathsf{E}_t(X),\, \mathsf{E}_t(Y)\big) \iff (X, Y) \in S \qquad \text{for all } X, Y \in \mathrm{IMetaD}^{(t)}.$$

Let $M = (V_M, A_M, s_M, t_M, \lambda_M) \in \mathrm{IMetaD}^{(t+1)}$. Define $\mathsf{E}_{t+1}(M)$ to be the Meta-Bidigraph

$$\big(V_{\mathbb{M}}, E_{\mathbb{M}}, \partial_{\mathbb{M}}, \tau_{\mathbb{M}}, \lambda_{\mathbb{M}}\big)$$

with

$$V_{\mathbb{M}} := \{\ \mathsf{E}_t(v) \mid v \in V_M\ \} \ \subseteq\ \mathfrak{B}^{(t)}, \quad E_{\mathbb{M}} := A_M, \quad \partial_{\mathbb{M}}(a) := \big\{\mathsf{E}_t(s_M(a)),\ \mathsf{E}_t(t_M(a))\big\},$$

$$\tau_{\mathbb{M}}\big(\mathsf{E}_t(s_M(a)), a\big) = -1, \qquad \tau_{\mathbb{M}}\big(\mathsf{E}_t(t_M(a)), a\big) = +1, \qquad \lambda_{\mathbb{M}}(a) := \lambda_M(a)^{\flat} \in \mathcal{R}^{(t)}.$$

This is well-defined: the local signs are $\{-1,+1\}$ at the two incident meta-vertices and 0 elsewhere. For the witnessing constraint at level $t+1$, fix $a \in E_{\mathbb{M}}$ and write $X := \mathsf{E}_t(s_M(a))$, $Y := \mathsf{E}_t(t_M(a))$. By construction, the demand set is $\mathrm{Dem}(a) = \{(X,Y)\}$. Since $(s_M(a), t_M(a)) \in \lambda_M(a) \in \mathcal{Q}^{(t)}$, the transport property gives

$$(X,Y) \in \lambda_M(a)^{\flat} = \lambda_{\mathbb{M}}(a),$$

so $\mathrm{Dem}(a) \subseteq \lambda_{\mathbb{M}}(a)$, as required.

Directed shadow and injectivity. The directed shadow $\overrightarrow{\mathbb{M}}$ of $\mathsf{E}_{t+1}(M)$ has vertex set $V_{\mathbb{M}}$ and arc set in bijection with A_M, preserving sources/targets and labels; hence $\overrightarrow{\mathbb{M}} \cong M$. Distinct M yield distinct $\mathsf{E}_{t+1}(M)$, so E_{t+1} is injective.

Compatibility of lifted relations. By construction of $\mathcal{R}^{(t+1)}$ from $\mathcal{R}^{(t)}$ and of $\mathcal{Q}^{(t+1)}$ from $\mathcal{Q}^{(t)}$ via the same existential vertex-witness rule, the transport $(\cdot)^{\flat}$ commutes with lifting:

$$\left(S^{\uparrow}\right)^{\flat} \;=\; \left(S^{\flat}\right)^{\uparrow}.$$

Thus the label family at level $t+1$ matches the embedding above.

This completes the induction and proves the claim. □

2.9. *Meta-Neutrosophic Graph*

A Meta-Neutrosophic Graph organizes neutrosophic graphs as vertices, with edges reflecting truth, indeterminacy, and falsity components of higher-level relational uncertainty.

Let NG be a fixed universe of (finite, undirected, loopless unless stated) *neutrosophic graphs* G with vertex-membership $\sigma_G : V(G) \to [0,1]^3$ and edge-membership $\mu_G : V(G) \times V(G) \to [0,1]^3$, written

$$\sigma_G(v) = (T_\sigma(v), I_\sigma(v), F_\sigma(v)), \qquad \mu_G(u,v) = (T_\mu(u,v), I_\mu(u,v), F_\mu(u,v)),$$

satisfying for all distinct u, v:

$$T_\mu(u,v) \le \min\{T_\sigma(u), T_\sigma(v)\}, \quad I_\mu(u,v) \ge \max\{I_\sigma(u), I_\sigma(v)\}, \quad F_\mu(u,v) \ge \max\{F_\sigma(u), F_\sigma(v)\}.$$

Let $\mathcal{R} \subseteq ([0,1]^3)^{\mathsf{NG}\times\mathsf{NG}}$ be a nonempty family of *neutrosophic relations* $R(X,Y) = (T_R, I_R, F_R)$.

Definition 2.44 (Meta-Neutrosophic Graph)**.** A *Meta-Neutrosophic Graph* over $(\mathsf{NG}, \mathcal{R})$ is a quadruple

$$\mathbb{N} = (V, \Sigma_M, M_N, L_M)$$

with $V \subseteq \mathsf{NG}$, $\Sigma_M : V \to [0,1]^3$, $M_N : V \times V \to [0,1]^3$, and $L_M : V \times V \to \mathcal{P}_{\text{fin}}(\mathcal{R})$, such that for all $X, Y \in V$:

$$T_{M_N}(X,Y) \le \min\{T_{\Sigma_M}(X), T_{\Sigma_M}(Y)\}, \tag{6}$$

$$I_{M_N}(X,Y) \ge \max\{I_{\Sigma_M}(X), I_{\Sigma_M}(Y)\}, \tag{7}$$

$$F_{M_N}(X,Y) \ge \max\{F_{\Sigma_M}(X), F_{\Sigma_M}(Y)\}, \tag{8}$$

and the *label witnessing* bounds

$$T_{M_N}(X,Y) \le \sup_{R \in L_M(X,Y)} T_R(X,Y), \tag{9}$$

$$I_{M_N}(X,Y) \ge \inf_{R \in L_M(X,Y)} I_R(X,Y), \tag{10}$$

$$F_{M_N}(X,Y) \ge \inf_{R \in L_M(X,Y)} F_R(X,Y), \tag{11}$$

with conventions $\sup \emptyset := 0$ and $\inf \emptyset := 1$ (componentwise).

Example 2.45 (Hospital Data-Sharing under Uncertainty as a Meta-Neutrosophic Graph)**.** Let NG contain three hospital-level neutrosophic graphs $A =$ (Tokyo General), $B =$ (Osaka Central), $C =$ (Nagoya West), each internally describing clinical entities (labs, encounters) with neutrosophic memberships (omitted here). Define the meta-vertex neutrosophic memberships (institution-level reliability/uncertainty):

$$\Sigma_M(A) = (0.85,\ 0.10,\ 0.05), \qquad \Sigma_M(B) = (0.75,\ 0.20,\ 0.10), \qquad \Sigma_M(C) = (0.65,\ 0.25,\ 0.15).$$

Let $\mathcal{R}$ contain two neutrosophic relations on $\mathsf{NG} \times \mathsf{NG}$:

$$R_{\text{align}}(X,Y) = (T_{\text{al}}(X,Y), I_{\text{al}}(X,Y), F_{\text{al}}(X,Y)) \quad \text{(policy \& coding alignment)},$$

$$R_{\text{share}}(X,Y) = (T_{\text{sh}}(X,Y), I_{\text{sh}}(X,Y), F_{\text{sh}}(X,Y)) \quad \text{(data-sharing readiness)}.$$

For (A, B) assume (symmetric values suffice here):

$$R_{\text{align}}(A,B) = (0.70,\ 0.25,\ 0.10), \qquad R_{\text{share}}(A,B) = (0.60,\ 0.15,\ 0.20).$$

Set the label set $L_M(A,B) = \{R_{\text{align}}, R_{\text{share}}\}$ and define the meta-edge membership

$$M_N(A,B) = (0.68,\ 0.22,\ 0.12).$$

Verification of the Meta-Neutrosophic constraints. First, vertex bounds (6)–(8):

$$\min\{T_{\Sigma_M}(A), T_{\Sigma_M}(B)\} = \min\{0.85, 0.75\} = 0.75 \ \ge\ T_{M_N}(A,B) = 0.68,$$

$$\max\{I_{\Sigma_M}(A), I_{\Sigma_M}(B)\} = \max\{0.10, 0.20\} = 0.20 \ \le\ I_{M_N}(A,B) = 0.22,$$

$$\max\{F_{\Sigma_M}(A), F_{\Sigma_M}(B)\} = \max\{0.05, 0.10\} = 0.10 \ \le\ F_{M_N}(A,B) = 0.12.$$

Next, witnessing bounds (9)–(11) with $L_M(A, B)$:

$$\sup_{R\in L_M} T_R(A,B) = \max\{0.70, 0.60\} = 0.70 \ \geq \ 0.68 = T_{M_N}(A,B),$$
$$\inf_{R\in L_M} I_R(A,B) = \min\{0.25, 0.15\} = 0.15 \ \leq \ 0.22 = I_{M_N}(A,B),$$
$$\inf_{R\in L_M} F_R(A,B) = \min\{0.10, 0.20\} = 0.10 \ \leq \ 0.12 = F_{M_N}(A,B).$$

All inequalities hold, so with $V = \{A, B, C\}$ and L_M defined likewise on other pairs, $\mathbb{N} = (V, \Sigma_M, M_N, L_M)$ is a concrete *Meta-Neutrosophic Graph* modeling hospital-to-hospital data-sharing under uncertainty.

Theorem 2.46 (Generalization)**.** *(i)* Neutrosophic graph ⇒ meta. *Given $G \in \mathsf{NG}$ with vertex set $V(G)$, for each $v \in V(G)$ let A_v be the one-vertex neutrosophic graph with $\sigma_{A_v}(v) = \sigma_G(v)$ and no edges. Define*

$$V := \{A_v : v \in V(G)\}, \quad \Sigma_M(A_v) := \sigma_G(v), \quad M_N(A_u, A_v) := \mu_G(u, v),$$

and $L_M(A_u, A_v) := \{R_{u,v}\}$ where $R_{u,v}(A_u, A_v) := \mu_G(u, v)$ and $R_{u,v}(\cdot, \cdot) = (0, 0, 0)$ otherwise.
(ii) Meta-Fuzzy ⇒ meta-neutrosophic. *For a Meta-Fuzzy Graph $\mathbb{M} = (\sigma_M, \mu_M, L)$ on a fuzzy-graph universe FG, define the lift*

$$a \mapsto a^\sharp := (a, 0, 1 - a) \quad \text{on } [0, 1].$$

Set $V := \mathrm{supp}(\sigma_M)$, $\Sigma_M(F) := \sigma_M(F)^\sharp$, $M_N(F, G) := \mu_M(F, G)^\sharp$, and $L_M(F, G) := \{R^\sharp : R \in L(F, G)\}$ where $(R^\sharp)_T = R$, $(R^\sharp)_I = 0$, $(R^\sharp)_F = 1 - R$.
The constructions in (i) and (ii) embed, respectively, neutrosophic graphs and Meta-Fuzzy Graphs into Meta-Neutrosophic Graphs. Hence Meta-Neutrosophic Graphs generalize both classes.

Proof. (i) For A_u, A_v,

$$T_{M_N} = T_{\mu_G}(u, v) \leq \min\{T_{\sigma_G}(u), T_{\sigma_G}(v)\} = \min\{T_{\Sigma_M}(A_u), T_{\Sigma_M}(A_v)\},$$

and similarly (7)–(8). For witnessing, $R_{u,v}(A_u, A_v) = \mu_G(u, v)$ gives (9)–(11) with equality.
(ii) Since $\mu_M \leq \min\{\sigma_M, \sigma_M\}$, we obtain

$$T_{M_N} = \mu_M \leq \min\{\sigma_M, \sigma_M\} = \min\{T_{\Sigma_M}, T_{\Sigma_M}\},$$
$$I_{M_N} = 0 \geq \max\{0, 0\},$$
$$F_{M_N} = 1 - \mu_M \geq \max\{1 - \sigma_M, 1 - \sigma_M\}.$$

For witnessing, with $Q = R^\sharp$,

$$T_{M_N} \leq \sup_{R\in L} R = \sup_{Q\in L_M} T_Q,$$
$$I_{M_N} = 0 \geq \inf_{Q\in L_M} I_Q = 0,$$

$$F_{M_N} = 1 - \mu_M \geq \inf_{R \in L} (1 - R) = \inf_{Q \in L_M} F_Q.$$

□

2.10. *Iterated Meta-Neutrosophic Graph*

An Iterated Meta-Neutrosophic Graph recursively applies neutrosophic meta-construction, forming multi-level structures representing layered uncertain interactions among complex neutrosophic networks.

Definition 2.47 (Neutrosophic lifting of relations)**.** Let each level-t object X have a vertex-set V_X and $\Sigma_X : V_X \to [0,1]^3$. For R on the previous level define, for X, Y,

$$T_{R^\uparrow}(X,Y) := \sup_{u \in V_X,\ v \in V_Y} \min\{T_{\Sigma_X}(u), T_{\Sigma_Y}(v), T_R(u,v)\},$$
$$I_{R^\uparrow}(X,Y) := \inf_{u \in V_X,\ v \in V_Y} \max\{I_{\Sigma_X}(u), I_{\Sigma_Y}(v), I_R(u,v)\},$$
$$F_{R^\uparrow}(X,Y) := \inf_{u \in V_X,\ v \in V_Y} \max\{F_{\Sigma_X}(u), F_{\Sigma_Y}(v), F_R(u,v)\}.$$

Definition 2.48 (Iterated universes and objects)**.** Fix $\mathsf{NG}^{(0)} := \mathsf{NG}$ and $\mathcal{R}^{(0)} \subseteq ([0,1]^3)^{\mathsf{NG}^{(0)} \times \mathsf{NG}^{(0)}}$. Recursively for $t \geq 0$,

$$\mathsf{NG}^{(t+1)} := \{\text{ Meta-Neutrosophic Graphs over } (\mathsf{NG}^{(t)}, \mathcal{R}^{(t)}) \ \}, \qquad \mathcal{R}^{(t+1)} := \{R^\uparrow : R \in \mathcal{R}^{(t)}\}.$$

Any element of $\mathsf{NG}^{(t+1)}$ is an *Iterated Meta-Neutrosophic Graph of depth t.*

Example 2.49 (Regional Health Consortia as an Iterated Meta-Neutrosophic Graph)**.** Form two level-1 meta-neutrosophic vertices (consortia):

$$X = \text{East Consortium on } \{A, C\}, \qquad Y = \text{West Consortium on } \{B\}.$$

Give level-1 vertex memberships (institutional fitness at the consortium level):

$$\Sigma^{(1)}(X) = (0.82,\ 0.18,\ 0.12), \qquad \Sigma^{(1)}(Y) = (0.90,\ 0.15,\ 0.10).$$

For lifting (Definition 2.47), we need the *level-0* memberships of the inner vertices. Specify (componentwise) for X and Y:

$$\Sigma_X(A) = (0.80,\ 0.15,\ 0.10), \quad \Sigma_X(C) = (0.65,\ 0.25,\ 0.15), \quad \Sigma_Y(B) = (0.88,\ 0.20,\ 0.10).$$

Assume base-level relation values on pairs with B:

$$R_{\text{align}}(A,B) = (0.60,\ 0.30,\ 0.20), \qquad R_{\text{align}}(C,B) = (0.50,\ 0.35,\ 0.25),$$

$$R_{\text{share}}(A,B) = (0.55,\ 0.25,\ 0.25), \qquad R_{\text{share}}(C,B) = (0.40,\ 0.40,\ 0.30).$$

Lifted relations to level 1. Using Definition 2.47, compute for $R^{\uparrow}_{\text{align}}$:

$$T_{R^{\uparrow}_{\text{align}}}(X,Y) = \sup_{u\in\{A,C\},\, v=B} \min\{T_{\Sigma_X}(u), T_{\Sigma_Y}(v), T_{R_{\text{align}}}(u,v)\}$$
$$= \max\{\min(0.80, 0.88, 0.60),\ \min(0.65, 0.88, 0.50)\} = \max\{0.60,\ 0.50\} = 0.60,$$

$$I_{R^{\uparrow}_{\text{align}}}(X,Y) = \inf_{u,v} \max\{I_{\Sigma_X}(u), I_{\Sigma_Y}(v), I_{R_{\text{align}}}(u,v)\}$$
$$= \min\{\max(0.15, 0.20, 0.30),\ \max(0.25, 0.20, 0.35)\} = \min\{0.30,\ 0.35\} = 0.30,$$

$$F_{R^{\uparrow}_{\text{align}}}(X,Y) = \inf_{u,v} \max\{F_{\Sigma_X}(u), F_{\Sigma_Y}(v), F_{R_{\text{align}}}(u,v)\}$$
$$= \min\{\max(0.10, 0.10, 0.20),\ \max(0.15, 0.10, 0.25)\} = \min\{0.20,\ 0.25\} = 0.20.$$

Hence $R^{\uparrow}_{\text{align}}(X,Y) = (0.60,\ 0.30,\ 0.20)$.
Similarly for $R^{\uparrow}_{\text{share}}$:

$$T_{R^{\uparrow}_{\text{share}}}(X,Y) = \max\{\min(0.80, 0.88, 0.55),\ \min(0.65, 0.88, 0.40)\} = \max\{0.55,\ 0.40\} = 0.55,$$
$$I_{R^{\uparrow}_{\text{share}}}(X,Y) = \min\{\max(0.15, 0.20, 0.25),\ \max(0.25, 0.20, 0.40)\} = \min\{0.25,\ 0.40\} = 0.25,$$
$$F_{R^{\uparrow}_{\text{share}}}(X,Y) = \min\{\max(0.10, 0.10, 0.25),\ \max(0.15, 0.10, 0.30)\} = \min\{0.25,\ 0.30\} = 0.25.$$

Thus $R^{\uparrow}_{\text{share}}(X,Y) = (0.55,\ 0.25,\ 0.25)$.
Level-1 meta-edge and verification. Take the meta-label set $L^{(1)}(X,Y) = \{R^{\uparrow}_{\text{align}}, R^{\uparrow}_{\text{share}}\}$ and define

$$M_N^{(1)}(X,Y) = (0.58,\ 0.26,\ 0.21).$$

Vertex bounds:

$$\min\{T_{\Sigma^{(1)}}(X), T_{\Sigma^{(1)}}(Y)\} = \min\{0.82, 0.90\} = 0.82\ \geq\ 0.58,$$
$$\max\{I_{\Sigma^{(1)}}(X), I_{\Sigma^{(1)}}(Y)\} = \max\{0.18, 0.15\} = 0.18\ \leq\ 0.26,$$
$$\max\{F_{\Sigma^{(1)}}(X), F_{\Sigma^{(1)}}(Y)\} = \max\{0.12, 0.10\} = 0.12\ \leq\ 0.21.$$

Witnessing with lifted labels:

$$\sup_{R\in L^{(1)}} T_R(X,Y) = \max\{0.60, 0.55\} = 0.60\ \geq\ 0.58,$$
$$\inf_{R\in L^{(1)}} I_R(X,Y) = \min\{0.30, 0.25\} = 0.25\ \leq\ 0.26,$$
$$\inf_{R\in L^{(1)}} F_R(X,Y) = \min\{0.20, 0.25\} = 0.20\ \leq\ 0.21.$$

Therefore $\mathbb{N}^{(1)} = (\{X,Y\},\ \Sigma^{(1)},\ M_N^{(1)},\ L^{(1)})$ is a valid *Iterated Meta-Neutrosophic Graph*: a concrete hospital-pair evidence at level 0 lifts to a consortium-to-consortium relation at level 1 with all neutrosophic constraints satisfied componentwise.

Theorem 2.50 (Depth 1). $\mathsf{NG}^{(1)}$ *equals the class of Meta-Neutrosophic Graphs over* $(\mathsf{NG}^{(0)}, \mathcal{R}^{(0)})$.

Proof. Unfold Definition 2.48 at $t = 0$. □

Theorem 2.51 (IMNG generalizes IMFG and MNG)**.** *Let* $\mathsf{FG}^{(0)}$ *be a fuzzy-graph universe with fuzzy relations* $\mathcal{S}^{(0)}$*. Define the levelwise lift* $\sharp$ *by* $a \mapsto (a, 0, 1-a)$ *on memberships and relations, and extend recursively:*

$$\sharp: \ \mathsf{FG}^{(t)} \hookrightarrow \mathsf{NG}^{(t)}, \qquad \sharp: \ \mathcal{S}^{(t)} \hookrightarrow \mathcal{R}^{(t)}.$$

Then for all $t \geq 0$*:*

(1) $\sharp$ *embeds Iterated Meta-Fuzzy Graphs (depth* t*) into Iterated Meta-Neutrosophic Graphs (depth* t*).*

(2) At $t = 0$ *this reduces to Theorem 2.46; at* $t = 1$ *to the Theorem.*

Proof. For any $R \in \mathcal{S}^{(t)}$ and $X, Y \in \mathsf{FG}^{(t)}$, using $a^\sharp = (a, 0, 1-a)$:

$$T_{(R^\sharp)^\uparrow}(\sharp X, \sharp Y) = \sup_{u,v} \min\{\Sigma_X(u), \Sigma_Y(v), R(u,v)\} = T_{R^\uparrow}(X,Y),$$

$$I_{(R^\sharp)^\uparrow}(\sharp X, \sharp Y) = \inf_{u,v} \max\{0,0,0\} = 0,$$

$$F_{(R^\sharp)^\uparrow}(\sharp X, \sharp Y) = \inf_{u,v} \max\{1-\Sigma_X(u), 1-\Sigma_Y(v), 1-R(u,v)\} = 1 - T_{R^\uparrow}(X,Y),$$

hence $(R^\sharp)^\uparrow = (R^\uparrow)^\sharp$ and the label families match levelwise. Edge/vertex bounds are preserved exactly as in Theorem 2.46(ii), now at level t. □

2.11. *Meta-Weighted Graph*

A meta-weighted graph has vertices that are graphs, edges labeled by relations, and real weights encoding costs, capacities, or strengths.

Definition 2.52 (Universe and relation family)**.** Fix a nonempty universe $\mathfrak{G}$ of finite (undirected, loopless by default) graphs and a nonempty family

$$\mathcal{R} \ \subseteq \ \mathcal{P}\big(\mathfrak{G} \times \mathfrak{G}\big)$$

of binary relations on $\mathfrak{G}$ (e.g. subgraph, homomorphism, minor, isomorphism).

Definition 2.53 (Meta-Weighted Graph over $(\mathfrak{G}, \mathcal{R})$)**.** A *Meta-Weighted Graph* is a directed, labeled multidigraph with edge weights

$$\mathbb{M} \ = \ (V, E, s, t, \lambda, w),$$

where $V \subseteq \mathfrak{G}$, $s, t : E \to V$, $\lambda : E \to \mathcal{R}$, and $w : E \to \mathbb{R}$, such that

$$\forall e \in E: \qquad (\, s(e), \, t(e) \,) \in \lambda(e) \quad \text{(incidence witnessing).}$$

Elements of V are *meta-vertices* (each is itself a graph $G \in \mathfrak{G}$). For $e \in E$ we write

$$s(e) \xrightarrow[w(e)]{\lambda(e)} t(e),$$

and call $w(e)$ the *meta-weight* of e. If every $R \in \mathcal{R}$ is symmetric and for each unordered pair $\{x, y\}$ the multiset of arcs $x \to y$ equals that of $y \to x$ with identical weights, $\mathbb{M}$ can be regarded as an undirected weighted, labeled meta-multigraph.

Remark 2.54 (Forgetting weights and labels)**.** There are natural forgetful maps:

$$\mathrm{U_w}: \ (V, E, s, t, \lambda, w) \longmapsto (V, E, s, t, \lambda), \qquad \mathrm{U_{lab}}: \ (V, E, s, t, \lambda, w) \longmapsto (V, E, s, t, w),$$

which discard, respectively, weights and labels.

Example 2.55 (Inter–city Transport Corridors as a Meta–Weighted Graph)**.** Let $\mathfrak{G}$ be the universe of finite *city–level* transportation graphs, each encoding local stations/airports and routes. Fix a family of binary relations $\mathcal{R} = \{\mathrm{Rail}, \mathrm{Air}, \mathrm{Hwy}\}$ on $\mathfrak{G}$, where

$$(X, Y) \in \mathrm{Rail} \iff \text{there exists a direct rail corridor between cities represented by } X \text{ and } Y,$$

and analogously for Air (direct scheduled flight) and Hwy (limited–access highway).
Consider three city graphs G_T (Tokyo), G_O (Osaka), G_N (Nagoya) in $\mathfrak{G}$. Define the meta–weighted graph

$$M = (V, E, s, t, \lambda, w), \qquad V = \{G_T, G_O, G_N\},$$

as a directed, labeled multigraph whose meta–edges record the type of corridor and whose weights are *door–to–door median travel times (hours)*:

$$\begin{aligned}
e^{\mathrm{rail}}_{TO}: \ & s(e^{\mathrm{rail}}_{TO}) = G_T, \ t(e^{\mathrm{rail}}_{TO}) = G_O, \ \lambda(e^{\mathrm{rail}}_{TO}) = \mathrm{Rail}, \ w(e^{\mathrm{rail}}_{TO}) = 2.5, \\
e^{\mathrm{air}}_{TO}: \ & s(e^{\mathrm{air}}_{TO}) = G_T, \ t(e^{\mathrm{air}}_{TO}) = G_O, \ \lambda(e^{\mathrm{air}}_{TO}) = \mathrm{Air}, \ \ w(e^{\mathrm{air}}_{TO}) = 1.0, \\
e^{\mathrm{rail}}_{ON}: \ & s(e^{\mathrm{rail}}_{ON}) = G_O, \ t(e^{\mathrm{rail}}_{ON}) = G_N, \ \lambda(e^{\mathrm{rail}}_{ON}) = \mathrm{Rail}, \ w(e^{\mathrm{rail}}_{ON}) = 1.8, \\
e^{\mathrm{hwy}}_{TN}: \ & s(e^{\mathrm{hwy}}_{TN}) = G_T, \ t(e^{\mathrm{hwy}}_{TN}) = G_N, \ \lambda(e^{\mathrm{hwy}}_{TN}) = \mathrm{Hwy}, \ \ w(e^{\mathrm{hwy}}_{TN}) = 3.1.
\end{aligned}$$

Each meta–edge e satisfies the incidence constraint $\big(s(e), t(e)\big) \in \lambda(e)$ by construction (e.g. $(G_T, G_O) \in \mathrm{Air}$ and $(G_T, G_O) \in \mathrm{Rail}$), while the weight $w(e)$ numerically encodes the operational cost/time of that corridor. Multiple edges between a pair (e.g. rail and air) capture alternative modalities.

Theorem 2.56 (Meta-Weighted Graphs generalize MetaGraphs)**.** *Let $M_0 = (V_0, E_0, s_0, t_0, \lambda_0)$ be a MetaGraph over $(\mathfrak{G}, \mathcal{R})$. Define*

$$\iota_{\mathrm{MG}}(M_0) \ := \ (V_0, E_0, s_0, t_0, \lambda_0, w_1), \qquad w_1(e) \equiv 1 \quad (\forall e \in E_0).$$

Then $\iota_{\mathrm{MG}}(M_0)$ is a Meta-Weighted Graph and $\mathrm{U_w}\big(\iota_{\mathrm{MG}}(M_0)\big) = M_0$. Hence Meta-Weighted Graphs strictly extend MetaGraphs.

Proof. Incidence witnessing for $\iota_{\mathrm{MG}}(M_0)$ is identical to that of M_0, and constant weights pose no additional constraint. The equality under $\mathrm{U_w}$ is immediate. Strictness follows since different weightings of the same metagraph yield distinct Meta-Weighted Graphs. □

Definition 2.57 (Singleton-graph embedding)**.** For a set X, write $\mathsf{pt}(x)$ for the one-vertex graph with vertex x and no edges.

Theorem 2.58 (Meta-Weighted Graphs generalize Weighted Graphs)**.** *Let $G = (V_G, E_G, w_G)$ be a (finite, undirected, loopless) weighted graph with $w_G : E_G \to \mathbb{R}$. Fix any nonempty $\mathcal{R}$ and, for each unordered pair $\{u, v\} \subseteq V_G$, introduce a label*

$$R_{u,v} \ \in \ \mathcal{R} \qquad \textit{with} \qquad (\mathsf{pt}(u), \mathsf{pt}(v)) \in R_{u,v}.$$

Define a Meta-Weighted Graph over $(\mathfrak{G}, \mathcal{R})$ by

$$V := \{\mathsf{pt}(v) \mid v \in V_G\}, \quad E := \{e_{u\to v}, \, e_{v\to u} \mid \{u, v\} \in E_G\},$$

$$s(e_{u\to v}) = \mathsf{pt}(u), \quad t(e_{u\to v}) = \mathsf{pt}(v), \quad \lambda(e_{u\to v}) = R_{u,v}, \quad w(e_{u\to v}) = w_G(\{u, v\}),$$

and symmetrically for $e_{v\to u}$. Then:

(1) Incidence is witnessed by construction, so (V, E, s, t, λ, w) is a Meta-Weighted Graph.

(2) Collapsing opposite arcs into a single undirected edge and keeping the common weight recovers G.

Thus weighted graphs embed into Meta-Weighted Graphs.

Proof. (1) By definition $(\mathsf{pt}(u), \mathsf{pt}(v)) \in R_{u,v} = \lambda(e_{u\to v})$; similarly for the reverse arc. (2) The map $\Psi : V_G \to V$, $v \mapsto \mathsf{pt}(v)$ is a bijection. For each $\{u, v\} \in E_G$, the two arcs $e_{u\to v}$ and $e_{v\to u}$ have identical weight $w_G(\{u, v\})$, so the undirected identification yields an edge of the same weight between $\Psi(u)$ and $\Psi(v)$. This gives a canonical isomorphism between G and the undirected quotient of (V, E, s, t, λ, w). □

2.12. *Iterated Meta-Weighted Graphs*

An iterated meta-weighted graph uses metagraphs as vertices, recursively repeating labeling and weighting to form multi-level graph-of-graphs structures across hierarchies.

Definition 2.59 (Relation lifting)**.** Given $\mathcal{R}$ on $\mathfrak{G}$, define its *lift* $\mathcal{R}^{\uparrow}$ on finite Meta-Weighted Graphs over $(\mathfrak{G}, \mathcal{R})$ by

$$\mathcal{R}^{\uparrow} := \{R^{\uparrow} \mid R \in \mathcal{R}\}, \qquad (M_1, M_2) \in R^{\uparrow} \iff \exists\, x \in V(M_1),\, y \in V(M_2) : \ (x, y) \in R.$$

(Weights play no role in witnessing; they are additional structure on edges.)

Definition 2.60 (Iterated universes)**.** Define recursively for $t \in \mathbb{N}_0$:

$$\mathfrak{G}^{(0)} := \mathfrak{G}, \qquad \mathcal{R}^{(0)} := \mathcal{R},$$

$$\mathfrak{G}^{(t+1)} := \Big\{ \text{all finite Meta-Weighted Graphs over } \big(\mathfrak{G}^{(t)}, \mathcal{R}^{(t)}\big) \Big\}, \qquad \mathcal{R}^{(t+1)} := \big(\mathcal{R}^{(t)}\big)^{\uparrow}.$$

Definition 2.61 (Iterated Meta-Weighted Graph of depth t)**.** For $t \in \mathbb{N}_0$, an *Iterated Meta-Weighted Graph of depth t* is a tuple

$$\mathbb{M}^{(t)} = (V^{(t)}, E^{(t)}, s^{(t)}, t^{(t)}, \lambda^{(t)}, w^{(t)})$$

with $V^{(t)} \subseteq \mathfrak{G}^{(t)}$, $\lambda^{(t)} : E^{(t)} \to \mathcal{R}^{(t)}$, $w^{(t)} : E^{(t)} \to \mathbb{R}$, and

$$\forall e \in E^{(t)} : \qquad \big(s^{(t)}(e),\, t^{(t)}(e)\big) \in \lambda^{(t)}(e).$$

Example 2.62 (Division–Level Planning as an Iterated Meta–Weighted Graph)**.** Start from the meta–weighted graph M above. Form two *level–1 meta–vertices*, each of which is itself a meta–weighted graph:

$$X := \text{“East” corridor view on } \{G_T, G_N\}, \qquad Y := \text{“West” corridor view on } \{G_O\}.$$

Lift the relation family $\mathcal{R}$ to $\mathcal{R}^{\uparrow}$ by the usual existential witness rule:

$$(X, Y) \in R^{\uparrow} \iff \exists\, x \in V(X),\, y \in V(Y) : \ (x, y) \in R, \quad R \in \mathcal{R}.$$

Define the *iterated meta–weighted graph of depth* 1

$$M^{(1)} = \big(V^{(1)}, E^{(1)}, s^{(1)}, t^{(1)}, \lambda^{(1)}, w^{(1)}\big), \qquad V^{(1)} = \{X, Y\},$$

with two meta–edges whose labels are lifted relations and whose weights aggregate underlying corridor weights (minimum over witnessing pairs, i.e. best available time):

$$\begin{aligned} e^{(1)}_{\text{air}} :\ & s^{(1)} = X,\ t^{(1)} = Y,\ \lambda^{(1)}(e^{(1)}_{\text{air}}) = \text{Air}^{\uparrow}, \\ & \qquad w^{(1)}(e^{(1)}_{\text{air}}) = \min\{\, w(e^{\text{air}}_{TO})\,\} = 1.0, \\ e^{(1)}_{\text{rail}} :\ & s^{(1)} = X,\ t^{(1)} = Y,\ \lambda^{(1)}(e^{(1)}_{\text{rail}}) = \text{Rail}^{\uparrow}, \\ & \qquad w^{(1)}(e^{(1)}_{\text{rail}}) = \min\{\, w(e^{\text{rail}}_{TO}),\ w(e^{\text{rail}}_{ON})\,\} = 1.8. \end{aligned}$$

Incidence holds: $\text{Air}^{\uparrow}$ is witnessed by the pair (G_T, G_O) with a direct flight, and $\text{Rail}^{\uparrow}$ by (G_O, G_N) (or (G_T, G_O)). The weights $w^{(1)}$ summarize lower–level options into division–level best travel times, enabling hierarchical planning across meta–vertices X and Y.

Theorem 2.63 (Depth 1 recovers the meta level)**.**

$$\Big\{ \textit{Meta-Weighted Graphs over } (\mathfrak{G}, \mathcal{R}) \Big\} \ = \ \mathfrak{G}^{(1)}.$$

Proof. By Definition, $\mathfrak{G}^{(1)}$ is exactly the class of Meta-Weighted Graphs over $(\mathfrak{G}, \mathcal{R})$. □

Theorem 2.64 (Iterated Meta-Weighted Graphs generalize Iterated MetaGraphs and Meta-Weighted Graphs)**.** *For every $t \geq 0$:*

(1) The assignment

$$(V^{(t)}, E^{(t)}, s^{(t)}, t^{(t)}, \lambda^{(t)}) \longmapsto (V^{(t)}, E^{(t)}, s^{(t)}, t^{(t)}, \lambda^{(t)}, \mathbf{1})$$

(where $\mathbf{1}$ is the constant-1 weight on $E^{(t)}$) embeds Iterated MetaGraphs of depth t into Iterated Meta-Weighted Graphs of depth t, and forgetting weights inverts this embedding.

(2) The case $t = 1$ reduces to the Theorem; hence Iterated Meta-Weighted Graphs strictly extend Meta-Weighted Graphs.

Proof. (1) Incidence witnessing is unchanged; the extra constant weight satisfies the definition of an Iterated Meta-Weighted Graph. The forgetful map $\mathrm{U_w}$ applied levelwise recovers the original Iterated MetaGraph, giving a left inverse and hence an embedding.
(2) Immediate from Definition 2.61 and the Theorem. □

3. Conclusion

In this paper, we extended the frameworks of fuzzy graphs, neutrosophic graphs, multigraphs, digraphs, and bidirected graphs by embedding them into the unified setting of MetaGraphs and Iterated MetaGraphs. In the future, we intend to investigate extended systems of the concepts defined in this paper by employing Plithogenic Sets [40], Intuitionistic Fuzzy Sets [41], Bipolar Fuzzy Sets [42], HyperGraphs [43,44], and SuperHyperGraphs [45,46].

Funding

No external funding was received for this work.

Conflicts of Interest

The authors declare no conflicts of interest regarding the publication of this work.

Acknowledgments

We thank all colleagues, reviewers, and readers whose comments and questions have greatly improved this manuscript. We are also grateful to the authors of the works cited herein for providing the theoretical foundations that underpin our study. Finally, we appreciate the institutional and technical support that enabled this research.

Data Availability

This paper is theoretical and did not generate or analyze any empirical data. We welcome future studies that apply and test these concepts in practical settings.

Research Integrity

The authors confirms that this manuscript is original, has not been published elsewhere, and is not under consideration by any other journal.

Use of Computational Tools

All proofs and derivations were performed manually; no computational software (e.g., Mathematica, SageMath, Coq) was used.

Code Availability

No code or software was developed for this study.

Ethical Approval

This research did not involve human participants or animals, and therefore did not require ethical approval.

Use of Generative AI and AI-Assisted Tools

We use generative AI and AI-assisted tools for tasks such as English grammar checking, and we do not employ them in any way that violates ethical standards.

Supplementary Information

No supplementary materials accompany this paper.

Disclaimer

The ideas presented here are theoretical and have not yet been validated through empirical testing. While we have strived for accuracy and proper citation, inadvertent errors may remain. Readers should verify any referenced material independently. The opinions expressed are those of the authors and do not necessarily reflect the views of their institutions.

References

[1] Reinhard Diestel. *Graph theory.* Springer (print edition); Reinhard Diestel (eBooks), 2024.

[2] RB Azevedo, Rolf Lohaus, and Tiago Paixão. Networking networks. *Evol Dev*, 10:514–515, 2008.

[3] T. Fujita. Metahypergraphs, metasuperhypergdynaraphs, and iterated metagraphs: Modeling graphs of graphs, hypergraphs of hypergraphs, superhypergraphs of superhypergraphs, and beyond. *Current Research in Interdisciplinary Studies*, 4(5):1–23, 2025.

[4] Claire Donnat and Susan Holmes. Tracking network dynamics: A survey using graph distances. *The Annals of Applied Statistics*, 12(2):971–1012, 2018.

[5] Jiaqi Cao, Shengli Zhang, Qingxia Chen, Houtian Wang, Mingzhe Wang, and Naijin Liu. Network-wide task offloading with leo satellites: A computation and transmission fusion approach. *arXiv preprint arXiv:2211.09672*, 2022.

[6] Takaaki Fujita. Molecular metagraph and molecular iterated metagraph in chemistryand biochemistry. *Journal of Applied Mathematics and Symbolic Science*, 1(1):43–57, 2025.

[7] Takaaki Fujita and Florentin Smarandache. *HyperGraph and SuperHyperGraph Theory with Applications.* Neutrosophic Science International Association (NSIA) Publishing House, 2026.

[8] Takaaki Fujita. Metastructure, meta-hyperstructure, and meta-superhyper structure. *Journal of Computers and Applications*, 1(1):1–22, 2025.

[9] Lotfi A Zadeh. Fuzzy sets. *Information and control*, 8(3):338–353, 1965.

[10] Hans-Jürgen Zimmermann. *Fuzzy set theory—and its applications.* Springer Science & Business Media, 2011.

[11] Takaaki Fujita, Ajoy Kanti Das, Sankar Prasad Mondal, and Suman Das. A short note on interval-valued bipolar fuzzy superhypergraphs. *Galoitica: Journal of Mathematical Structures and Applications*, 12(2):51–58, 2025.

[12] Azriel Rosenfeld. Fuzzy graphs. In *Fuzzy sets and their applications to cognitive and decision processes*, pages 77–95. Elsevier, 1975.

[13] Takaaki Fujita, Ajoy Kanti Das, Suman Das, and Sankar Prasad Mondal. Fuzzy Off-SuperHyperGraphs: Extending uncertainty modeling beyond classical boundaries. *Neutrosophic Knowledge*, 9:14–30, 2026.

[14] Muhammad Akram and Anam Luqman. *Fuzzy hypergraphs and related extensions.* Springer, 2020.

[15] Florentin Smarandache. *Neutrosophic Overset, Neutrosophic Underset, and Neutrosophic Offset. Similarly for Neutrosophic Over-/Under-/Off-Logic, Probability, and Statistics.* Infinite Study, 2016.

[16] Florentin Smarandache. Operators for uncertain over/under/off-sets/-logics/probabilities/-statistics. *Neutrosophic Sets and Systems*, 79:493–500, 2025.

[17] Said Broumi, Mohamed Talea, Assia Bakali, and Florentin Smarandache. Single valued neutrosophic graphs. *Journal of New theory*, (10):86–101, 2016.

[18] Said Broumi, Mohamed Talea, Assia Bakali, and Florentin Smarandache. Interval valued neutrosophic graphs. *Critical Review, XII*, 2016:5–33, 2016.

[19] Said Broumi, Assia Bakali, Mohamed Talea, and Florentin Smarandache. An isolated bipolar single-valued neutrosophic graphs. In *Information Systems Design and Intelligent Applications: Proceedings of Fourth International Conference INDIA 2017*, pages 816–822. Springer, 2018.

[20] Sunil Mathew and MS Sunitha. Cycle connectivity in weighted graphs. *Proyecciones (Antofagasta)*, 30(1):1–17, 2011.

[21] A. Buck and James M. Keller. Evaluating path costs in multi-attributed fuzzy weighted graphs. *2019 IEEE International Conference on Fuzzy Systems (FUZZ-IEEE)*, pages 1–6, 2019.

[22] Chris Cornelis, Pieter M. M. De Kesel, and Etienne E. Kerre. Shortest paths in fuzzy weighted graphs. *International Journal of Intelligent Systems*, 19, 2004.

[23] P. Sinthamani. Mathematical modeling of optimizing television cable network using fuzzy weighted graph. *Malaya Journal of Matematik*, 2019.

[24] Shinji Umeyama. An eigendecomposition approach to weighted graph matching problems. *IEEE transactions on pattern analysis and machine intelligence*, 10(5):695–703, 1988.

[25] Michael B Teitz and Polly Bart. Heuristic methods for estimating the generalized vertex median of a weighted graph. *Operations research*, 16(5):955–961, 1968.

[26] Takaaki Fujita. Extensions of multidirected graphs: Fuzzy, neutrosophic, plithogenic, rough, soft, hypergraph, and superhypergraph variants. *International Journal of Topology*, 2(3):11, 2025.

[27] Adam L. Buchsbaum, Emden R. Gansner, and Suresh Venkatasubramanian. Directed graphs and rectangular layouts. *2007 6th International Asia-Pacific Symposium on Visualization*, pages 61–64, 2007.

[28] Frank Gurski and Carolin Rehs. Comparing linear width parameters for directed graphs. *Theory of Computing Systems*, 63:1358–1387, 2019.

[29] Ping Zhang and Gary Chartrand. Introduction to graph theory. *Tata McGraw-Hill*, 2:2–1, 2006.

[30] Takaaki Fujita. Review of plithogenic directed, mixed, bidirected, and pangene offgraph. *Advancing Uncertain Combinatorics through Graphization, Hyperization, and Uncertainization: Fuzzy, Neutrosophic, Soft, Rough, and Beyond*, page 120, 2025.

[31] Rui Xu and Cun-Quan Zhang. On flows in bidirected graphs. *Discrete mathematics*, 299(1-3):335–343, 2005.

[32] Jack Edmonds and Ellis L Johnson. Matching: A well-solved class of integer linear programs. In *Combinatorial Optimization-Eureka, You Shrink! Papers Dedicated to Jack Edmonds 5th International Workshop Aussois, France, March 5–9, 2001 Revised Papers*, pages 27–30. Springer, 2003.

[33] Laura Gellert and Raman Sanyal. On degree sequences of undirected, directed, and bidirected graphs. *European Journal of Combinatorics*, 64:113–124, 2017.

[34] Landon Butler, Alejandro Parada-Mayorga, and Alejandro Ribeiro. Convolutional learning on multigraphs. *IEEE Transactions on Signal Processing*, 71:933–946, 2023.

[35] Gordon F Royle. Graphs and multigraphs. In *Handbook of Combinatorial Designs*, pages 757–765. Chapman and Hall/CRC, 2006.

[36] Hiroshi Nagamochi and Toshihide Ibaraki. Computing edge-connectivity in multigraphs and capacitated graphs. *SIAM Journal on Discrete Mathematics*, 5(1):54–66, 1992.

[37] Vijay Ingalalli, Dino Ienco, and Pascal Poncelet. Mining frequent subgraphs in multigraphs. *Information Sciences*, 451:50–66, 2018.

[38] Oana Andrei and Hélene Kirchner. A rewriting calculus for multigraphs with ports. *Electronic Notes in Theoretical Computer Science*, 219:67–82, 2008.

[39] Fujita Takaaki and Arif Mehmood. Iterative multifuzzy set, iterative multineutrosophic set, iterative multisoft set, and multiplithogenic sets. *Neutrosophic Computing and Machine Learning*, 41:1–30, 2025.

[40] Florentin Smarandache. Plithogeny, plithogenic set, logic, probability, and statistics. *arXiv preprint arXiv:1808.03948*, 2018.

[41] Krassimir T Atanassov. Circular intuitionistic fuzzy sets. *Journal of Intelligent & Fuzzy Systems*, 39(5):5981–5986, 2020.

[42] Wen-Ran Zhang. Bipolar fuzzy sets and relations: a computational framework for cognitive modeling and multiagent decision analysis. *NAFIPS/IFIS/NASA '94. Proceedings of the First International Joint Conference of The North American Fuzzy Information Processing Society Biannual Conference. The Industrial Fuzzy Control and Intellige*, pages 305–309, 1994.

[43] Alain Bretto. Hypergraph theory. *An introduction. Mathematical Engineering. Cham: Springer*, 1, 2013.

[44] Yifan Feng, Haoxuan You, Zizhao Zhang, Rongrong Ji, and Yue Gao. Hypergraph neural networks. In *Proceedings of the AAAI conference on artificial intelligence*, volume 33, pages 3558–3565, 2019.

[45] Takaaki Fujita, Ajoy Kanti Das, and Suman Das. Molecular line HyperGraphs and SuperHyperGraphs. *Neutrosophic Knowledge*, 9:31–65, 2026.

[46] Florentin Smarandache. *Extension of HyperGraph to n-SuperHyperGraph and to Plithogenic n-SuperHyperGraph, and Extension of HyperAlgebra to n-ary (Classical-/Neutro-/Anti-) HyperAlgebra*. Infinite Study, 2020.

Neutrosophic Knowledge (NK) is an academic journal, published quarterly online and on paper, that has been created for publishing in all scientific and literary fields. Papers Published in Arabic, Turkish, English and French.
ISSN (print): 2767-0619, ISSN (online): 2767-0627

The papers should be professional, in good Arabic, Turkish, English and French, containing a brief review of a problem and obtained results. All submissions should be designed in MS Word format using our template file:
http://fs.unm.edu/NK/

Submit your paper by email to: neutrosophic.knowledge@gmail.com. To order printed issues, contact the Editor-in Chief. This journal is non-commercial, academic edition. It is printed from private donations. The neutrosophics website at UNM is: http://fs.unm.edu/neutrosophy.htm

The home page of the journal is accessed on:
http://fs.unm.edu/NK/

Editors in Chief